

ENVIRONMENTAL INFLUENCE ON COLD-CLIMATE GRAPEVINE (*VITIS*  
SPP.) FALL ACCLIMATION RESPONSE AND FRUIT RIPENING

A Dissertation  
Submitted to the Graduate Faculty  
of the  
North Dakota State University  
of Agriculture and Applied Science

By

John Edward Stenger

In Partial Fulfillment of the Requirements  
for the Degree of  
DOCTOR OF PHILOSOPHY

Major Department:  
Plant Sciences

October 2016

Fargo, North Dakota

North Dakota State University  
Graduate School

---

**Title**  
ENVIRONMENTAL INFLUENCE ON COLD-CLIMATE GRAPEVINE  
(*VITIS* SPP.) FALL ACCLIMATION RESPONSE AND FRUIT  
RIPENING

---

**By**

John Edward Stenger

---

The Supervisory Committee certifies that this *disquisition* complies with North Dakota State University's regulations and meets the accepted standards for the degree of

**DOCTOR OF PHILOSOPHY**

SUPERVISORY COMMITTEE:

Dr. Harlene Hatterman-Valenti

Chair

Dr. Todd West

Dr. Tom DeSutter

Dr. Juan Osorno

Dr. Jim Hammond

Deceased – Aug 9, 2016

Approved:

Oct. 19, 2016

Date

Richard Horsley

Department Chair

## ABSTRACT

Two experiments were conducted to determine differences in sensitivity to temperature among cold-climate grapevine genotypes in fall-acclimation response. One experiment utilized a growth chamber to compare grapevine plantlets under reducing photoperiod in two static temperatures through the quantification of seven predictor variables. Reduction models were compared for their effectiveness in interpreting the interaction among cultivars, traits, photoperiodic times, and temperatures. All models identified three similar axes relating the genotypes. Tucker decomposition was better able to separate wild genotypes from hybrids, was more consistent in the subspace defined, and was more readily interpretable, thus was preferred over SVD. Adapted types, *V. riparia* and ‘Frontenac’, showed increased tip responsiveness to temperature while *V. riparia* and ‘MN 1131’ more temperature response in their relative active growth to tissue maturation compared with marginal types including ‘Marquette’. Overall, it seems at least one strategy for temperature adaptive response is required in addition to early onset of acclimation for successful adaptation to the Northern Plains Region. In a second study, mature plants of three locally important cultivars were evaluated under five environmental conditions for similar acclimation traits along with fruit maturation traits under naturally decreasing photoperiod and temperature regimes. Reductions of phenotypic and temperature trends lead to a correlation between axes contrasting investigated years. Unique responses to temperature reduction were found in all cultivars, while ‘Marquette’ was additionally more responsive under temperature increases as it reverted to an active growth state. These alterations were speculated to be caused by differential partitioning of phloem resources within the plant through control of stomatal conductance. Lastly, a unique genotype was discovered. The genotype was determinate in both growth and reproduction in contrast to the indeterminate vining growth habit that defines members

of *Vitis*. The natural mutant may have use in research on plant reproductive and vegetative growth regulation. Overall, insight was gained into the contrasts among acclimation processes within *Vitis* hybrids, and the use of growth chamber based evaluations of *V. riparia* derived progeny for background selection may lead to more rapid introgression of adaptive traits into favorable quality backgrounds in cold-climate *Vitis* breeding.

## ACKNOWLEDGMENTS

I would like to thank Dr. Harlene Hatterman-Valenti for all her help during my graduate career at NDSU. I thank her for her patience, guidance, and for believing in me. I have thoroughly enjoyed my time here as a member of her NDSU HVC team.

I would like to thank Collin Auwarter for his help with all my projects and tangent pursuits. Collin works diligently to help accomplish all that Dr. Hatterman-Valenti pursues, this includes my project thus I am grateful. I would additionally like to thank the many members of the NDSU High Value Crops project who have helped me throughout my graduate experience.

I would like to express my appreciation of the efforts of my graduate committee members, Drs. Todd West, Tom DeSutter, and Juan Osorno. They have aided me in during the design of my study as well as in making this dissertation possible. Additionally, I would like express my deepest gratitude for the efforts of the late Dr. Jim Hammond, who served on my graduate committee until his death in 2016. Through Dr. Hammond I was taught many lessons in statistics and research ethics that have greatly influenced me as a researcher. He lives on through all those he kindly mentored and assisted throughout his life and career.

Additionally, I would like to thank the entire NDSU department of plant sciences faculty for the numerous lessons learned both in and out of the classroom. In particular, I thank the members of the breeding faculty for their help with my many questions.

I would like to thank my wife, Brianna, for her constant support and assistance. I would also like to thank my parents John and Mary for always guiding me down the right path, and my brother, Craig, and sister, Kristy, for their help and support throughout my life.

Lastly, I would like to acknowledge the funding support of the North Dakota Department of Agriculture as well as the NDSU graduate school for making this research possible.

## TABLE OF CONTENTS

ABSTRACT.....	iii
ACKNOWLEDGEMENTS.....	v
LIST OF TABLES .....	x
LIST OF FIGURES .....	xii
LIST OF EQUATIONS .....	xv
LIST OF APPENDIX TABLES .....	xvi
LIST OF APPENDIX FIGURES .....	xvii
CHAPTER I. LITERATURE REVIEW .....	1
CHAPTER II. COMPARISON OF ACCLIMATION RESPONSES IN <i>V. RIPARIA</i> AND DERIVED HYBRID GRAPEVINE THROUGH BI-LINEAR AND MULTIWAY DECOMPOSITIONS OF HIGH-ORDER INTERACTION.....	8
Abstract.....	8
Introduction.....	9
Materials and methods .....	15
Plant material .....	15
Growing conditions.....	17
Experimental design .....	18
Acclimation measures.....	19
Statistical analysis.....	19
Singular value decomposition.....	20
Tucker decomposition.....	20
Multidimensional scaling.....	21
Model comparisons.....	22
Results.....	23

Singular value decomposition.....	23
Varimax rotation of loadings and scores .....	27
Tucker decomposition .....	32
Non-rotated .....	32
Temperature .....	33
Measures .....	33
Photoperiods .....	34
Variable weights .....	35
Genotypes .....	36
Varimax mode-rotation .....	40
Measures .....	41
Photoperiods .....	42
Variable weights .....	42
Genotypes .....	43
Rotation to maximum core variance .....	47
Measures .....	48
Photoperiods .....	49
Variable weights .....	50
Genotypes .....	50
Multidimensional scaling .....	54
Non-metric multidimensional scaling .....	54
Metric multidimensional scaling .....	58
Comparison of model relationships .....	63
Discussion.....	67
Identified axes.....	67

Comparison of reduction methods .....	79
Identified axes .....	79
Effect on genotypic means .....	80
Ability to separate <i>V. riparia</i> from non- <i>V. riparia</i> genotypes .....	81
SVD and Tucker decomposition solution stability .....	84
Comparison of SVD and Tucker decompositions with MDS .....	84
Conclusions.....	87
<b>CHAPTER III. CONTRASTING RESPONSES TO ENVIRONMENTAL CONDITIONS BY THREE COLD-CLIMATE WINEGRAPE CULTIVARS GROWN IN THE UNITED STATES UPPER PLAINS REGION .....</b>	<b>89</b>
Abstract.....	89
Introduction.....	90
Materials and methods .....	96
Plant materials.....	96
Test vineyards .....	96
Sample collection times .....	97
Traits .....	97
Acclimation predictors.....	97
Fruit quality predictors.....	98
Environmental conditions .....	98
Statistical analysis.....	99
Results.....	100
Vine response.....	100
Cultivars.....	101
Traits .....	101
Photoperiodic time .....	102



Environments .....	103
Inter-connections among modes .....	104
Temperature conditions .....	107
Time .....	107
Temperature parameters.....	108
Environments .....	108
Inter-connections among modes .....	109
Inter-connections between temperature and phenotypic alterations .....	110
Discussion .....	121
<b>CHAPTER IV. A NOVEL DETERMINATE FORM INTERSPECIFIC GRAPEVINE FOR GENETIC AND PHYSIOLOGICAL STUDY AS WELL AS BREEDING APPLICATIONS .....</b>	<b>131</b>
Abstract .....	131
Introduction.....	132
Origin .....	132
Description.....	134
Growth habit .....	134
Reproduction.....	137
Comparison of growth habit with a wild type S1 sibling .....	140
Material and methods.....	140
Results.....	140
Future study and application.....	141
<b>CHAPTER V. OVERALL CONCLUSIONS.....</b>	<b>144</b>
<b>LITERATURE CITED .....</b>	<b>150</b>
<b>APPENDIX A. TABLES .....</b>	<b>162</b>
<b>APPENDIX B. FIGURES .....</b>	<b>181</b>

## LIST OF TABLES

<u>Table</u>	<u>Page</u>
1. Clonal genotypes utilized and their origins .....	16
2. SVD singular values, eigenvalues, proportions and cumulative proportions of the total dataset variance.....	24
3. Effect of accessions for the retained axes scores following SVD .....	24
4. SVD mean genotype scores .....	25
5. Counter-rotated relational matrix of varimax rotated scores and loadings.....	28
6. Effect of accessions for the retained axes scores following varimax rotation .....	29
7. Varimax-rotated SVD mean genotype scores .....	30
8. Tucker core-array of relationships among genotype, measure, and photoperiod axes.....	33
9. Tucker loadings for measured variables .....	34
10. Tucker loadings for photoperiodic times .....	35
11. Effect of accessions for the retained axes scores following Tucker decomposition .....	36
12. Tucker mean genotype scores .....	37
13. Mode-rotated Tucker core-array of relationships among genotype, measure, and photoperiod axes .....	41
14. Mode-rotated Tucker loadings for measured variables .....	41
15. Mode-rotated Tucker loadings for photoperiodic times .....	42
16. Effect of accessions for the retained axes scores following mode-rotation .....	43
17. Mode-rotated Tucker mean genotype scores .....	45
18. Core-rotated Tucker core-array of relationships among genotype, measure, and photoperiod axes .....	48
19. Core-rotated Tucker loadings for measured variables .....	48
20. Core-rotated Tucker loadings for photoperiodic times.....	49
21. Effect of accessions for the retained axes scores following core-rotation .....	50

22.	Core-rotated Tucker mean genotype scores .....	51
23.	Effect of accessions for the retained axes scores following NMS .....	55
24.	NMS mean genotype scores .....	56
25.	Effect of accessions for the retained axes scores following metric-MDS .....	59
26.	Metric-MDS mean genotype scores .....	60
27.	Estimated sum of squared deviations from observed and predicted values .....	64
28.	Correlation among derived genotype sample scores from the three axes of each of the seven solutions .....	65
29.	Correlations among derived weights (W) such that $X*W$ equates to the genotype sample scores of the model .....	66
30.	ANOVA sources of variation for fixed effects of the field evaluation of acclimation .....	100
31.	Tucker scores for cultivars along the two retained axes .....	101
32.	Tucker loadings for measured traits along the five retained axes .....	102
33.	Tucker loadings for photoperiodic times along the four retained axes .....	103
34.	Tucker loadings for phenotypic environments along the four retained axes .....	103
35.	Tucker core-array singular-values of the reduced four-way cultivar-by-trait-by-photoperiod-by-environment interaction .....	105
36.	Tucker core-array eigenvalues of the reduced four-way cultivar-by-trait-by-photoperiod-by-environment interaction .....	106
37.	Tucker loadings for temperature parameters along the two retained axes .....	108
38.	Tucker loadings for temperature environments along the three retained axes .....	109
39.	Temperature core-array of relationships among time, temperature parameter, and environment axes .....	110
40.	Correlation coefficients among environmental axes from the reduction of phenotypic and temperature datasets, respectively .....	111
41.	Effect of determinant form on growth characteristics .....	141

## LIST OF FIGURES

<u>Figure</u>	<u>Page</u>
1. Cluster of Euclidean distances between genotypic means for the three retained axes from the non-rotated SVD solution using Ward’s minimum variance method of linkage...27	27
2. Cluster of Euclidean distances between genotypic means for the three retained axes from the rotated SVD solution using Ward’s minimum variance method of linkage .....31	31
3. Cluster of Euclidean distances between genotypic means for the two axes having significant genotypic variation from the rotated SVD solution using Ward’s minimum variance method of linkage .....32	32
4. Cluster of Euclidean distances between genotypic means for the three retained axes of The Tucker solution using Ward’s minimum variance method of linkage .....39	39
5. Cluster of Euclidean distances between genotypic means for the two axes having significant genotypic variation from the Tucker solution using Ward’s minimum variance method of linkage .....40	40
6. Cluster of Euclidean distances between genotypic means for the three retained axes of the mode-rotated Tucker solution using Ward’s minimum variance method of linkage ....46	46
7. Cluster of Euclidean distances between genotypic means for the two axes having significant genotypic variation from the mode-rotated Tucker solution using Ward’s minimum variance method of linkage .....47	47
8. Cluster of Euclidean distances between genotypic means for the three retained axes of the core-rotated Tucker solution using Ward’s minimum variance method of linkage .....53	53
9. Cluster of Euclidean distances between genotypic means for the two axes having significant genotypic variation from the core-rotated Tucker solution using Ward’s minimum variance method of linkage .....54	54
10. Cluster of Euclidean distances between genotypic means for the three retained axes of the NMS solution using Ward’s minimum variance method of linkage .....57	57
11. Cluster of Euclidean distances between genotypic means for the two axes having significant genotypic variation from the NMS solution using Ward’s minimum variance method of linkage .....58	58
12. Cluster of Euclidean distances between genotypic means for the three retained axes of the metric-MDS solution using Ward’s minimum variance method of linkage .....62	62
13. Cluster of Euclidean distances between genotypic means for the two axes having significant genotypic variation from the metric-MDS solution using Ward’s minimum variance method of linkage .....63	63

14.	Plotted mean four-way interaction effect trends through photoperiodic time (15 – 10h of daylight) averaged across tested <i>V. riparia</i> .....	69
15.	Difference in effect between temperatures (27 – 10°C) for the seven measured traits through photoperiodic time (15 – 10h of daylight) averaged across the tested <i>V. riparia</i> vines .....	70
16.	Difference in effect between temperatures (27 – 10°C) for the seven measured traits through photoperiodic time (15 – 10h of daylight) averaged across the tested ‘Frontenac’ vines .....	70
17.	Difference in effect between temperatures (27 – 10°C) for the seven measured traits through photoperiodic time (15 – 10h of daylight) averaged across the tested ‘917’ vines .....	71
18.	Difference in effect between temperatures (27 – 10°C) for the seven measured traits through photoperiodic time (15 – 10h of daylight) averaged across the tested ‘MN 1131’ vines .....	71
19.	Difference in effect between temperatures (27 – 10°C) for the seven measured traits through photoperiodic time (15 – 10h of daylight) averaged across the tested ‘900’ vines .....	72
20.	Difference in effect between temperatures (27 – 10°C) for the seven measured traits through photoperiodic time (15 – 10h of daylight) averaged across the tested ‘Marquette’ vines .....	72
21.	Comparison of the trends in differences of response across temperatures for the seven predictor variables across photoperiodic time (15 – 10h of daylight) for the mean of <i>V. riparia</i> , ‘917’, and ‘Marquette’ .....	75
22.	Temperature time-axes loadings across the 40 evaluated dates .....	107
23.	Temperature progress in Absaraka, ND (A) and Wyndmere, ND (W) during the years of 2012-2014 .....	113
24.	Estimated effect of temperature derived environmental axis 2 for environmental parameter axes 1 and 2 from August, 8 through September, 17 .....	114
25.	Estimated cultivar four-way interaction effects across photoperiodic time for environmental axis 2 for stem growth characteristics .....	115
26.	Estimated cultivar four-way interaction effects across photoperiodic time for environmental axis 2 for traits related to growth cessation .....	116
27.	Estimated cultivar four-way interaction effects across photoperiodic time for environmental axis 2 for traits relating to tissue maturation .....	118

28.	Estimated cultivar four-way interaction effects across photoperiodic time for environmental axis 2 for traits relating to berry growth .....	119
29.	Estimated cultivar four-way interaction effects across photoperiodic time for environmental axis 2 for traits relating to fruit ripening .....	120
30.	<i>Vitis</i> ‘ND 733’ showing typical A) node and inflorescence development as well as B) tip growth .....	133
31.	Stem displaying both normal nodes (having leaves, axial, and resting buds), and altered nodes (having leaves, tendrils and inflorescences) on the same plant .....	134
32.	Vegetative buds altered to reproductive structures with singly borne flowers .....	135
33.	A.) Plant displaying altered form with B.) altered shoot tip .....	136
34.	Determinant form vine displaying shrub habit .....	137
35.	A) Plant resuming growth following induced dormancy, and B) Inflorescence showing normal development .....	138
36.	A) Cuttings of <i>Vitis</i> ‘ND Mutant 1’ showing profuse rooting, B) rooted cuttings, and C) propagule showing the same growth habit of the mother vine .....	139

## LIST OF EQUATIONS

<u>Equation</u>	<u>Page</u>
1. Principal Components Analysis.....	13
2. Singular Value Decomposition.....	13
3. Decomposition of $X'X$ .....	13
4. Decomposition of $XX'$ .....	13
5. Estimate of singular value sample scores and loadings.....	13
6. The Tucker3 model.....	14
7. Alternate expression of the Tucker3 model for $X_b$ .....	14
8. Alternate expression of the Tucker3 model for $X_c$ .....	14
9. Multidimensional scaling stress formula.....	15
10. Multidimensional scaling raw stress formula.....	15
11. Single Value Decomposition variable weights.....	20
12. The generalization of the Tucker3 model to four modes.....	20
13. Tucker4 model variable weights.....	21

## LIST OF APPENDIX TABLES

<u>Table</u>	<u>Page</u>
A1. ANOVA for stem length .....	162
A2. ANOVA for number of nodes .....	162
A3. ANOVA for number of mature nodes .....	163
A4. ANOVA for number of lateral shoots .....	163
A5. ANOVA for tip abscission progress .....	164
A6. ANOVA for periderm development (length of shoot) .....	164
A7. ANOVA for periderm development (nodes enveloped) .....	165
A8. Factor weights of predictor variables for non-rotated SVD axis 1 .....	166
A9. Factor weights of predictor variables for non-rotated SVD axis 2 .....	167
A10. Factor weights of predictor variables for non-rotated SVD axis 3 .....	168
A11. Factor weights of predictor variables for rotated SVD axis 1 .....	169
A12. Factor weights of predictor variables for rotated SVD axis 2 .....	170
A13. Factor weights of predictor variables for rotated SVD axis 3 .....	171
A14. Factor weights of predictor variables for Tucker axis 1 .....	172
A15. Factor weights of predictor variables for Tucker axis 2 .....	173
A16. Factor weights of predictor variables for Tucker axis 3 .....	174
A17. Factor weights of predictor variables for mode-rotated Tucker axis 1 .....	175
A18. Factor weights of predictor variables for mode-rotated Tucker axis 2 .....	176
A19. Factor weights of predictor variables for mode-rotated Tucker axis 3 .....	177
A20. Factor weights of predictor variables for core-rotated Tucker axis 1 .....	178
A21. Factor weights of predictor variables for core-rotated Tucker axis 2 .....	179
A22. Factor weights of predictor variables for core-rotated Tucker axis 3 .....	180



## LIST OF APPENDIX FIGURES

<u>Figure</u>	<u>Page</u>
B1. Metric-MDS three axis solution fit .....	181
B2. NMS three axis solution fit .....	181
B3. SVD A.) quartile-quartile plot and B.) distribution of residuals from ANOVA of each retained axis .....	182
B4. Varimax rotated SVD A.) quartile-quartile plot and B.) distribution of residuals from ANOVA of each retained axis .....	182
B5. Tucker decomposition A.) quartile-quartile plot and B.) distribution of residuals from ANOVA of each retained axis .....	183
B6. Mode-rotated Tucker A.) quartile-quartile plot and B.) distribution of residuals from ANOVA of each retained axis .....	183
B7. Core-rotated Tucker A.) quartile-quartile plot and B.) distribution of residuals from ANOVA of each retained axis .....	184
B8. Metric-MDS A.) quartile-quartile plot and B.) distribution of residuals from ANOVA of each retained axis .....	184
B9. NMS A.) quartile-quartile plot and B.) distribution of residuals from ANOVA of each retained axis .....	185
B10. Plotted mean four-way interaction effect trends averaged across tested ‘64’ .....	185
B11. Plotted mean four-way interaction effect trends averaged across tested ‘73’ .....	186
B12. Plotted mean four-way interaction effect trends averaged across tested ‘900’ .....	186
B13. Plotted mean four-way interaction effect trends averaged across tested ‘903’ .....	187
B14. Plotted mean four-way interaction effect trends averaged across tested ‘906’ .....	187
B15. Plotted mean four-way interaction effect trends averaged across tested ‘909’ .....	188
B16. Plotted mean four-way interaction effect trends averaged across tested ‘911’ .....	188
B17. Plotted mean four-way interaction effect trends averaged across tested ‘913’ .....	189
B18. Plotted mean four-way interaction effect trends averaged across tested ‘914’ .....	189
B19. Plotted mean four-way interaction effect trends averaged across tested ‘917’ .....	190

B20. Plotted mean four-way interaction effect trends averaged across tested ‘920’ .....	190
B21. Plotted mean four-way interaction effect trends averaged across tested ‘924’ .....	191
B22. Plotted mean four-way interaction effect trends averaged across tested ‘936’ .....	191
B23. Plotted mean four-way interaction effect trends averaged across tested ‘937’ .....	192
B24. Plotted mean four-way interaction effect trends averaged across tested ‘938’ .....	192
B25. Plotted mean four-way interaction effect trends averaged across tested ‘939’ .....	193
B26. Plotted mean four-way interaction effect trends averaged across tested ‘940’ .....	193
B27. Plotted mean four-way interaction effect trends averaged across tested ‘956’ .....	194
B28. Plotted mean four-way interaction effect trends averaged across tested ‘958’ .....	194
B29. Plotted mean four-way interaction effect trends averaged across tested ‘961’ .....	195
B30. Plotted mean four-way interaction effect trends averaged across tested ‘962’ .....	195
B31. Plotted mean four-way interaction effect trends averaged across tested ‘965’ .....	196
B32. Plotted mean four-way interaction effect trends averaged across tested ‘1001’ .....	196
B33. Plotted mean four-way interaction effect trends averaged across tested ‘1002’ .....	197
B34. Plotted mean four-way interaction effect trends averaged across tested ‘1003’ .....	197
B35. Plotted mean four-way interaction effect trends averaged across tested ‘Frontenac’ .....	198
B36. Plotted mean four-way interaction effect trends averaged across tested ‘MN 1131’ .....	198
B37. Plotted mean four-way interaction effect trends averaged across tested ‘Marquette’ .....	199
B38. Plotted mean four-way interaction effect trends averaged across tested ‘1004’ .....	199
B39. Plotted mean four-way interaction effect trends averaged across tested ‘SD 62-8-160’ ....	200
B40. Plotted mean four-way interaction effect trends for averaged ‘St. Croix’ in Absaraka, ND in 2012.....	200
B41. Plotted mean four-way interaction effect trends for averaged ‘St. Croix’ in Wyndmere, ND in 2012.....	201
B42. Plotted mean four-way interaction effect trends for averaged ‘St. Croix’ in Absaraka, ND in 2013.....	201

B43. Plotted mean four-way interaction effect trends for averaged ‘St. Croix’ in Wyndmere, ND in 2013.....	202
B44. Plotted mean four-way interaction effect trends for averaged ‘St. Croix’ in Absaraka, ND in 2014.....	202
B45. Plotted mean four-way interaction effect trends for averaged ‘Marquette’ in Absaraka, ND in 2012.....	203
B46. Plotted mean four-way interaction effect trends for averaged ‘Marquette’ in Wyndmere, ND in 2012.....	203
B47. Plotted mean four-way interaction effect trends for averaged ‘Marquette’ in Absaraka, ND in 2013.....	204
B48. Plotted mean four-way interaction effect trends for averaged ‘Marquette’ in Wyndmere, ND in 2013. ....	204
B49. Plotted mean four-way interaction effect trends for averaged ‘Marquette’ in Absaraka, ND in 2014.....	205
B50. Plotted mean four-way interaction effect trends for averaged ‘Frontenac Gris’ in Absaraka, ND in 2012.....	205
B51. Plotted mean four-way interaction effect trends for averaged ‘Frontenac Gris’ in Wyndmere, ND in 2012.....	206
B52. Plotted mean four-way interaction effect trends for averaged ‘Frontenac Gris’ in Absaraka, ND in 2013.....	206
B53. Plotted mean four-way interaction effect trends for averaged ‘Frontenac Gris’ in Wyndmere, ND in 2013.....	207
B54. Plotted mean four-way interaction effect trends for averaged ‘Frontenac Gris’ in Absaraka, ND in 2014 .....	207
B55. Daily average temperatures in Absaraka, ND (A) and Wyndmere ND (W) in 2012 – 2014 .....	208

## CHAPTER I. LITERATURE REVIEW

Breeding advancements have made commercial winegrape production possible in the Northern Plains Region of the United States including North Dakota. However, continued breeding efforts will be needed to stabilize production, as adaptation of germplasm to the Northern Plains' climate will be critical to the success of viticulture in North Dakota. Though winegrape cultivars are available to producers, these cultivars tend to be unpredictable in local adaptation and lack necessary fruit quality traits (Hatterman-Valenti et al., 2016). One species used in hybrid winegrape breeding is *Vitis vinifera* (Garris et al., 2009). *Vitis vinifera* is considered the traditional wine grape species (Myles et al., 2011). The species is used to impart fruit quality characteristics to progeny. Though this species is ideal in fruit quality, it is not adapted to the region. The species is insufficiently winter hardy to survive North Dakota winters with a threshold ranging from -17.8°C (0°F) to -23.3°C (-10°F) (Dami et al., 2005). To improve the adaptation of *V. vinifera* to broader environments, breeders have taken to interspecific hybridization with other *Vitis* species from North America and Asia (Garris et al., 2009). One species that has become an important source of adapted genetics in the breeding of hardy wine grape cultivars is *V. riparia* or the riverbank grape. This species is native to the central and eastern portions of North America, including North Dakota. Most notable of its adaptations is acclimation to winter conditions and overall winter hardiness. *Vitis riparia* is noted as the hardiest *Vitis* species with tolerances to winter cold temperatures below -40°C (-40°F).

Many traits are important for proper acclimation to winter conditions. One such trait is photoperiodicity, or photoperiodic response. Photoperiodicity is the triggering of a response in an organism based on the ratio of daylight to night-time hours. Hardy grapevine breeders have been aware of the importance of photoperiodicity in dormancy response in *Vitis* for many years (Fennell

and Hoover, 1991; Schnabel and Wample, 1987). In a 2009 article by Garris et al., the photoperiodic responses of 'Seyval', *V. riparia*, and their F1 and F2 populations were investigated. The investigator displayed data which alluded to a stringent response by the *V. riparia* vine in regard to the induction of dormancy as a result of photoperiodic response. This response was less defined within the inter-specific hybrid cultivar Seyval. Overall, the differing responses suggest that the stringency of the dormancy triggering mechanism may vary depending on the origin of the parents utilized in a cross, though this has gone on uninvestigated. In regions of large climactic changes or climactic uncertainty, photoperiod recognition is a powerful adaptation. Photoperiod induced responses allow organisms to, in a way, predict the future (Lagercrantz, 2009). Though the conditions of fall may not exist physically, individuals are selected as a result of their ability to utilize the optimal ratio of daylight hours to night-time hours to respond at a time for which dormancy will consistently occur prior to harsh winter conditions. This selection pressure aids in evolution of ecotypes to local climactic regimes.

Photoperiodicity's importance to woody plant growth and acclimation has been more fundamentally explored using the model organism *Populus spp.* In 2006, Böhlenius et al. reported that photoperiodicity was involved in the cessation of growth. The authors described the involvement of CONSTANS (CO) and FLOWERING LOCUS T (FLT) genes in the annual dormancy cycling in *P. trichocarpa*. Though it is understood that photoperiod is critical in signaling through the alteration of CO, other factors play important roles in vegetative reproductive cycling in woody plants. In 2011, Hsu et al. used transgenic incorporation of two divergent paralogs of the FLT locus, FLOWERING LOCUS T1 (FT1) and FLOWERING LOCUS T2 (FT2), into *P. tremula x P. tremuloides* 353 and demonstrated differential regulation of FT2 by either photoperiod or temperature. FT2 was found to inhibit acclimation response in favor of continued

vegetative growth under long-day high temperature conditions. Homologous genes to FT and TERMINAL FLOWER 1 (TFL1) have been described in grapevine (*V. vinifera*) (Boss et al, 2006; Sreekantan and Thomas, 2006; Carmona et al., 2007). Carmona et al. (2007) reported the gene family consisted of five gene homologs with additional genes described by others. The polygenic nature of the FT, TFL1, SUPPRESSOR OF OVEREXPRESSION OF CONSTANS 1 as well as the described MADS genes with their known link to both reproductive and vegetative growth and dormancy suggest acclimation of woody plants to winter conditions is a complex trait likely to exhibit environmental variation in its expression.

Soolanayakanahally et al. (2013) demonstrated local variation in photoperiodic response in a common garden experiment of differing genotypes at locations with similar latitudes having differing climates. They found variation over the differing environments in the setting of dormant terminal buds as well as leaf senescence. They noted that those plants at the milder site (Vancouver, British Columbia) showed earlier fall phenology than those at Indian Head, Saskatchewan. Though photoperiodism is known to have control over fall plant phenology, the environmental conditions under which these plants were grown also contributed the effect. Li, in 2003, found that silver birch (*Betula pendula*) exhibited latitudinal variation among ecotypes in critical photoperiod as well as photoperiodic sensitivity quantified as the slope of the photoperiodic response curve. The northern ecotype tested had a longer critical photoperiod as well as it was also more photoperiodically sensitive when compared to the southern ecotype. This builds evidence for the need of background selection in both the critical photoperiod of acclimation response as well as stringency or sensitivity of that response in breeding woody plant cultivars for northern continental regions. To this point cold-climate grapevine breeding has largely focused on early response without due attention to the stringency of such responses.

North Dakota is classified as having a continental climate ranging from dry sub-humid in the west to sub-humid in the east (Stoner et al., 1993). Continental climates lack large mediating bodies of water, thus weather and temperature patterns are relatively unpredictable when compared to weather patterns of more coastal areas. Such stochastic conditions may increase the importance of stringent responses as variable environmental conditions may be present at static photoperiodic times over years and locations. This may cause a relative need of native *V. riparia* vines to have a more stringent dormancy induction mechanism when compared to other coastal species of *Vitis*. Coastal species, such as *V. vinifera*, may be increasingly dependent on environmental signals such as temperature and soil moisture due to their relative seasonal predictability when compared to continental temperature and moisture regimes.

Grape acclimation response to photoperiod has been identified as a critical trait for vines intended for the northern reaches of the production range. However, just as early acclimation is important to cultivar success, it is equally important that this response be consistent across environmental conditions over years. The trait's interaction with other environmental factors important for the cessation of growth leading to dormancy could also be important for overwintering success in North Dakota. It is also very likely that relationships or the dependence upon a signal varies among the different species utilized in breeding of hardy grapevines. The stringency of genotypic performance in single traits has largely been investigated through trait stability analysis. Trait stability analysis is a broad class of methodologies that may take many forms (Flores et al., 1998). Generally, such models use different methods to understand and partition genotype-by-environment interaction into meaningful variance of individuals relative to the mean response of the population as they relate to specific environmental patterns. Within mixed model approaches, such methods are implemented by defining the residual variance-covariance

structure of the model (Piepho, 1999). Many common models may be implemented using factor analytic structures to define commonalities that account for the greatest portion of variance within the interaction.

Expanding factor analytic models to facilitate more complex datasets has been discussed and implemented. In the past, data having greater than two modes was generally either ‘flattened’ or ‘matricized’ (Kroonenberg, 2008). Flattening is accomplished by averaging a two-mode matrix over a third mode. An example would be averaging matrices of genotypic values in a number of environments over a third mode relating data collection times. In such a way, the information held within time trends is lost as only the average value over time is investigated. Matricizing data is accomplished through concatenating modes of the dataset together to effectively obtain a single matrix. In such a method, each matrix of genotypic values at each environment would be concatenated for each collection time such that all time-by-environment combinations are treated as variable vectors. In such a method the intercorrelation among times is lost in the analysis. It has been argued that application of two mode analytic modes to higher order datasets does not utilize the structure of the data appropriately. This study looks to investigate time dependent reactions of individuals to dynamically applied stimuli. This makes the correlation of trait responses among times critical in interpretation. With the prior concerns relating to loss of information from concatenated or averaged higher order modes, comparisons will be made between higher order models and wide combination-mode matrix bi-linear methods to ensure that higher order methods are justified and beneficial.

Higher-order models have been used to facilitate evaluation of more complex traits, having more complex outcomes. In such models, several traits of importance, and presumed involvement in processes, are assessed and reduced to generalized trends through analytic models. Chapman et



al. (1997) evaluated several traits in maize in order to evaluate the effectiveness of selection of the complex trait drought resistance. Such a model resolved the poly-trait, multi-environment input data to latent traits that differed among progeny facing differing degrees of drought stress. Varela et al. (2006) outlined the advantages and three mode factor analytic models in additive main effect and multiplicative interaction (AMMI) modeling relative to previously used two-way AMMI models of concatenated-mode matrices in the interpretation of three-way interaction in plant breeding. It was found that more useful information about the interaction was obtained from the higher-order model relative to the concatenated form. The flexibility of such models will be helpful moving forward as the attention of breeders shifts from the quantification of end products, such as yield, to comparisons among genotypes in the process used to obtain such end products. Many metabolic routes may lead to a similar end, however, each route may have differences in dependability in the presence of dynamic stimuli or influence on or covariance with other desirable or detrimental traits.

Future research will require, additions of multiple modes to resolve more complex situations. The creation of a normalized response of grapes to a stimulus in order to infer time related effects on latent traits is needed to fully understand the effects of stochastic temperature effects on acclimation. Such a generalization of three-way analysis to a fourth mode is natural in the use of multiway decompositions (Kroonenberg, 2008). The determination of how to center and scale the data is a challenge. Centering of all modes removes all offsets as well as all low level interactions. In the detection of an instance reaction as a process proceeds, such analysis of the four-way interaction is intuitive. The interaction between traits and times can be interpreted as generalized processes of latent constructs that represent the acclimation process. The differences in this average acclimation process as they are unique to each genotype would be the three-way

interaction and represent the average relative response curves of each genotype as they differ from the average response of all cultivars. The four-way interaction can be considered the change in shape of a three-way interaction along a fourth axis. In this instance, the three-way interaction is the described reaction norm involving the traits and time trends unique to individual genotypes while the fourth axis would be interpreted as the change in shape of this curve across tested environments.

The overriding goal of this study was to interpret acclimation response under differing environmental conditions and to assist in the identification of traits important to the Northern adaptation of *V. riparia*. A method for *ex situ* testing of *V. riparia* derived progeny for background selection of *V. riparia*-type responses to temperature alteration was constructed. Such a test could expedite the incorporation of adapted traits from *V. riparia* into high fruit quantity and quality backgrounds from *V. vinifera* sources through an accelerated greenhouse-based advancement or backcrossing system. Differing models were compared and contrasted for their ability to separate native wild-type vines from hybrid progeny, as well as in the reproducibility and interpretability of their results regarding relative trait trends. Additionally, known cultivars will be evaluated under field conditions to offer evidence that the observed associations under controlled conditions could be re-obtained in a natural setting. Lastly, through this research a novel determinate form natural mutant was identified, which may aid to elucidate underlying genetic and metabolic structures that define *Vitis* spp. growth and reproductive development and expression in the future.

**CHAPTER II. COMPARISON OF ACCLIMATION RESPONSES IN *V. RIPARIA* AND  
DERIVED HYBRID GRAPEVINE THROUGH BI-LINEAR AND MULTIWAY  
DECOMPOSITIONS OF HIGH-ORDER INTERACTION**

**Abstract**

Methods of determining *V. riparia*-like acclimation responses in related interspecific progeny were compared in a growth chamber using fixed temperature regimes. Thirty genotypes were evaluated for seven predictor phenotypic traits relating to stem growth under eleven decreasing photoperiodic time points in the presence of either 10 or 27°C. The four-way interaction effects among genotype samples, traits, times, and temperatures was isolated and further examined through bi-linear singular value decomposition (SVD) and multiway Tucker decomposition data reduction models to determine if the use of the full structure of the data resulted in a more practical interpretation of vine reactions. Rotated solutions were also investigated as all modes were varimax rotated. The Tucker solution was also core rotated to maximize core variance. All models were compared to metric-multidimensional scaling (MDS) as well as non-metric multidimensional scaling (NMS) solutions to determine their ability to retain point-wise distances among data points. Regardless of model, a similar set of three traits were identified. These traits related to tip abscission reactivity across temperatures, the rate of transition from active growth to tissue maturation, and the timing of initiation of the transition from active growth to tissue maturation. Of the tested models, non-rotated and core-rotated versions of the Tucker model led to better separation between wild-type vines and non-wild-type vines, were more consistent in the subspace identified, and were more readily interpretable. The study identified distinct strategies of two regionally adapted cultivars ('MN 1131' and 'Frontenac') as well as a deficiency in *V. riparia*-like reactions in the regionally unpredictable cultivar 'Marquette'. The findings of the study indicate

that traits of acclimation beyond photoperiodicity are present in *V. riparia*, and these traits should be further investigated for their utility in breeding cold-climate adapted genotypes.

## **Introduction**

Interspecific hybrid cold-climate grapevines have been bred to facilitate production in the Upper-Midwestern United States. Such cultivars are largely based on the adaptation genetics of the native Riverbank grape (*V. riparia*). Such wild material was combined with more traditional domesticated grape germplasm including *V. vinifera*, *V. labrusca*, as well as other non-domesticated types in order to facilitate adaptation along with adequate fruit quality. Several species additional species of grapevine exist including *V. californica*. *Vitis californica* is a particular novelty as it is native to America, native to a region of Mediterranean climate similar to that of the Eurasian species, *V. vinifera*, and clusters uniquely away from *V. vinifera* and continental American species in phylogenetic evaluations (Pèros et al., 2011; Tröndel et al. 2010; Wan et al., 2013; Zecca et al., 2012). In the current study, the species was included as an out group as well as help elucidate the origin of responses identified.

Acclimation to winter conditions is an example of a biological process. Moreover, acclimation to winter conditions, for all purposes, is a latent construct. Many environmental cues act upon a vine causing a cascade of physiological and physical alterations leading to a tolerance of winter stresses with the ability to survive these stresses and reinitiate growth upon the return of favorable conditions. In many ways, the quantification of fall acclimation response is synonymous with batch processes of industrial fields. The fall of a given season is of pseudo-finite duration. Under average conditions, vines exhibit a normal response to decreasing photoperiod. This response is likely to have normal variation that has little consequential effect, however; the

response is likely to also include particular variation which results from rare anomalies in environmental conditions. These particular variations are likely to influence the end status of the individual and alter its survival and may effect particular genotypes differentially. Methods in batch process monitoring used to determine faults often look to use multiway extensions of components modeling to project complex datasets into a lower dimension subspace which generalizes past batch runs into a model from which to judge deviations of new runs (Nomikos and MacGregor, 1995). The following study will look to investigate if similar methodologies applied to fault detection in industrial batch process monitoring can provide insight into alteration in acclimation regimes of grapevines. The responses of a sample of native *V. riparia* will be used as the process standard, or the desired response pattern. Interspecific types showing minimal deviations or ‘faults’ from the desired response pattern will be considered most suited for the region in comparison to those showing more deviations. The study will also look to compare two data reduction methods in the ability to construct a sub-space for such fault detection to occur. Bi-linear reduction will be used as the current standard procedure, and will be compared with a higher order model which utilizes the full structure of the data to evaluate cross mode axis combinations. The model that most consistently constructs a subspace able to separate *V. riparia* vines from those of interspecific types will be regarded as the preferred model.

The quantification of process data is inherently difficult. A process involves many inputs leading to outcomes that may or may not be directly quantifiable. These inputs and outcomes are likely to have multiple levels of co-integration with one another with varying degrees of co-variation over time. When applied to a natural setting, the influencing entities are not applied at a constant rate nor do all occur at predictable timings. This causes difficulties in the analysis and interpretation of results. To facilitate selection in process data, processes have been analyzed as a

single cause leading to a single effect (Garris et al, 2009, Fennell et al, 2005; Wake and Fennell, 2000; Fennell and Hoover, 1991). This method has also been employed in other multivariate areas such as metabolomics alongside multivariate methods (Goodacre et al., 2007). Though this methodology has effective enough in several instances to make progress, in reality only a portion of the genetic potential is being exploited as the inter-correlation of predictor variables, the inter-correlation of outcomes, as well as any cross relationships that are difficult to perceive as a result of the multi-collinear nature the data are ignored as the quantitative trait is forced into a qualitative solution. Additionally, when multivariate analysis is used, generally, multiway data sets are ‘flattened’ or ‘matricized’ in order to facilitate the use of bi-linear methods (Kroonenberg, 2008). Such flattening is carried out through either the averaging of individual variables over a third mode, such as collection times, to obtain the mean variable response of the variable across the second gradient. In this case, the effect of time on each variable is lost. Matricizing, or stringing-out, variables is accomplished through concatenating each variable-by-time observation or each sample-by-time observation together to consider each combination as a variable or sample in a bi-linear (matrix) form. In this method, the covariance that exists among variable observations or samples taken a differing times is ignored. Either method facilitates the use of bi-linear reduction methods on the multiway dataset at the cost of knowledge of the covariance of a variable with itself at a differing level of a second mode. In the pursuit of quantifying reactions, the information about the status of a variable, relative to itself, at differing times or under differing conditions becomes highly important. A reaction can be defined as a deviance to some kind of internal standard or status-quo, generally occurring at differing time periods. The concatenation of either variables and time or variables and environmental stimuli would result in a loss of information regarding time specific effects or differential responses across environmental stimuli critical in

defining the reactionary deviation from the status-quo within an individual genotype for use in comparisons among genotypes. The following study will look to compare these methods as applied to reaction quantification in process traits for plant breeding to determine if the use of the full structure of the data through multiway decomposition aids in extracting information useful in adaptation selection.

Acclimation is only one of several important processes needed for vine longevity, production, and ability to create a consistent product. The following study utilizes acclimation response as a particularly difficult case study, however, it is likely many other processes important in cultivar development, including fruit ripening, phenolic development, disease progression, horizontal disease resistance, and other physiological stresses could be investigated and selections made using similar methodologies. While methodologies used to investigate the genotypic specific effects to environmental conditions exist, the expansion of such methodologies to support multi-mode data is likely to be necessary to integrate transcriptomic data as genomic association moves to include time trends in expression (Conesa et al., 2010). To expedite the transition, the current study evaluates a flexible multiway data reduction method that extends to multi-mode data, in comparison with that of a more traditional bi-linear model used in many studies today.

To utilize the full dataset, multiple methods were used to dissect high-level interactions in the data. Principal components analysis (PCA) was used on a concatenated-mode wide matrix to represent a more typical handling of multi-mode data reduction. PCA was first described by Pearson (1901) and later by Hotelling (1933). PCA is used to detect patterns in multivariate data. Through this procedure, the number of dimensions of the data set is reduced to a smaller subspace accounting for the largest portion of the original variance. One beneficial property of PCA is that uncorrelated, orthogonal components are created from correlated datasets. One detriment is that

PCA is based on a linear transformation, thus non-linear data may cause a poor model fit. Each component is described as a linear combination of the original (p) variables ( $x_1, x_2, \dots, x_p$ ) (Kroonenberg, 2008):

$$X = AF' + E \quad (1)$$

Where X is an n by p matrix containing the original data of n samples by p variables. F is a matrix of size p by k containing the factor loadings of the p variables pertaining to the k retained components. A is a matrix of size n by k containing the sample scores of the n samples for the k retained components. E is a matrix of size n by p containing the residuals of the model caused by the loss of the p minus k dimensions of the full PCA decomposition. For the current study, PCA was conducted through the use of single value decomposition (SVD) as a result of the datasets large number of variables per sample genotype. SVD takes the form:

$$X = U\Sigma V' \quad (2)$$

Where X is any n by p matrix containing the original data. U is a n by k matrix containing the sample scores,  $\Sigma$  is a diagonal k by k matrix containing the singular values relating U to V, and V is a p by k matrix containing the variable loadings (weights) of the k reduced dimensions. Singular values equate to standard deviations thus relate to the eigenvalues of the decompositions of the covariance matrix  $X'X$  and the matrix  $XX'$ :

$$X'X = V\Sigma^2V' \quad (3)$$

$$XX' = U\Sigma^2U' \quad (4)$$

The subsequent sample scores then can be computed as:

$$U = XV\Sigma^{-1} \text{ and } V = XU\Sigma^{-1} \quad (5)$$

The procedure is considered a linear transformation of X into a reduced k dimensional subspace.



Though SVD can be effective to reduce two dimensional data sets, and has also been used to reduce multiway data arrays through the concatenation of multiple modes of the dataset into combination mode matrices. The use of bi-linear modeling on multi-mode data is not without consequence, as the covariance among concatenated modes is ignored. For this reason, the current study investigated the use of higher-order decomposition in comparison with bi-linear SVD on concatenated mode matrices. Higher-order decompositions are extensions of bi-linear methods to facilitate multi-mode datasets. Here, the Tucker decomposition model was compared with the previous bi-linear model. The Tucker3 model (Kroonenberg, 2008):

$$X_a = AG_a(C' \otimes B') + E_a \quad (6)$$

Where  $X_a$  is an  $n$  by  $p$  by  $m$  multiway array containing the original data of the  $n$  samples, from  $p$  variables and  $m$  occasions.  $A$ ,  $B$ , and  $C$  are matrices containing the loadings or scores of dimensions  $n$  by  $a$ ,  $p$  by  $b$ , and  $m$  by  $c$ , respectively, and are created from the reduced axes of each mode of the original dataset  $X_a$ .  $\otimes$  represents the Kronecker product of two matrices.  $G_a$  is an  $a$  by  $b$  by  $c$  core-array containing the weights, standard deviations or singular values, of the relationships between the  $a$  axes of  $A$ , the  $b$  axes of  $B$ , and the  $c$  axes of  $C$  obtained from the reductions of  $n$ ,  $p$  and  $m$ , respectively.  $E_a$  is an  $n$  by  $p$  by  $m$  multiway array containing the residuals which result from the reduction of the model. This model is equally expressed as:

$$X_b = BG_b(A' \otimes C') + E_b \quad (7)$$

$$X_c = CG_c(B' \otimes A') + E_c \quad (8)$$

These alternate configurations result from the differences in unfolding  $X$  and  $G$  along the two alternate modes through the alternating least-squares estimation procedure.

Another method that has been used in range and ecological studies of organism community data is multi-dimensional scaling (MDS). MDS utilizes pairwise dissimilarity distances between

observations to reduce a data set to a specified dimensionality while best preserving the distances between observations in variable space through the minimization of a measure called stress. (Kenkel and Orłóci, 1986). Kruskal (1964) defined stress as:

$$STRESS = \sqrt{\frac{S^*}{\sum \sum d_{ij}^2}} \quad (9)$$

Where  $d_{ij}$  is the element of the distance matrix relating to the  $i^{\text{th}}$  row and  $j^{\text{th}}$  column and  $S^*$  is the raw stress:

$$S^* = \sum \sum (d_{ij} - \hat{d}_{ij})^2 \quad (10)$$

This raw stress is normalized by  $\sum \sum d_{ij}^2$  and rescaled to a standard deviation through the use of the square root. Stress values near zero indicate a perfect fit of the distances among data points in the original and reduced spaces, while stress values near one indicate poor fits among the sets. MDS was included as to make comparisons between SVD and Tucker decomposition solutions on their ability to preserve pairwise distance between the original data points into their respective reduced spaces. In metric MDS, the absolute Euclidean distances are used to minimize the stress coefficient, while in Non-Metric MDS (NMS) the ordinal ranks of distances are used.

## Materials and methods

### *Plant material.*

In order to understand the contribution of temperature effects on the dormancy response to short day length in grapevine, a growth chamber study was conducted. Thirty genotypes were propagated (Table 1). Included in the study were several individuals derived from S1 populations from single S0 progenitors. These S1 progeny were derived from parent vines ‘Valiant’, ‘MN 1131’, ‘St. Croix’, ‘ES 8-2-24’ and ‘ES 8-2-43’. ‘Valiant’ and ‘St. Croix’ are of *V. labrusca*, *V.*

Table 1. Clonal genotypes utilized and their origins.

Genotype	Origin	Origin of S1 parent vine
64	‘Valiant’ x ‘Valiant’	‘Fredonia’ x <i>V. riparia</i> <sup>a</sup>
73	‘Valiant’ x ‘Valiant’	‘Fredonia’ x <i>V. riparia</i> <sup>a</sup>
900	‘MN 1131’ x ‘MN 1131’	<i>V. riparia</i> ‘89’ x ‘Seyval’ <sup>b</sup>
903	‘MN 1131’ x ‘MN 1131’	<i>V. riparia</i> ‘89’ x ‘Seyval’ <sup>b</sup>
906	‘MN 1131’ x ‘MN 1131’	<i>V. riparia</i> ‘89’ x ‘Seyval’ <sup>b</sup>
909	‘St. Croix’ x ‘St. Croix’	‘ES 283’ x ‘ES 193’ <sup>c</sup>
911	‘St. Croix’ x ‘St. Croix’	‘ES 283’ x ‘ES 193’ <sup>c</sup>
913	‘St. Croix’ x ‘St. Croix’	‘ES 283’ x ‘ES 193’ <sup>c</sup>
914	‘St. Croix’ x ‘St. Croix’	‘ES 283’ x ‘ES 193’ <sup>c</sup>
917	‘ES 8-2-24’ x ‘ES 8-2-24’	<i>V. riparia</i> ‘89’ x ‘SV 23-657’ <sup>d</sup>
920	‘ES 8-2-24’ x ‘ES 8-2-24’	<i>V. riparia</i> ‘89’ x ‘SV 23-657’ <sup>d</sup>
924	‘ES 8-2-24’ x ‘ES 8-2-24’	<i>V. riparia</i> ‘89’ x ‘SV 23-657’ <sup>d</sup>
936	‘ES 8-2-43’ x ‘ES 8-2-43’	<i>V. riparia</i> x ‘SV 23-657’ <sup>d</sup>
937	‘ES 8-2-43’ x ‘ES 8-2-43’	<i>V. riparia</i> x ‘SV 23-657’ <sup>d</sup>
938	‘ES 8-2-43’ x ‘ES 8-2-43’	<i>V. riparia</i> x ‘SV 23-657’ <sup>d</sup>
939	‘ES 8-2-43’ x ‘ES 8-2-43’	<i>V. riparia</i> x ‘SV 23-657’ <sup>d</sup>
940	‘ES 8-2-43’ x ‘ES 8-2-43’	<i>V. riparia</i> x ‘SV 23-657’ <sup>d</sup>
‘Frontenac’	<i>V. riparia</i> ‘89’ x ‘Landot Noir’ <sup>a</sup>	-
‘MN1131’	<i>V. riparia</i> ‘89’ x ‘Seyval’ <sup>b</sup>	-
‘Marquette’	‘MN 1094’ x ‘Ravat 626’ <sup>a</sup>	-
1001	<i>V. riparia</i> , Whapeton, ND	-
1002	<i>V. riparia</i> , Kindred, ND	-
1003	<i>V. riparia</i> , Fargo, ND	-
1004	<i>V. riparia</i> Burlington, ND	-
‘SD 62-8-160’	<i>V. riparia</i> , Culberson, MT	-
956	<i>V. californica</i> OP	-
958	<i>V. californica</i> OP	-
961	<i>V. californica</i> OP	-
962	<i>V. californica</i> OP	-
965	<i>V. californica</i> OP	-

<sup>a</sup> – (Hemstad, 2015)

<sup>b</sup> – (Hemstad and Luby, 2000)

<sup>c</sup> – (Swenson, 1982)

<sup>d</sup> – (National Plant Germplasm System, 2009)

*riparia*, and *V. vinifera* descent, whereas ‘MN 1131’, ‘ES 8-2-24’ and ‘ES 8-2-43’ are largely of *V. riparia* and *V. vinifera* descent having less *V. labrusca* parentage. ‘Valiant’, ‘MN 1131’, ‘ES 8-2-24’ and ‘ES 8-2-43’ were derived from first generation crosses of *V. riparia* with other material, whereas ‘St. Croix’ was derived from a cross between interspecific types. ‘MN 1131’, ‘Marquette’, and ‘Frontenac’ were used as industry standard checks. ‘MN 1131’ and ‘Frontenac’ are derived from first generation crosses of *V. riparia* with interspecific types including *V. vinifera* parentage, whereas ‘Marquette’ was derived from the crossing of two interspecific hybrids (‘Ravat 262’ and ‘MN 1094’) types; one of which, ‘MN 1094’, had *V. riparia* descent (Hemstad and Luby, 2008). Several natively collected *V. riparia* vines were included to provide directionality to results and to compare genotype responses to the native wild-type response. The contained *V. riparia* were collected to emulate the diversity seen in regionally adapted wild-type vines. Genotype 1002 was collected near the Sheyenne River near Kindred, ND. Genotypes 1001 and 1003 were collected near the Red River of the North near Abercrombie, ND and Fargo, ND, respectively. Genotype 1004 was received under the designation ‘Rip 821’ and originated from near Burlington, ND. Genotype ‘SD 62-8-160’ is documented as have originated near the Missouri River near Culbertson, MT (National Plant Germplasm System, 2009). A collection of *V. californica* was added as an out-group. *V. californica* is not known to be in the pedigrees of any of the tested vines as well it is a North American species of grapevine from a Mediterranean climate of California. The seed used to obtain the original parent plants of the *V. californica* used in this study was obtained commercially (Sheffield Seed Co., Locke, NY).

#### *Growing conditions.*

Whether parent plants were initially grown from seed or asexually propagated, single plants were obtained for each genotype tested. Propagules were rooted using green shoot tip cuttings in

100% perlite under mist with bottom heat and 1000 ppm IBA to obtain clones for subsequent tests. Rooted vines were planted in D40H Deepots (Stuewe and Sons, Inc., Tangent, Oregon) in Sunshine Mix #1 (Sungro Horticulture, Agawam, MA). Plants were vernalized for six weeks in a cooler at 3°C (37.4°F). Upon removal from vernalization, plants were root pruned to a length of approximately 10cm (4in) to prevent root binding and were replanted in the same Deepot. Vines were allowed to grow for 3 weeks at a photoperiod of 16h daylight and a temperature of 27°C (80.6°F) prior to the initiation of each study. Each plant was restricted to a single shoot trained to a bamboo stake. Plants were placed in a Percival growth chamber (Model no. WE-95, ~500  $\mu\text{mol}\cdot\text{m}^{-2}\cdot\text{s}^{-1}$ ; Percival Scientific Inc., Perry, IA) for the duration of the experiment and given weekly fertilizer applications of 20-10-20 NPK at a rate of 400 ppm N to support growth.

#### *Experimental design.*

Two temperatures were tested (10°C (50.0°F) and 27°C (80.6°F)). Order in which the temperatures were applied was confounded with the two runs of the experiment. The first run was confounded with the order 27°C followed by 10°C, while the second run of the experiment was 10°C followed by 27°C. Four replications of each cultivar were randomly assigned to four blocks within each run-by-temperature combination. Dormancy was evaluated similarly to what has been described previously with modifications (Garris et al.; 2009; Fennell et al, 2005; Wake and Fennell, 2000; Fennell and Hoover, 1991). For each of the four run-by-temperature combinations, test plants were subjected to decreasing photoperiod starting with 15h light followed by 9h darkness. Light hours were reduced weekly by 0.5h for 10 weeks to an ending photoperiod of 10h light and 14h darkness. Acclimation measures were quantified at the end of the week for each half-hour decrease in photoperiod resulting in 11 photoperiodic time periods.

*Acclimation measures.*

Measures taken included shoot length (cm), number of nodes (count), number of mature nodes (count), number of lateral shoots (count), tip growth cessation (visual rating 0 (fully active growth) to 5 (complete tip abscission)), and periderm development (cm and count of nodes encompassed). Each week, plants were removed from the growth chamber for evaluation. After data collection vines were arbitrarily replaced within their designated replications to ensure overall homogenous conditions for each vine.

*Statistical analysis.*

Traits were initially analyzed separately using the mixed procedure of SAS statistical software 9.4 (SAS Institute Inc., Cary, NC). Each trait was analyzed as a randomized complete block design with repeated photoperiodic measurements with four replications. For each trait, all factors were considered fixed effects as the goal of the analysis was to obtain mean values for further deconstruction. Following ANOVA, mean values for each run-by-temperature-by-cultivar-by-photoperiodic time combination in each evaluated trait were obtained and combined for further analysis.

To deconstruct the interaction, data were rearranged as a 60x7x11x2 multiway array (run-by-genotype, measures, photoperiods, and temperatures). The run and cultivar modes were concatenated to retain runs of the experiment as a replication for further comparison of reduction methods. Data was centered for each of the four obtained data modes and scaled to a variance of one for measures using the nprocess function of the N-way Toolbox for MATLAB in MATLAB R2015a (The MathWorks, Inc., Natick, MA) (Andersson and Bro, 2000). Measures were scaled to equally weight their differences in measurement units (lengths, counts, classes). The quadruple centering of the data effectively removed all main effects and lower level interactions leaving only

the effects of the four-way interaction. As the comparison across genotypes of relative reaction norms of the vines was the focus of this study the lower-level interactions were not reintroduced to the dataset and only four-way interaction was interpreted.

Singular value decomposition.

When SVD was used, the modes of measures, photoperiods and temperatures were concatenated resulting in a wide combination-mode matrix of dimension 60x154. Singular value decomposition was carried out using the svds function of MATLAB R2015a statistical software. The number of retained axes was determined as the best compromise between explained variance and complexity of the model by the visual evaluation of a scree plot. Both the loadings and scores of the solution were varimax rotated using the rotatefactors function of MATLAB R2015a. The relational matrix linking the two matrices was, in both cases, counter rotated using the inverse of the rotation matrices used to derive the rotated versions of the loadings and scores. The rotated and non-rotated models were compared. In all cases variable weights were calculated as:

$$W = V\Sigma^{-1} \tag{11}$$

Where W is a matrix of weights relating the predictor variables to the reduced U axes of sample scores such that:

$$XW = U$$

Tucker decomposition.

A Tucker4 decomposition, an extension of the Tucker3 model, was applied to the four-mode data array (genotypes\*runs (A) x measures (B) x photoperiods (C) x temperatures (D)) of dimension 60x7x11x2 using the tucker function of the N-way Toolbox for MATLAB in MATLAB R2015a. The Tucker4 model was calculated as:

$$X_a = AG_a(D \otimes (C \otimes B))' + E_a \tag{12}$$

Where  $X_a$  is the multiway array of centered and scaled interaction effects,  $G_a$  is a multiway array containing the singular values of the associations between mode matrices A, B, C, and D, while  $E_a$  is a multiway array containing the residuals of the model. The number of retained factors was determined visually as a compromise between explained variance and model complexity using the plotted values of explained variance for all combinations of components for each mode. After fitting the initial model, the A, B, and C matrices were varimax rotated independently using the rotatefactors function of MATLAB R2015a. The D matrix was not rotated as it was reduced to a single vector and thus was not included in the  $G_a$  array. The core-array,  $G_a$ , was counter rotated for each respective mode rotation by applying the inverse function of the rotation to the proper axis of  $G_a$ . Attempts were also made to simplify the relationships between the axes among modes. The  $G_a$  core-array was rotated to maximize its variance using the maxvar3 function of the N-way Toolbox for MATLAB R2015a. Upon convergence to a rotated solution, each mode matrix was counter rotated accordingly. All three solutions (non-rotated, mode-rotated, and core-rotated) were reported and compared. For each solution variable weights were calculated to compare the associations of the resulting sample scores with the initial set of predictor variables. Variable weights were calculated as:

$$W = (G_a(D \otimes (C \otimes B)))'^+ \quad (13)$$

Where W is a matrix of weights relating the relating the predictor variables to the reduced A axes and  $^+$  is the Moore-Penrose pseudoinverse such that:

$$XW = A$$

#### Multidimensional scaling.

Both metric-MDS and NMS were investigated as empirical solutions of best fit. In either case, the model was applied to the same combination mode matrix of size 60x154 as used for SVD



using the mds procedure of SAS statistical software. The input dataset was calculated as a Euclidean distance matrix using the SAS distance procedure. In both cases, the number of *a priori* dimensions sought was three to enable comparisons among reduction methods. Metric-MDS was conducted using absolute differences among data points whereas NMS was conducted using ordinal (rank) differences among data points.

#### Model comparisons.

No matter how the data was reduced the sample scores were interpreted using ANOVA. The interpretation of factors from decomposition has been accomplished in this manner in the past and has been termed PCA-ANOVA (Teh et al., 2010; Luciano and Næs, 2009; Légère and Samson, 1999; Nomme and Harrison, 1991). ANOVA was completed using the mixed procedure of SAS as an RCBD with two runs of the experiment treated as random replications and thirty genotypes considered fixed effects. Mean values for S1 families, species, combined S1s, Checks, and all non-*V. riparia* entries were estimated. Single degree of freedom contrasts were used to compare estimated mean values of genotypes and groups of interest with the mean value of tested *V. riparia*.

To visually evaluate the grouping of *V. riparia*, data were also clustered using the distance and cluster procedures of SAS statistical software. All resulting solutions were clustered using Euclidean distance measure between the mean values of the thirty genotypes with Ward's minimum variance method of linkage. To compare the overall stability of Tucker decomposition in comparison with SVD, sum of squared deviations from observed values as well as from full model solutions were estimated for each of 10,000 iterations of resampling of samples with replacement. Mean deviations were calculated and compared using estimated 95% confidence intervals. Lastly, to compare the solutions of the given models. Correlations between sample scores

as well as variable weights were completed using the corr procedure of SAS. Correlation was determined to be significant at  $\alpha=0.05$ .

## Results

### *Singular value decomposition.*

When SVD was applied to the centered and scaled data, the optimum number of axes was three from visual inspection of the scree plot of explained variance (Table 2). These components combined to recover 74.4% of the variation in the centered and scaled data. Tabulated variable weights were evaluated visually and determined that the first axis related to relative differences in tip progress through photoperiodic time from 15.0 to 10.5h of daylight across the two temperatures (Table A8). The second axis related to the relative transition in relative amounts of active growth and tissue maturation from early to late season across the two temperatures two temperatures (Table A9). Additionally, this axis contrasted tip abscission progress at 14.5h of daylight with that of 11.0h of daylight. Lastly, the third axis was associated with a parabolic distortion of the second axis through photoperiodic time across the two tested temperatures (Table A10). The axis additionally contrasted tip abscission progress at 12.5h of daylight with that of 10.0h of daylight. When these axes were tested with ANOVA, using runs of the experiment as replications, significant variance was found among genotypes in their scores for all three retained axes (Table 3).

When means of genotypes, populations, groups, and species were compared to the mean of tested *V. riparia*, significant deviations occurred along all three axes (Table 4). *V. riparia* was positively associated with all three axes. Of the check vines, 'Frontenac' did not significantly differ from the mean of tested *V. riparia* along any axis. Both 'MN 1131' and 'Marquette' deviated from

the response of the tested native vines along axis 1, while ‘Marquette’ also deviated along axis 2. Axis 1 tended to be most associated with the vines ‘Frontenac’ and ‘917’, while it was most negatively associated with ‘MN 1131’ and its progeny. Only vines having large negative values differed in response from *V. riparia* along this axis.

Table 2. SVD singular values, eigenvalues, proportions and cumulative proportions of the total dataset variance.

Axis	Singular Values	Eigenvalues	Proportion (%)	Cumulative (%)
<b>1</b>	<b>9.81</b>	<b>96.2</b>	<b>34.1</b>	<b>34.1</b>
<b>2</b>	<b>9.12</b>	<b>83.1</b>	<b>29.5</b>	<b>63.6</b>
<b>3</b>	<b>5.52</b>	<b>30.5</b>	<b>10.8</b>	<b>74.4</b>
4	3.41	11.6	4.1	78.5
5	3.07	9.4	3.3	81.9
6	2.93	8.6	3.0	84.9
7	2.41	5.8	2.1	87.0
8	2.27	5.1	1.8	88.8
... <sup>x</sup>	...	...	...	...
Total (154)	67.92	282.0	1.0	1.0

Bolded components were retained for further interpretation.

<sup>x</sup> – rows relating to axes 9-154 were omitted.

Table 3. Effect of accessions for the retained axes scores following SVD.

Axis	F Value	Pr > F
1	2.52	0.0076 **
2	2.16	0.0211 *
3	1.91	0.0432 *

\* and \*\* signify significance at  $\alpha=0.05$  and 0.01, respectively.

Axis 2 tended to be positively associated with ‘MN 1131’, its progeny ‘900’, and the mean *V. riparia*. The axis was negatively associated with progeny of ‘ES 8-2-43’, with the exception of ‘937’. All vines that significantly differed from *V. riparia* had negative values along the axis. Four-of-five genotypes derived from ‘ES 8-2-43’, ‘73’ as well as ‘Marquette’ also significantly differed

Table 4. SVD mean genotype scores.

Entry	Axis 1	Axis 2	Axis 3
64	-0.008	-0.034	-0.152 **
73	0.139	-0.088 *	0.053
900	-0.164 **	0.195	0.102
903	-0.164 **	0.039	0.055
906	-0.097 *	0.064	-0.121 **
909	-0.133 **	-0.022	-0.057 *
911	0.019	-0.023	-0.158 **
913	-0.050	0.079	-0.056 *
914	-0.127 *	0.026	-0.031
<b>917</b>	<b>0.155</b>	<b>0.033</b>	<b>-0.047</b>
920	0.059	-0.046	-0.129 **
924	0.087	-0.061	-0.052 *
936	-0.024	-0.137 **	-0.055 *
937	-0.136 **	0.045	-0.130 **
938	-0.004	-0.089 *	0.042
939	-0.079 *	-0.143 **	-0.017
940	0.013	-0.090 *	-0.128 **
<b>Frontenac</b>	<b>0.157</b>	<b>-0.053</b>	<b>0.009</b>
MN 1131	-0.192 **	0.101	0.018
Marquette	-0.106 *	-0.083 *	0.043
S1 Valiant	0.065	-0.061 *	-0.049 *
S1 MN 1131	-0.141 ****	0.100	0.012
S1 St. Croix	-0.073 **	0.015	-0.076 ***
S1 ES 8-2-24	0.100	-0.025 *	-0.076 **
S1 ES 8-2-43	-0.046 **	-0.083 ***	-0.058 ***
Checks	-0.047 *	-0.011	0.023
All S1s	-0.030 **	-0.015 **	-0.052 ****
All	-0.015 *	-0.018 **	-0.020 **
<i>V. californica</i>	0.057	-0.034 **	0.063
<i>V. riparia</i>	0.074 -	0.091 -	0.099 -

\*, \*\*, \*\*\*, and \*\*\*\* signify that the value is significantly different from that of the mean of *V. riparia* within the associated component at alpha = 0.05, 0.01, 0.001, and 0.0001, respectively.

Bolded individuals have mean values not significantly different than the mean of *V. riparia* for all significant components showing variation for genotypes.

from the mean of *V. riparia* along the axis. The final retained axis was predominately associated with *V. riparia* as well as '900', and was negatively associated with several genotypes arising from diverse families ('64', '906', '911', '920', '937', and '940'). All individuals showing significant differences from the tested *V. riparia* had negative values along the axis. Of the included checks, all three were found to have positive values and none were found to significantly depart from the values of the tested native vines. Of the tested genotypes only two, 'Frontenac' and '917', showed no significant departures from the mean of tested native vines across all three retained axes, while all other tested vines significantly differed from the mean of *V. riparia* along at least one axis.

When the mean values of the thirty tested genotypes were clustered using Euclidean distance with Ward's minimum variance method of linkage, two distinct groups formed (Fig. 1). Check vines were separated as 'Marquette' and 'Frontenac' clustered together while 'MN 1131' differed. The tested *V. riparia* were split among the two groups; however, representatives in either group tended to cluster together within sub-groups. In the group associated with 'Marquette' and 'Frontenac', *V. riparia* 'SD62-8-160' and '1002' grouped with 'Frontenac', '917', '73', and two *V. californica* vines, while 'Marquette' was associated with four of the five members of the 'ES 8-2-43' family, '920', '911', and the *V. californica* accession '958'. The group associated with 'MN 1131' was also sub-divided into two subgroups pertaining to *V. riparia* and non-*V. riparia* classes. The three remaining *V. riparia* clustered with the two remaining *V. californica* accessions, while 'MN 1131' clustered tightly with its progeny as well as the remaining accessions derived from other families.

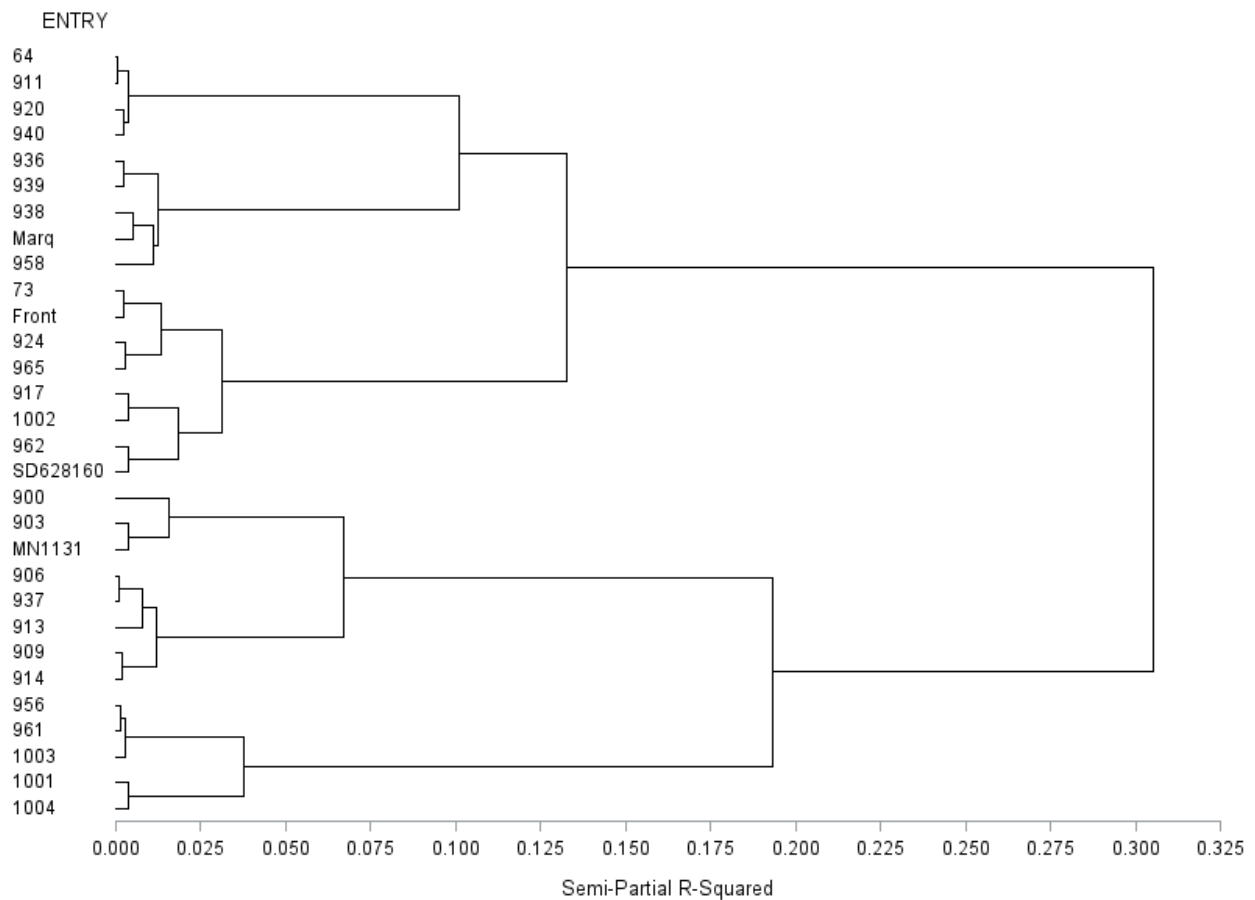


Figure 1. Cluster of Euclidean distances between genotypic means for the three retained axes from the non-rotated SVD solution using Ward's minimum variance method of linkage. Marq = 'Marquette' and Front = 'Frontenac'.

Varimax rotation of loadings and scores.

When the resulting scores and loadings matrices were varimax rotated to simple solution, the relational matrix was counter rotated to form off-diagonal covariates among predictors and sample scores (Table 5). The new axes contributed 32.52%, 29.11%, and 12.77% to the total variation of the dataset, respectively.

**Bolded values contribute greatest to the variation of the dataset**

Tabulated variable weights were evaluated visually. The axes retained similar relationships with the tested variables as was determined in the non-rotated solution; however, the relationship

of axes with photoperiodic time was altered. The first axis related to relative tip progress through photoperiodic time from 14.5h to 10.5h of daylight across temperatures putting increased emphasis on late season differences. (Table A11). The second axis related to the relative transition in relative amounts of active growth and tissue maturation between 15.0 and 12.0h of daylight across the two tested temperatures, relating to trends early in the simulated season (Table A12). Lastly, the third axis was associated with parabolic distortion of the second axis through photoperiodic time across the two temperatures, however the emphasis was shifted away from the influence of tip abscission progress (Table A13).

Table 5. Counter-rotated relational matrix of varimax rotated scores and loadings.

Genotypes	Measure					
	Axis 1	Axis 2	Axis 3	Axis 1	Axis 2	Axis 3
	----- Weight -----			----- Sq. weight -----		
Axis 1	<b>8.76</b>	-0.69	3.81	<b>76.71</b>	0.47	14.52
Axis 2	2.54	<b>7.81</b>	-3.83	6.44	<b>61.00</b>	14.65
Axis 3	-0.42	2.00	<b>5.64</b>	0.18	4.01	<b>31.82</b>

When the scores of the rotated axes were evaluated using ANOVA with runs of the experiment as replicates, only two of the three retained components had significant variation among genotypes (Table 6). When the resulting mean genotype scores were compared to the mean of tested native vines, significant differences were found in each of the axes with significant variation across genotypes. *V. riparia* was moderately positively associated with either axis (Table 7). The first axis was associated with ‘917’, ‘Frontenac’, and ‘73’. The axis was predominantly negatively associated with ‘MN 1131’ and its progeny, specifically ‘900’ and ‘903’. The remaining check vine, ‘Marquette’, was also moderately negative along the axis. All vines that significantly differed from that of the mean of *V. riparia* had negative values. These vines tended to arise from ‘MN 1131’ (‘900’ and ‘903’) as well as ‘St. Croix’ (‘909’ and ‘914’).

Table 6. Effect of accessions for the retained axes scores following varimax rotation.

Axis	F Value	Pr > F
1	2.49	0.0082 **
2	2.40	0.0108 *
3	1.77	0.0652

\* and \*\* signify significance at  $\alpha=0.05$  and  $0.01$ , respectively.

The second axis was positively associated with ‘900’, ‘MN 1131’, and the mean of *V. riparia*. The axis was negatively associated with the progeny of ‘ES 8-2-43’ with the exception of ‘937’, and to a lesser extent the descendants of ‘Valiant’. The additional included checks, ‘Frontenac’ and ‘Marquette’, were both negatively associated with the axis and significantly differed from the mean of riparian vines.

Several vines were found not to significantly differ from *V. riparia* along the two axes found to have significant variation among cultivars. These individuals were derived from included families, with the exception of ‘Valiant’ progeny, which both significantly differed from *V. riparia* along axis 2. While several S1 progeny were identified, none of the examined species F1 parental types had both qualities in common with *V. riparia*. ‘MN 1131’ and ‘Marquette’ significantly differed along axis 1 and ‘Frontenac’ significantly differed along axis 2 from the native types.

When all three retained axes were used to cluster the thirty tested genotypes, groups related to *V. riparia* and non-*V. riparia* genotypes were identified (Fig. 2). The *V. riparia* group contained all five tested wild vines, along with three *V. californica* genotypes (‘956’, ‘961’, and ‘962’), ‘Frontenac’, ‘917’, and ‘73’. The non-*V. riparia* group was subdivided into two sub-classes related to either the check vines ‘Marquette’ or ‘MN 1131’. The ‘MN 1131’ subclass additionally contained all ‘MN 1131’ progeny along with three of the four descendants of ‘St. Croix’ with ‘937’, while all other accessions grouped with ‘Marquette’.



Table 7. Varimax-rotated SVD mean genotype scores.

Entry	Axis 1	Axis 2	Axis 3
64	0.031	-0.056 *	-0.142
73	0.119	-0.075 *	0.100
900	-0.183 **	0.203	0.026
903	-0.172 **	0.042	0.005
<b>906</b>	<b>-0.061</b>	<b>0.044</b>	<b>-0.150</b>
909	-0.114 *	-0.033	-0.086
<b>911</b>	<b>0.059</b>	<b>-0.045</b>	<b>-0.143</b>
<b>913</b>	<b>-0.033</b>	<b>0.069</b>	<b>-0.078</b>
914	-0.115 *	0.018	-0.066
<b>917</b>	<b>0.162</b>	<b>0.030</b>	<b>-0.009</b>
920	0.091	-0.062 *	-0.101
924	0.097	-0.066 *	-0.019
936	-0.010	-0.144 **	-0.039
<b>937</b>	<b>-0.097</b>	<b>0.022</b>	<b>-0.166</b>
938	-0.016	-0.082 *	0.052
939	-0.073	-0.146 **	-0.017
940	0.045	-0.107 **	-0.106
Frontenac	0.149	-0.047 *	0.057
MN 1131	-0.189 **	0.098	-0.047
Marquette	-0.114 *	-0.079 *	0.025
S1 Valiant	0.075	-0.065 **	-0.021
S1 MN 1131	-0.138 ***	0.096	-0.040
S1 St. Croix	-0.051 *	0.002 *	-0.093
S1 ES 8-2-24	0.116	-0.033 **	-0.043
S1 ES 8-2-43	-0.030	-0.092 ****	-0.055
Checks	-0.052 *	-0.009 *	0.012
All S1s	-0.016	-0.023 ***	-0.055
All	-0.009	-0.021 ***	-0.020
<i>V. californica</i>	0.038	-0.023 **	0.080
<i>V. riparia</i>	0.046 -	0.106 -	0.101 -

\*, \*\*, \*\*\*, and \*\*\*\* signify that the value is significantly different from that of the mean of *V. riparia* within the associated component at alpha = 0.05, 0.01, 0.001, and 0.0001, respectively.

Bolded individuals have mean values not significantly different than the mean of *V. riparia* for all significant components showing variation for genotypes.

When only the two axes containing significant variation among genotypes were used to cluster, *V. riparia* accessions were subdivided (Fig. 3). Check vines were divided as with ‘MN 1131’ and ‘Marquette’ grouped together, while ‘Frontenac’ grouped separately. Grouped with ‘MN 1131’ and ‘Marquette’ were the *V. riparia* ‘1001’, ‘1003’, and ‘1004’, while ‘SD 62-8-160’ and ‘1002’ grouped with ‘Frontenac’.

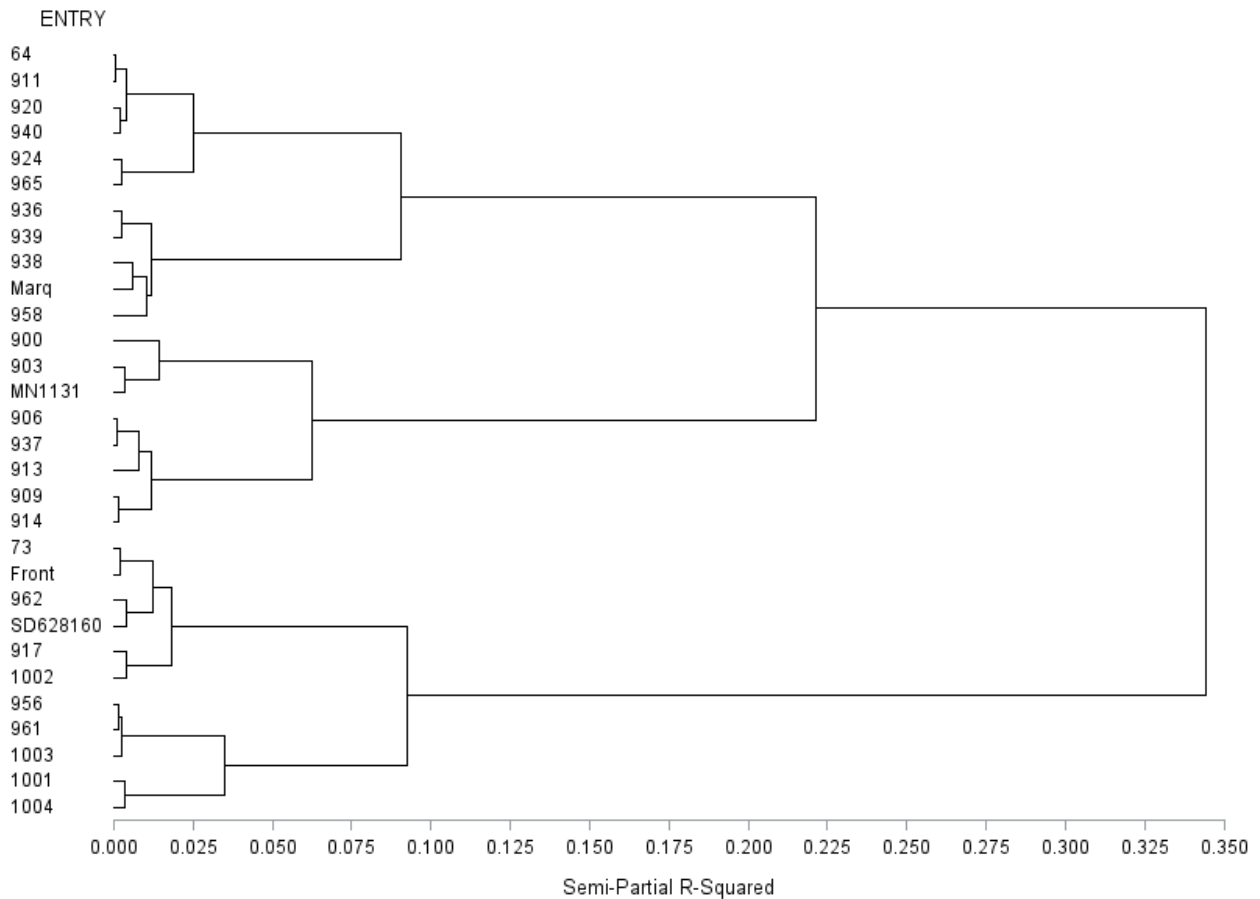


Figure 2. Cluster of Euclidean distances between genotypic means for the three retained axes from the rotated SVD solution using Ward’s minimum variance method of linkage. Marq = ‘Marquette’ and Front = ‘Frontenac’.

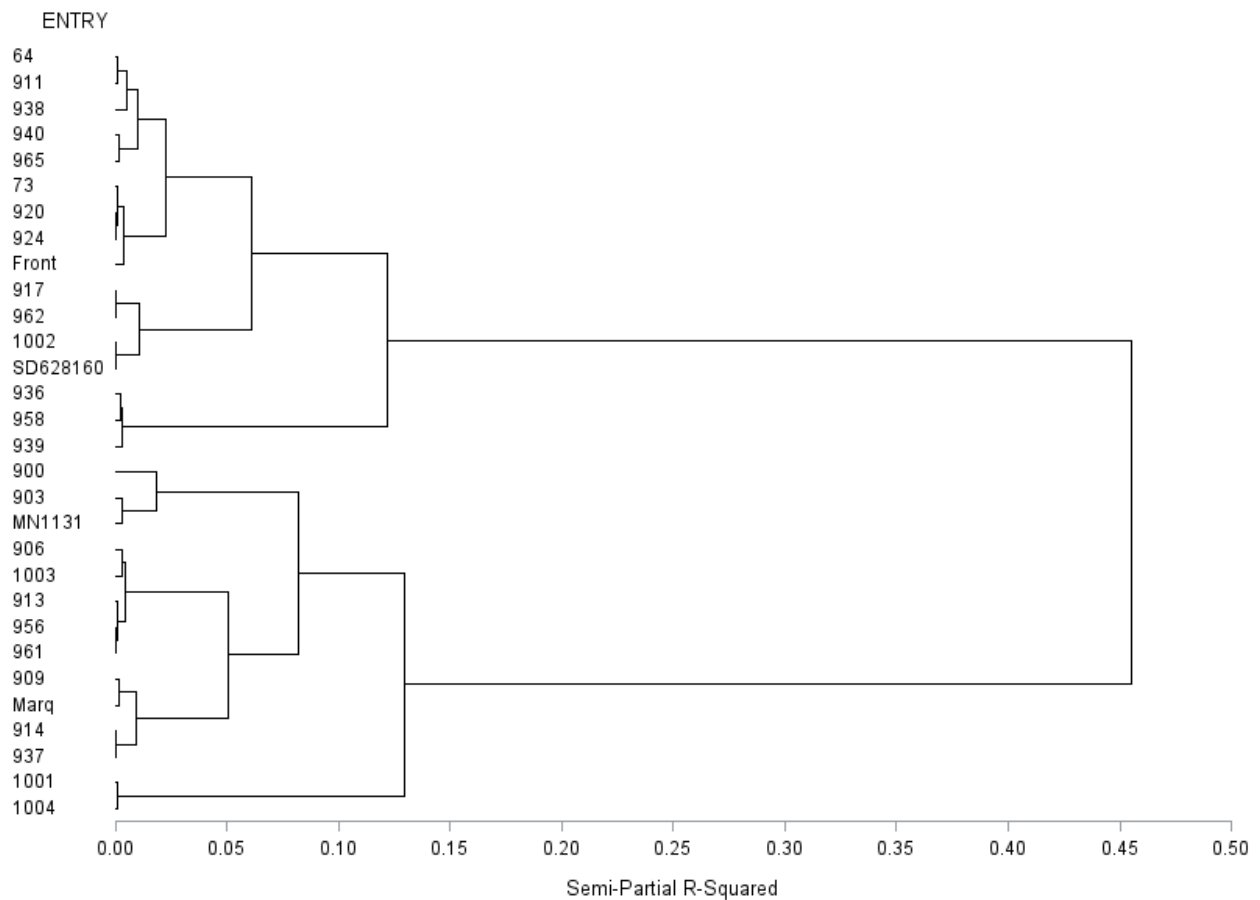


Figure 3. Cluster of Euclidean distances between genotypic means for the two axes having significant genotypic variation from the rotated SVD solution using Ward's minimum variance method of linkage. Marq = 'Marquette' and Front = 'Frontenac'.

*Tucker decomposition.*

Non-rotated.

Upon visual evaluation of the explained variance all combinations of components for all modes, it was determined that the best fit was found using the reduced dimensions of 3x2x2x1 for the original 60x7x11x2 dataset. This solution explained 72.0% of the variation that existed in the original interaction data. The solution's core-array suggested that four relationships among the resulting components had the greatest influence on the dataset (Table 8).

Table 8. Tucker core-array of relationships among genotype, measure, and photoperiod axes.

Photoperiod	Genotypes	----- Measure -----			
		Axis 1	Axis 2	Axis 1	Axis 2
<i>Axis 1</i>		----- Weight -----		----- Sq. weight -----	
	Axis 1	<b>-3.89</b>	<b>8.40</b>	<b>15.11</b>	<b>70.62</b>
	Axis 2	<b>8.19</b>	2.97	<b>67.14</b>	8.82
	Axis 3	0.60	1.87	0.36	3.51
<i>Axis 2</i>					
	Axis 1	-3.04	0.18	9.26	0.03
	Axis 2	-2.28	-0.15	5.18	0.02
	Axis 3	<b>4.50</b>	1.64	<b>20.28</b>	2.70

Bolded combinations contributed greatest to the variation of the dataset.

### Temperature.

A single vector was found to describe the relationship between the two included temperatures. As only two levels of temperature were investigated, and the resulting data was centered along each mode, the data for the two temperatures were reduced to exact inverses as either was equally and oppositely distanced from the mean. All data observed over the two temperatures then related to the relative difference between the two temperatures. This was the case for all investigated data regardless of the method used (SVD, Tucker, or MDS).

### Measures.

Using the Tucker model, two components were extracted from the initial seven phenotypic traits measured (Table 9). The first axis largely contrasted measures of growth and tissue maturation. Stem length, number of nodes, and number of lateral shoots were positively associated with the axis, whereas the number of mature buds and the measures of periderm development were negatively associated with the axis. The strongest positive association was with the number of lateral shoots, whereas the axis was most strongly negatively associated with measures of periderm development. Progress toward tip abscission was not associated with the axis. For interpretations,

the first axis was considered the relative progress the transition from active growth (negative) to the maturation of tissues (positive).

The second axis had a strong, positive association with progress toward tip abscission. The axis was marginally, negatively associated with the number of nodes each vine had, and was not associated with all remaining predictor variables. The second axis was interpreted as progress toward tip abscission and the cessation tip-growth.

Table 9. Tucker loadings for measured variables.

Measure	Axis 1	Axis 2
Stem Length (cm)	<b>-0.313</b>	-0.144
Nodes (count)	<b>-0.350</b>	<b>-0.297</b>
Mature Buds (count)	<b>0.346</b>	-0.029
Lateral Shoots (count)	<b>-0.544</b>	-0.037
Tip Abscission (0-5 scale)	0.010	<b>0.901</b>
Periderm (cm)	<b>0.456</b>	-0.208
Periderm (node count)	<b>0.394</b>	-0.186
Portion of total variation (%)	41.61	30.39

Bolded values indicate local minimums and maximums for each axis.

### Photoperiods.

Two significant axes were found for photoperiodic time from the original eleven time points for which data was collected (Table 10). The first axis was interpreted to be general progress through time with photoperiod 14.5h of daylight being positively and 10.5h of daylight begin negatively associated with the axis with a gradual transition between these photoperiodic extremes. The second component was interpreted as a parabolic distortion from the linear trend through time, and was centered around 12.5h of daylight.

Variable weights.

When variable weights were evaluated visually the axes retained similar relationships with the tested variables as determined with SVD; however, the photoperiodic timing of events was altered. The first axis related to relative tip progress through photoperiodic time from 15.0 - 14.5h of daylight to 11.0 - 10.5h of daylight across the tested temperatures (Table A14). The second axis contrasted the relative amounts of active growth and tissue maturation early in the season to those late in the season (Table A15). This axis also showed tip abscission progress to have a similar trend to that of tissue maturation in contrast with the SVD model. Lastly, the third axis was associated with a parabolic distortion of the second axis through linear time across the two tested temperatures (Table A16). The axis also was related to contrasts of late tip abscission progress between 13.0 and 10.0h of daylight.

Table 10. Tucker loadings for photoperiodic times.

Photoperiodic time (hours of daylight)	Axis 1	Axis 2
15.0	<b>0.384</b>	<b>-0.384</b>
14.5	0.387	-0.248
14.0	0.340	-0.045
13.5	0.284	0.154
13.0	0.166	0.408
12.5	-0.045	<b>0.445</b>
12.0	-0.199	0.383
11.5	-0.291	0.079
11.0	-0.355	-0.110
10.5	-0.354	-0.295
10.0	<b>-0.318</b>	<b>-0.387</b>
Portion of total variation (%)	58.71	13.28

Bolded values indicate local minimums and maximums within each axis.

Genotypes.

When the Tucker model was used, three significant axes, contributing 33.69%, 28.78%, and 9.52% of the total variation, respectively, were found to describe the sixty genotype-by-run combination samples. ANOVA was used to investigate the variance attributable to differences among genotypes using runs as replicates. Two of the three retained axes showed significant variation among genotypes (Table 11).

Genotype, population, group, and species means were estimated (Table 12). The resulting components had similar relationships as those discovered through SVD. The first axis was positively associated with ‘Frontenac’, ‘917’, and ‘73’ while being negatively associated with ‘MN 1131’, its progeny (‘900’, ‘903’, and ‘906’), ‘909’, ‘914’, and ‘937’. The mean of tested *V. riparia* was found to be moderately positively associated with the axis and all vines that statistically differed from this mean tended to have negative values. The remaining check vine, ‘Marquette’, was moderately negatively associated with the axis and did significantly differ from *V. riparia*.

Table 11. Effect of accessions for the retained axes scores following Tucker decomposition.

Axis	F Value	Pr > F
1	2.54	0.0072 **
2	2.09	0.0254 *
3	1.63	0.0976

\* and \*\* signify significance at  $\alpha=0.05$  and 0.01, respectively.

The second axis was associated with ‘900’, ‘MN 1131’ and *V. riparia*. This axis was negatively associated with four of the five progeny derived from ‘ES 8-2-43’, ‘73’ and ‘Marquette’. All genotypes that differed significantly from the tested wild vines were negative along the axis. The remaining check vine, ‘Frontenac’, was slightly negative along the axis, however, it did not significantly differ from the mean of wild riparian vines.

Table 12. Tucker mean genotype scores.

Entry	Axis 1	Axis 2	Axis 3
<b>64</b>	<b>-0.005</b>	<b>-0.027</b>	0.145
73	0.142	-0.084 *	-0.042
900	-0.168 **	0.186	-0.086
903	-0.163 **	0.034	-0.030
906	-0.099 *	0.064	0.116
909	-0.131 **	-0.019	0.027
<b>911</b>	<b>0.019</b>	<b>-0.023</b>	0.157
<b>913</b>	<b>-0.051</b>	<b>0.072</b>	0.047
914	-0.130 *	0.020	0.035
<b>917</b>	<b>0.153</b>	<b>0.038</b>	0.042
<b>920</b>	<b>0.060</b>	<b>-0.040</b>	0.139
<b>924</b>	<b>0.088</b>	<b>-0.055</b>	0.043
936	-0.019	-0.135 **	0.045
937	-0.138 **	0.044	0.126
938	-0.002	-0.091 *	-0.047
939	-0.076	-0.145 **	0.037
940	0.016	-0.089 *	0.129
<b>Frontenac</b>	<b>0.159</b>	<b>-0.045</b>	-0.014
MN 1131	-0.198 ***	0.092	-0.020
Marquette	-0.106 *	-0.090 *	-0.048
S1 Valiant	0.069	-0.055 *	0.052
S1 MN 1131	-0.143 ****	0.095	0.000
S1 St. Croix	-0.073 **	0.012	0.067
S1 ES 8-2-24	0.100	-0.019 *	0.075
S1 ES 8-2-43	-0.044 *	-0.083 ***	0.058
Checks	-0.048 *	-0.014 *	-0.027
All S1s	-0.030 **	-0.015 **	0.052
All	-0.014 *	-0.019 **	0.021
<i>V. californica</i>	0.058	-0.037 **	-0.054
<i>V. riparia</i>	0.071	0.095	-0.106

\*, \*\*, \*\*\*, and \*\*\*\* signify that the value is significantly different from that of the mean of *V. riparia* within the associated component at  $\alpha = 0.05, 0.01, 0.001, \text{ and } 0.0001$ , respectively. Bolded individuals have mean values not significantly different than the mean of *V. riparia* for all significant components showing variation for genotypes.



Overall, several vines were not statistically different from *V. riparia* along both axes having significant variation among genotypes. Included in these vines were accessions derived from ‘St. Croix’ (‘911’ and ‘913’) and ‘ES 8-2-24’ (‘917’, ‘920’, and ‘924’) along with ‘64’ as well as the check vine ‘Frontenac’. When all three retained components were clustered using the Euclidean distance and Ward’s minimum variance linkage, distinct *V. riparia* and non-*V. riparia* groups were defined (Fig. 4). The solution largely mimicked that of the rotated SVD solution having ‘Frontenac’ along with sub-classes of the non-*V. riparia* group. ‘MN 1131’ again had a propensity to cluster with its all five wild *V. riparia* clustering together, while each of ‘MN 1131’ and ‘Marquette’ defined progeny, while ‘Marquette’ has a tended to cluster with members of the ‘ES 8-2-43’ family.

When only the two axes containing significant genotypic variation were evaluated, those genotypes with similar responses to ‘MN 1131’ clustered away from all other genotypes, identifying it as an outgroup (Fig. 5). This group included ‘MN 1131’, its progeny, three of the four progeny of ‘St. Croix’, ‘937’, and two *V. californica* genotypes. The remaining genotypes were sub-divided into *V. riparia*-like and ‘Marquette’-like sub-classes. The *V. riparia* sub-grouping included four of the five included wild riparian vines, *V. californica* ‘962’, ‘Frontenac’, ‘917’, and ‘73’. All remaining genotypes clustered with ‘Marquette’ including one wild-type vine ‘1003’.

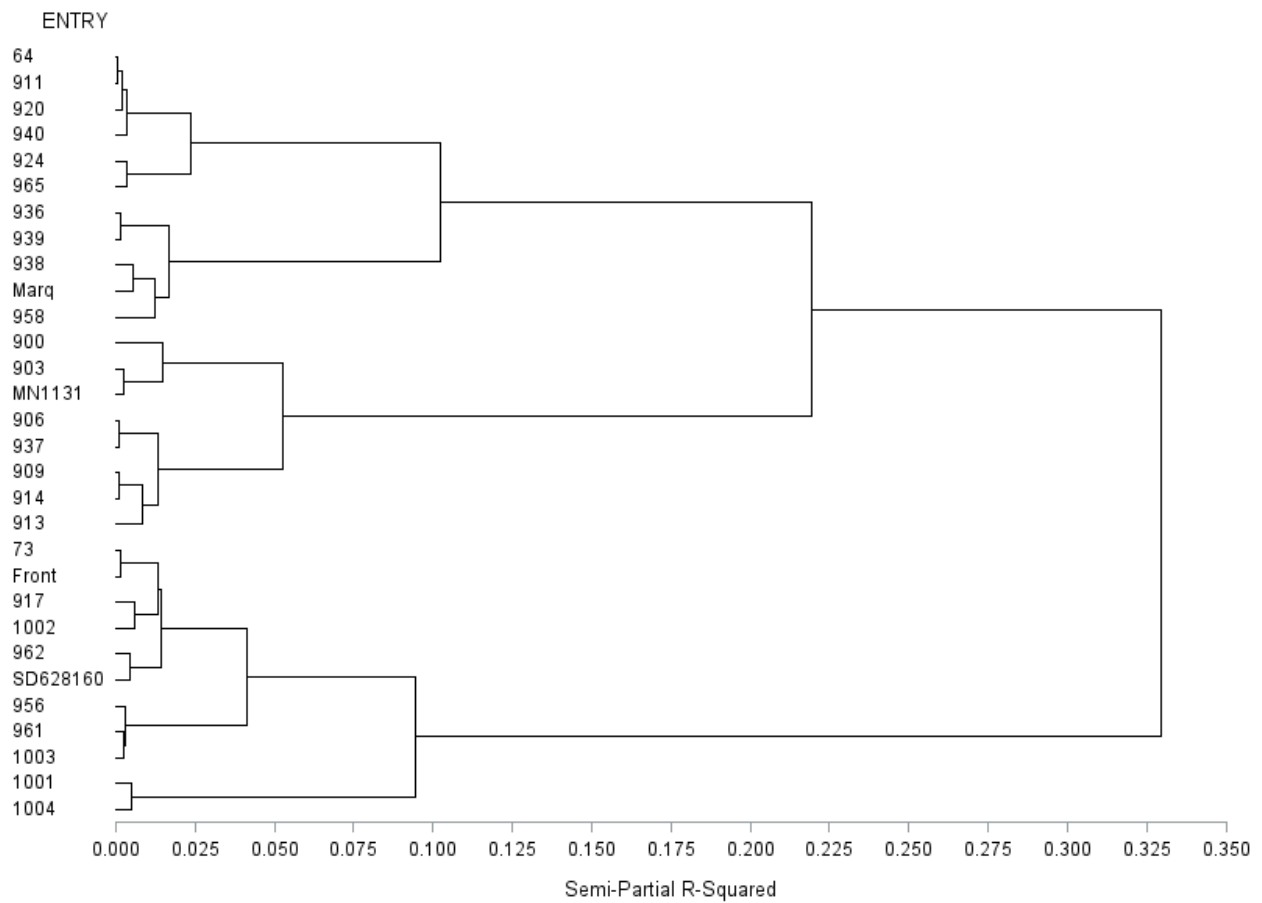


Figure 4. Cluster of Euclidean distances between genotypic means for the three retained axes of the Tucker solution using Ward's minimum variance method of linkage. Marq = 'Marquette' and Front = 'Frontenac'.

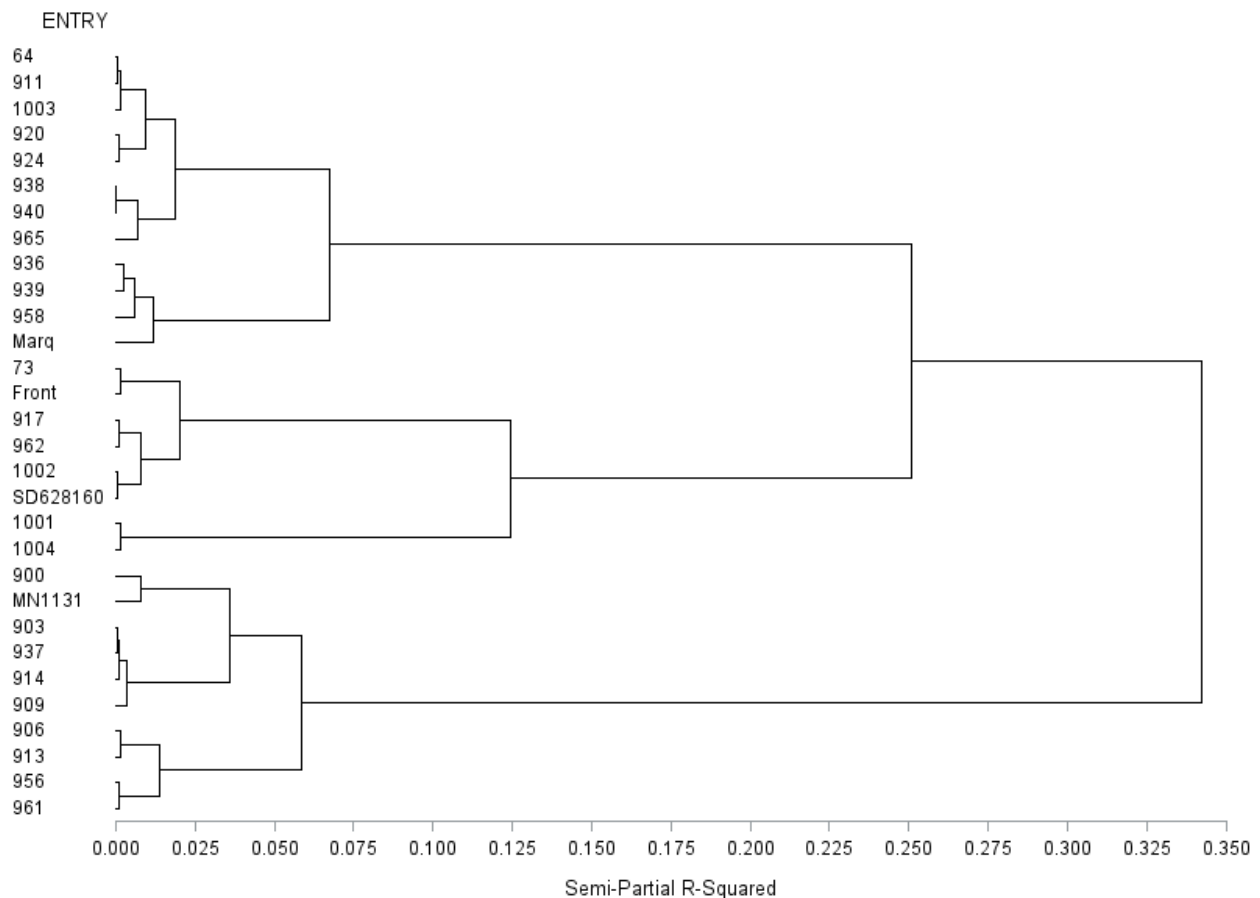


Figure 5. Cluster of Euclidean distances between genotypic means for the two axes having significant genotypic variation from the Tucker solution using Ward's minimum variance method of linkage. Marq = 'Marquette' and Front = 'Frontenac'.

Varimax mode-rotation.

When the modes of genotypes, measures, and photoperiodic timings were varimax rotated independently, a more diffuse core-array of associations among mode axes was obtained (Table 13). The strongest relationship among the derived axes was between genotype axis 2, measure axis 1, and photoperiodic time axis 1. This accounted for 22.4% of the retained variation of the reduced model. A second tier of associations included the associations between genotype axes 1 and 2 with measure axis 1 and time axis 1, genotype axis 1 with photoperiodic time axis 2 across both measure axes, as well as genotype axis 1 with measure axis 1 and time axis 2.

Table 13. Mode-rotated Tucker core-array of relationships among genotype, measure, and photoperiod axes.

Photoperiod	Genotypes	----- Measure -----			
		Axis 1	Axis 2	Axis 1	Axis 2
<i>Axis 1</i>		----- Weight -----		----- Sq. weight -----	
	Axis 1	-2.58	<b>5.28</b>	6.65	<b>27.89</b>
	Axis 2	<b>6.74</b>	<b>4.47</b>	<b>45.48</b>	<b>20.01</b>
	Axis 3	-0.30	-1.63	0.09	2.65
<i>Axis 2</i>					
	Axis 1	<b>-5.06</b>	<b>5.24</b>	<b>25.64</b>	<b>27.46</b>
	Axis 2	2.86	2.19	8.20	4.82
	Axis 3	<b>5.23</b>	2.61	<b>27.34</b>	6.79

Bolded combinations contributed greatest to the variation of the dataset.

Measures.

Following varimax-rotation, similar associations among measures and the resulting two axes as seen in the non-rotated solution were found. Axis 1 contrasted the differences in measures of growth and tip abscission with measures of tissue maturation (Table 14). Tip abscission was negatively associated with the axis in contrast to the lack of association found in the non-rotated solution. Axis two was strongly associated with shoot tip abscission and was contrasted by the number of nodes similar to that was seen in the non-rotated solution.

Table 14. Mode-rotated Tucker loadings for measured variables.

Measure	Axis 1	Axis 2
Stem Length (cm)	-0.243	-0.245
Nodes (count)	-0.223	<b>-0.401</b>
Mature Buds (count)	<b>0.334</b>	0.095
Lateral Shoots (count)	<b>-0.496</b>	-0.226
Tip Abscission (0-5 scale)	<b>-0.307</b>	<b>0.847</b>
Periderm (cm)	<b>0.500</b>	-0.034
Periderm (node count)	<b>0.435</b>	-0.035
Portion of total variation (%)	40.22	31.78

Bolded values indicate local minimums and maximums for each axis.

### Photoperiods.

Rotation of photoperiodic time axes lead to differing results when compared with those found in the non-rotated solution. The rotation identified two timelines equating to early (Axis 1: 15.0-12.0h of daylight) and late (Axis 2: 13.0-10.0h of daylight) (Table 15). The variation was more evenly distributed along the two axes with either contributing similarly to the variation of the dataset (36.45% and 35.55%, respectively).

Table 15. Mode-rotated Tucker loadings for photoperiodic times.

Photoperiodic time (hours of daylight)	Axis 1	Axis 2
15.0	<b>0.543</b>	-0.005
14.5	0.450	0.094
14.0	0.274	0.206
13.5	0.095	0.308
13.0	-0.167	<b>0.408</b>
12.5	-0.343	0.286
12.0	<b>-0.410</b>	0.134
11.5	-0.263	-0.147
11.0	-0.177	-0.327
10.5	-0.046	-0.459
10.0	0.043	<b>-0.499</b>
Portion of total variation (%)	36.45	35.55

<sup>z</sup> Bolded values indicate local minimums and maximums for each axis.

### Variable weights.

When variable weights were evaluated visually the axes retained similar relationships with the tested variables as determined with other models however the photoperiodic timing of events was altered. The first axis related to relative tip progress through photoperiodic time between early season (prior to 12.5h of daylight) and late season (after 12.5h of daylight) across the tested temperatures (Table A17). The second axis related to the relative amounts of active growth and

tissue maturation across temperatures early in the season, contrasting photoperiodic times between 15.0 - 14.0h of daylight with those at 12.0h of daylight (Table A18). Lastly, the third axis was parabolic through time centering between 13.0 and 12.5h of daylight contrasting the amounts of active growth with the amount of mature tissue development and tip abscission progression across the tested temperatures, however, emphasized the contrast between the traits from mid-season to late season (Table A19).

Genotypes.

Following the rotation of the sample axes, the three axes contributed 31.08%, 27.84%, and 13.08% of the variation of the dataset, respectively. When genotypic scores were tested using ANOVA utilizing runs of the experiment as replications, axes 1 and 2 showed significant variation among genotypes (Table 16).

Table 16. Effect of accessions for the retained axes scores following mode-rotation.

Axis	F Value	Pr > F
1	2.29	0.0147 *
2	2.44	0.0095 **
3	1.59	0.1087

\* and \*\* signify significance at  $\alpha=0.05$  and  $0.01$ , respectively

When the means of genotypes, families, and species were compared to the mean of *V. riparia*, significant differences occurred along both axes (Table 17). The first axis was mildly associated with *V. riparia*. However, the axis did contrast groups of the derived families. The axis tended to be positively associated with progeny of ‘ES 8-2-24’ and ‘Valiant’ as well as the industry check ‘Frontenac’. The highest positive values along the axis were associated with ‘917’, ‘Frontenac’ and ‘73’. Those genotypes most negative association with the axis were found to be related to ‘MN 1131’, as well as the check vine ‘Marquette’.

The second axis was positively associated with *V. riparia*. This axis was strongly associated with '900' as well as with 'MN 1131' and was most negatively associated with members of the 'ES 8-2-43' family ('936', '939', and '940'). Overall, only four hybrid genotypes out of the twenty evaluated did not statistically differ from the mean of *V. riparia* across both axes containing significant variation among genotypes. These individuals included '906', '913', '917' and '937'.

When all three retained axes were used to cluster genotype means, entries were sub-divided into *V. riparia* and non-*V. riparia* groups (Fig 6). All five tested *V. riparia* belonged to the *V. riparia* group. Additional genotypes included three of the five *V. californica* accessions, 'Frontenac', '917', and '73'. The non-*V. riparia* group was sub-divided into 'Marquette' and 'MN 1131' like sub-classes. 'MN 1131' was most similar to its progeny, three of the four 'St. Croix' progeny, and '937', while all other genotypes grouped with 'Marquette'.

When only the two axes having significant variation among genotypes were included in the cluster analysis, the wild-type *V. riparia* vines were divided among groups (Fig 7). The two groups that were identified represented a 'Frontenac'-like as well as a 'MN 1131'/'Marquette'-like group. 'Frontenac' grouped with the riparian vines 'SD 62-8-160' as well as '1002'. Additionally, all progeny from 'Valiant' and 'ES 8-2-24' as well as four of the five members of the 'ES 8-2-43' family, two *V. californica* progeny, and '911'. All other genotypes grouped with 'MN 1131' and 'Marquette', including the wild-type vines '1003', '1001', and '1004'.

Table 17. Mode-rotated Tucker mean genotype scores.

Entry	Axis 1	Axis 2	Axis 3
64	0.039	-0.058 *	0.130
73	0.110	-0.080 *	-0.103
900	-0.162 **	0.209	0.015
903	-0.158 **	0.049	0.035
<b>906</b>	<b>-0.047</b>	<b>0.042</b>	<b>0.153</b>
909	-0.117 *	-0.017	0.066
911	0.066	-0.059 *	0.134
<b>913</b>	<b>-0.024</b>	<b>0.063</b>	<b>0.074</b>
914	-0.108 *	0.018	0.081
<b>917</b>	<b>0.162</b>	<b>0.019</b>	<b>-0.007</b>
920	0.096	-0.073 *	0.099
924	0.090	-0.068 *	-0.002
936	-0.020	-0.140 **	0.022
<b>937</b>	<b>-0.083</b>	<b>0.022</b>	<b>0.171</b>
938	-0.028	-0.078 *	-0.060
939	-0.078	-0.145 **	0.032
940	0.046	-0.116 **	0.096
Frontenac	0.139	-0.049 *	-0.076
MN 1131	-0.181 **	0.105	0.068
Marquette	-0.126 *	-0.071 *	-0.025
S1 Valiant	0.074	-0.069 **	0.013
S1 MN 1131	-0.122 **	0.100	0.067
S1 St. Croix	-0.046 *	0.001 *	0.089
S1 ES 8-2-24	0.116	-0.040 **	0.030
S1 ES 8-2-43	-0.033	-0.091 ****	0.052
Checks	-0.056 *	-0.005 *	-0.011
All S1s	-0.013	-0.024 ***	0.055
All	-0.009	-0.022 ***	0.021
<i>V. californica</i>	0.033	-0.027 **	-0.077
<i>V. riparia</i>	0.044	0.112	-0.104

\*, \*\*, \*\*\*, and \*\*\*\* signify that the value is significantly different from that of the mean of *V. riparia* within the associated component at alpha = 0.05, 0.01, 0.001, and 0.0001, respectively.

Bolded individuals have mean values not significantly different than the mean of *V. riparia* for all significant components showing variation for genotypes.



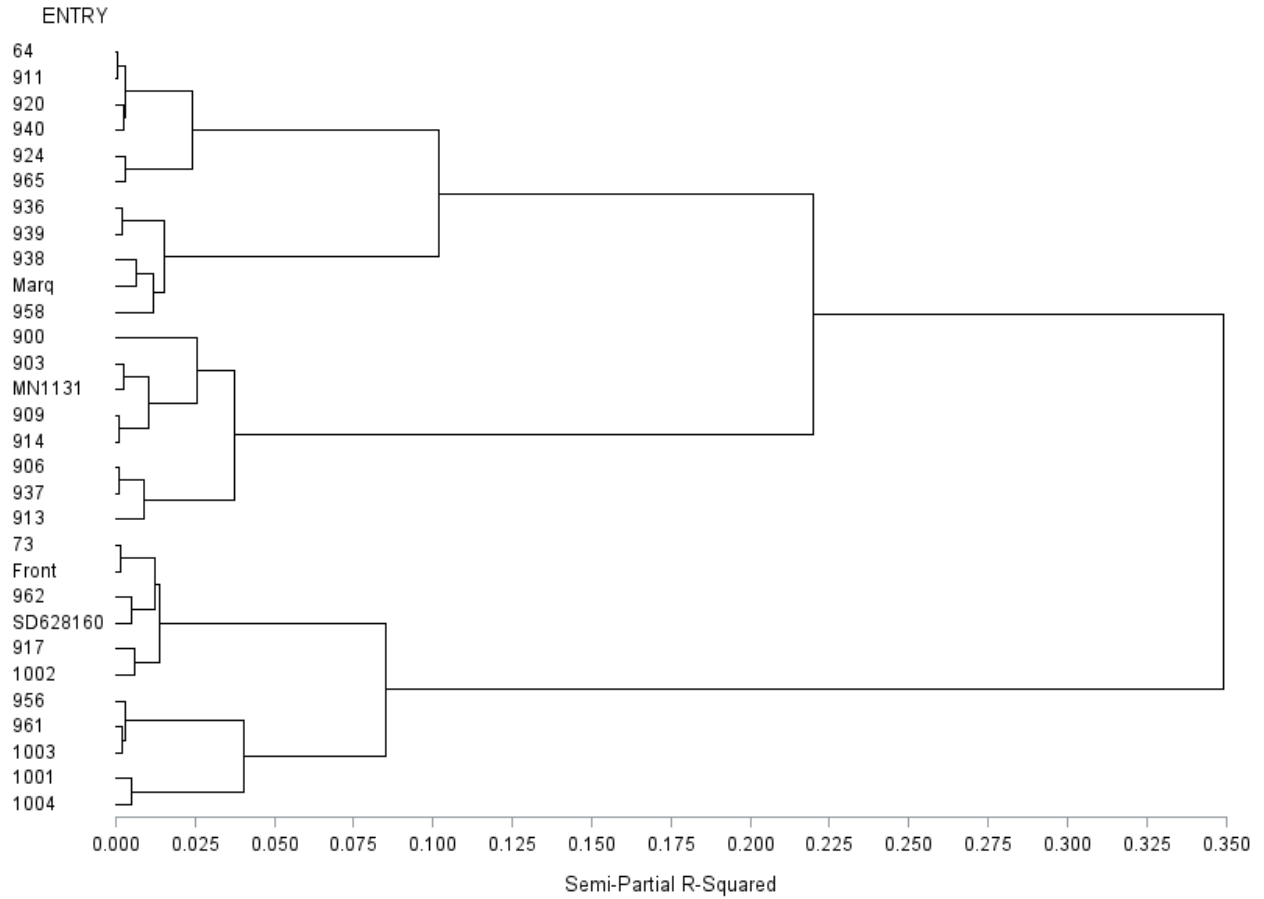


Figure 6. Cluster of Euclidean distances between genotypic means for the three retained axes of the mode-rotated Tucker solution using Ward's minimum variance method of linkage. Marq = 'Marquette' and Front = 'Frontenac'.

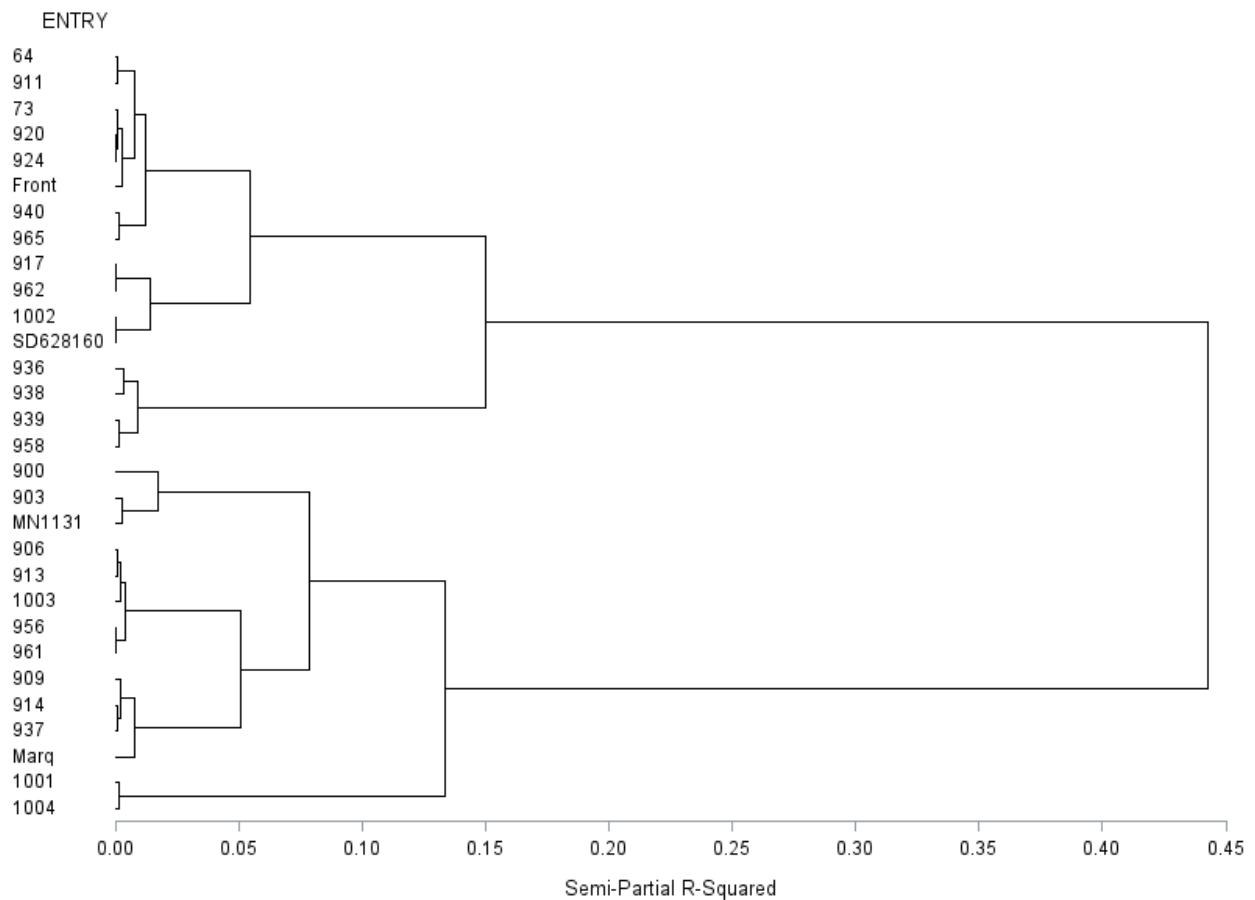


Figure 7. Cluster of Euclidean distances between genotypic means for the two axes having significant genotypic variation from the mode-rotated Tucker solution using Ward's minimum variance method of linkage. Marq = 'Marquette' and Front = 'Frontenac'.

Rotation to maximum core variance.

When the resulting core-array was rotated to maximize its variance, the relationship among mode axes was simplified and three primary combinations of axes were identified to contribute the majority of variation to the dataset (Table 18). The first axis relating to genotype samples was highly related to axis 2 of measures along axis 1 of photoperiodic time. The second genotypic axis was highly associated with axis 1 of measures along axis 1 of photoperiodic time. The final genotypic axis was most highly associated with axis 2 of measures along axis 2 of photoperiodic time.

Table 18. Core-rotated Tucker core-array of relationships among genotype, measure, and photoperiod axes.

Photoperiod	Genotypes	----- Measure -----			
		Axis 1	Axis 2	Axis 1	Axis 2
<i>Axis 1</i>		----- Weight -----		----- Sq. weight -----	
	Axis 1	0.28	<b>8.77</b>	0.08	<b>76.92</b>
	Axis 2	<b>9.39</b>	0.34	<b>88.14</b>	0.11
	Axis 3	0.33	-0.32	0.11	0.10
<i>Axis 2</i>					
	Axis 1	0.61	1.29	0.37	1.67
	Axis 2	-0.98	-1.74	0.95	3.02
	Axis 3	-0.49	<b>-5.59</b>	0.24	<b>31.30</b>

Bolded combinations contributed greatest to the variation of the dataset.

Measures.

Following the core-rotation similar axes were identified for measures as found in the non-rotated Tucker solution. Axis 1 was strongly associated with tip abscission with a moderate negative association with periderm development (Table 19). Axis 2 was positively associated with measures related to active growth, while it was negatively associated with measures of tissue maturation and progress toward an acclimated state.

Table 19. Core-rotated Tucker loadings for measured variables.

Measure	Axis 1	Axis 2
Stem Length (cm)	-0.020	<b>0.344</b>
Nodes (count)	-0.149	<b>0.435</b>
Mature Buds (count)	-0.153	-0.312
Lateral Shoots (count)	0.164	<b>0.520</b>
Tip Abscission (0-5 scale)	<b>0.835</b>	<b>-0.338</b>
Periderm (cm)	<b>-0.360</b>	<b>-0.349</b>
Periderm (node count)	<b>-0.317</b>	-0.300
Portion of total variation (%)	31.88	40.12

Bolded values indicate local minimums and maximums for each axis.

Photoperiods.

Similar photoperiodic time axes were identified as found with the initial Tucker decomposition. The first axis was related to a linear trend through time (Table 20). The axis was most strongly associated with 10.5h of daylight and was most negatively associated with 14.5h of daylight. The axis showed a general progression from negative association to positive association through photoperiodic time centering at 12.5h of daylight where little correlation existed with the axis. The second axis was again interpreted as a parabolic distortion from this linear trend through time. The axis again had a large positive association where axis 1 was uncorrelated (12.5h of daylight) with gradual trends toward negative associations at either extreme (15.0 and 10.0h of daylight).

Table 20. Core-rotated Tucker loadings for photoperiodic times.

Photoperiodic time (hours of daylight)	Axis 1	Axis 2
15.0	-0.374	<b>-0.394</b>
14.5	<b>-0.380</b>	-0.258
14.0	-0.339	-0.054
13.5	-0.288	0.146
13.0	-0.177	0.404
12.5	0.033	<b>0.446</b>
12.0	0.189	0.388
11.5	0.289	0.087
11.0	0.357	-0.100
10.5	<b>0.362</b>	-0.286
10.0	0.329	<b>-0.378</b>
Portion of total variation (%)	58.68	13.32

Bolded values indicate local minimums and maximums for each axis.

Variable weights.

When variable weights were evaluated visually the axes retained similar relationships with the tested variables as determined with other models. The first axis related to the relative amounts of active growth and tissue maturation early (prior to 12.5h of daylight) versus late (after 12.5h of daylight) in the season across tested temperatures (Table A20). The second axis related to the relative progress in tip abscission and contrasted early and late photoperiods across temperatures (Table A21). Lastly, the third axis was parabolic through time centering between at 12.5h of daylight contrasting the amount of active growth with the amount of mature tissue development and tip abscission progression across the tested temperatures (Table A22). The axis also contrasted differences in tip progress across the two tested temperatures between 13.0h of daylight and 10.0h of daylight.

Genotypes.

Following the rotation of the core to maximal variance the three axes relating to the genotypes explained 28.03%, 32.71%, and 11.26% of the variation of the dataset, respectively. When genotypes were tested using ANOVA with runs of the experiment as replications, genotype axes 2 and 3 were found to significantly vary across genotypes (Table 21).

Table 21. Effect of accessions for the retained axes scores following core-rotation.

Axis	F Value	Pr > F
1	1.77	0.0653
2	2.47	0.0089 **
3	2.03	0.0305 *

\* and \*\* signify significance at  $\alpha=0.05$  and 0.01, respectively.

When the means of genotypes, families, and species were compared to the mean of *V. riparia*, significant differences occurred along both axes (Table 22). The mean of *V. riparia* was moderately, negative along axis 2. Those genotypes showing the greatest negative values along

Table 22. Core-rotated Tucker mean genotype scores.

Entry	Axis 1	Axis 2	Axis 3
64	0.003	-0.024	0.146 **
<b>73</b>	<b>-0.096</b>	<b>-0.131</b>	<b>-0.051</b>
900	0.172	0.181 **	-0.087
903	0.034	0.165 **	-0.004
906	0.090	0.073	0.118 **
909	-0.008	0.123 *	0.056 *
911	0.008	-0.051	0.152 ***
913	0.082	0.041	0.040 *
914	0.032	0.120 *	0.056 *
<b>917</b>	<b>0.039</b>	<b>-0.158</b>	<b>0.003</b>
920	-0.014	-0.087	0.129 **
924	-0.049	-0.095	0.035 *
936	-0.123	0.010	0.074 *
937	0.073	0.110 *	0.139 **
<b>938</b>	<b>-0.098</b>	<b>0.011</b>	<b>-0.026</b>
939	-0.132	0.068	0.080 *
940	-0.062	-0.042	0.139 **
<b>Frontenac</b>	<b>-0.053</b>	<b>-0.153</b>	<b>-0.036</b>
MN 1131	0.095	0.198 **	0.002
Marquette	-0.093	0.114 *	-0.007
S1 Valiant	-0.047	-0.078	0.047 **
S1 MN 1131	0.099	0.140 ***	0.009 **
S1 St. Croix	0.028	0.058 *	0.076 ****
S1 ES 8-2-24	-0.008	-0.113	0.055 ***
S1 ES 8-2-43	-0.068	0.031	0.081 ****
Checks	-0.017	0.053 *	-0.014 *
All S1s	-0.003	0.019	0.059 ****
All	-0.014	0.010	0.027 ****
<i>V. californica</i>	-0.049	-0.046	-0.056
<i>V. riparia</i>	0.069	-0.049	-0.135

\*, \*\*, \*\*\*, and \*\*\*\* signify that the value is significantly different from that of the mean of *V. riparia* within the associated component at alpha = 0.05, 0.01, 0.001, and 0.0001, respectively. Bolded individuals have mean values not significantly different than the mean of *V. riparia* for all significant components showing variation for genotypes.

the axis included '917', 'Frontenac', and '73'. Those vines having the greatest positive association with the axis included 'MN 1131' and its progeny '900' and '903'. All genotypes that significantly differed from the mean of the tested *V. riparia* were positive along the axis. Members of the 'ES 8-2-24' and 'Valiant' families did not differ from *V. riparia* along the axis while members of all other families, including '900', '903', '909', '914', and '937', did. In addition, both 'MN 1131' and 'Marquette' significantly differed from the tested *V. riparia*, whereas 'Frontenac' was the only tested check which did not.

*V. riparia* tended to be strongly negative along genotype axis 3, which related to the parabolic trend through time of the relationship to between active growth and measure of tissue maturation. All vines that significantly differed from the mean of these wild vines tended to have positive values along the axis. Those genotypes having the strongest positive values included '909', '64', '936', and '940'. Those having the most negative values along the axis included '900', members of the *V. californica* family, '73', '938', and 'Frontenac'. In addition, genotypes 'MN 1131', 'Marquette', '903', and '917' were not found to significantly differ from the mean of tested *V. riparia*. Overall, only three individuals ('73', '917', and 'Frontenac') were found to not significantly differ from the average of tested *V. riparia* for both retained axes having significant variation across the genotypes.

When means of the included thirty entries were clustered using Euclidean distances and Ward's minimum variance method linkage using all three retained axes, distinct *V. riparia* and non-*V. riparia* groups were defined (Fig. 8). The *V. riparia* group contained all five tested *V. riparia* vines. In addition, four of the five *V. californica* entries, 'Frontenac' '924', '917', and '73' were contained within the group. The non-*V. riparia* group was subdivided into 'MN1131' and

‘Marquette’ like genotypes. ‘MN 1131’ grouped with all three of its progeny, three of the four progeny of ‘St. Croix’, and ‘937’. All remaining genotypes grouped with ‘Marquette’.

When only those axes containing significant variation were used to cluster the genotypes, differences between *V. riparia* and non-*V. riparia* genotypes remained well defined. All *V. riparia* entries cluster together along with four of the five *V. californica* genotypes, ‘Frontenac’, ‘938’, ‘917’, and ‘73’ (Fig. 9). The opposing group related to accessions more similar to ‘MN 1131’ and Marquette’. ‘MN 1131’ and ‘Marquette’ grouped tightly together along with ‘914’, ‘909’, ‘900’, and ‘903’.

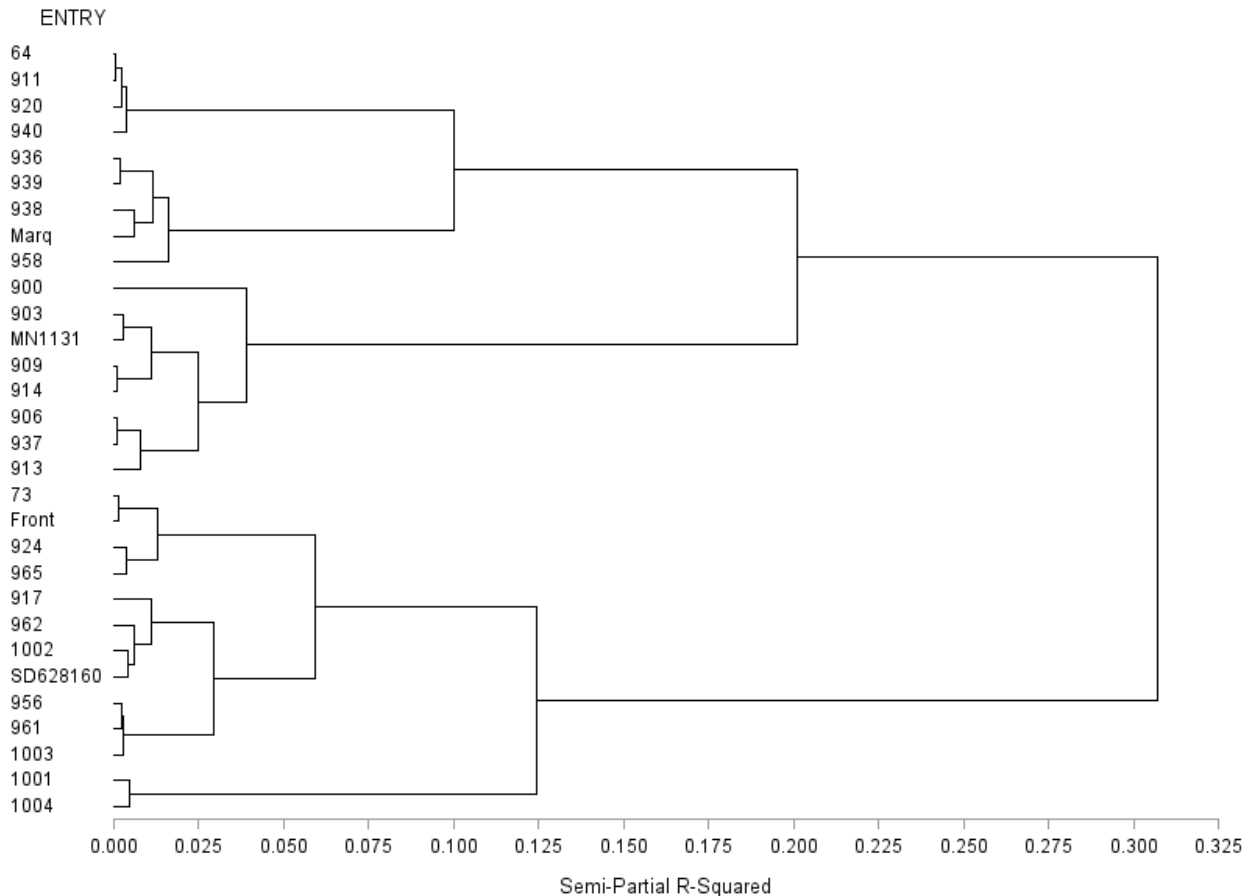


Figure 8. Cluster of Euclidean distances between genotypic means for the three retained axes of the core-rotated Tucker solution using Ward’s minimum variance method of linkage. Marq = ‘Marquette’ and Front = ‘Frontenac’.



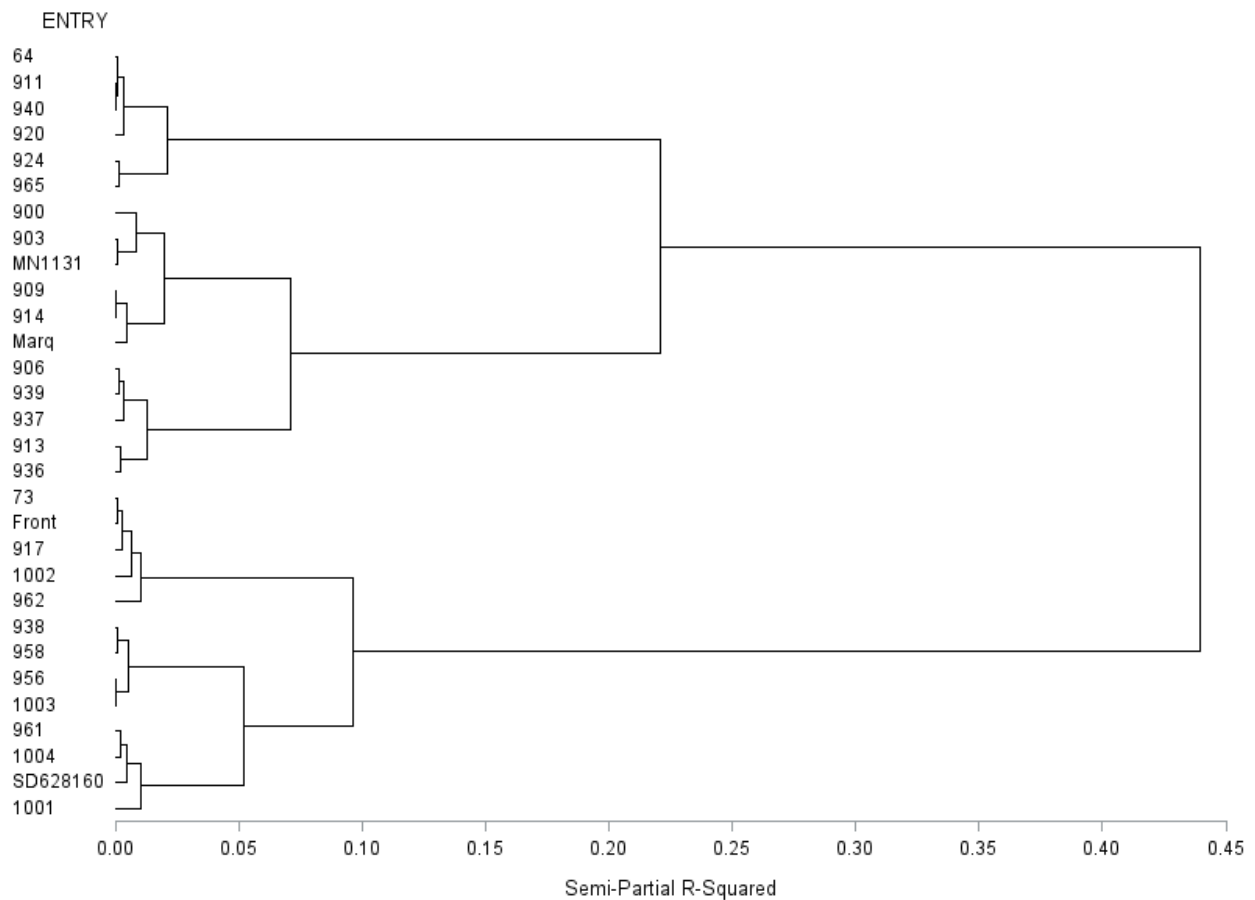


Figure 9. Cluster of Euclidean distances between genotypic means for the two axes having significant genotypic variation from the core-rotated Tucker solution using Ward's minimum variance method of linkage. Marq = 'Marquette' and Front = 'Frontenac'.

*Multidimensional scaling.*

Non-metric multidimensional scaling.

Non-metric multidimensional scaling was applied to the data as a best representative of pairwise distance conservation as well as best representation for distortion reduction in the presence of non-linear data. When the resulting scores along the estimated three dimensions were tested for genotypic effects using the two runs of the experiment as replications, the first two obtained axes contained significant variation among genotypes (Table 23).

When the calculated mean scores were compared to the mean value of tested *V. riparia*, both axes showed departures by tested genotypes. The first axis was negatively associated with the average of *V. riparia*. Accessions being particularly negative in value along the axis included ‘Frontenac’, ‘917’, and ‘73’. Genotypes ‘MN 1131’, ‘903’, and ‘900’ and ‘914’ tended to have high positive values along the axis. All individuals having significantly different value from the average of tested *V. riparia* (9) had positive values along the axis. This group included the check vines ‘MN 1131’ as well as ‘Marquette’.

Table 23. Effect of accessions for the retained axes scores following NMS.

Axis	F Value	Pr > F
1	2.35	0.0121 *
2	2.15	0.0217 *
3	1.75	0.0686

\* signifies significance at  $\alpha=0.05$

The mean of *V. riparia* was also negative in value along the second axis. Individual genotypes having means strongly negative along the axis included ‘900’, ‘MN1131’ and ‘913’. Individual genotypes being strongly positively associated with the axis included ‘936’, ‘939’, and ‘73’. All accessions statistically differing from the mean of *V. riparia* (6) had positive values along the axis and included the check vine ‘Marquette’.

Overall, many of the vines tested did not statistically differ from *V. riparia* across both identified axes containing significant variation across cultivars. These accessions included ‘64’, ‘911’, 913, all three progeny of ‘ES 8-2-24’ (‘917’, ‘920’, and ‘924’), as well as ‘Frontenac’. Few accessions departed from *V. riparia* for both axes and included ‘939’ and ‘Marquette’.

When genotype mean axis scores from the three retained axes were used to cluster the investigated genotypes, two clusters relating to *V. riparia*-like and non-*V. riparia*-like groups were

Table 24. NMS mean genotype scores.

Entry	Axis 1	Axis 2	Axis 3
<b>64</b>	<b>0.068</b>	<b>0.334</b>	-0.843
73	-1.176	0.755 *	0.202
900	1.365 **	-1.718	0.517
903	1.522 **	-0.398	0.459
906	0.771 *	-0.504	-0.553
909	1.296 **	0.186	-0.371
<b>911</b>	<b>-0.197</b>	<b>0.237</b>	-0.813
<b>913</b>	<b>0.468</b>	<b>-0.762</b>	-0.265
914	1.310 **	-0.372	-0.423
<b>917</b>	<b>-1.314</b>	<b>-0.150</b>	-0.258
<b>920</b>	<b>-0.525</b>	<b>0.434</b>	-0.625
<b>924</b>	<b>-0.683</b>	<b>0.553</b>	-0.248
936	0.197	1.102 **	-0.240
937	1.235 **	-0.306	-0.648
938	0.042	0.670 *	0.150
939	0.709 *	1.178 **	-0.163
940	-0.063	0.688 *	-0.627
<b>Frontenac</b>	<b>-1.369</b>	<b>0.515</b>	0.035
MN 1131	1.651 **	-0.890	0.171
Marquette	0.862 *	0.647 *	0.236
S1 Valiant	-0.554	0.545 *	-0.321
S1 MN 1131	1.219 ****	-0.873	0.141
S1 St. Croix	0.719 **	-0.178	-0.468
S1 ES 8-2-24	-0.841	0.279 *	-0.377
S1 ES 8-2-43	0.424 **	0.666 ***	-0.306
Checks	0.381 *	0.091	0.148
All S1s	0.296 **	0.113 **	-0.279
All	0.145 **	0.147 **	-0.100
<i>V. californica</i>	-0.507	0.295 **	0.362
<i>V. riparia</i>	-0.727	-0.735	0.500

\*, \*\*, \*\*\*, and \*\*\*\* signify that the value is significantly different from that of the mean of *V. riparia* within the associated component at alpha = 0.05, 0.01, 0.001, and 0.0001, respectively. Bolded individuals have mean values not significantly different than the mean of *V. riparia* for all significant components showing variation for genotypes.

identified (Fig. 10). ‘MN 1131’ clustered with four of the five *V. riparia* and three of the five included *V. californica* along with two of its progeny (‘900’ and ‘903’) as a sub-class in the *V. riparia*-like group. All other entries, including the *V. riparia* ‘1002’, clustered separately.

When only the two axes showing significant variation among cultivars were clustered *V. riparia* were split among the two broadest groups (Fig. 11). ‘1001’ and ‘1004’ clustered along with ‘MN 1131’, while ‘SD 62-8-160’, ‘1002’ and ‘1003’ clustered along with ‘Frontenac’ and ‘Marquette’.

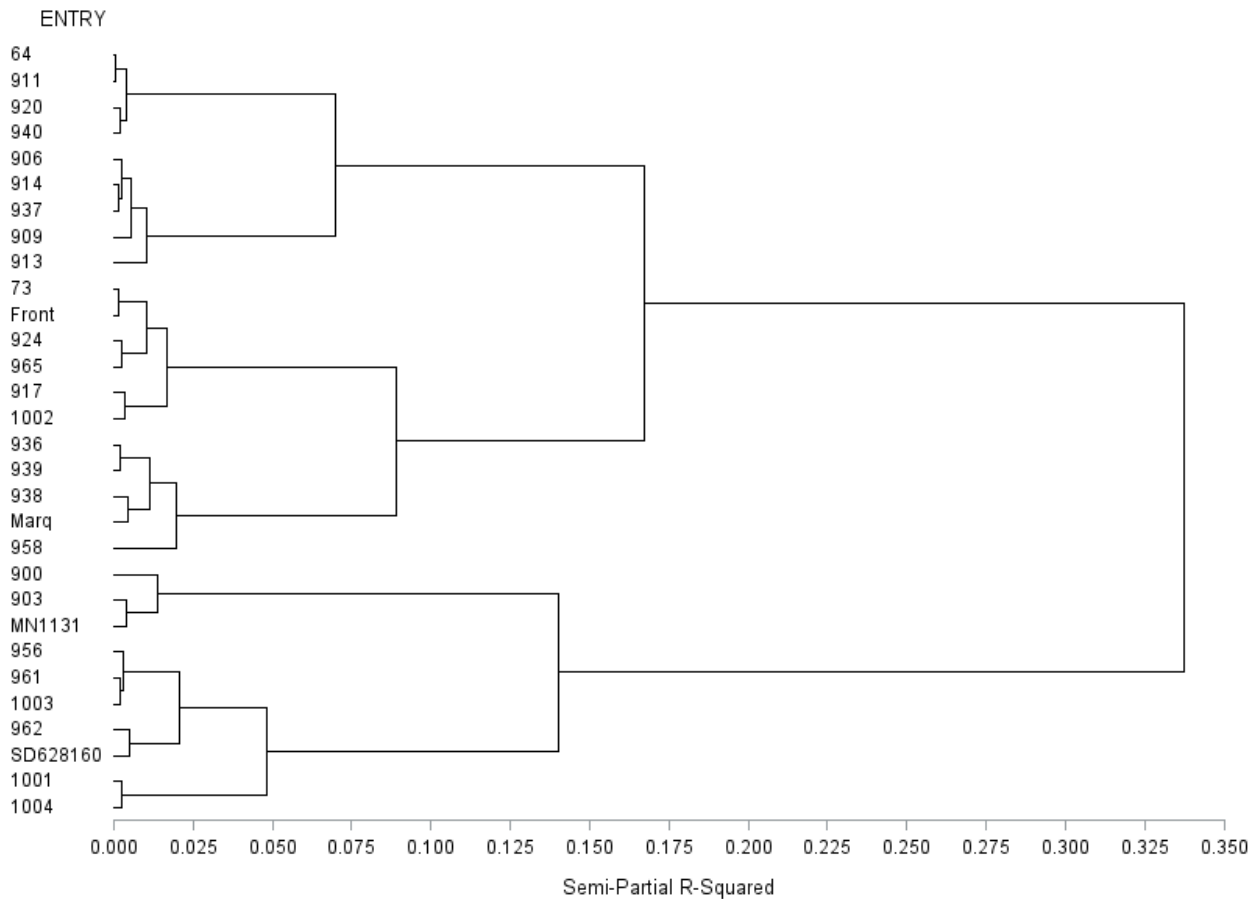


Figure 10. Cluster of Euclidean distances between genotypic means for the three retained axes of the NMS solution using Ward’s minimum variance method of linkage. Marq = ‘Marquette’ and Front = ‘Frontenac’.

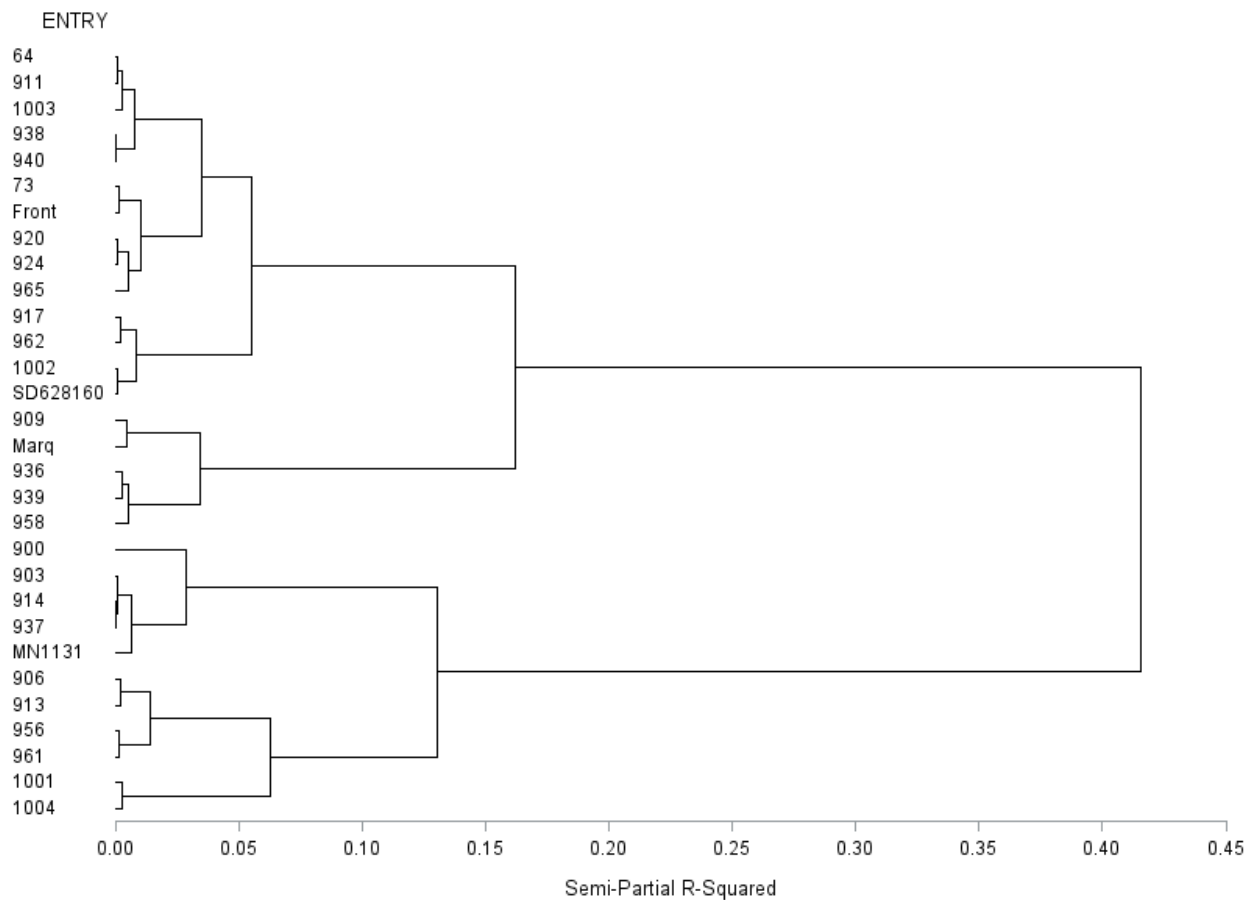


Figure 11. Cluster of Euclidean distances between genotypic means for the two axes having significant genotypic variation from the NMS solution using Ward's minimum variance method of linkage. Marq = 'Marquette' and Front = 'Frontenac'.

Metric multidimensional scaling.

When metric-MDS was used with Euclidean distances between data points the resulting scores along the estimated three dimensions were tested for genotypic effects using the two runs of the experiment. The first two obtained axes contained significant variation among genotypes (Table 25).

When the calculated mean scores were compared to the mean value of tested *V. riparia*, significant differences were found along both axes. The first axis was negatively associated with the average of *V. riparia*. Accessions that were particularly negative in value along the axis

included ‘Frontenac’, ‘917’, ‘73’, and ‘924’. Genotypes ‘MN 1131’, ‘903’, and ‘900’, ‘909’, and ‘914’ tended to be highly positively associated with the axis. All nine individuals having significantly different values from the average of tested *V. riparia*, including ‘MN 1131’ and ‘Marquette’, were positive in value.

Table 25. Effect of accessions for the retained axes scores following metric-MDS.

Axis	F Value	Pr > F
1	2.53	0.0074 **
2	2.31	0.0137 *
3	1.75	0.0698

\* and \*\* signify significance at  $\alpha=0.05$  and 0.01, respectively.

The mean of *V. riparia* was also negative in value along the second axis. Individual genotypes having strong negative means along the axis included ‘900’, ‘MN1131’ and ‘913’. Individual genotypes that had a strong positive association with the axis included ‘936’, ‘939’, and ‘73’. All seven individuals that statistically differed from the mean of *V. riparia* had positive values along the axis, including the check vine ‘Marquette’. Overall, six of the genotypes tested (‘64’, ‘911’, ‘913’, ‘917’, ‘920’, as well as ‘Frontenac’) did not statistically differ from *V. riparia* across both identified axes containing significant variation among genotypes. Only two accessions, ‘939’ and ‘Marquette’ departed from *V. riparia* for both axes.

When genotype mean axis scores from the three retained axes were used to cluster the investigated genotypes, two clusters relating to ‘MN 1131’ and non-‘MN 1131’ types were identified. ‘MN 1131’ clustered with three of the five *V. riparia* and two of the five included *V. californica*. ‘MN 1131’ tightly clustered with two of its progeny (‘900’ and ‘903’), while also clustering with members of the ‘St. Croix’ family (‘909’, 913, and ‘914’), ‘937’ and ‘906’. All other entries, including the *V. riparia* ‘1002’ and ‘SD 62-8-160’ and the check vines ‘Frontenac’

Table 26. Metric-MDS mean genotype scores.

Entry	Axis 1	Axis 2	Axis 3
<b>64</b>	<b>0.081</b>	<b>0.483</b>	-1.290
73	-1.487	0.900 *	0.349
900	1.632 **	-2.058	0.682
903	1.850 **	-0.515	0.649
906	0.970 *	-0.589	-0.716
909	1.613 **	0.233	-0.581
<b>911</b>	<b>-0.262</b>	<b>0.316</b>	-1.092
<b>913</b>	<b>0.668</b>	<b>-1.011</b>	-0.277
914	1.578 **	-0.413	-0.474
<b>917</b>	<b>-1.672</b>	<b>-0.221</b>	-0.364
<b>920</b>	<b>-0.624</b>	<b>0.500</b>	-1.011
924	-0.902	0.685 *	-0.385
936	0.285	1.396 **	-0.416
937	1.437 **	-0.379	-0.875
938	0.094	0.889 *	0.302
939	0.938 *	1.449 **	-0.233
940	-0.089	0.909 *	-0.769
<b>Frontenac</b>	<b>-1.685</b>	<b>0.565</b>	0.100
MN 1131	1.904 **	-1.079	0.218
Marquette	1.105 *	0.755 *	0.341
S1 Valiant	-0.703	0.692 **	-0.470
S1 MN 1131	1.484 ****	-1.054	0.205
S1 St. Croix	0.899 **	-0.219	-0.606
S1 ES 8-2-24	-1.066	0.321 *	-0.587
S1 ES 8-2-43	0.533 **	0.853 ***	-0.398
Checks	0.441 *	0.080	0.220
All S1s	0.360 **	0.151 **	-0.382
All	0.173 **	0.181 **	-0.134
<i>V. californica</i>	-0.621	0.341 **	0.498
<i>V. riparia</i>	-0.866	-0.904	0.670

\*, \*\*, \*\*\*, and \*\*\*\* signify that the value is significantly different from that of the mean of *V. riparia* within the associated component at alpha = 0.05, 0.01, 0.001, and 0.0001, respectively. Bolded individuals have mean values not significantly different than the mean of *V. riparia* for all significant components showing variation for genotypes.

and ‘Marquette’, clustered in the alternate group. Within this second group, ‘Frontenac’ tended to cluster with the remaining *V. riparia*, *V. californica*, the ‘ES 8-2-24’ progeny ‘917’ and ‘924’, as well as ‘73’. ‘Marquette’ tended to cluster tightest with descendants of the ‘ES 8-2-43’.

When only the two axes containing significant variation among genotypes were used, three groups were identified (Fig. 13). An out-group relating to ‘MN 1131’ like vines was identified. This group included ‘MN 1131’, its three progeny, as well as ‘913’, ‘914’, and ‘937’. The remaining accessions were split into *V. riparia*-like vines and non-*V. riparia*-like vines. The *V. riparia*-like vines contained all five *V. riparia* types, three of the five tested *V. californica*, as well as ‘917’. The final group contained vines more similar to ‘Marquette’ or ‘Frontenac’. The subgroup relating to ‘Marquette’ additionally included ‘958’, ‘939’, ‘936’, and ‘909’, while all additional genotypes were more similar to ‘Frontenac’.



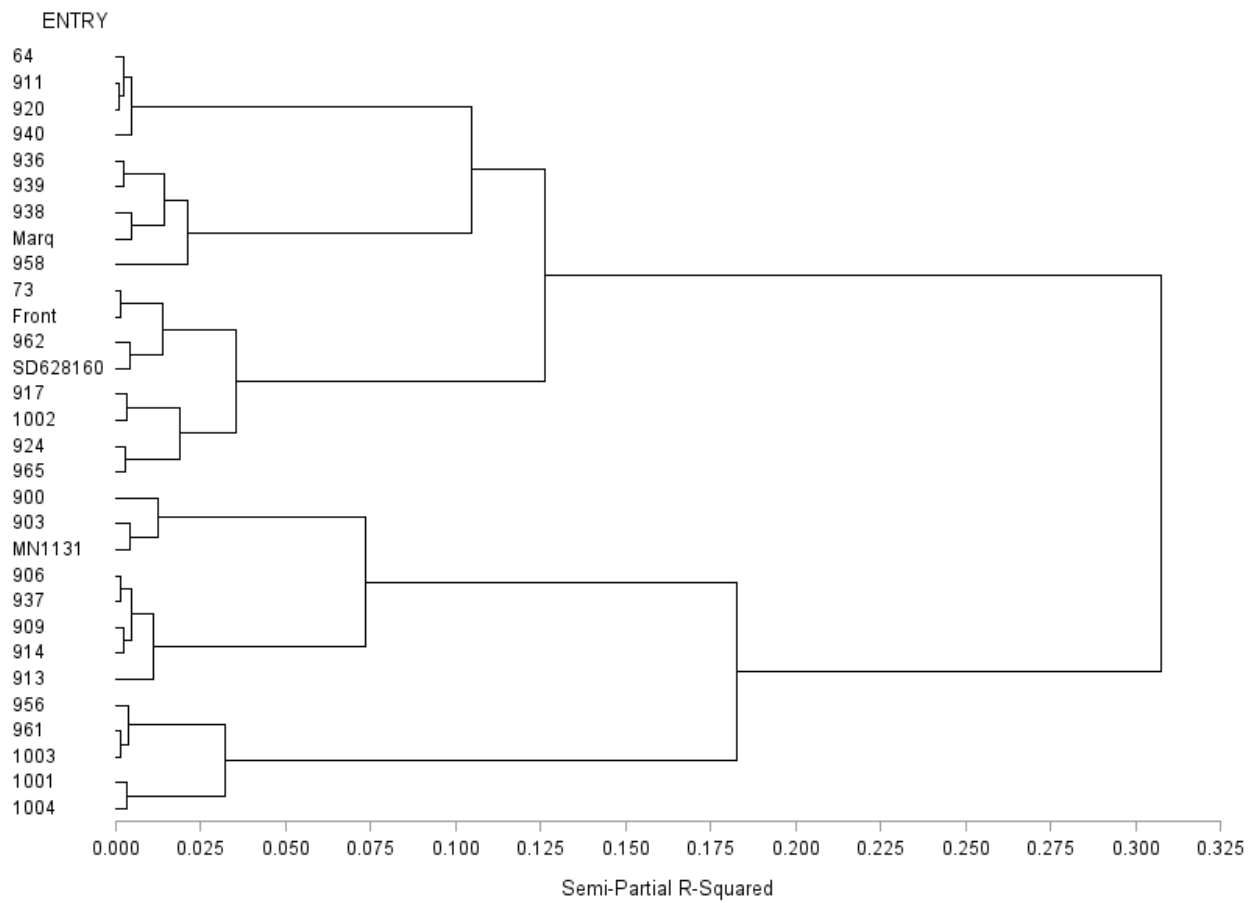


Figure 12. Cluster of Euclidean distances between genotypic means for the three retained axes of the metric-MDS solution using Ward's minimum variance method of linkage. Marq = 'Marquette' and Front = 'Frontenac'.

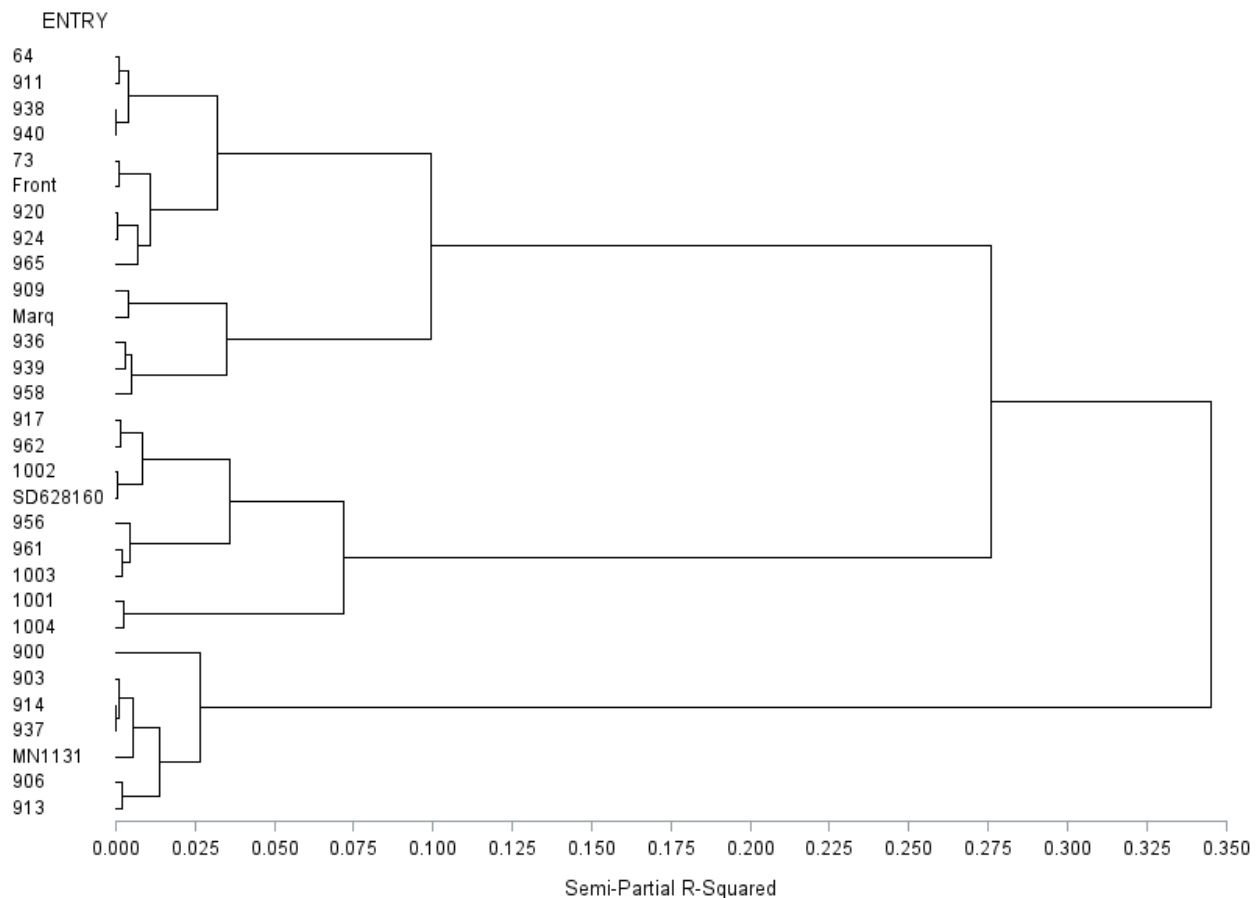


Figure 13. Cluster of Euclidean distances between genotypic means for the two axes having significant genotypic variation from the metric-MDS solution using Ward's minimum variance method of linkage. Marq = 'Marquette' and Front = 'Frontenac'.

*Comparison of model relationships.*

When resampling of the samples with replacement was used to test the consistency of the predictions, the sum of squared deviations from observed values was significantly higher and sum of squared deviations from the full model solution using all samples was lower for the Tucker model when compared to SVD (Table 27).

Sample scores of non-rotated SVD, non-rotated Tucker, core-rotated Tucker, metric-MDS as well as NMS tended to be highly correlated and had no significant cross-axis correlation (Table 28). The rotated SVD and mode-rotated Tucker models also tended to be highly correlated, again

having no significant cross-axis correlation among their axes. While the scores were consistent across all non-rotated models, the derived weights of the predictor variables differed among most tested models. The non-rotated version of SVD as well as the initial Tucker model were the only two models which did not show significant cross-axis correlation, and correlated well with one another for all three axes (Table 29). The mode-rotated version of the Tucker solution showed the greatest amount of cross-axis correlation within any given solution.

Both SVD and Tucker deconstruction of the variable scaled four-way interaction lead to similar solutions. Scores correlated well across the three axes as well as variable weights. While initial solutions were similar, rotation to simple structure in either model caused differences in interpretation. Intuitively, the rotation of the highly correlated genotype scores of the two models yielded highly correlated scores among their rotated solutions; however, the rotation of the combination mode loadings and the independent rotation of the trait and photoperiod loading matrices of the Tucker model yielded differing results. The rotation of the SVD loadings resulted in the creation of significant correlation among axes 1 and 3 of the SVD solution. The mode or core-rotation of the Tucker solution introduced significant negative correlation between axis 1 and 2, while caused positive correlation between axes 3 and 1.

Table 27. Estimated sum of squared deviations<sup>x</sup> from observed and predicted values.

	Observed values	Full model prediction <sup>y</sup>
	SSD <sup>z</sup>	SSD
Tucker Decomposition	13.876 ± 0.046	0.11679 ± 0.00187
SVD	13.687 ± 0.045	0.28998 ± 0.00324

<sup>x</sup>Estimated using 10,000 iterations of resampling with replacement (50 train: 10 test).

<sup>y</sup>Predicted values through decompositions using all observed samples

<sup>z</sup>Averages sum of squared deviations (SSD) ± 95% confidence interval.

Table 28. Correlation among derived genotype sample scores from the three axes of each of the seven solutions.

Model	Axis	---- SVD ----			---- Rot ----			---- TD ----			---- Mode ----			---- Core ----			---- MDS ----			---- NMS ----			
		1	2	3	1	2	3	1	2	3	1	2	3	1	2	3	1	2	3	1	2	3	
SVD	1	<b>1.0</b>	0.0	0.0																			
	2	0.0	<b>1.0</b>	0.0																			
	3	0.0	0.0	<b>1.0</b>																			
Rot	1	<b>1.0</b>	0.0	<b>-0.3</b>	<b>1.0</b>	0.0	0.0																
	2	0.0	<b>1.0</b>	0.1	0.0	<b>1.0</b>	0.0																
	3	<b>0.3</b>	-0.1	<b>1.0</b>	0.0	0.0	<b>1.0</b>																
TD	1	<b>1.0</b>	0.0	0.0	<b>1.0</b>	0.0	<b>0.3</b>	<b>1.0</b>	0.0	0.0													
	2	0.0	<b>1.0</b>	0.0	0.0	<b>1.0</b>	-0.1	0.0	<b>1.0</b>	0.0													
	3	0.0	0.0	<b>-1.0</b>	<b>0.3</b>	-0.1	<b>-0.9</b>	0.0	0.0	<b>1.0</b>													
Mode	1	<b>0.9</b>	0.1	<b>-0.3</b>	<b>1.0</b>	0.1	-0.1	<b>0.9</b>	0.1	<b>0.3</b>	<b>1.0</b>	0.0	0.0										
	2	0.0	<b>1.0</b>	0.2	-0.1	<b>1.0</b>	0.1	-0.1	<b>1.0</b>	-0.2	0.0	<b>1.0</b>	0.0										
	3	<b>-0.3</b>	0.2	<b>-0.9</b>	-0.1	0.1	<b>-1.0</b>	<b>-0.3</b>	0.2	<b>0.9</b>	0.0	0.0	<b>1.0</b>										
Core	1	0.0	<b>1.0</b>	-0.2	0.1	<b>0.9</b>	<b>-0.3</b>	0.0	<b>1.0</b>	0.2	0.1	<b>0.9</b>	<b>0.4</b>	<b>1.0</b>	0.0	0.0							
	2	<b>-1.0</b>	0.0	0.2	<b>-1.0</b>	0.0	-0.1	<b>-1.0</b>	0.0	-0.2	<b>-1.0</b>	0.1	0.2	0.0	<b>1.0</b>	0.0							
	3	-0.2	-0.2	<b>-0.9</b>	0.1	<b>-0.3</b>	<b>-0.9</b>	-0.2	-0.2	<b>1.0</b>	0.1	-0.4	<b>0.9</b>	0.0	0.0	<b>1.0</b>							
MDS	1	<b>-1.0</b>	0.0	0.0	<b>-1.0</b>	-0.1	<b>-0.3</b>	<b>-1.0</b>	-0.1	0.0	<b>-0.9</b>	0.0	<b>0.3</b>	0.0	<b>1.0</b>	0.2	<b>1.0</b>	0.0	0.0				
	2	0.0	<b>-1.0</b>	0.0	0.0	<b>-1.0</b>	0.1	0.1	<b>-1.0</b>	0.0	-0.1	<b>-1.0</b>	-0.2	<b>-1.0</b>	-0.1	0.2	0.0	<b>1.0</b>	0.0				
	3	0.0	0.0	<b>1.0</b>	<b>-0.3</b>	0.1	<b>0.9</b>	0.0	0.0	<b>-1.0</b>	<b>-0.3</b>	0.2	<b>-0.9</b>	-0.2	0.2	<b>-0.9</b>	0.0	0.0	<b>1.0</b>				
NMS	1	<b>-1.0</b>	0.0	0.0	<b>-1.0</b>	-0.1	<b>-0.3</b>	<b>-1.0</b>	-0.1	0.0	<b>-0.9</b>	0.0	<b>0.3</b>	0.0	<b>1.0</b>	0.2	<b>1.0</b>	0.0	0.0	<b>1.0</b>	0.0	0.0	
	2	0.0	<b>-1.0</b>	0.0	0.0	<b>-1.0</b>	0.1	0.1	<b>-1.0</b>	0.0	0.0	<b>-1.0</b>	-0.2	<b>-1.0</b>	-0.1	0.2	0.0	<b>1.0</b>	0.0	0.0	<b>1.0</b>	0.0	
	3	0.0	0.0	<b>1.0</b>	<b>-0.3</b>	0.1	<b>0.9</b>	0.0	0.0	<b>-1.0</b>	<b>-0.3</b>	0.2	<b>-0.9</b>	-0.2	0.2	<b>-0.9</b>	0.0	0.0	<b>1.0</b>	0.0	0.0	<b>1.0</b>	

SVD, Single Value Decomposition; Rot, Rotated SVD; TD, Tucker decomposition; Mode, Mode-rotation of Tucker4; Core, Core-rotation of the Tucker4; MDS, Metric Multidimensional Scaling; NMS, Non-Metric Multidimensional Scaling.

Bolded values indicate significance at  $\alpha = 0.05$

Shading indicates model combinations where no off diagonal correlation was found among the three retained axes across models

Table 29. Correlations among derived weights (W) such that  $X*W$  equates to the genotype sample scores of the model.

		----- SVD -----			----- Rot -----			----- TD -----			----- Mode -----			----- Core -----		
		1	2	3	1	2	3	1	2	3	1	2	3	1	2	3
SVD	1	<b>1.0</b>	0.0	0.0												
	2	0.0	<b>1.0</b>	0.0												
	3	0.0	0.0	<b>1.0</b>												
Rot	1	<b>0.9</b>	0.0	<b>-0.4</b>	<b>1.0</b>	-0.1	<b>-0.3</b>									
	2	0.0	<b>1.0</b>	<b>0.2</b>	-0.1	<b>1.0</b>	0.1									
	3	0.2	-0.1	<b>1.0</b>	<b>-0.3</b>	0.1	<b>1.0</b>									
TD	1	<b>1.0</b>	0.0	0.0	<b>0.9</b>	0.0	0.2	<b>1.0</b>	0.0	0.0						
	2	0.0	<b>1.0</b>	0.0	0.0	<b>1.0</b>	-0.1	0.0	<b>1.0</b>	0.0						
	3	0.0	0.0	<b>-0.9</b>	<b>0.4</b>	<b>-0.2</b>	<b>-0.9</b>	0.0	0.0	<b>1.0</b>						
Mode	1	<b>0.8</b>	0.1	<b>-0.5</b>	<b>1.0</b>	0.0	<b>-0.4</b>	<b>0.8</b>	0.1	<b>0.5</b>	<b>1.0</b>	-0.1	<b>0.4</b>			
	2	0.0	<b>0.9</b>	<b>0.3</b>	-0.2	<b>1.0</b>	<b>0.2</b>	-0.1	<b>0.9</b>	<b>-0.4</b>	-0.1	<b>1.0</b>	<b>-0.2</b>			
	3	<b>-0.2</b>	0.1	<b>-0.9</b>	<b>0.2</b>	-0.1	<b>-0.9</b>	<b>-0.2</b>	0.1	1.0	<b>0.4</b>	<b>-0.2</b>	<b>1.0</b>			
Core	1	0.0	<b>0.9</b>	<b>-0.3</b>	0.1	<b>0.8</b>	<b>-0.4</b>	0.0	<b>0.9</b>	<b>0.3</b>	<b>0.3</b>	<b>0.8</b>	<b>0.4</b>	<b>1.0</b>	-0.1	<b>0.2</b>
	2	<b>-0.9</b>	0.0	<b>0.3</b>	<b>-1.0</b>	0.1	<b>0.2</b>	<b>-0.9</b>	0.0	<b>-0.4</b>	<b>-1.0</b>	<b>0.2</b>	<b>-0.2</b>	-0.1	<b>1.0</b>	<b>-0.3</b>
	3	-0.1	-0.1	<b>-0.9</b>	<b>0.3</b>	<b>-0.3</b>	<b>-0.9</b>	-0.1	-0.1	<b>1.0</b>	<b>0.4</b>	<b>-0.5</b>	<b>1.0</b>	<b>0.2</b>	<b>-0.3</b>	<b>1.0</b>

SVD, Single Value Decomposition; Rot, Rotated SVD; TD, Tucker decomposition; Mode, Mode-rotation of Tucker4; Core,

Core-rotation of the Tucker4; MDS, Metric Multidimensional Scaling; NMS, Non-Metric Multidimensional Scaling.

Bolded values indicate significance at  $\alpha = 0.05$ .

Shading indicates model combinations where no off diagonal correlation was found among the three retained components.

## **Discussion**

### *Identified axes.*

For all investigated methods a similar set of three genotypic axes were obtained. Generally, for each solution, factors relating to relative tip abscission progress through time, progression from active growth to maturation of tissue through time, and parabolic trend through time of growth and tissue maturation were important among the tested genotypes across the tested temperatures. Following quadruple centering of the data, all that remained was the effect of the four-way interaction as all main-effect means, two-way interactions, and three-way interactions were removed (Kroonenberg, 2008). Through the quadruple centering of data, the two investigated temperatures reduced to reciprocals of one another. As either was equidistant from the mean, the results related to either temperature were equivalent to one-half the difference in response across the tested temperatures. This effectively reduced the solutions of each analysis to a three-mode dataset of differences across temperatures. This three-mode dataset represented the differences in relative trait trends through photoperiodic time of the tested genotypes relative to the mean of all tested genotypes. The trait identified to explain the largest portion of the variance of the dataset was the differences in relative tip progress through photoperiodic time across temperature for the tested genotypes relative to the average of genotypes. The trend had linear trend through time generally centering at 12.5h of daylight. This trend distinguished those vines which tended to have relatively small differences in tip abscission progress across the two temperatures relative to the mean of all tested genotypes early in the season compared to late in the season from vines that had relatively large differences in tip abscission progress early in the season when compared to late in the season.

The contrast between relative amounts of growth versus amounts of tissue maturation was generally split into a linear and a parabolic trend in non-rotated or core-rotated solutions. The varimax rotation of the modes of the either dataset created joint trends relating to early and late progress. The linear trend contrasted the amounts of either trait, relative to the average vine, as it differed across the two temperatures early versus late in the season. The parabolic trend was evaluated as a distortion from this linear trend comparing the relative ratio of growth to tissue maturation as a result of the differing photoperiodic induction timings of acclimation responses across the tested genotypes.

*V. riparia* tended to have below average differences across the tested temperatures in tip abscission progress relative to the average of vines early in the season, while having relatively high differences in the measure across the two temperatures late in the season compared to other genotypes (Fig. 14). When the linear trend of the relative ratio of active growth to mature tissue development was investigated, *V. riparia* had increased differences in growth versus tissue maturation early in the season across the two temperatures relative to late in the season when compared to the average of vines. This indicated a relatively accelerated rate of transition early with a relative plateauing of differences among environments late. Lastly, the parabolic relationship through time between the relative amounts of growth and tissue maturation across temperatures when compared to the average of all vines indicated that *V. riparia* tended to have higher than average differences in growth across the tested temperatures when compared to the average vine both early and late in the season. During mid-fall, *V. riparia* vines had lower than averaged differences in growth across the two temperatures relative to other tested vines. The inverse of this trend was true for measures of tissue maturation.

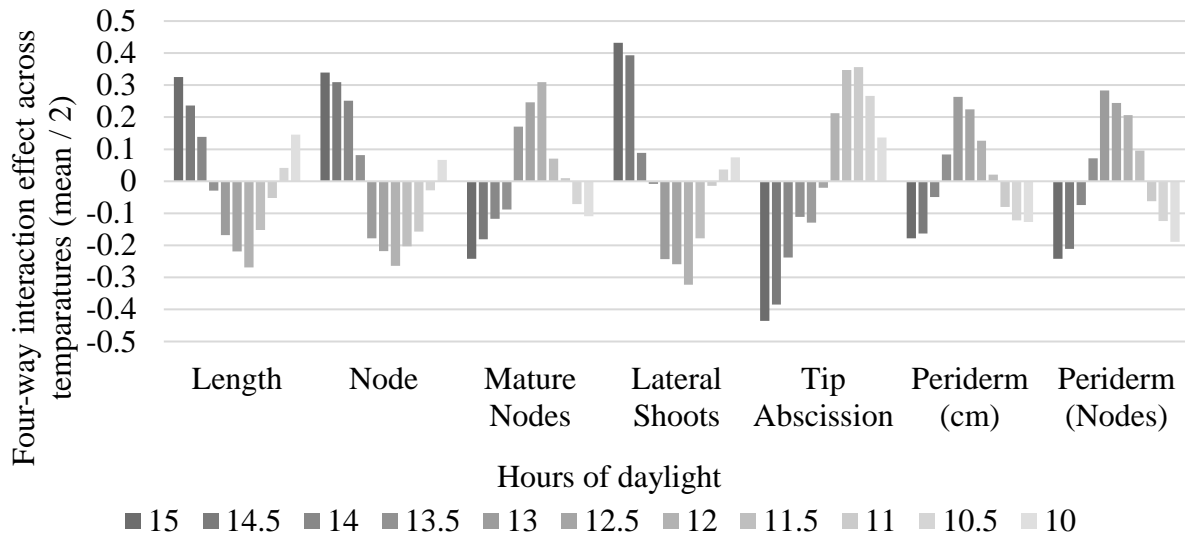


Figure 14. Plotted mean four-way interaction effect trends through photoperiodic time (15 – 10h of daylight) averaged across tested *V. riparia*.

The plotted differences in mean values across the two tested temperatures were reviewed to draw conclusions about the basis for the identified axes (Figs. 15-20). Tip abscission was decided to indicate temperature reactive and non-reactive types. *V. riparia*, ‘Frontenac’, and ‘917’, all exhibited increasing differences in tip abscission progress through photoperiodic time under warm conditions when compared to cool conditions, whereas tip abscission progress was similar across the two investigated temperatures for non-riparian types including ‘Marquette’, ‘939’, and ‘MN 1131’.

‘MN 1131’, and ‘917’ were identified to be similar to *V. riparia*, whereas ‘Frontenac’, ‘Marquette’ and ‘939’ differed along the axis related to the identified linear trend contrasting growth and tissue maturation. Upon review of the graphed differences between temperatures of each trait over photoperiodic time for each genotype it was determined that two possible trends explained the difference. *V. riparia*-like genotypes tended to have initially high relative differences in numbers of lateral shoots between temperatures with a decreasing trend as the simulated fall



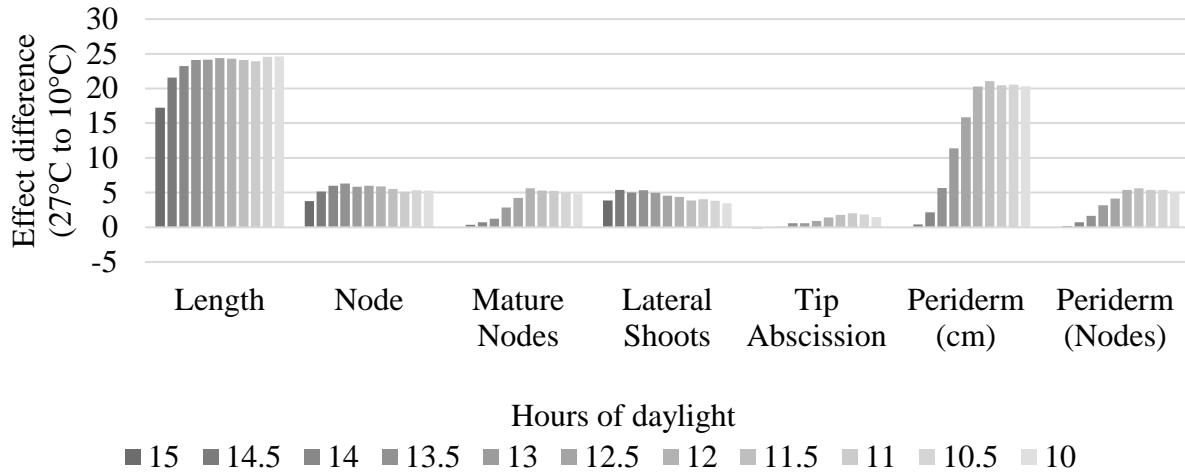


Figure 15. Difference in effect between temperatures (27 – 10°C) for the seven measure traits through photoperiodic time (15 – 10h of daylight) averaged across the tested *V. riparia* vines.

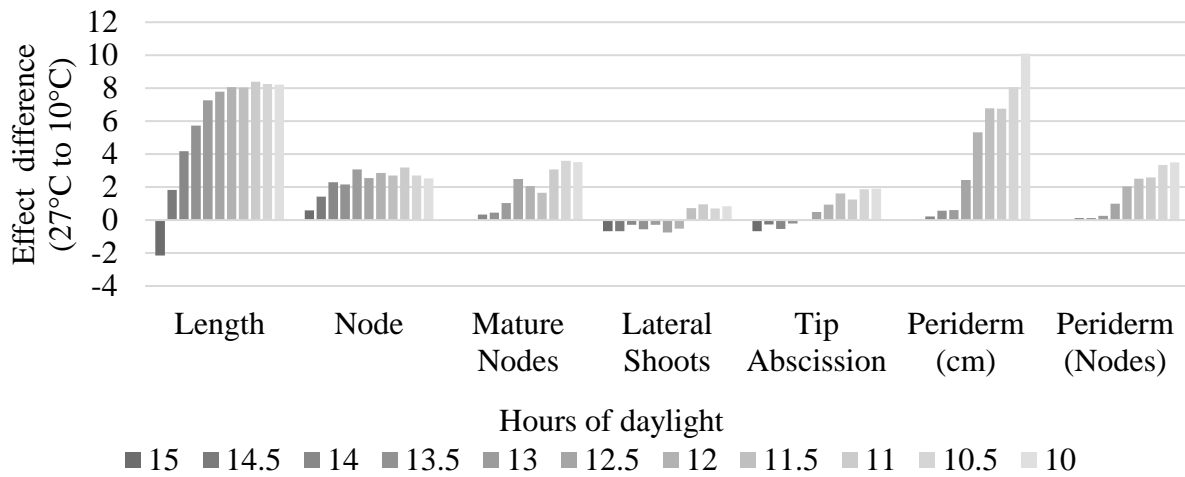


Figure 16. Difference in effect between temperatures (27 – 10°C) for the seven measured traits through photoperiodic time (15 – 10h of daylight) averaged across the tested 'Frontenac' vines.

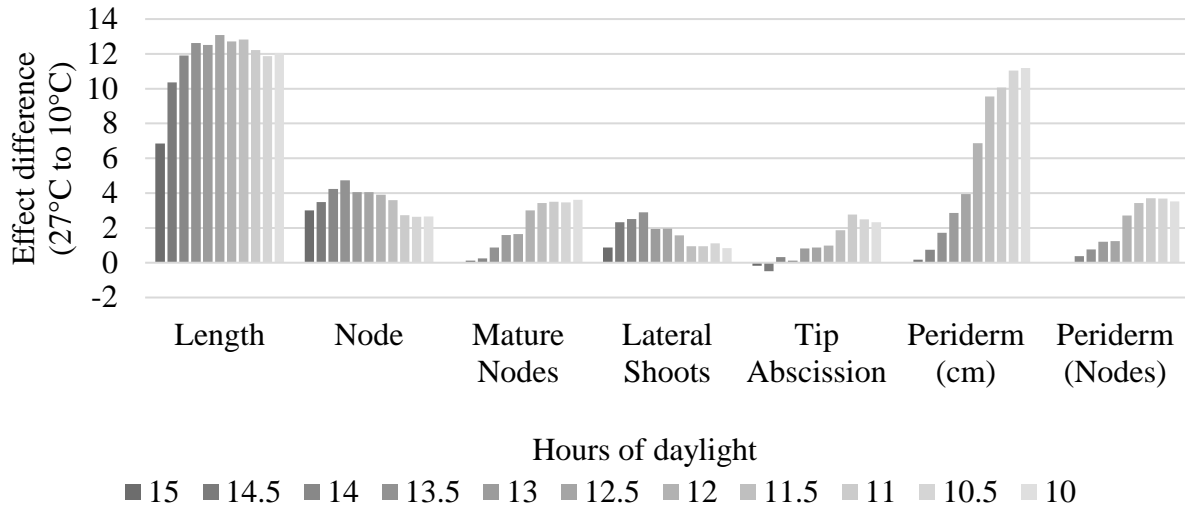


Figure 17. Difference in effect between temperatures (27 – 10°C) for the seven measured traits through photoperiodic time (15 – 10h of daylight) averaged across the tested ‘917’ vines.

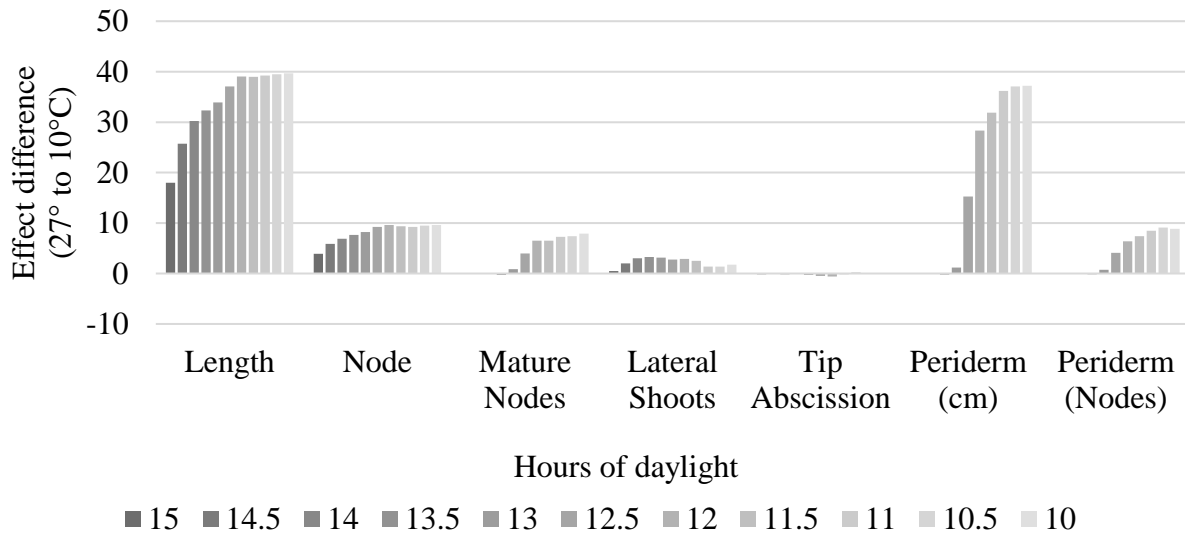


Figure 18. Difference in effect between temperatures (27 – 10°C) for the seven measured traits through photoperiodic time (15 – 10h of daylight) averaged across the tested ‘MN 1131’ vines.

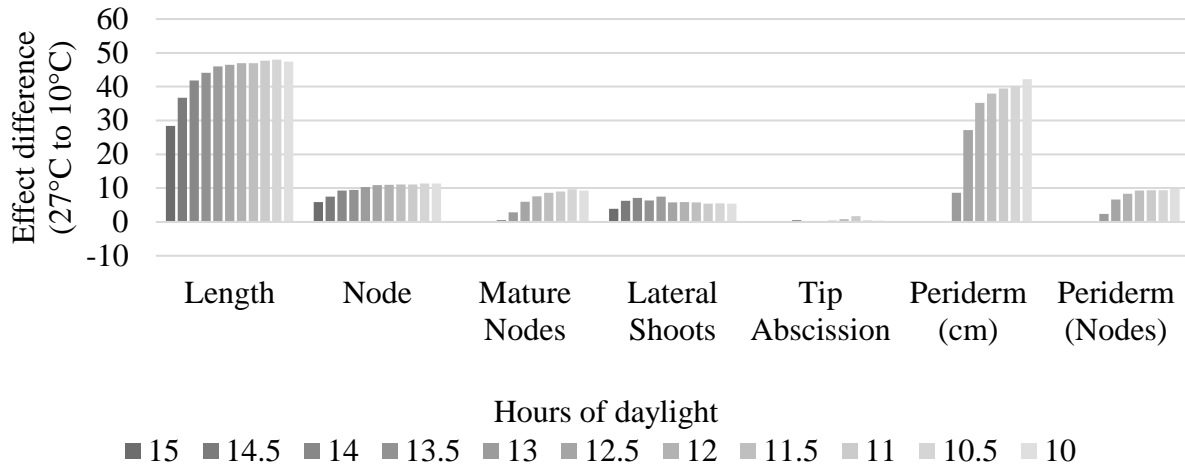


Figure 19. Difference in effect between temperatures (27 – 10°C) for the seven measured traits through photoperiodic time (15 – 10h of daylight) averaged across the tested ‘900’ vines.

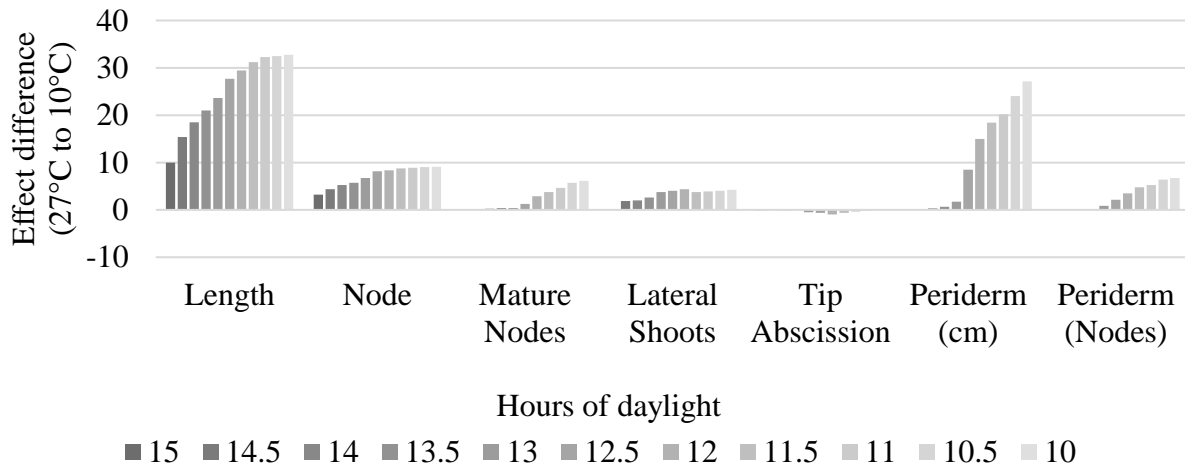


Figure 20. Difference in effect between temperatures (27 – 10°C) for the seven measured traits through photoperiodic time (15 – 10h of daylight) averaged across the tested ‘Marquette’ vines.

progressed. Those types not associated with the wild-type species tended to have initially low differences between the two temperatures for the trait with an overall increasing trend as the simulated season progressed. The other trait that differed between the extreme types along the axis

was the trend of differences in periderm development. Types identified to be similar to *V. riparia* along the axis tended to have plateauing of periderm development differences across the tested temperatures through photoperiodic time indicating a cessation of tissue maturation early in the season. No such plateau was identified in non-*V. riparia* type vines as increasing differences among the temperatures continued until late in the simulated season beyond reasonable season length for northern vineyards.

Along the axis related to the parabolic trend contrasting growth and tissue maturation identified to contain significant variation in the non-rotated SVD solution as well as the core-rotated Tucker solution, *V. riparia* was found to be similar in response to '73' and '900', while '940', '939', and '920' differed. Upon review of the plotted differences in trait values between the two tested temperatures across photoperiodic time, those vines similar to *V. riparia* had increased differences in periderm development and bud maturation between tested temperatures early in the simulated season when compared to those vines that differed. The difference in mature nodes across the temperatures also plateaued earlier in vines found to be similar to *V. riparia* compared to those that differed along the axis. Acclimation initiation time differences coupled with the effects of the linear trend of these traits, also identified in this study, caused individuals with similar reactions, which occurred at differing times to become dissimilar from one another.

When *V. riparia* was compared with the vine '917', which was most commonly identified to be *V. riparia*-like, and the vine 'Marquette', which most commonly identified to significantly differ from the wild-type, stark differences were seen along these described trends (Fig. 21). '917' tended to follow similar shaped response curves, independent of scale, in comparison with wild type vines. While 'Marquette' was not statistically different in its timing of initiation of growth

cessation and tissue maturation in comparison with wild-type vines, overall progress in the identified traits took comparatively different shapes across the two temperature regimes.

The parabolic trend relating growth and tissue maturation was likely related to the previously described photoperiodic response of *V. riparia* (Garris et al., 2009; Fennell et al., 2005; Wake and Fennell, 2000; Fennell and Hoover, 1991). The axis was interpreted as the distortion from the progress through linear photoperiodic time of relative growth and tissue maturation. The axis was related to the lateral shoot development, a critical trait determined by the previous studies. Through comparisons of mean differences in trait values across the tested temperatures through photoperiodic time, it was observed that the axis tended to contrast those types that initiated phenotypic alterations early in the simulated season when compared to late. This parabolic trend through time in conjunction with the linear trend through time relating to the traits, likely jointly characterize the transition from active growth to tissue maturation. The parabolic trend identified the earliness of the initiation of acclimation response, while the linear trend tended to identify the rate at which the transition occurred. The current study separated the two confounded factors into distinguishable traits; however, this is not to say that the two axes are independent of one another. The two trends likely arise from a single non-linear trait relating to growth cessation and mature tissue development, thus it may be more appropriate to consider each trait as a responses given the known condition of the alternate trait.

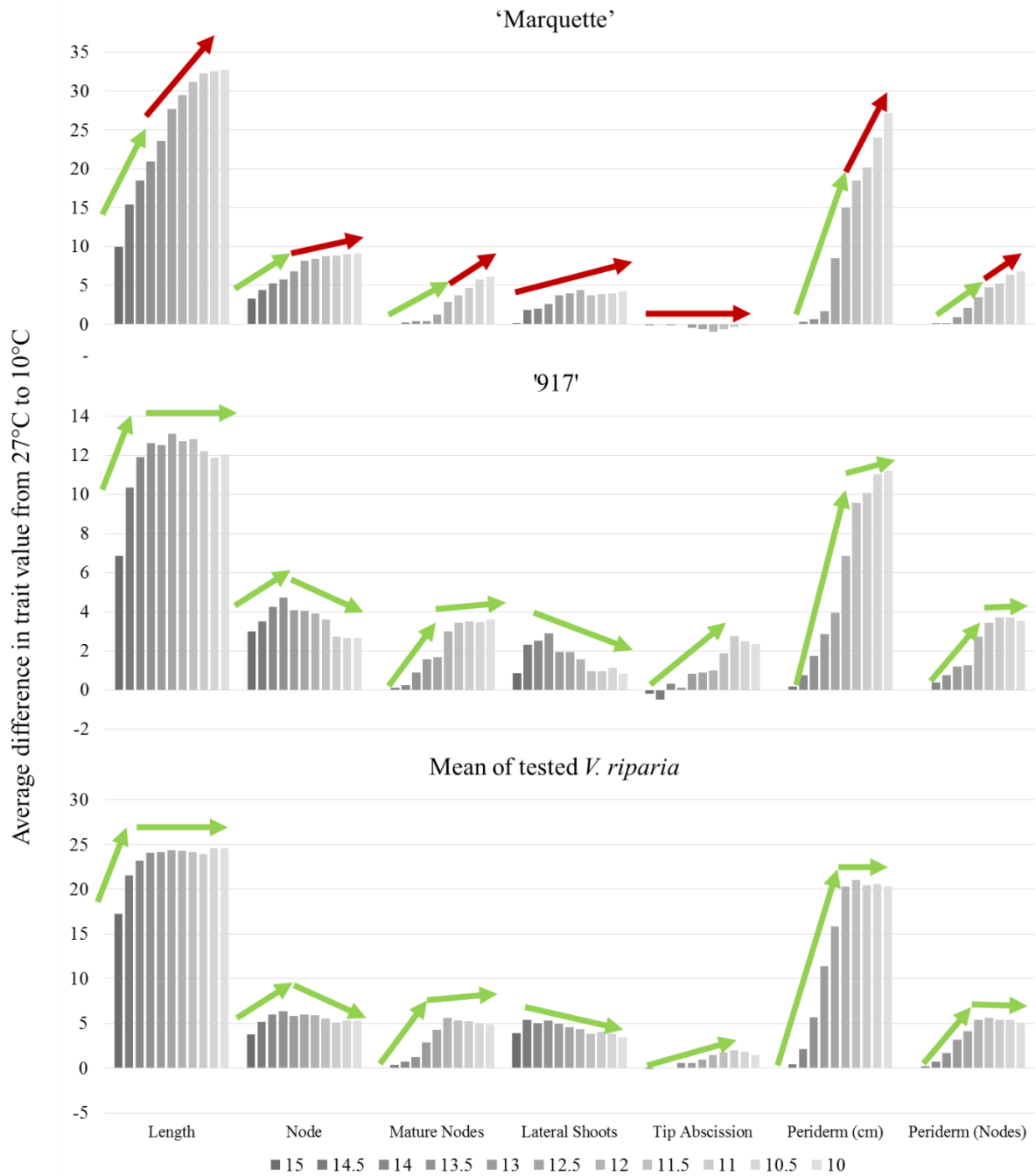


Figure 21. Comparison of the trends in differences of response across temperatures for the seven predictor variables across photoperiodic time (15 – 10h of daylight) for the mean of *V. riparia*, ‘917’, and ‘Marquette’. Green arrows indicate trends similar to that of *V. riparia*, while red lines indicate those trends that tended to differ.

The lack of identification of these separate trends in previous research may stem from the evaluation of a single *V. riparia* by ‘Seyval’ derived F2 family created from a single F1 progenitor vine (Garris et al., 2009). Neither parent of the F1 progenitor was homozygous, thus each contained allelic variation derived from their progenitors. This population may be better characterized, with terminology commonly used in maize breeding, as an S0 progenitor giving rise to S1 progeny (Hallauer et al., 2010). The lack of homozygosity in the parental types may have led to a loss of alleles important for the success of *V. riparia*. In the current study, progeny derived from the same parent types were variable in their likeness in response to *V. riparia* along the axis relating to the parabolic distortion that contrasted active growth and tissue maturation, which is being considered here as the timing of acclimation initiation. However, all individuals derived from this family had relatively similar values for the linear axis relating to the trait considered in this study as the rate of acclimation across the tested temperatures and all were similar in response compared to *V. riparia*. When other hybrids containing *V. riparia* parentage were investigated, diversity in response was found within the derived progeny. Family means of progeny derived from ‘MN 1131’ and ‘St. Croix’ did not differ from *V. riparia*, while the family means of all other tested families did. Within the check vines tested, the adapted types ‘MN 1131’ and ‘Frontenac’ had similar responses to *V. riparia* in their acclimation rate across the two temperatures when compared to ‘Marquette’ which differed. While similar timing of acclimation response to *V. riparia* was found in all tested check vines, those cultivars that have shown to be more adapted to the region additionally possessed the ability to complete these alterations at an increased rate under warm conditions when compared to the less reliable check ‘Marquette’ (Hatterman-Valenti et al., 2016). ‘MN 1131’ was always similar to *V. riparia* along such axes, while ‘Frontenac’ was at times similar to the average of the wild-type vines. Additionally, when ‘Frontenac’ was not found

to differ from *V. riparia*, its mean opposed the wild-type relative to the mean of all tested vines, thus it is likely that the response was more characteristically found in ‘MN 1131’ and opposed that found in ‘Marquette’.

*V. riparia* was also tied to temperature adaptive responses in tip growth, as it tended to have increased progress toward tip abscission under warmer conditions when compared to cool conditions and compared to the average tested vines; where non-*V. riparia* types had more similar responses across the two temperatures compared to the average tested vines. This trait was found to be an alternative method of adaptation in hardy interspecific cultivars, such as the regionally adapted type ‘Frontenac’ as neither ‘Marquette’ nor ‘MN 1131’ exhibited a similar response. Prior to the study, ‘Frontenac’ was included as an adapted industry standard, and overall exhibited the greatest similarity to *V. riparia* as it was rarely found to be dissimilar from the wild vines for any axis, and was the only control to have similar tip abscission response across the temperatures, a trait found to explain the majority of the variation in the interaction.

In a review and research article by Tanino et al. (2010), two methods of temperature-photoperiod related dormancy induction were outlined. In their investigation into *Populus* hybrids, the authors found, night temperature was correlated with days to growth cessation, rate of growth cessation, depth of dormancy and both the rate and depth of cold hardiness, while only rate of dormancy development was significantly correlated with daytime temperatures. In the current study, the environmental responses of *V. riparia* derived hybrids were similar with those found in *Populus* hybrids. The northern adapted species, *V. riparia*, showed a large increase in responsiveness when temperature was increased, particularly in tip abscission and the rate of growth cessation and mature tissue development, across the two temperatures when compared to those vines exhibiting alternate responses. In hybrid progeny of *V. riparia* crossed with non-



adapted types, these abilities were separable, with adapted types ‘Frontenac’ and ‘MN 1131’ displaying alternate temperature based responses that were found in common with *V. riparia* in rate of tip abscission and the rate of growth cessation and mature tissue development in the cultivars, respectively.

The connections among plant reactions and temperature have been researched in-depth through model organisms. Links have been made between the seasonal cycling of *Populus* spp. homologs and paralogs of genes identified in *Arabidopsis* spp. as CONSTANS (CO) and FLOWERING LOCUS T (FT) (Böhlenius et al. 2006). More recently Hsu et al. (2011) discovered two functionally diverged paralogs of FT within the genus, FT1 and FT2, respectively. Through a manipulative experiment, the authors discovered shifts in expression patterns caused by the temporally separated regulation of the genes’ expression that allowed for the cycling of reproductive and vegetative states. Both genes’ expression were highly influenced by temperature as FT1 was expressed under low temperature conditions and repressed under warm conditions and FT2 was expressed under low stress conditions including warm temperatures and long-days. As stressful conditions arise during late spring and summer including high temperature and dry conditions or the onset of short day conditions with cool temperatures the expression of FT2 is suppressed leading to growth cessation, bud set, and dormancy. Critically, the trait is effected by two paths for dormancy induction; both fall-like conditions as well as stressful conditions lead to a reduction in growth and eventual dormant state. A homologous gene to FT has been described in grapevine (*V. vinifera*) as VvFT (Boss et al, 2006; Sreekantan and Thomas, 2006; Carmona et al., 2007). VvFT, is also speculated to have a similar role in grapevine as FT2 has in *Populus* (Carmona et al., 2007). In investigations using progeny from *V. riparia* and the interspecific hybrid ‘Seyval’, homologous genes VvPHYA VvPHYB VvPHYC, VvPHYE, VvCO and VvCRY were

able to be mapped; however, the grape FT homolog VvFT was as a result of extreme segregation distortion (Garris et al., 2009). Within the current study, the resulting effects of temperature on *V. riparia* growth rate, tissue maturation rate, and tip abscission rate were consistent with the effects of FT2 described effects by Hsu et al. (2011) as both photoperiod as well as temperature were involved in the alterations of these phenotypic traits. The rate of trait response in the current study was also dictated by temperature and the degree of difference in response among temperatures was influenced by the genotype. Within the tested vines, *V. riparia* and similar hybrids were linked together through their ability to increase vine alterations due to the rise in temperature over the average of tested vines when compared to non-*V. riparia* types. This was demonstrated in greater increases in tissue alteration progress between temperatures 10°C to 27°C. Vines better able to capitalize on the increased temperatures tended to be more similar to wild collected vines than those unable to do so. While responses were similar to that described by Tanino et al. (2010) and Hsu et al. (2011), further characterization and additional information about gene expression would be needed to confirm these similarities.

#### *Comparison of reduction methods.*

##### Identified axes.

Of the tested reduction methods and subsequent rotations, only the non-rotated SVD model had significant variation along all three retained axes. All other tested models only contained significant variation along two axes. In most cases, these were the first two axes which related to linear progression of both tip abscission and relative amounts of active growth versus tissue maturation. This was not true following the rotation of the core-array of the Tucker solution to maximize its variance. In this case, the axes that contained significant variation related to linear

progress of tip abscission through time as well as the parabolic distortion from the linear trend of comparative active growth and tissue maturation among the tested genotypes.

#### Effect on genotypic means.

When mean genotype scores along their respective axes were compared with the mean score of tested *V. riparia* using ANOVA, the only genotype to never significantly differ from *V. riparia* across all axes having genotypic variation across tested all models was '917'. Other entries that tended to have the fewest deviations from *V. riparia* across axes and models were 'Frontenac', '911' and '913'. Other accessions that did not differ along any axes showing genotypic variation in select models were '64', '73', '906', '920', '924', '937' and '938'. The tested genotype that tended to differ significantly from *V. riparia* along two evaluated axes was 'Marquette', while '906', '909', '914', '936', '937', '939', and '940' also differed from *V. riparia* along two axes for specific models. These results are consistent with the hypothesized relationships of 'Frontenac' and 'Marquette' in their relative adaptation to the North Dakota climate (Hatterman-Valenti et al., 2016). The results may, in part, describe the reasons for the ability of 'Frontenac' to reliably survive and produce in the Northern Great Plains Region, while survival and production of 'Marquette' has been inconsistent. The largest trait that separated the two cultivars was the difference in the trend of tip abscission among the two temperatures. In general, 'Frontenac' tended to have values more similar to *V. riparia* along such axes while 'Marquette' tended to significantly differ as did 'MN 1131'. 'MN 1131' has also shown promise to be an adapted genotype for production in the region. The primary differences between 'MN 1131' and 'Marquette' was along axes relating to linear progress in relative amounts of active growth and tissue maturation through photoperiodic time. From the results of this study, it seems the combination of the three identified traits are what typify *V. riparia* upon the onset of fall conditions as they relate to the effects of

temperature. For the contrasting results seen between ‘Frontenac’ and ‘MN 1131’, it was concluded that the relative deficiency of either trait, relating to temperature sensitivity in tip abscission rate or relative growth versus dormant tissue development transition rate, and their relative progress through photoperiodic time may be overcome. However, the loss of both, as in the case of ‘Marquette’, may not allow for adaptation to North Dakota and the Upper Plains Region of the United States even if acclimation is initiated early in the season.

Ability to separate *V. riparia* from non-*V. riparia* genotypes.

Upon clustering of the retained axes for each solution, *V. californica* did not create an out-group as intended despite its lack of relation to the remaining accessions on the species level. At times, ‘MN 1131’ or the combination of the species accessions, *V. riparia* along with *V. californica*, grouped separately from most other tested hybrids. Prior to the initiation of this study it was hypothesized that the two tested species would react differently due to the differing climates of their geographic origins. The results of this study suggest commonality among *V. riparia* and *V. californica* acclimation responses, particularly along axes relating to linear progression of tip abscission through time as well as the parabolic distortion from the linear trend of the transition from active growth to tissue maturation tested across the two temperatures. Included was the suspected photoperiodic response, which was identified as a parabolic distortion in time and tied to differences in genotypic trends in lateral shoot development (Garris et al., 2009; Fennell et al., 2005; Wake and Fennell, 2000; Fennell and Hoover, 1991). Previous research has shown *V. californica* to be genetically distinct from either the North American or Eurasian species of *Vitis* (Pèros et al., 2011; Tröndel et al., 2010; Wan et al., 2013; and Zecca et al., 2012). This study demonstrates a similar early occurrence of feed-forward response to photoperiod in the Mediterranean species *V. californica* as was found in continental species *V. riparia*. *V. californica*

tended to be distinct from *V. riparia* along the axis relating to rate of transition from active growth to tissue maturation as their axes differed for every tested model where significant variation existed along the axis. This adaptation may afford *V. californica* the ability to take advantage of extended cool seasons as growth and tissue maturation were allowed to progress, where *V. riparia* had increased benefit in growth cessation and tissue maturation when temperatures were increased.

When clusters using all three retained axes for each model were compared, differences existed in the ability of the model to retain logical clusters of the tested *V. riparia*. All three Tucker solutions and the rotated SVD solution clearly grouped all *V. riparia* together while all other models split these accessions among groupings. When clusters were created using only those axes having significant variation among genotypes, differing results were obtained. Of the tested models, only the core-rotated variant of the Tucker solution and the metric-MDS solution clustered all tested *V. riparia* together. In addition, the non-rotated Tucker solution clustered all *V. riparia* together, however this cluster did not cluster away from most observed genotypes as groupings largely separated 'MN 1131' types from all others.

Overall, the most concise clustering was created through the use of the Tucker model when compared to the SVD based on the goal of identifying *V. riparia*-like accessions. The three retained components of SVD split *V. riparia* across groups. The rotated version of SVD was adequately able to distinguish *V. riparia* from most other types tested; however, upon clustering using the two axes containing significant variation, *V. riparia* were split among groupings. When the non-rotated Tucker or core-rotated solutions were used with either three or two components, reasonable separation of *V. riparia* from other accessions was obtained, with the core-rotated being the most accurate. The results obtained draw the conclusion that the tip abscission environmental sensitivity and early photoperiodic based initiation of acclimation response are the two most defining features

of *V. riparia* of the axes investigated, as two axis solutions had difficulty in grouping *V. riparia* when the axis relating to the rate of transition from active growth to tissue maturation was included.

When clustering resulted in an identifiable *V. riparia* group, ‘917’ as well as ‘Frontenac’, ‘73’, and several *V. californica* seedlings tended to most consistently cluster with the tested *V. riparia*. Prior to the initiation of the study, it was hypothesized that ‘Frontenac’ would be the most similar to *V. riparia*, as it has been a long-time, stable cultivar for production in North Dakota, the origin of all the included *V. riparia*. Comparatively, ‘Marquette’, through its relatively short production period in North Dakota, has been less predictable in winter survival and in-turn production. The findings from the current study support overwintering observations and provide an explanation for the observed differences among northerly adapted cultivars. ‘Frontenac’ tended to identify with wild vines when discernable wild-type groups were found, while ‘Marquette’ did not. In particular, the greatest contrast of the two cultivars was in the adaptability of tip abscission in the presence of differing temperatures. When ‘MN 1131’, an additional adapted type, was compared, the cultivar tended to react differently than the other included industry checks. Model dependent, ‘MN 1131’-like vines acted as an out-group, being more different from all other tested accessions when compared the tested *V. riparia*. In the past, populations derived from crosses between *V. riparia* and ‘Seyval’, as is ‘MN 1131’, have been used as the basis of photoperiodic induction of acclimation response studies (Garris et al, 2009, Fennell et al, 2005; Wake and Fennell, 2000; Fennell and Hoover, 1991). The current study indicates that ‘MN 1131’ has a unique acclimation response when compared to other *V. riparia* derived hybrids as well as compared to the mean of *V. riparia* itself. Beyond this, it’s progeny, in particular ‘900’ and ‘903’, reacted similarly. The findings of the current study suggest a larger exploration of possible *V. riparia* derived hybrid populations is needed in order to ensure that genetic associations discovered in *V.*

*riparia* x ‘Seyval’ derived populations are transmissible and remain stable over a broader range of cold-climate grapevine breeding germplasm. Further, an expansion may lead to the identification of more traits needed for northern adaptation that may not have been identified or were masked in the previously studied population.

#### SVD and Tucker decomposition solution stability.

Following iterative resampling, SVD consistently recovered more variation, having lower sums of square deviation among estimated and observed sample values, when compared with the Tucker model. However, Tucker solutions were more consistent, as squared deviations from the solution obtained using the full complement of samples was lower than that obtained using SVD. This led to the conclusion that SVD was over fitting the model to the data presented. Overall, the Tucker model was more consistent in the subspace it defined regardless of samples used, and likely better reflects repeatable variation that may be used to predict trait reactions among *V. riparia* derived hybrids when compared to SVD.

#### Comparison of SVD and Tucker decomposition with MDS.

NMS and metric-MDS were included as standards for use in comparing the ability of SVD and Tucker decomposition to retain pairwise point distances. NMS and metric-MDS correlated near identically. Both models’ scores correlated well with the non-rotated solutions derived from SVD and the Tucker model as well as with the core-rotated solution of the Tucker model, where no significant cross-axis correlations were found indicating that all three models identified similar orthonormal axes relating the sample vines’ reactions. Of the three *a priori* dimensions specified, two were found to contain significant variance across genotypes for both models. This was consistent with the results obtained using varimax rotation of the SVD solution as well as with all versions of the Tucker solution.

In the non-rotated Tucker solution, the linear trend was found to contain significant variation among the genotypes, as the core-rotated model detected only the variation among genotypes along the axis related to the parabolic distortion. Using MDS, metric or non-metric, the axes with significant variation among genotypes were similar to those previously described relating to the temperature adaptability in tip abscission as well as the rate of transition between active growth and cessation of tissue maturation. The varimax rotation of the SVD solution, the Tucker solution, as well as the mode-rotated Tucker solution also identified significant variation in similar axes, whereas the non-rotated SVD solution identified significant variation in all three axes and the core-rotated Tucker solution was similar only in its identification of significant variation in the trait related to tip abscission adaptability.

It has been previously reported that the flattening of higher dimensional data into combination-mode matrices causes the loss of effects (Kroonenberg, 2008). The loss would occur from unaccounted inter-relationships between the concatenated modes, such as the loss of information between the time dependence of a trait's expression when exposed to a specific temperature. In the current study, the end result of SVD and Tucker modeling were very similar, however models differed in their ability to separate genotypes in their similarity to *V. riparia* in a reduced space and the consistency of mapping to this reduced space. The three components modeled by each method had similar relevance to the data set, correlations between their resulting axis scores were high and significant, while no significant cross-axis correlation was identified between the two models. The variable weights applied to the original data set to obtain the axes were also similar, as they were also highly correlated with no cross-axis correlation between the two models. Bi-linear modeling accounted for a greater proportion of the overall variance and resulted in significant genotypic variation in all three resulting axes following ANOVA, whereas



only two axes were identified to vary in the Tucker solution. While increased variance was accounted for in the bi-linear model, the number of axes found using the Tucker model were similar to that of the included metric-MDS and NMS standard models. Tucker and SVD results clustered observed vines differently when all three axes were used. The Tucker solution had similarities to the NMS solution when the two axes containing significant genotypic variation were used. The mode-rotation of either the SVD or Tucker solution led to alterations in the interpretation of the axes in similar ways. The linear response with parabolic distortion found prior to rotation was interpreted as a joint response of alterations occurring early and late in the simulated season following mode-rotation. The rotation of the core-array to maximize variance using the Tucker model led to differing axes contributing significantly to genotypic differences and thus an altered its interpretation. However, it was best able to separate *V. riparia* types from other genotypes even when reduced to a two axis solution.

The similarity among bi-linear and multiway methods has also been reported previously (Dyrby et al., 2005). The authors concluded that multiway analysis was still advantageous, even though similar results were obtained. The methodology allows for more interpretable results as the number of modes are increased, as each mode is decomposed separately. In agreement with the previous study, the overall trends identified between the opposing data reduction methods was similar, however the reasoning for these trends were more readily interpretable when using the Tucker model. Upon rotation of the core-array to maximize its variance, a reasonable separation of the axes occurred as the core-array was approximately superdiagonalized. This allowed for independent interpretation of the resulting sample scores based on individual combinations of traits and time trends. Three unique contributing combinations were found, each associated with a sample axis with minimal offsets. While this allowed for easier interpretation of the resulting axes,

it also led to results that opposed other tested models as differing axes were found to contribute significantly to the variation among tested genotypes, which indicated a redistribution variance and error among the axes. Also, while these results tended to best separate *V. riparia* accessions from all other tested genotypes, the resulting axes defining variance among the genotypes differed from the NMS solution that was thought to present the best fit in the case of non-linear trends as well as best preservation the point-wise distances among data points. However, MDS and NMS were applied to the same wide combination-mode matrix as used in the SVD reduction, which may bias the comparison as multiway generalizations of the procedures were not compared.

## **Conclusions**

Overall, beyond early photoperiod based induction previously described, the rate of transition from active growth to tissue maturation was a discernable acclimation trait of *V. riparia*. Additionally, the trait contributing greatest to the variation in the dataset was the differences in tip abscission progress rate between the two temperatures over photoperiodic time. *V. riparia*-like accessions tended to be temperature sensitive in their responses, having greater increases in reaction across the two temperatures when compared to the average vine, where non-*V. riparia* types tended to be less responsive. ‘MN 1131’ was found to have an adaptive type response that combined early acclimation response with rapid progression of the transition from active growth to tissue maturation, while ‘Frontenac’ displayed an alternative method as it had early induction of acclimation response coupled with temperature adaptive tip abscission rate across the tested temperatures. ‘Marquette’ did not differ from *V. riparia* in acclimation initiation timing where the trait was found to statistically differ across genotypes; however, it did differ for the additional adaptive responses involving rate of progress of either tip progression and the transition from

active growth to tissue maturation across the two temperatures. The conclusions of this study indicate, in part, that the inclusion of either rate adaptive response with early acclimation initiation may enable consistent productivity in riparian-based interspecific grape cultivars in North Dakota and the Northern Plains Region. However, the exclusion of both rate adaptive responses, even with early acclimation initiation, may leave cultivars unreliable in the region.

The study was also able to identify a *V. riparia*-like hybrid vine, '917', which was not distinguishable from the mean of *V. riparia* along all investigated axis using all tested modeling methods, suggesting that one may be able to recombine the identified traits in future cultivar releases having greater adaptation to the region. The use of either linear modeling method, SVD and Tucker decomposition, led to similar axes, however the total percent variation and the allocation of error in these axes differed as all three axes contained significant variation in SVD where the Tucker model resulted in a reduced set of two axes containing significant variation. While SVD was able to consistently account for a greater percent of variation in resampled test datasets using models derived from independent training sets, the Tucker model showed less indication of overfitting, as solutions showed comparatively less variation from the full model solution. Overall, the non-rotated and core-rotated versions of the Tucker solution were better able to separate *V. riparia* accessions into distinguishable groupings when compared to bi-linear modeling or MDS using the combination mode matrix. The similarity of the identified axes, increased ability to differentiate *V. riparia* from other accessions, increased consistency in resampled solutions, and the increased ease of interpretation of the identified axes lends Tucker modeling more practical in this particular application when compared to bi-linear modeling.

# CHAPTER III. CONTRASTING RESPONSES TO ENVIRONMENTAL CONDITIONS BY THREE COLD-CLIMATE WINEGRAPE CULTIVARS GROWN IN THE UNITED STATES UPPER PLAINS REGION

## Abstract

Three cold-climate winegrape cultivars ('Frontenac Gris', 'Marquette', and 'St. Croix') were investigated for environmental effects on fall-acclimation and fruit quality. Twelve measures were taken at five photoperiodic times under five environments. Mean values of environment-by-trait-by-cultivar-by-photoperiodic time combinations were used to reduce the interaction from a 3x12x5x5 dataset to dimensions of 2x5x4x4 while retaining 90.70% of the original variation using the Tucker model. Additionally, three temperature parameters at each site were obtained for a 40 day period coinciding with the phenotypic evaluation period and were also reduced to dimensions of 2x3x2 while retaining 94.71% of the total variance. Environmental axes derived from the temperature data correlated with two identified phenotypic environmental axes, one of which contributed highest to the variance of the phenotypic interaction. Temperature increases were found to be associated with relative increases to active growth and berry ripening in 'Marquette' compared with other cultivars. Temperature declines early in the season were associated with reduced berry growth, increased periderm development and increased berry ripening rate in 'St. Croix' relative to other cultivars. Overall, 'Frontenac Gris' had a moderated response in comparison with the other two cultivars, being less affected by individual temperature events in its progress in fall acclimation. Overall, it is speculated that relative differences in reaction of symplasmic unloading restriction to differing tissues in the face of differing perceived stressful conditions resulted in the cultivar differences. The uncompromising progress in bud maturation relative to other cultivars likely aids in the year-to-year reliability of 'Frontenac Gris' over the

other investigated cultivars in North Dakota, while the relative ability of ‘Marquette’ to return to active growth upon temperature increase may contribute to its relative unpredictability under the stochastic environmental conditions faced by Northern Plains producers from one year to the next.

## **Introduction**

Recent advances have occurred in the understanding of grape acclimation and dormancy response. Photoperiodic response has been found to contribute greatly to growth cessation in *V. riparia* allowing for entrance into a dormant state earlier relative to other grapevine species (Garris et al., 2009). However, after growth cessation, induction of dormancy may take several weeks (Cooke et al., 2012). Environmental conditions can influence the transition from active growth to an acclimated dormant state. Temperature has been found to contribute greatly to this transition. Alternate responses to the photoperiodicity of grapevines have been observed in *Malus* and *Pyrus* of Rosaceae as reduced temperature was found to be the primarily cue of acclimation (Heide and Persturd, 2005). These responses are not necessarily static across the diversity within genera nor across environmental gradients among individuals. Within *Prunus*, diverse responses have been found among species (Heide, 2008). While warm temperatures (21°C) induced continuation of growth under long or short-day conditions, under low-temperature conditions, *Prunus* species ranged in growth cessation responses from the need of short-day conditions in combination with low temperatures to the overcoming of long-day conditions through their response to low temperature alone. Investigations into the woody species *Populus* spp. and *Betula* spp. have provided evidence that increased temperature can lead to increased depth of dormancy (Kalcsits et al, 2009; Junttila et al, 2003). Hsu et al. (2011) investigated the alternate responses of two paralogous FT genes in *Populus* spp. linked with the annual cycling of growth and found them to

be influenced and alternatively expressed by contrasting temperatures during differing seasons. Tanino et al. (2010) evaluated two methods of temperature-photoperiod related dormancy induction found within woody plants. Responses in *Populus* spp. indicated that northerly adapted ecotypes had amplified responses to decreasing photoperiod in the presence of warm temperatures compared with other genotypes.

Similar temperature effects have been linked with other fall alterations affecting grape production. Implications of temperature differences in the fall extend to alterations in fruit quality. Temperature differences have been shown to alter malate concentrations leading to differences in titratable acidity in *V. vinifera* fruit (Sweetman et al., 2009; Kuhn et al., 2013). Pre-veraison temperature increase was associated with increases in malate concentrations, while temperature increases reduced malate content at veraison or post-veraison timings. Temperatures have also been known to affect ripening in other ways. Berry weight and volume were shown to be increased by high temperatures (Greer and Weston, 2010). High temperatures have been suggested to decrease the percent soluble solids as well as titratable acidity, while low temperatures increased berry soluble solid content and decreased titratable acidity (Greer and Weston, 2010; Carbonell-Bejerano et al., 2013; Mori et al., 2005). Through the effects of temperature, berry maturation and acclimation progress are partially linked with each other.

The alterations attributed to temperature differences have largely been tied to hormone biosynthesis alterations within the plant. Many of the positive effects on grapevine dormancy responses and fruit ripening have been found to be associated with increased abscisic acid (ABA) concentrations. ABA is a plant hormone predominantly expressed during seed ripening and stressful conditions (Xiong and Zhu, 2003). In the occurrence of either cue, ABA is associated with greater tolerance to environmental stressors. One of the several effects of increased ABA

synthesis is the regulation of turgor within the vine (Christmann et al., 2004). While either the re-distribution or increased biosynthesis of ABA may result in mediated responses to stimuli, baseline levels of ABA also contribute to overall growth regulation within plants (Christmann et al., 2004; Slovik et al., 1995; Wilkinson and Davies, 1997; Zeevaart and Creelman, 1988; Cheng et al., 2002). Exogenous concentrations of ABA have been shown to delay bud break and influence overall dormancy in *V. vinifera* (Zheng et al., 2015). Ecotypic variation in ABA concentration has been demonstrated in *Betula pendula*, as ABA concentrations in northern ecotypes were more responsive to low temperatures and short-day conditions in comparison with southerly adapted ecotypes (Li et al., 2002). Differences in the expression of a putative ABA-inducer protein, HVA22, were found in *V. riparia* under chilling (Mathiason et al., 2009). During the same treatment a gibberellic acid (GA) receptor was found to be up-regulated. The hormone is antagonistic to the effects of ABA. Involvement of ABA in fruit ripening has also been described in *Vitis* (Kuhn et al., 2013). The hormone provides a linkage between the processes of fall dormancy response and fruit ripening and maturation. The interconnection between berry diameter and ripening has also been tied to the effects of ethylene (Gómez-Cadenas et al., 2001). Though grape is considered a non-climacteric fruit, Chervin et al. (2004) found that ethylene signaling was involved in the onset of ripening. Application of a competitive ethylene inhibitor (1-methylcyclopropene) delayed berry growth as well as acidity reduction. Ethylene has also been shown to be antagonistic to the effects of ABA (Ghassemaian et al., 2000).

Water flow and turgor in sink organs that lack abundant photosynthetic tissues have been attributed to the effects of phloem (Wang et al., 1997; Lang, 1990; Lang and Thorpe, 1989; Ho et al., 1987). Unloading from the phloem occurs by two routes, symplasmic or apoplasmic (Patrick, 1997). Symplasmic unloading occurs as intracellular transport through plasmodesmata. Long-term

regulation of such passages has been speculated to be caused by the relative number or ultrastructure of plasmodesmata passages. Such passages, however, have not been found to be of fixed-size. Temporary alterations may occur through restriction of plasmodesmal opening size. In a comparison of maize ecotypes, chilling resulted in plasmodesmata restriction (Bilska and Sowiński, 2010). The two ecotypes in the comparison were identified as either chilling-sensitive or chilling-tolerant. The chilling-sensitive type was unable to relax plasmodesmata after a return to ambient temperatures following chilling, where the chilling-tolerant genotype could.

Many of the alterations which occur along with the onset of fall have been connected to alterations in water relations within plants. Fruit ripening has been studied in its relation to phloem unloading and its onset is marked by a transition from symplasmic to apoplasmic pathway (Zhang et al., 2006; Keller and Shrestha, 2014). Root restriction has been shown to affect water relations of a vine. Xie et al. (2009) found, following root restriction, that both berry diameter and total soluble solids were increased during berry development. This coincided with an increase in the number of plasmodesmata connections that existed between the sieve element/companion cell complexes and the phloem parenchyma cells when compared to vines that were not restricted. The effects on berry ripening were noted to potentially be due to the increase in symplasmic flow. Stem maturation has also been linked with water status of sink tissues. The color changes of stems during maturation was found to be associated with stem drying as well as increased freezing tolerance (Wolpert and Howell, 1986). Dormancy and hardiness of primary buds has also been tied to decreasing water content (Fennell and Wake, 1996; Wolpert and Howell, 1985). These linkages lead to the interpretation that water restriction to maturing tissues may be important in their preparation to winter conditions, and may have similar ties to symplasmic phloem unloading in such regions as in sink tissues of fruits.



In addition to stem maturation, the cessation of growth may have ties to relative water status and relative phloem unloading. The amount of symplasmic and apoplasmic transport of photo-assimilates has been speculated to have a role in stem elongation (Patrick, 1997). Additionally, the temporary blockage of symplasmic flow has been associated with rapid elongation of *Gossypium hirsutum* fibers (Raun et al., 2001). Stem elongation zones have been associated with the effects of both symplasmic and apoplasmic phloem unloading, possibly indicating a dynamic role of both methodologies (Patrick, 1997). These processes allude to a common linkage of traits related to stem growth with that of phloem unloading across plant tissues, while the dynamic control of unloading methodologies may allow for variance in environmental sensitivity across genotypes.

ABA has been tied with the regulation of growth within plants (Christmann et al., 2004). ABA has also been found to regulate turgor within plant tissues, most notably in the reduction of turgor in stomatal guard cells allowing for stomatal closure and water conservation under water stressful conditions (Wright and Hiron, 1969; Kriedemann et al., 1972). The increase in ABA production at the onset of acclimation may contribute to or be the cause of disproportionate water regulation to differing sink tissues of *Vitis*, affecting source-sink relationships as acclimation and fruit ripening proceed. Source-sink relationships of carbohydrate movement within plant tissues is, in part, responsible for increased freezing tolerance, as well as fruit maturation. The competition between these sink locations has also been investigated in grapevine (*V. vinifera*). Murcia et al. (2016) found that the exogenous application of ABA and GA<sub>3</sub> were able to alter relative sugar accumulation. The relative hormone applications were found to alter sugar transport, with ABA causing increases in glucose and fructose accumulation in berries and GA<sub>3</sub>, an ABA antagonist, causing increases in stem tissue. Sugar accumulation in stem tissue has also been shown to differ

among cold adapted and cold sensitive genotypes in the presence of cool, acclimation favorable conditions (Grant et al., 2009). As previous research has shown that sugar accumulation is required for resistance to cold temperature freezing as well as in fruit maturation, the reactions of vines to environmental signals affecting relative ABA or ABA antagonistic compound production may play a critical role in the tradeoffs between preparedness for winter conditions and ability to ripen fruit to acceptable levels for wine production.

Chapter 1 outlined a method for evaluation of temperature effect on vine specific reactions during a simulated fall at two static temperatures. This process decomposed a four-way interaction of genotypes, traits, photoperiodic times, and temperatures to uncover differences in instantaneous response to environmental differences through comparisons of vine trait trends relative to other genotypes as well as in comparison with a mean internal response. The differences in deviations from internal responses compared across the mean of tested genotypes was able to identify three important aspects of temperature adaptive response of *V. riparia* related accessions. A similar methodology will be applied here to ensure that similar contrasting responses of tested cultivars remain under field conditions and that instantaneous alterations may be explored, as well as additional basic fruit ripening characteristics will be included to attempt to help elucidate relationships that exist between temperature adaptive dormancy response and fruit ripening in hybrid grapevine among three cold-climate cultivars of differing perceived reliability in the Northern Plains Region of the United States (Hatterman-Valenti et al., 2016).

## Materials and methods

### *Plant materials.*

Three cultivars ('Frontenac Gris', 'Marquette', and 'St. Croix') were compared. 'Frontenac Gris' is a gris (gray) fruited sport mutant of the cultivar 'Frontenac', a red fruited unpatented cultivar for used for red wine production, which was developed at the University of Minnesota (Luby and Hemstad, 2006). 'Frontenac Gris' was patented by its inventors James Luby and Peter Hemstad in 2004. The cultivar was released for white wine production in the Upper Midwestern United States for which it is adapted. The vines have been described as vigorous, productive and winter hardy. 'Marquette' is a cold-climate grapevine variety for red wine production. The cultivar was released by Hemstad and Luby in 2006 and is described as very cold hardy ( $-37.8^{\circ}\text{C}$  ( $-36^{\circ}\text{F}$ )), disease resistant and of high quality. The cultivar was created from the intercrossing of 'MN 1094' and the French Hybrid 'Ravat 262' at the University of Minnesota (Hemstad and Luby, 2008). 'St. Croix' is a cold climate grapevine that was developed for red wine production. The vine was labeled ES-2-3-21 by its inventor Elmer Swenson and was released as 'St. Croix' in 1982 (Swenson, 1982). The vine was noted for its good winter hardiness, low acidity, high sugar content, and absence of foxy *V. labrusca* flavor.

### *Test vineyards.*

Test vineyards were used in Absaraka, ND as well as Wyndmere, ND. Vines used in Absaraka, ND were spaced 2.44 m (8 ft) apart in north-south facing rows spaced 3 m (10 ft) apart in 2004. Vines at Wyndmere, ND were planted in 2009 1.83 m (6 ft) apart in rows spaced 2.44 m (8 ft) apart. Both vineyards were trellised to a high cordon trellising system. Within-row areas were managed as bare-soil by the use of herbicide (combination of flumioxazin and glufosinate-ammonium with spot applications of glyphosate for perennial weed control) and tillage. Row

middles were managed as turfgrass (*Festuca rubra*, Creeping Red Fescue). Data were taken in 2012, 2013 and 2014 in both locations. Each year-by-location combination was considered an environment for the study. Severe winter dieback of ‘Marquette’ and ‘St. Croix’ in 2014 at the Wyndmere location caused the data from this environment to be excluded from analysis. Each test vineyard was sub-divided into three replications containing each of the three investigated cultivars. Four-vine experimental plots of each cultivar were evaluated in each replication, and data was collected on the middle two vines within each experimental plot.

#### *Sample collection times.*

Fruit samples were collected and plant measurements were taken from each test vineyard for each half-hour decline in photoperiod from 14.5 to 12.5h of daylight constituting five data collection times within each environment. Initially, data was taken for a longer duration within particular environments; however, data were reduced to include only time periods for the frost-free period at all included test environments.

#### *Traits.*

##### Acclimation predictors.

Stem acclimation measures were taken on each of two individual stems arising from each of the two investigated vines to constitute four stems for each experimental unit. Each stem was measured for seven predictors of fall-acclimation response. Stem length was measured as length (cm) from the point of bud emergence on the spur to the tip of the newly developing cane. The number of nodes was determined through direct count along the entire cane. Number of mature nodes was determined by direct count as the number of nodes showing mature brown tissue. Tip abscission, was measured on a zero to five scale, where zero was full active growth and five was loss of the shoot tip. Values of 1-2 were progressively reduced turgidity of the shoot tip and values

3-4 were marked by progressively greater browning. Lateral shoots were assessed through direct count as the number of stem nodes possessing lateral shoots having at least one unfurled leaf. Periderm development was measured as both the length (cm) of mature woody stem, as well as the number of nodes this mature region enveloped.

#### Fruit quality predictors.

A ten-berry sample was collected from each experimental unit at each data collection time. Attempts were made to make each sample as homogenous as possible. Samples were taken from five representative clusters across the cordon expanse and berries selected from multiple positions on clusters to represent multiple degrees of light exposure. After taken, fruit samples were stored frozen until evaluation. Five predictor variables of fruit quality were quantified and evaluated. Berry size was evaluated by measures of berry weight and diameter. Each was quantified as an average of the 10 berry sample. In addition, basic quality parameters were tracked as the combined juice of each homogenized sample was evaluated for soluble solid content (brix, refractometer), pH (electronic pH meter), and titratable acidity (burette using a 3 ml juice sample).

#### *Environmental conditions.*

Ambient air temperatures (°C) was collected throughout the experiment using Decagon Em5b analog data loggers with RT-1 thermistors (Decagon Devices, Inc; Pullman, WA). Nine separate loggers were used at each test environment. Sensors were placed at cordon level and were covered with an open-bottomed expanded polystyrene foam surround to protect against solar influence. Data was collected every 1.5h from July 5<sup>th</sup> through the duration of the study. Daily minimum, maximum and average temperatures were extracted for further analysis. For daily average temperature, the 16 daily readings were averaged within each day for each logger. For all measures the data for the nine loggers in each environment were averaged for analysis.

### *Statistical analysis.*

Data were initially subjected to ANOVA to confirm higher-order interactions among the investigated components using the mixed procedure of SAS 9.4 statistical software (SAS Institute Inc.; Cary, NC). The data were treated as a randomized complete block design with a split-plot in time and space arrangement combined over the five evaluated environments with three replications within each environment. The 12 multivariate predictors as well as the five photoperiodic sampling dates were treated as blocking gradients. Upon confirmation of the presence of higher-order interaction the least-squared means were used to deconstruct the interaction.

The resulting dataset of estimated means was deconstructed with the Tucker model using the N-Way toolbox for MATLAB with MATLAB R2015a (The MathWorks, Inc.; Natick, MA) (Andersson and Bro, 2000). The initial data set was a 3x12x5x5 multiway array with modes relating to cultivars, traits, environments, and photoperiodic times, respectively. To isolate the four-way interaction each mode was sequentially centered to a mean of zero and traits were scaled to equal variances due to their differing scales (lengths, counts, and scales) using `nprocess` function (Kroonenberg, 2008). The number of retained axes from each mode was determined using a compromise between explained variance and model complexity using the `tucktest` function. The decomposition was done using the `tucker` function with the chosen reduced dimensions of 2x5x4x4.

To determine any possible relationship between the environmental axes and ambient temperature, for each date from Aug, 9 through Sept, 19 in each of the five test environments, seven-day moving-averages were calculated for daily average temperature, daily minimum temperature, and daily maximum temperature. The resulting 40x5x3 dataset was centered for days and environments leaving only environment-by-day and environment-by-day-by-temperature

parameter interactions and was reduced by the Tucker3 model using the N-way toolbox for MATLAB in MATLAB R2015a. The number of axes for each mode was determined as the best compromise between explained variance and model complexity through visual evaluation of plotted explained variance for each combination of retained mode levels. The reduced phenotypic and temperature environmental axes were compared using correlation between environmental scores of the respective models using the corr procedure of SAS 9.4 statistical software.

## Results

### *Vine response.*

The full model was tested using ANOVA. The resulting analysis identified significant variance in the four-way interaction among cultivars, traits, photoperiodic times, and environments (Table. 30). Upon confirmation of this higher-level interaction, the Tucker model was used to

Table 30. ANOVA sources of variation for fixed effects of the field evaluation of acclimation.

Effect	DF	Den DF	F-value	p-value
Env	4	-	-	-
Cult	2	20	1.91	0.1741
Env*Cult	8	20	0.56	0.7951
Photo	4	40	103.72	<.0001 *
Env*Photo	16	40	1.87	0.0551
Cult*Photo	8	80	5.32	<.0001 *
Env*Cult*Photo	32	80	1.66	0.0357 *
Trait	11	110	391.03	<.0001 *
Env*Trait	44	110	1.97	0.0023 *
Cult*Trait	22	220	5.44	<.0001 *
Env*Cult*Trait	88	220	1.00	0.4995
Photo*Trait	44	440	134.60	<.0001 *
Env*Photo*Trait	176	440	3.76	<.0001 *
Cult*Photo*Trait	88	879	12.55	<.0001 *
Env*Cult*Photo*Trait	353	879	1.69	<.0001 *

Env = Environment, Cult = Cultivar, and Photo = Photoperiod.

\* indicates significance at  $\alpha = 0.05$ .

reduce the resulting multiway dataset of means to a reduced set of orthonormal axes from each mode. To determine the number of axis from each mode to retain, the explained variation as a percent was plotted against the complexity of the model as the total number of axes. The solution relating to the reduced dimensionality of 2x5x4x4 was determined to be the most appropriate. This model explained 90.70% of the original variation of the interaction and reduced the dimensionality of the model considerably.

### Cultivars.

The first mode of the data relating to cultivars was reduced to two axes and was interpreted as differences occurring between ‘Frontenac Gris’ and ‘Marquette’ (Table 31). The axis was positively associated with ‘Marquette’ while negatively associated with ‘Frontenac Gris’ and was relatively unassociated with ‘St. Croix’. The second retained axis related to differences in the responses of ‘St. Croix’ and the remaining two cultivars. This axis was positively associated with ‘St. Croix and was negatively associated with ‘Marquette’ as well as ‘Frontenac Gris’.

Table 31. Tucker scores for cultivars along the two retained axes.

Cultivar	Axis 1	Axis 2
‘Frontenac Gris’	<b>-0.6221</b>	<b>-0.5288</b>
‘Marquette’	<b>0.7690</b>	<b>-0.2743</b>
‘St. Croix’	-0.1469	<b>0.8032</b>

Bolded values relate to contrasting associations within each retained axis.

### Traits.

The second mode relating to the measured traits was reduced from twelve original dimensions to five retained axes (Table 32). The first retained axis was interpreted as tissue maturation. Periderm development as well as number of mature buds were associated with the axis. This tended to contrast measures of vine growth as well as berry size and quality parameters.



The second retained axis was interpreted as progress toward tip abscission as it was negatively associated with the trait. The axis was also negatively associated with berry size, both weight and diameter, and was inversely related to berry total soluble solids and berry pH as well as the number of lateral shoots. The third axis was negatively associated with the number of mature nodes and titratable acidity which contrasted tip abscission progress and berry pH and soluble solids. The fourth axis generally contrasted berry size with titratable acidity and tip abscission progress. Lastly, the final axis contrasted bud maturation, berry diameter, and berry pH with berry titratable acidity, berry weight, and periderm development.

Table 32. Tucker loadings for measured traits along the five retained axes.

Trait	Axis 1	Axis 2	Axis 3	Axis 4	Axis 5
Stem Length (cm)	-0.161	0.140	0.022	-0.120	0.000
Number of Nodes (#)	-0.136	0.218	-0.092	-0.113	0.004
Mature buds (#)	<b>0.503</b>	-0.029	<b>-0.493</b>	0.012	<b>0.483</b>
Lateral Shoots (#)	-0.213	<b>0.316</b>	-0.185	-0.083	-0.070
Tip Abscission Progress (0-5)	0.090	<b>-0.582</b>	<b>0.374</b>	<b>-0.561</b>	0.216
Periderm (cm)	<b>0.437</b>	0.083	0.288	0.169	-0.278
periderm (# nodes)	<b>0.470</b>	0.043	0.062	0.281	-0.246
Berry wt. (g)	-0.234	<b>-0.415</b>	0.112	<b>0.341</b>	<b>-0.366</b>
Berry dia. (cm)	<b>-0.357</b>	<b>-0.332</b>	-0.216	<b>0.504</b>	<b>0.332</b>
pH	-0.135	0.270	0.255	-0.069	0.289
Soluble solids (brix)	-0.158	<b>0.353</b>	<b>0.358</b>	0.047	0.122
Titratable Acidity (g/L)	-0.107	-0.064	<b>-0.485</b>	<b>-0.408</b>	<b>-0.485</b>

Bolded values relate to contrasting associations within each retained axis.

#### Photoperiodic time.

The original five photoperiodic times were reduced to a set of four orthonormal axes (Table 33). Axis 1 was determined to represent general progress through time. The axis was negatively associated with long-day photoperiods, and transitioned to positive associations with the short-day photoperiods later in the season. The axis had its strongest negative and positive associations at 14.0 and 12.5h of daylight, respectively. The second axis was related to differences early in the

season as 14.5h of daylight was most negatively associated with the axis and 13.5h was most positively associated with the axis. The third retained axis was parabolic and spanned the middle portion of the season, with 14.0 and 13.0h being most positively associated and 13.5h being most negatively associated with the axis. The final axis was also parabolic and spanned the later portion of the season from 14.0 to 12.5h of daylight.

Table 33. Tucker loadings for photoperiodic times along the four retained axes.

Photoperiodic Time (hours of daylight)	Axis 1	Axis 2	Axis 3	Axis 4
14.5	<b>-0.444</b>	<b>-0.682</b>	-0.260	0.265
14.0	<b>-0.483</b>	0.216	<b>0.461</b>	<b>-0.555</b>
13.5	-0.106	<b>0.669</b>	<b>-0.505</b>	0.294
13.0	<b>0.404</b>	-0.002	<b>0.609</b>	<b>0.516</b>
12.5	<b>0.629</b>	-0.201	-0.306	<b>-0.520</b>

Bolded values relate to contrasting associations within each retained axis.

### Environments.

The original five test environments were reduced to four orthogonal axes. The first axis contrasted the locations observed in 2013 (Table 34). The second axis largely contrasted the years of the experiment, identifying differing trends between 2012 and other years. The third axis contrasted

Table 34. Tucker loadings for phenotypic environments along the four retained axes.

--- Environment ---		Axis 1	Axis 2	Axis 3	Axis 4
Year	Location				
<i>2012</i>					
	Absaraka, ND	0.179	<b>0.625</b>	<b>0.534</b>	<b>-0.304</b>
	Wyndmere, ND	0.069	<b>0.418</b>	<b>-0.751</b>	0.239
<i>2013</i>					
	Absaraka, ND	<b>0.683</b>	<b>-0.504</b>	0.129	0.251
	Wyndmere, ND	<b>-0.643</b>	-0.136	0.300	<b>0.538</b>
<i>2014</i>					
	Absaraka, ND	-0.288	<b>-0.403</b>	-0.212	<b>-0.714</b>

Bolded numbers relate to contrasting associations within each retained axis.

the locations in 2012, while the final axis contrasted the commonalities among the Absaraka, ND locations in 2012 and 2014 with that of the Wyndmere, ND location in 2013.

Inter-connections among modes.

When plotted core-array eigenvalues were investigated, it was determined that four combinations of mode axes contributed greatest to the solution (Table 35-36). Both cultivar axes were represented as the contrast between ‘Frontenac Gris’ and ‘Marquette’ contributed greatest along photoperiodic time axis 1, trait axes 1 and 2, and environmental axes 1 and 2 while the contrast of ‘St. Croix’ with the two remaining cultivars contributed greatest to the variation of the dataset along photoperiodic time axes 1, trait axes 1 and 2, and environmental axes 1 and 2. The single combination contributing greatest to the dataset was the contrasts of linear time trends between ‘Marquette’ and ‘Frontenac Gris’ in tissue maturation among the trial locations in 2013.

Table 35. Tucker core-array singular-values of the reduced four-way cultivar-by-trait-by-photoperiod-by-environment interaction.

Axis combination			Trait Axis				
Photoperiod	Environment	Cultivar	1	2	3	4	5
1	1	1	<b>-1.854</b>	-0.608	0.314	-0.023	-0.022
1	1	2	<b>-0.846</b>	0.333	-0.037	-0.447	-0.258
1	2	1	<b>0.895</b>	<b>-0.713</b>	-0.279	-0.088	0.241
1	2	2	-0.503	<b>0.720</b>	-0.608	-0.300	0.483
1	3	1	0.164	0.632	-0.122	-0.086	0.253
1	3	2	-0.455	0.428	-0.072	-0.185	-0.087
1	4	1	0.043	-0.059	-0.172	0.252	-0.085
1	4	2	0.066	0.150	-0.423	-0.213	-0.280
2	1	1	0.205	-0.669	-0.337	-0.162	0.036
2	1	2	0.513	0.221	0.437	0.261	-0.089
2	2	1	0.427	-0.342	0.197	-0.489	0.023
2	2	2	-0.117	0.502	0.543	0.447	0.270
2	3	1	-0.175	0.048	-0.559	0.585	-0.227
2	3	2	0.309	0.105	0.229	0.025	-0.026
2	4	1	-0.386	-0.112	0.048	-0.033	0.093
2	4	2	-0.060	-0.135	-0.213	0.086	0.073
3	1	1	-0.110	-0.040	0.259	-0.290	0.039
3	1	2	-0.561	-0.200	-0.008	0.116	0.283
3	2	1	-0.475	-0.331	0.119	0.337	0.187
3	2	2	0.101	0.197	0.558	-0.127	-0.235
3	3	1	-0.295	0.146	-0.230	0.190	0.034
3	3	2	0.113	0.113	0.032	0.137	0.311
3	4	1	0.085	0.085	-0.112	-0.116	-0.054
3	4	2	-0.040	-0.065	-0.011	0.074	0.154
4	1	1	0.101	0.081	0.096	-0.091	0.019
4	1	2	-0.028	0.179	-0.254	0.257	-0.012
4	2	1	0.027	-0.100	0.109	0.041	0.071
4	2	2	-0.435	-0.120	-0.258	0.086	-0.248
4	3	1	-0.062	-0.243	-0.190	0.034	0.042
4	3	2	-0.040	-0.039	0.120	-0.218	0.489
4	4	1	-0.140	-0.289	-0.063	0.053	0.239
4	4	2	0.081	0.103	-0.097	-0.009	-0.226

Bolded values indicate the highest five component combination weights.

Table 36. Tucker core-array eigenvalues of the reduced four-way cultivar-by-trait-by-photoperiod-by-environment interaction.

Photoperiod	Axis combination		Trait Axis				
	Environment	Cultivar	1	2	3	4	5
1	1	1	<b>3.438</b>	0.370	0.098	0.001	0.001
1	1	2	<b>0.716</b>	0.111	0.001	0.200	0.067
1	2	1	<b>0.801</b>	<b>0.508</b>	0.078	0.008	0.058
1	2	2	0.253	<b>0.519</b>	0.370	0.090	0.233
1	3	1	0.027	0.399	0.015	0.007	0.064
1	3	2	0.207	0.183	0.005	0.034	0.008
1	4	1	0.002	0.003	0.029	0.063	0.007
1	4	2	0.004	0.022	0.179	0.045	0.078
2	1	1	0.042	0.447	0.114	0.026	0.001
2	1	2	0.263	0.049	0.191	0.068	0.008
2	2	1	0.182	0.117	0.039	0.239	0.001
2	2	2	0.014	0.252	0.294	0.200	0.073
2	3	1	0.031	0.002	0.312	0.342	0.051
2	3	2	0.095	0.011	0.052	0.001	0.001
2	4	1	0.149	0.013	0.002	0.001	0.009
2	4	2	0.004	0.018	0.045	0.007	0.005
3	1	1	0.012	0.002	0.067	0.084	0.002
3	1	2	0.314	0.040	0.000	0.013	0.080
3	2	1	0.226	0.109	0.014	0.114	0.035
3	2	2	0.010	0.039	0.312	0.016	0.055
3	3	1	0.087	0.021	0.053	0.036	0.001
3	3	2	0.013	0.013	0.001	0.019	0.097
3	4	1	0.007	0.007	0.013	0.013	0.003
3	4	2	0.002	0.004	0.000	0.005	0.024
4	1	1	0.010	0.007	0.009	0.008	0.000
4	1	2	0.001	0.032	0.065	0.066	0.000
4	2	1	0.001	0.010	0.012	0.002	0.005
4	2	2	0.189	0.014	0.067	0.007	0.061
4	3	1	0.004	0.059	0.036	0.001	0.002
4	3	2	0.002	0.002	0.014	0.047	0.239
4	4	1	0.019	0.083	0.004	0.003	0.057
4	4	2	0.007	0.011	0.009	0.000	0.051

Bolded values indicate the highest five component combination weights.

*Temperature conditions.*

To determine any relationship that existed among environmental axes and ambient conditions, temperature was tracked throughout the data collection period. The Tucker model was used to reduce the 40x5x3 dimensioned dataset to size 3x2x2 while retaining 94.71% of the original variation.

Time.

Time points, as seven-day moving averages, were reduced to three axes contributing 64.99%, 26.16%, and 3.56% of the total variance, respectively (Fig. 22). The first axis largely defined contrasts between temperature regimes of mid-August with those of periods during late-August and mid-September. The second axis generally was negatively associated with conditions of early to mid-August as well as for periods of early and mid-September and was positively associated with time periods of mid-August and mid-September. The final axis was positively related with the period from early-August, late-August and mid-September, while it was negatively associated with times in mid-August, late-August, and early-September.

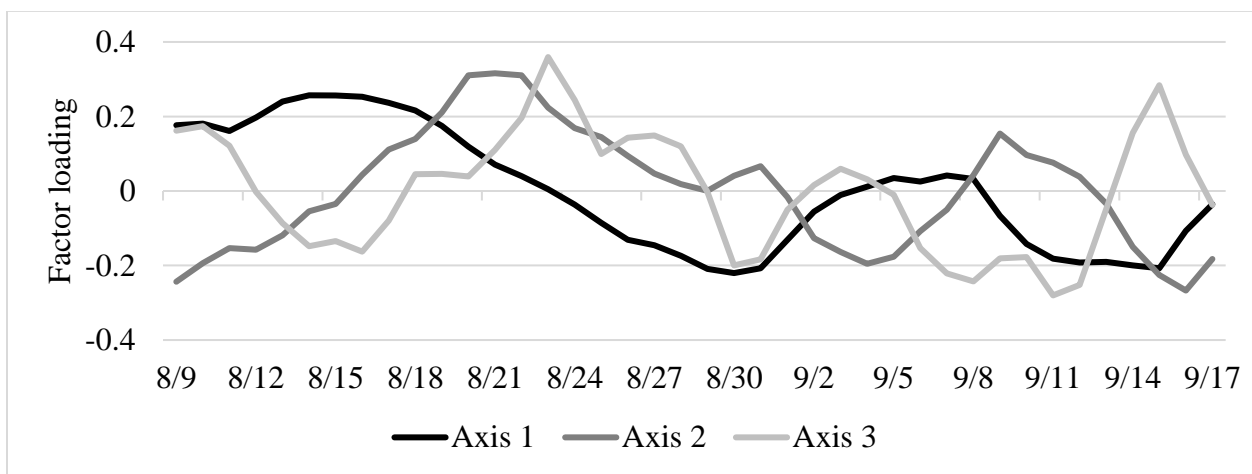


Figure 22. Temperature time-axes loadings across the 40 evaluated dates.

Temperature parameters.

The three tested parameters of temperature were reduced to two axes contributing 80.73% and 14.00% of the variance of the dataset, respectively (Table 37). All temperature parameters were negatively associated with the first axis; thus the axis was considered the overall mean temperature effect. The second axis contrasted daily high temperature and daily minimum temperature while it was relatively unassociated with daily average temperature. Positive and negative values along the axis indicate relatively lower or greater than average daily range in temperature, respectively. Jointly, this was interpreted as the rate of temperature change through time as periods of temperature increase or decrease related to greater or lower daily minimum or maximum temperatures when compared with the alternate parameter.

Table 37. Tucker loadings for temperature parameters along the two retained axes.

Year	Axis 1	Axis 2
Daily Minimum	<b>-0.630</b>	<b>0.675</b>
Daily Average	<b>-0.758</b>	-0.079
Daily Maximum	<b>-0.518</b>	<b>-0.733</b>

Bolded numbers relate to minimum and maximum associations within each retained axis.

Environments.

The five tested environments were reduced to a subset of two axes contributing to 57.43% and 37.28% of the total variance, respectively (Table 38). The first axis characterized the differences between the conditions of Absaraka, ND in 2014 with those of other environments, particularly those of 2013. The second axis contrasted the temperature regime found in either location in 2012 and with that of other years.

Table 38. Tucker loadings for temperature environments along the three retained axes.

--- Environment ---			
Year	Location	Axis 1	Axis 2
<i>2012</i>			
	Absaraka, ND	-0.071	<b>0.509</b>
	Wyndmere, ND	-0.103	<b>0.570</b>
<i>2013</i>			
	Absaraka, ND	<b>-0.310</b>	<b>-0.453</b>
	Wyndmere, ND	<b>-0.380</b>	<b>-0.398</b>
<i>2014</i>			
	Absaraka, ND	<b>0.863</b>	-0.228

Bolded numbers relate to minimum and maximum associations within each retained axis.

Inter-connections among modes.

Three combinations of axes among the three modes contributed greatest to the overall variation of the dataset (Table 39). Two of these combinations were found to be related to the overall temperature. The highest contributing combination of axes related the contrasts in overall temperature of 2014 with those in other years during early through mid-August with those in late-August and mid-September. Alone this combination contributed to 53.50% of the variation that existed in the data. The second combination of axes that contributed greatly to the dataset related the trend of overall temperature and contrasted environments in 2012 with other environments in their temperatures during early-August as well as for periods of early and mid-September with times of mid-August and mid-September. The final axis contrasted 2012 with other years in daily temperature transitioned from times in early to mid-august to those in late-August and mid-September. Overall, the majority of differences of temperature patterns among the tested environments related to how overall temperature transitioned from late-summer to early-fall. Generally, differences in shifts of temperatures were among particular years, with less emphasis being placed on differences between the test locations. While most of the variance in the dataset



was attributed to trends of overall temperature, at times the daily range in temperature was important. In particular, differences between minimum and maximum temperatures between 2012 and other tested years.

Table 39. Temperature core-array of relationships among time, temperature parameter, and environment axes.

Parameter	Time	----- Environment -----			
		Axis 1	Axis 2	Axis 1	Axis 2
<i>Axis 1</i>		----- Weight -----		----- Sq. weight -----	
	Axis 1	<b>-33.99</b>	-5.66	<b>1155.29</b>	32.02
	Axis 2	-4.79	<b>22.82</b>	22.98	<b>520.68</b>
	Axis 3	-3.01	-1.82	9.07	3.33
<i>Axis 2</i>					
	Axis 1	-3.81	<b>14.20</b>	14.48	<b>201.63</b>
	Axis 2	4.46	-1.19	19.87	1.41
	Axis 3	4.29	-6.79	18.42	46.04

Bolded combinations contributed greatest to the variation of the dataset.

*Inter-connections between temperature and phenotypic alterations.*

Through the reductions of both datasets, linkages among phenotypic reactions as well as temperature regimes differences were evaluated through correlation of resulting environmental scores of each model. When the sets of environmental scores were correlated across the two reductions, two combination of axes among the two sets were found to be significant (Table 40). Significant correlation was found between temperature environmental axis 2 and phenotypic environmental axis 2. The similarities among the axes were the contrasts of environments in 2012 with those of other years. The first temperature environmental axis was found to correlate well with the observed phenotypic environmental axis 4. The two axes obtained from differing data sets generally described differences occurring between 2014 and other environments.

While phenotypic environmental axis 1 was found to account for a relatively large portion of the variance that described differences in reactions of the investigated cultivars, no

combinations of axes obtained through the reduction of temperature data were found to correlate. Additionally, while temperature environmental axis 1 contributed greatest to the overall variation in the temperature data, it's associated phenotypic axis contributed very little to the variance of the phenotypic data set. For these reasons, the effect of temperature trend differences on vine responses was determined to be phenotypic environmental axis 2, and will thus it will be discussed further.

Table 40. Correlation coefficients among environmental axes from the reduction of phenotypic and temperature datasets, respectively.

Phenotypic environmental axis	Temperature environmental axis			
	----- 1 -----		----- 2 -----	
	r	p>r	r	p>r
1	-0.236	0.702	0.142	0.819
2	-0.228	0.712	<b>0.930</b>	<b>0.022</b>
3	-0.297	0.627	-0.286	0.641
4	<b>-0.897</b>	<b>0.039</b>	-0.179	0.773

Bolded combinations indicate significant relationships among the dataset axes ( $\alpha = 0.05$ ).

Differences among cultivars in their reactions to differing environments were attributed to temperature trend differences among the tested years, particularly contrasting 2012 with other environments (Fig. 23). These contrasting environments were also associated with contrasting responses in ‘Marquette’ compared with ‘Frontenac Gris’ as well as ‘St. Croix’ with the other tested cultivars. The majority of this response could be categorized into two latent trait trends. The first contrasted the relative rate of tissue maturation with that of shoot growth berry growth and increases in berry pH and soluble solid content. The second trend contrasted the rates of tip abscission and berry growth with the number of lateral shoots as well as berry soluble solid and pH increase. While the majority of differences in temperature trends in 2012 relative to other environments could be attributed to differences in overall temperatures at times during the season, the transition of daily temperature fluctuations from late summer into fall was also important, and tended to be confounded with periods of temperature increase or decreases. It is logical that these

measures are not unrelated as periods of temperature change would also tend to skew relative differences in minimum to average and average to maximum ranges (Fig. 24).

Stem length, number of nodes, and lateral production reacted similarly while tip abscission rate was inversely affected by the contrasting environments (Figs. 25-26). As temperature declined in 2012 relative to other years, 'St. Croix' maintained similar rates of growth, lateral shoot production, and tip abscission across the contrasting climates. The relative rate of growth in 'Frontenac Gris' was higher than 'Marquette' during temperature decline relative to the more static conditions of other years. Tip abscission was found to be reduced in 'Marquette' under these cool conditions relative to the other tested cultivars. As temperature increased in 2013 and 2014 relative to 2012, the rate of growth in 'Marquette' increased relative to other cultivars and was accompanied by a relative reduction in tip abscission progress when compared to other environments. This temperature increase had an opposite effect on 'St. Croix', as tip abscission rate increased relative to other cultivars. This coincided with relatively decreased rates of growth when compared to other cultivars relative to 2012. As temperature cooled in 2013 and 2014 relative to 2012, shoot growth in 'Marquette' continued to increase as shoot growth continued to decrease in 'St. Croix' relative to the mean of cultivars. Late in the season, as temperature rose then fell in most years, while it remained relatively static in 2012, relative growth, in comparison to 2012, was increased in 'Frontenac Gris' relative to other cultivars. This rise in growth was associated with a reduction in tip abscission progress relative to the more static season of 2012.

Differences were seen between the relative reaction trends for periderm development and bud maturation across the contrasting temperature regimes (Fig. 27). As temperature fell in 2012 relative to other years, periderm development increased while bud maturation decreased in 'St.

Croix’ compared with other cultivars relative to other environments. As temperature increased in 2013 and 2014 relative to 2012, bud maturation increased in ‘Frontenac Gris’ relative to other cultivars. During this time, the rate of periderm development continued to increase in ‘St. Croix’ relative to other cultivars in spite of relatively increasing temperature. With increases in temperature, tissue maturation rate decreased in ‘Marquette’ in both bud maturation as well as periderm development while its relative active growth increased and tip abscission decreased in comparison with other cultivars. As temperature began to decrease in 2013 and 2014 relative to 2012, the relative rate of bud maturation increased in ‘St. Croix’, while periderm development slowed in ‘Frontenac Gris’ compared with other cultivars. As temperature increased then decreased rapidly late in the season, bud maturation increased in ‘Frontenac Gris’ relative to ‘St. Croix’, as periderm development occurred more slowly in ‘Marquette’ compared to other cultivars relative to 2012.

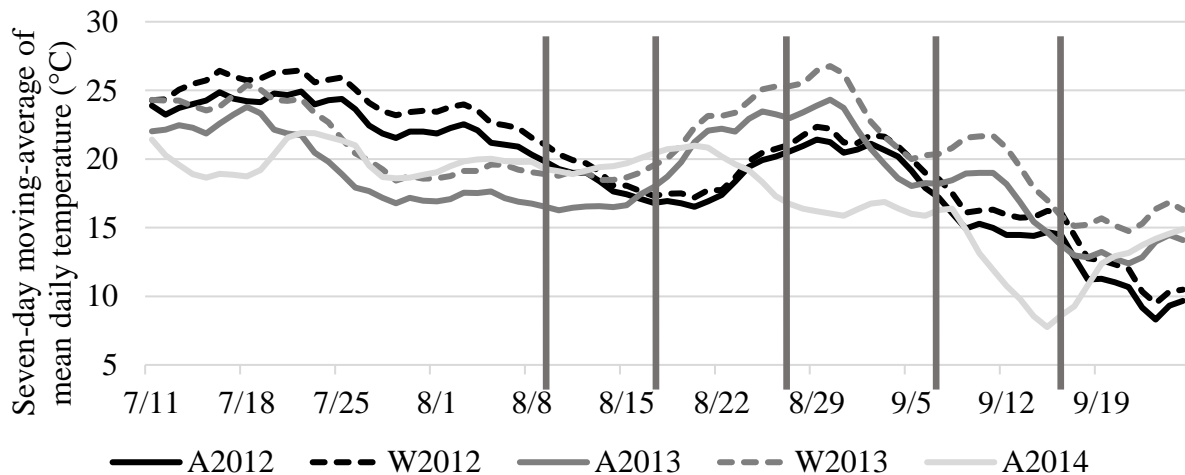


Figure 23. Temperature progress in Absaraka, ND (A) and Wyndmere, ND (W) during the years of 2012-2014. Vertical lines indicate approximate half-hour photoperiodic data collection times 14.5h – 12.5h, respectively.

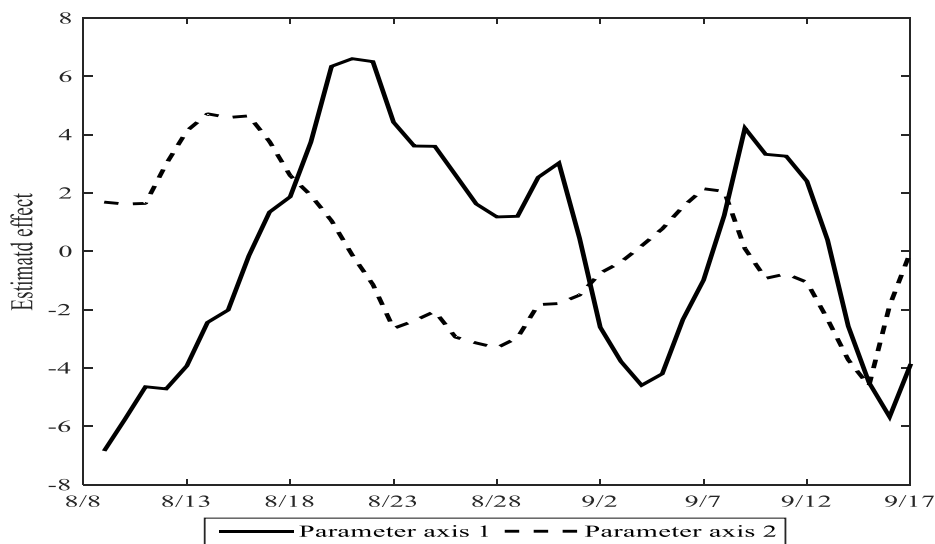


Figure 24. Estimated effect of temperature derived environmental axis 2 for environmental parameter axes 1 and 2 from August, 8 through September, 17.

Differences in berry parameters were also associated with relative temperature trend that occurred among the investigated years (Fig. 28). A decline in berry growth, in both diameter and weight, was associated with early season temperature decline in ‘St. Croix’ compared with other cultivars relative to other environments. As temperature increased between 14.0 and 13.5h of daylight, ‘St. Croix’ had relatively similar rates of berry weight increase across the tested environments, while its relative rate of berry diameter growth decreased. Rising temperature was also associated with increases in berry growth, both in weight and diameter, in ‘Marquette’ relative to other cultivars in contrast with other environments. ‘Frontenac Gris’ maintained relatively similar berry diameter increases across the contrasting environments, however, had a relatively decrease in berry weight during the temperature increase in comparison with other cultivars. As temperature decreased in 2013 and 2014 relative to 2012 between 13.5 and 13.0h of daylight, berry growth decreased in ‘Marquette’ relative to other cultivars. Later in the season, as temperature again peaked then declined relative to 2012, berry diameter increased in ‘Marquette’ while berry weight decreased in ‘Frontenac Gris’ relative to the mean of tested cultivars.

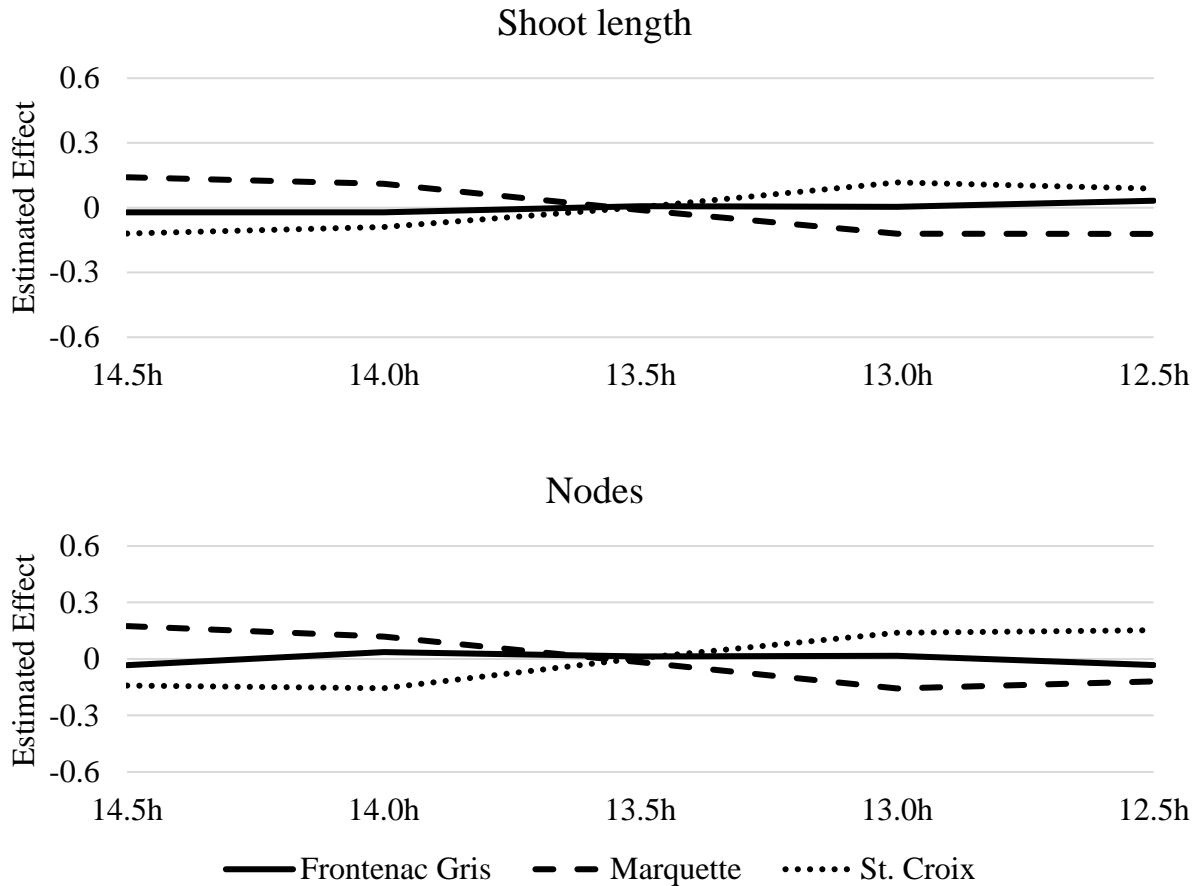


Figure 25. Estimated cultivar four-way interaction effects across photoperiodic time for environmental axis 2 for stem growth characteristics.

Relative trend differences in berry ripening parameters were also found to differ between the contrasting environmental types (Fig. 29). Early fall temperature decline was associated with increased early season ripening in ‘St. Croix’ as berry pH and total soluble solids increased and titratable acidity declined more rapidly in 2012 compared with other cultivars relative to other years. As temperature increased between 14.0 and 13.5h of daylight, rates of ripening became more similar across years in ‘St. Croix’ relative to other cultivars. In ‘Frontenac Gris’ the rate titratable acidity reduction was decreased while relative rates of berry pH increase and soluble solid content accumulation increased in ‘Marquette’ compared with other cultivars in 2013 and

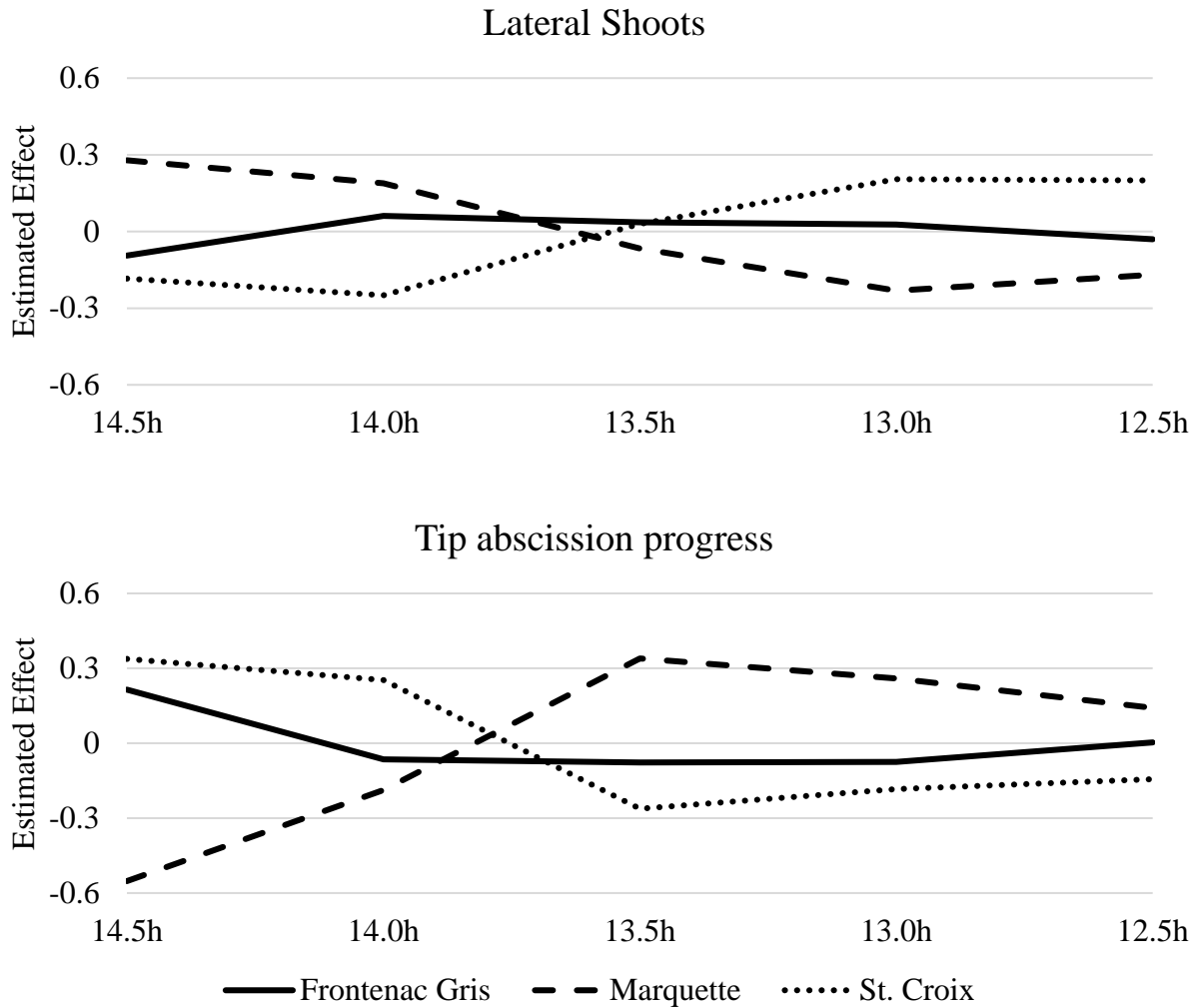


Figure 26. Estimated cultivar four-way interaction effects across photoperiodic time for environmental axis 2 for traits related to growth cessation.

2014 relative to 2012. As temperature decreased in 2013 and 2014 relative to 2012 after 13.5h of daylight, berry pH and soluble solid content continued to increase in ‘Marquette’ relative to other cultivars, while its titratable acidity reduced slowly relative to ‘St. Croix’. Following an increase in temperature after 13.0h of daylight, the rate of titratable acidity reduction was increased in ‘Marquette’ relative to other cultivars, while berry pH and soluble solid content continued to rise compared with environments in 2012. The rise in temperature tended to be associated with slowed titratable acidity reduction and soluble solid accumulation in ‘Frontenac Gris’ compared to the

mean of cultivars, relative to environments of 2012. During this same period acidity reduction was improved in 'Marquette' relative to the mean of cultivars, compared to other environments.

Overall, late summer decline in temperature tended to increase periderm development while reducing bud maturation in 'St. Croix' compared with other tested cultivars. This was associated with a relative berry size decrease and a relative increase in berry ripening in the cultivar compared to others. Similar conditions increased tip abscission rate in 'Marquette' compared with other cultivars, particularly 'Frontenac Gris'. This was associated with a faster rate of growth cessation and reduced bud maturation in 'Marquette' relative to 'Frontenac Gris'. Early season temperature increase was associated with increased active growth and reduced tissue maturation in 'Marquette' compared other cultivars. This was generally associated with reduced tip abscission, increased berry growth, and increased berry ripening rates. Under these same conditions, 'St. Croix' had increased rates of periderm development, increased tip abscission rate, reduced vegetative growth and reduced berry diameter growth relative to the mean of cultivars. Late season temperature decline slowed 'Marquette' berry growth and titratable acidity reduction relative to other cultivars, while 'St. Croix' had increased periderm development, reduced bud maturation, and hastened titratable acidity reduction. Late season temperature increase was associated with increased bud maturation, reduced berry weight, reduced total soluble solid accumulation and slowed titratable acidity reduction in 'Frontenac Gris'; reduced bud maturation and increased periderm development in 'St. Croix' and reduced periderm development, reduced bud maturation, increased berry diameter growth, and increased berry ripening in 'Marquette' compared with the mean of cultivars relative to other environments. Generally, increased temperature tended to reduce rates of measures of acclimation progress in 'Marquette' and



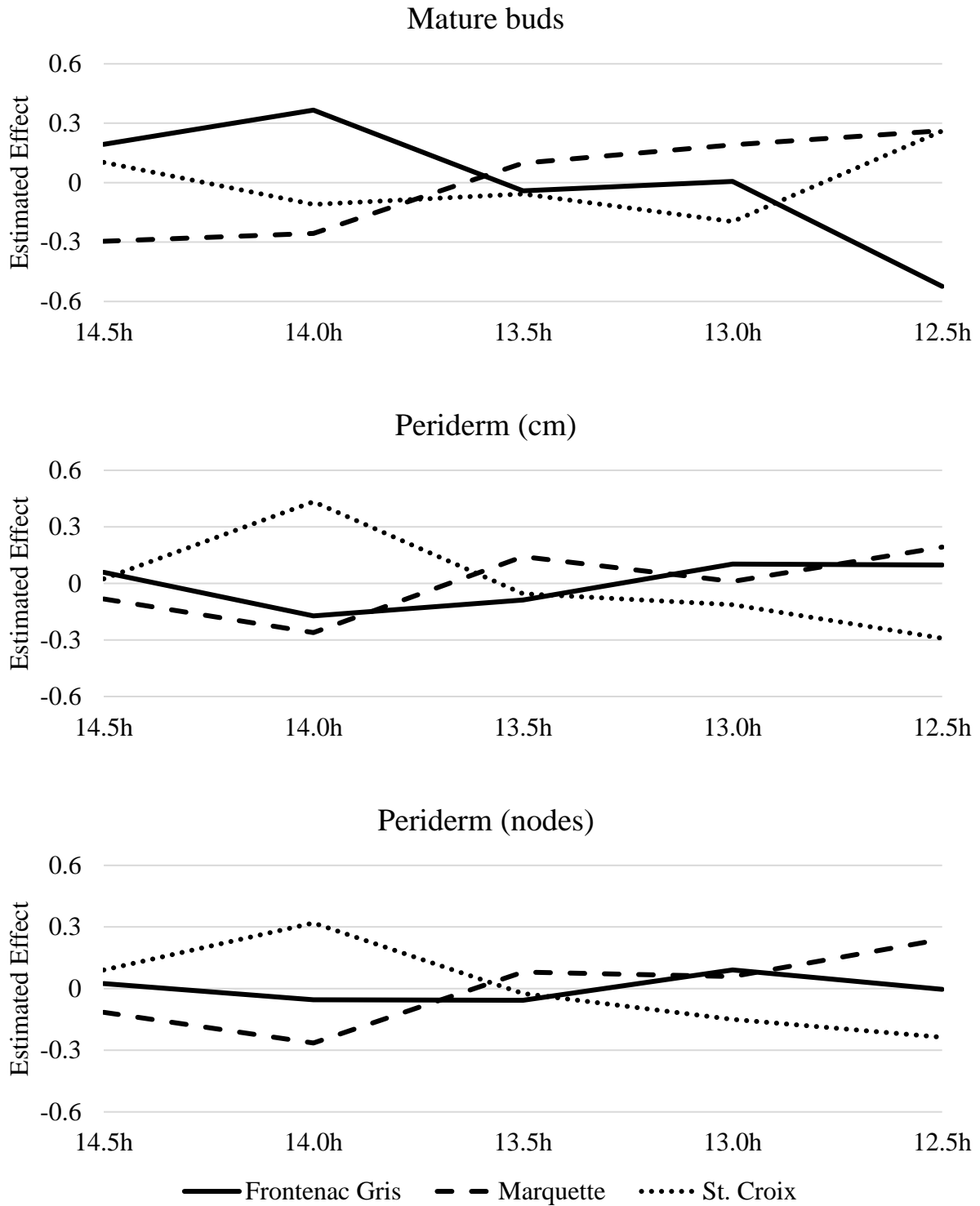


Figure 27. Estimated cultivar four-way interaction effects across photoperiodic time for environmental axis 2 for traits relating to tissue maturation.

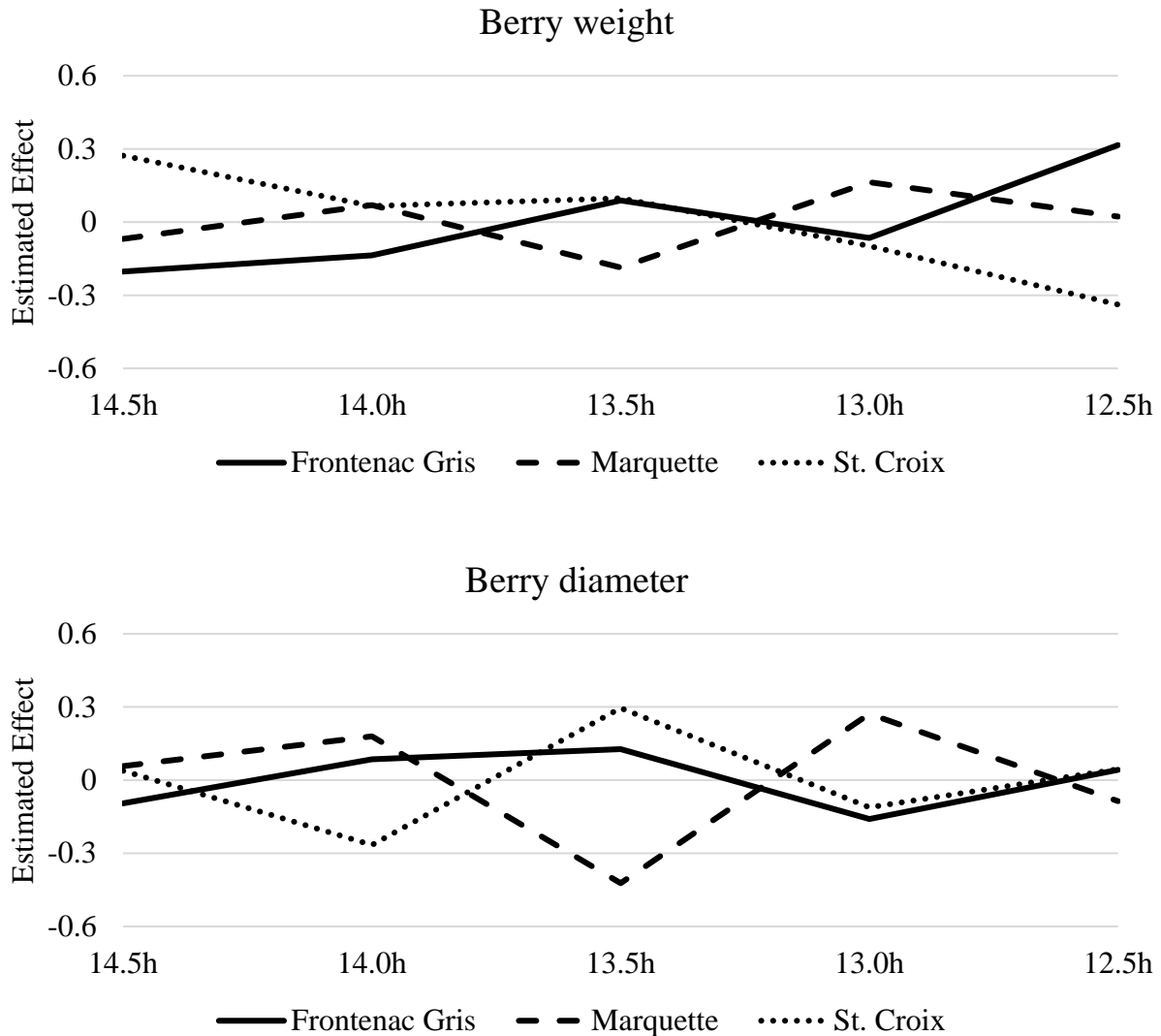


Figure 28. Estimated cultivar four-way interaction effects across photoperiodic time for environmental axis 2 for traits relating to berry growth.

promoted berry ripening, berry growth, and stem growth; while in ‘St. Croix’ increased temperature reduced berry growth, reduced tip abscission rate and promoted periderm development; and in ‘Frontenac Gris’ increased temperature promoted relative bud maturation and decreased the rate of titratable acidity reduction relative to other cultivars. Temperature reductions, tended to have greatest effect on ‘St Croix’ as bud maturation and berry growth were slowed and

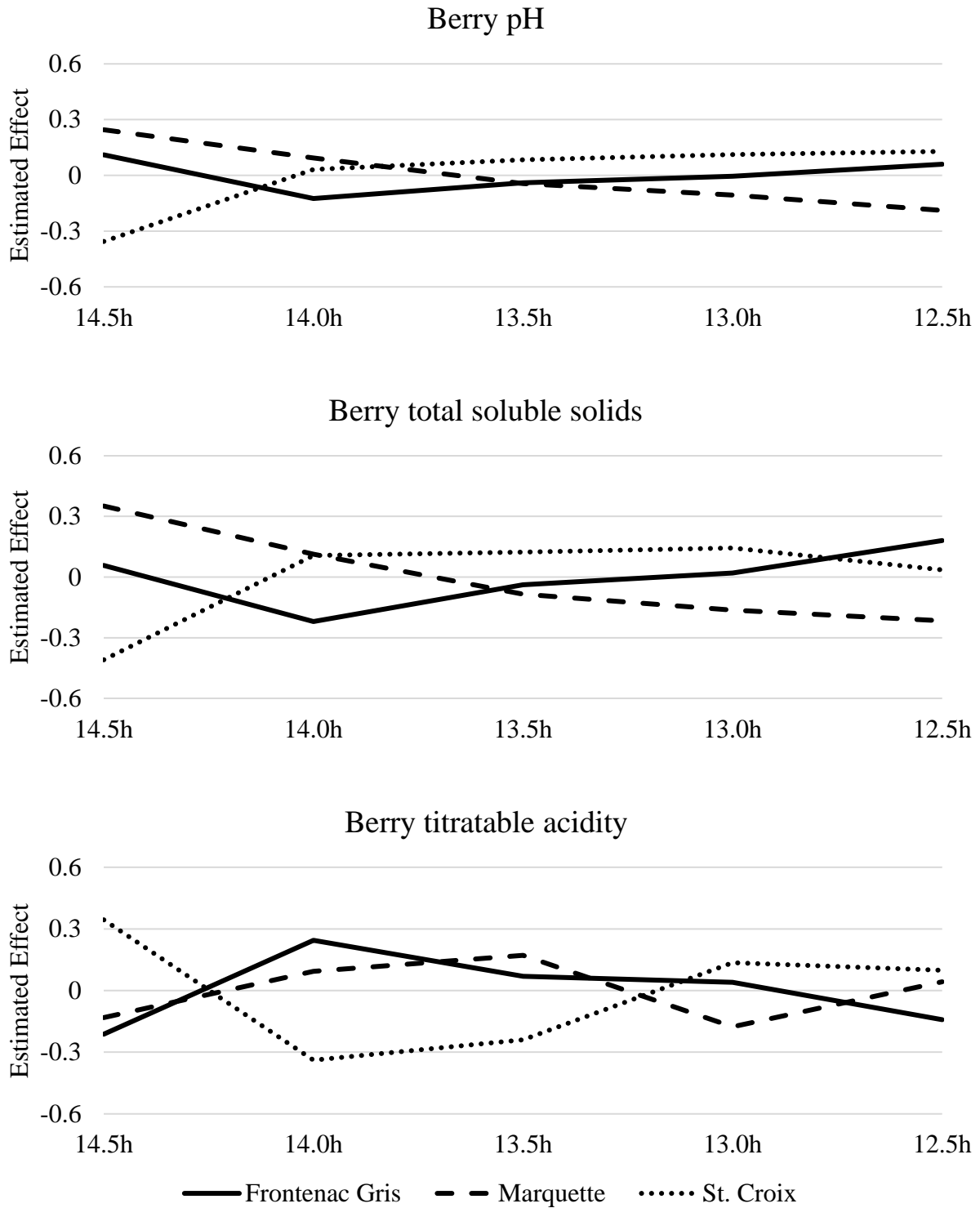


Figure 29. Estimated cultivar four-way interaction effects across photoperiodic time for environmental axis 2 for traits relating to fruit ripening.

periderm development and berry ripening were more rapid compared with other cultivars relative to alternate environments. The other two tested cultivars were affected less by temperature declines as ‘Marquette’ had increased tip abscission progress while ‘Frontenac Gris’ had increased lateral shoot development relative to other cultivars and alternate environments.

## **Discussion**

Though it was demonstrated that the majority of variation in the initiation of growth cessation response in a *V. riparia* based family was attributable to photoperiod through the cessation of lateral shoot emergence, it has been suggested that following growth cessation, bud growth and dormancy induction takes several weeks and is primarily controlled by temperature (Garris et al., 2009; Cooke et al., 2012). The overriding conclusion from this study is that temperature plays an important role in the alteration of tissues in cold-climate grapevines through the transition from summer active growth through preparation for winter conditions. Differences in how contrasting temperature regimes affected differing tissues among cultivars was demonstrated by isolating not only the performance of each cultivars’ traits relative to one another, but also relative to an internal standard through the reduction of the four-way interaction effects among cultivars, traits, photoperiodic times, and environments. Once reduced to relative differences in trait effects, relative vine responses to particular stimuli could be evaluated. A portion of these differences in relative trait trends were found to be associated with temperature trend differences that existed in environments in 2012 when compared with environments of other years. A significant correlation was found among the environmental axes derived from phenotypic trait trends and temperature trends. The effects of differences in daily temperature and relative difference in daily minimum and maximum temperature relative to the daily average temperature

were likely confounded and considered the relative change in temperature among the environmental types. The differences in temperature trend among the environmental types was typified by both the relative difference in temperature as well as the relative skewedness in the relative differences in temperature minimum and maximum relative to the mean temperature. These two effects taken together result in the conclusion that the environmental temperature cue of importance in vine reactions was relative temperature increase or decrease. The current study builds evidence for the importance of temperature change over that of average, minimum, or maximum daily temperature alone.

In general, 'St. Croix', was most reactive to temperature reductions relative to the mean of other cultivars. The cultivar had relatively hastened progress in acclimation under low temperature conditions consistent with a reaction to the presence of a stressor. This response to stress resulted in a relative reallocation of resources to periderm development and fruit ripening at the relative sacrifice of berry growth as well as bud maturation. The reduction in berry growth may suggest an alteration of the vine's translocative source-sink relationships, particularly for water relations. As transpiration potentials are low in sink-organs, their water relations are generally dictated by the phloem (Wang et al., 1997; Lang, 1990; Lang and Thorpe, 1989; Ho et al., 1987). Overall, as a result of its relative responsiveness to temperature declines, 'St. Croix' was considered to be a chilling sensitive cultivar.

The ratio of symplasmic and apoplasmic transport of photoassimilates has been speculated to have a role in stem elongation and evidence has been found that a temporary blockage of symplasmic flow through plasmodesmata is associated with the rapid elongation of cotton (*Gossypium hirsutum*) fibers (Patrick, 1997; Raun et al., 2001). During the onset of fruit ripening, a transition from symplasmic to apoplasmic phloem unloading occurs in grapevine (Zhang et al.,

2006). A similar response was observed by Keller and Shrestha (2014). The ability of vines to utilize symplasmic unloading, however, is not static and maybe dynamically controlled (Patrick, 1997). Xie et al. (2009) demonstrated that root restriction caused an increase in the number of plasmodesmata connections between the sieve element/companion cell complexes and the phloem parenchyma cells in comparison with non-restricted vines. This was noted to potentially increase symplasmic flow under root restriction, leading to an increase in both berry diameter and total soluble solid content during phase III of berry development. From the results of the current study, the onset of fruit ripening was triggered by temperature reduction in ‘St. Croix’ relative to other cultivars and had related responses in other trait characteristics. It is hypothesized that the blockage of symplasmic unloading to the fruits relative to other cultivars may account for the differences progress that occurred under temperature reduction in ‘St. Croix’. Such a transition from symplasmic to apoplasmic phloem unloading may account for the associated reduction in berry growth as water movement was restricted to fruit. Stem color change and maturation has been associated with stem drying as well as increased freezing tolerance (Wolpert and Howell, 1986). Increased periderm development may indicate a restriction of water content in stem tissues. While stem maturation proceeded rapidly under temperature decline, bud maturation was relatively slower in ‘St. Croix’ in comparison with the other tested vines. This may indicate a relatively greater restriction of symplasmic phloem unloading stem tissues relative to buds, and a relatively reduced ability to mature buds when compared to other cultivars under temperature reduction. In general, shoot tip growth was also relatively unaffected compared with other cultivars suggesting that particular tissues had differential responses to temperature decline, potentially having differing degrees of plasmodesmata restriction and subsequent blockage.

'Frontenac Gris' had contrasts with 'St. Croix' in its signaling of a stress response under periods of relative temperature reduction and differed in its relative allocation of resources under such conditions. While 'St. Croix' comparatively sacrificed bud maturation and berry growth to allow for periderm development and continued fruit ripening, 'Frontenac Gris' had slowed rates of titratable acidity reduction and periderm development to enable continued shoot and berry growth along with an increased bud maturation rate. While the cultivar did react through the reallocation of resources, this reallocation was differentially expressed. It was hypothesized that symplasmic flow continued in fruits under the temperature decline as berry size continued to increase relative to other cultivars and that this was due to continued symplasmic phloem unloading as plasmodesmata were less constricted under the temperature decline. Dormancy and hardiness of primary buds has been associated with decreasing water content (Fennell and Wake, 1996; Wolpert and Howell, 1985). This may allude to an overall relative greater propensity to restrict symplasmic flow or overall reduced plasmodesmata porosity to resting buds in 'Frontenac Gris' relative to other cultivars, as the drying of tissue would speed maturation relative to other cultivars. It was also hypothesized that continued symplasmic phloem unloading to other sink regions of the vine, meristem regions and fruits, allowed for continued tip elongation and berry size increase as turgor and flow of photosynthates were maintained. This was at the detriment of stem maturation, as the continued flow of photosynthates to stem tissues did not allow drying and maturation of stem tissues. This may allude to a differential effect on or size of plasmodesmata among the two contrasting cultivars in differing tissues.

Alternatively, 'Marquette', under temperature reduction, tended to sacrifice periderm development, shoot growth, and berry maturation in order to enable berry growth and tip abscission. Under the current hypothesis of differential phloem unloading among the investigated

cultivars, this would allude to a differential response or porosity difference in plasmodesmata among ‘Marquette’ sink organs in contrast with other cultivars. Stem elongation zones have been associated with the effects of both symplasmic and apoplasmic phloem unloading, possibly indicating a dynamic role of both unloading methodologies (Patrick, 1997). The restriction in cell elongation relative to other cultivars may be indicative of reduced symplasmic unloading to meristematic regions as an associated reduction in turgor may have inhibited cell expansion. In contrast, ‘Marquette’ berry size was comparatively increased relative to ‘St. Croix’ under such conditions, alluding to continued symplasmic flow to fruits accompanied by increased sugar accumulation. As with ‘Frontenac Gris’, stem tissues did not mature as rapidly as seen in ‘St. Croix’ under the reduced temperatures. Evidence for combined apoplasmic and symplasmic transport in mature stems also exists, with irreversible symplasmic isolation under low source-to-sink ratio conditions (Patrick, 1997). The loss of symplasmic flow allows carbohydrate loading of the tissues. This may lend to less acclimated stem tissues when compared with ‘St. Croix’ following temperature decline.

Under relative temperature increases, ‘Marquette’ was highly responsive compared to the other tested cultivars. These conditions were associated with a reallocation of physiological resources for continued vegetative growth, berry growth and berry ripening at the relative sacrifice of periderm and bud maturation. Under the current hypothesis of symplasmic unloading alterations, these reactions would be consistent with a return of symplasmic flow to sink organs upon the return of warm conditions. In maize, differing genotypes were found to be non-responsive or responsive in plasmodesmata relaxation with a return to warm temperatures following exposure to cool conditions and were referred to as chilling-sensitive (non-responsive) and chilling-tolerant (responsive) types (Bilska and Sowiński, 2010). This may demonstrate a chilling-tolerant type



reaction in ‘Marquette’, showing greater than average increase in activities associated with active symplasmic flow relative to those associated with blockage of plasmodesmata. Fruit expansion as well as soluble solid accumulation were similar to the effects of root restriction as described by Xie et al. (2009), where the number of plasmodesmata were increased over that of controls having less root restriction. In either case, relative berry expansion as well as berry ripening continued together, possibly illustrating continued symplasmic unloading alongside the initiation of apoplasmic unloading of solutes in a dynamic system.

Under the hypothesis of transition from symplasmic to apoplasmic unloading as the cause of the differences in investigated vines, ‘Frontenac Gris’ and ‘St. Croix’ had commonalities in the signaling of tissue maturation in the presence of temperature decline; however, the tissues affected by chilling induced restrictions of water flow differed among the two cultivars. Generally, ‘St. Croix’ tended to have contrasting reactions to ‘Marquette’ in stem growth, periderm development and berry diameter growth. ‘Frontenac Gris’ tended to differ from ‘Marquette’ in bud maturation, berry weight increase, and titratable acidity reduction. In either case, it was hypothesized that the cultivars were unable to return to symplasmic phloem unloading as temperatures increased, a common contrast from that of ‘Marquette’ which generally resumed active growth under periods of temperature increase.

Investigations into other woody plants, *Populus* and *Betula*, have provided evidence that increased temperature led to increased depth of dormancy (Kalcsits et al., 2009; Junttila et al., 2003). In the current study, temperature increases tended to impacted cultivars differently. Increases in temperature were associated with a reduction in progress in ‘Marquette’ toward tissue maturation as well as increases in traits indicative of active growth, while ‘St. Croix’ had accelerated rates of periderm development, and ‘Frontenac Gris’ had accelerated rates of bud

maturation. In *Populus* spp., Tanino et al. (2010) described an amplification of dormancy response in northern adapted types relative to those of southerly populations with increased temperature. While ‘St. Croix’ and ‘Frontenac’ continued respective indicators of tissue maturation consistent with progression to winter dormancy during periods of temperature increase, ‘Marquette’ had relatively reduced rates of dormancy related responses including tip abscission rate, growth cessation, and tissue maturation under similar conditions, suggesting similar contrasts to the northerly and southerly adapted ecotypes of *Populus*, respectively.

The perceived relative requirement for temperature decline of ‘St. Croix’ to signal increased maturation of tissues was more similar to the induction process found in members of Rosaceae (*Malus* and *Pyrus*). Within these species, alterations in photoperiod was not influential in acclimation response, however reduced temperatures were relied upon for induction signaling (Heide and Perstrud, 2005). Investigations into *Prunus* resulted in the most similar results as presented here. Through the investigation of several *Prunus* species, Heide (2008) found that under warm conditions (21°C) all species tested (*P. cerasus*, *P. insititia*, and *P. avium*) were not reactive to reductions in photoperiod as they maintained continuous growth. However, under reduced temperatures, diverse responses were found from those that overcame long-day conditions to the need of cold temperatures even under short-day conditions for cessation of growth.

The current study also had commonalities with previously described alterations related to ABA influence. Berry weight and volume were shown to be increased by high temperatures (Greer and Weston, 2010). High temperatures have also been suggested to decrease the percent soluble solids as well as titratable acidity while low temperatures increased soluble solid content and decreased titratable acidity (Greer and Weston, 2010; Carbonell-Bejerano et al., 2013; Mori et al., 2005). The positive effects of low temperatures have been linked with ABA concentration

increases (Kuhn et al., 2013). It has also been shown that exogenous ABA can induce a delay of bud break and influence dormancy in *V. vinifera*, while being concentration dependent (Zheng et al., 2015). Ecotypic variation in ABA concentration has also been demonstrated in *Betula pendula*, as ABA concentrations in northern ecotypes were more responsive to low temperatures and short-day conditions in comparison with southerly adapted ecotypes (Li et al., 2002). The authors speculated that these response differences may be important in controlling the rate at which trees are able to acclimate. The current study builds evidence for the causal linkage between superior acclimation adaptive response and low overall quality as well as the genotypic specificity and variation in this response. The amount of ABA or antagonists to the effects and synthesis of ABA within the plant are likely to be involved in the differing responses found in the current study. However, more expansive experiments to directly quantify ABA concentrations in differing tissues would be needed to confirm this speculation.

Overall findings of temperature effects on three cultivars of varying backgrounds and relative success in year-to-year survival, demonstrated differing responses to changing temperatures dynamically through contrasting seasons. ‘St. Croix’ was most greatly affected by cool temperatures and demonstrated reactions consistent with those of reduced water flow and turgor pressure in the sink regions of fruits as well as symptomology of drying and maturing of periderm tissues. Temperature increases had the greatest effect on ‘Marquette’ as it returned to active growth in comparison with the other tested cultivars. It is thought that the causation of these contrasting reactions was related to contrasting phloem unloading methods, cues, and relative reversibility among the tested genotypes. The adaptive response to temperature reduction of ‘Marquette’ was generally limited to reductions in growth and progress toward tip abscission and these responses were found to be reversible as temperatures increased. The other cultivars, at least

in part, were chilling sensitive, as water flow appeared to be restricted to differing organs, and these effects were relatively irreversible under temperature increases. The most adapted type, ‘Frontenac Gris’, demonstrated temperature insensitive response in bud maturation, which was unique from all other cultivars.

The key to the relative regional success of the cultivar ‘Frontenac Gris’ is suspected to be its unwavering promotion of bud maturation at expense of other alterations within the plant. Generally, temperature decreases promoted increased rates of bud maturation relative to other cultivars. Additionally, it was speculated that upon temperature increases, the cultivar was relatively unable to revert back to active symplasmic flow to maturing buds. Alternatively, the susceptibility of ‘Marquette’ and ‘St. Croix’ to continued symplasmic unloading in bud tissue may account reduced regional reliability. Additionally, ‘Marquette’ showed a differential response in its reaction to temperature increases when compared to the other tested cultivars. This may contribute to the cultivar’s stochastic year-to-year production and overwintering ability.

Through the findings of this study, it was hypothesized that the relative success of cultivars in North Dakota was, in part, related to the symplasmic porosity of sink-source relationships among the tested plants. This porosity is likely dictated by the number, size and/or the relative sensitivities to temperature increases or decreases of plasmodesmata leading to differential symplasmic phloem unloading, which differs among tissues within a single vine, while the relative ratios across tissues differs across genotypes. Though much information exists about individual trait responses in individual tissues of specific genotypes, the interrelationships among these tissues has been relatively unexplored. Additionally, the information that does exist is largely restricted to a few individual cultivars. As demonstrated in this current study, the effects of the environment on specific tissues is likely to enact alterations in the effects of the environment on

alternate tissues. Water relations within the plant are dictated by turgor pressure. Relative alterations in flow of the phloem to individual tissues are also likely to alter the relative flow to others. Additionally, these alterations are likely to not conform to a single methodology; however, will likely differ based on the specific genotype investigated. The phenotyping of broad germplasm on the relative reactions to dynamically applied stimuli will likely aid in the identification of dynamically adapted genotypes with necessary reactions to particular stimuli of differing growing regions. Future identification of such genotypes will be imperative to the long-term success and economic stability of wine production in the Northern Plains region of the United States.

**CHAPTER IV. A NOVEL DETERMINATE FORM INTERSPECIFIC GRAPEVINE  
FOR GENETIC AND PHYSIOLOGICAL STUDY AS WELL AS BREEDING  
APPLICATIONS**

**Abstract**

In 2013, a novel genotype of interspecific hybrid grapevine (*Vitis* spp.) was identified in the Agriculture Experiment Station (AES) Research Greenhouse Complex on the North Dakota State University campus. Upon the generation of an S1 population from a single progeny from a ‘Valiant’ x ‘Madeleine Angevine’ population a single mutant form was found. The vine, designated ‘ND Mutant 1’, was identified to be determinate in both growth and reproduction. The vine was vegetatively propagated to generate propagules showing the same unique phenotype as the mother plant, building evidence the phenotype is clonally stable and genetically based. The vine is seedless, thus its use as a seed parent was unsuccessful; however, its use as a pollen parent resulted in progeny. The unique vine’ early and continuous flowering nature may have use in applied breeding to hasten generation cycling time. Future research must confirm heritability of the unique phenotype and further investigate its genetic and physiological basis. It is thought that the likely reason for the unusual phenotype is a mutation in one or more of the previously described flowering related genes which regulate bud set and flowering. In particular, the effects may be related to the FLOWERING LOCUS T, TERMINAL FLOWER 1, LEAFY, and SUPPRESSOR OF OVEREXPRESSION OF CONSTANS 1 gene family of *Arabidopsis*. The answer to these questions may also help to address differences that exist between the vine and shrub functional plant groups as well as flowering initiation and control. *Vitis* ‘ND Mutant 1’ may open new doors as a model organism in woody plant physiology.

## **Introduction**

Within the North Dakota State University grapevine germplasm enhancement project a novel genotype with breeding, genetic, physiological, and taxonomic study implications was discovered. The genotype resulted from self-derived pollination of a vine designated *Vitis* ‘ND 733’ (unreleased) (Fig. 30). The resulting genotype displays a determinate, shrub-like growth and reproductive habit with continuous flowering capabilities (Fig. 31). These properties may have value in foundational research in inflorescence initiation and development as well as in the genetics differentiating determinate shrubs and indeterminate vines. Additionally, the vine may have application in applied breeding of seedless and cold-hardy wine and table grapes. The plant has been successfully replicated through green shoot tip cuttings. The resulting propagules demonstrated the same unique phenotype. Attempts to germinate seed were unsuccessful as seeds of the plant are poorly developed, thus the vine is considered at least semi-seedless. However, the vine’s use as a pollen parent has proven successful, and progeny have been developed. Further investigations will be made into the inheritance of the phenotype. Once inheritance is confirmed further experimentation into causation for the unique phenotype and into its genetic and physiological basis will be conducted.

## **Origin**

The genotype resulted from the self-pollination of a hybrid grapevine designated ‘ND 733’ within the North Dakota State University germplasm enhancement program. ‘ND 733’ is a vine produced by the controlled hybridization of the *V. vinifera*, *V. labrusca* and *V. riparia* hybrid grape ‘Valiant’ with the *V. vinifera* table grape cultivar ‘Madeleine Angevine’. The initial hybridization was conducted to create low acid early maturing white wine grape parents for future breeding

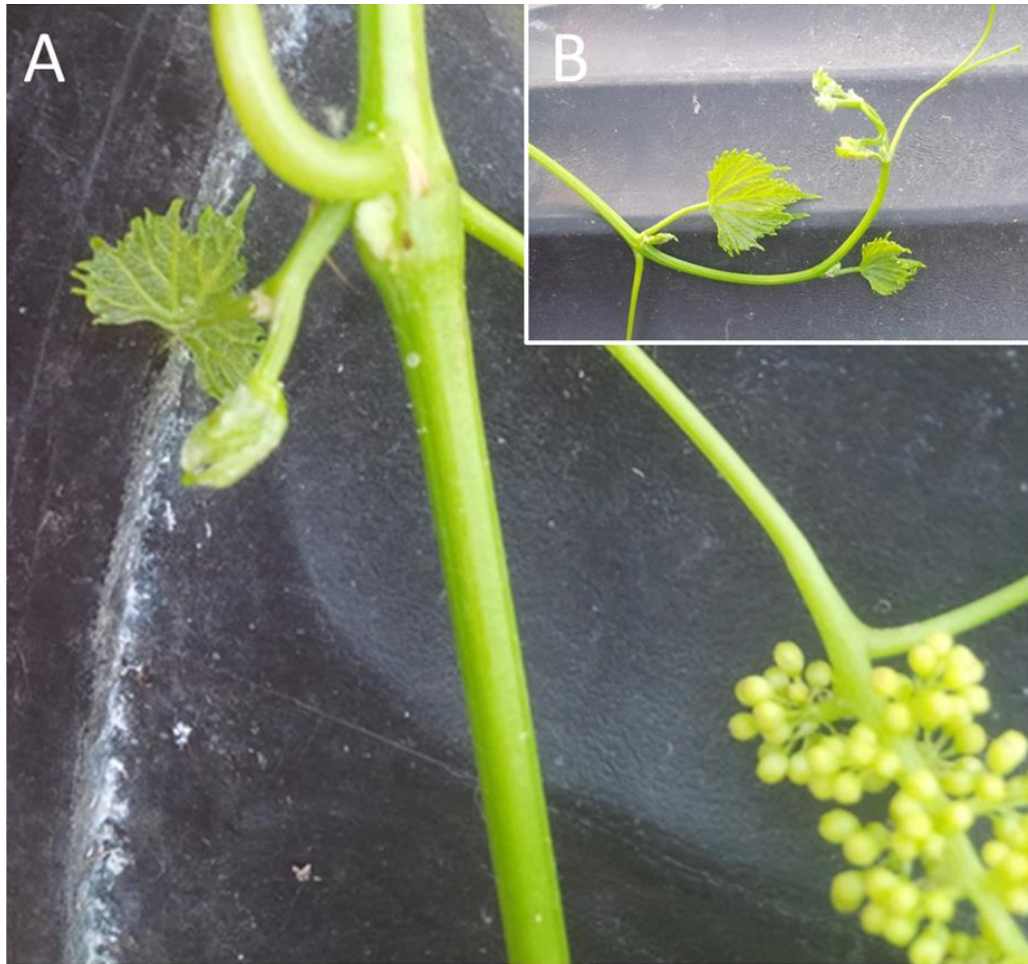


Figure 30. *Vitis* 'ND 733' showing typical A) node and inflorescence development as well as B) tip growth.

efforts for North Dakota. 'ND 733' was further investigated because of its uniquely low initial total titrateable acidity at veraison. With the intention of further improvement, 'ND 733' was self-pollinated to create a S1 population. Within, the resulting S1 population a single shrub-like grape was discovered displaying a determinate growth and reproductive form. This vine's form was thought to be the result of a natural mutation, thus given the designation 'ND Mutant 1'. Within the S1 population many siblings failed to grow due to perceived genetic abnormalities due to inbreeding depression. One sibling of 'ND Mutant 1' was also retained and did not display a determinate habit.





Figure 31. Stem displaying both normal nodes (having leaves, axial, and resting buds), and altered nodes (having leaves, tendrils and inflorescences) on the same plant.

## **Description**

### *Growth habit.*

The plant's shoots initiate normal vine growth through juvenility with nodes of normal appearance containing leaves, axillary buds and dormant resting buds. The vine's leaves are thick in nature and triangular to ovate in shape. The plant produces extensive aerial roots along its trunk and lower stems. After producing several phenotypically normal nodes the vine produces altered

nodes containing only leaves, tendrils, and reproductive inflorescence (Fig. 32). When altered nodes are formed, the reproductive structures are not of typical form. Instead, individual or grouped singly borne flowers are produced in place of lateral and resting buds. This is in contrast to the panicle-type altered tendrils typically seen in *Vitis*. Lastly, stem growth is ceased through conversion of the shoot tip to a tendril, inflorescence-like structure, giving the vine its unique determinate growth and reproductive habit (Fig 33).



Figure 32. Vegetative buds altered to reproductive structures with singly borne flowers.

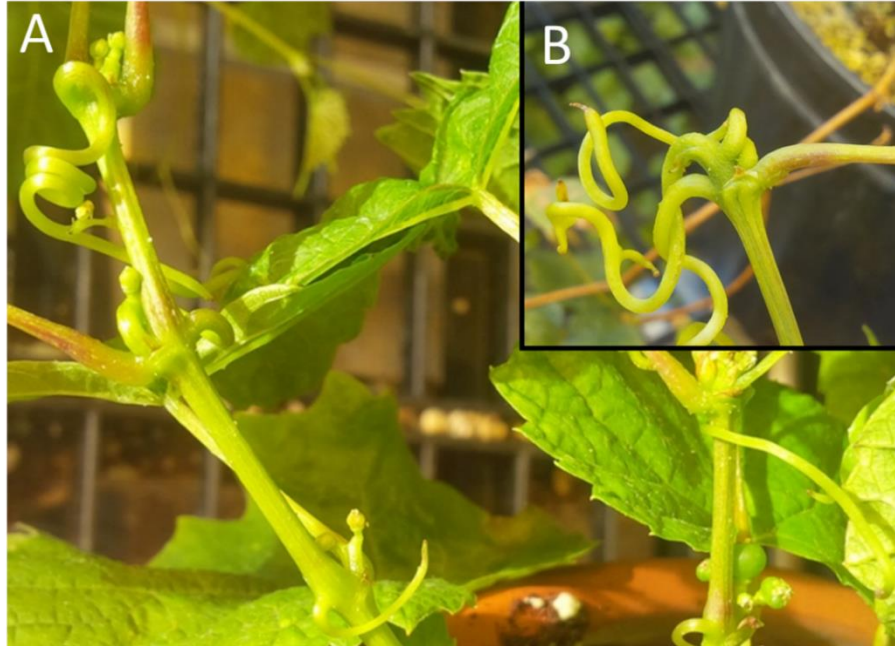


Figure 33. A.) Plant displaying altered form with B.) altered shoot tip.

The plant creates a number resting buds at the base of each new stem. These buds break over time, allowing for continuous growth under favorable conditions. Given proper conditions, the plant grows as a small shrub with waves of new shoots followed by flowering (Fig. 34). This unique growth pattern enables the plant to show all reproductive stages simultaneously from flowering to mature fruit, similar to the mutant *Vitis* ‘Pixie’ derived from the L1 layer from the L1/L2 periclinal chimera *Vitis* ‘Pinot Meunier’ (Boss and Thomas, 2002; Cousins and Tricoli, 2006).

The original vine was vernalized to evaluate its growth following a simulated winter. Through its growth, periderm and resting buds were able to mature allowing for overwintering. After placed in 3°C refrigeration for 45 days, resting buds broke dormancy normally. The shoots formed from resting buds appeared normal in their growth including the creation of relatively normal inflorescences (Fig. 35). However after the initial 4-5 nodes were created shoots again altered, reverting back to a determinate growth habit.



Figure 34. Determinant form vine displaying shrub habit.

### *Reproduction.*

To determine the stability of the phenotype the plant was asexually propagated using green shoot-tip cuttings (Fig. 36). Cuttings were treated with 0.01% indole-3-butyric acid (IBA) with mist and bottom heat in 100% perlite media. During the initial attempt to propagate the vine, two clonal propagules were created from 30 cuttings of the original vine (6.7% rooting success). Many other cuttings initiated roots, however, were unable to grow due to a lack unaltered vegetative nodes. The two resulting clones displayed the same phenotype as the mother plant and demonstrated that the phenotype was at least, in part, genetically and clonally stable. Second and third attempts to propagate cuttings from the determinant form vine and its propagules yielded better results. Out of ten cuttings attempted eight (80%) and seven (70%) initiated roots and seven

(70%) and five (50%) reinitiated vegetative growth. The increase in rooting success was attributed to obtaining cuttings at an earlier growth stage prior to bud morphogenesis into reproductive structures. Through visual inspection it was determined that all propagules maintained the same growth habit as the mother plant. Additionally, budding of the mutant onto rootstock did not cause a reversion to typical *Vitis* vining habit, and vegetative buds continued to be altered to reproductive structures, again confirming the phenotypic stability of the trait.

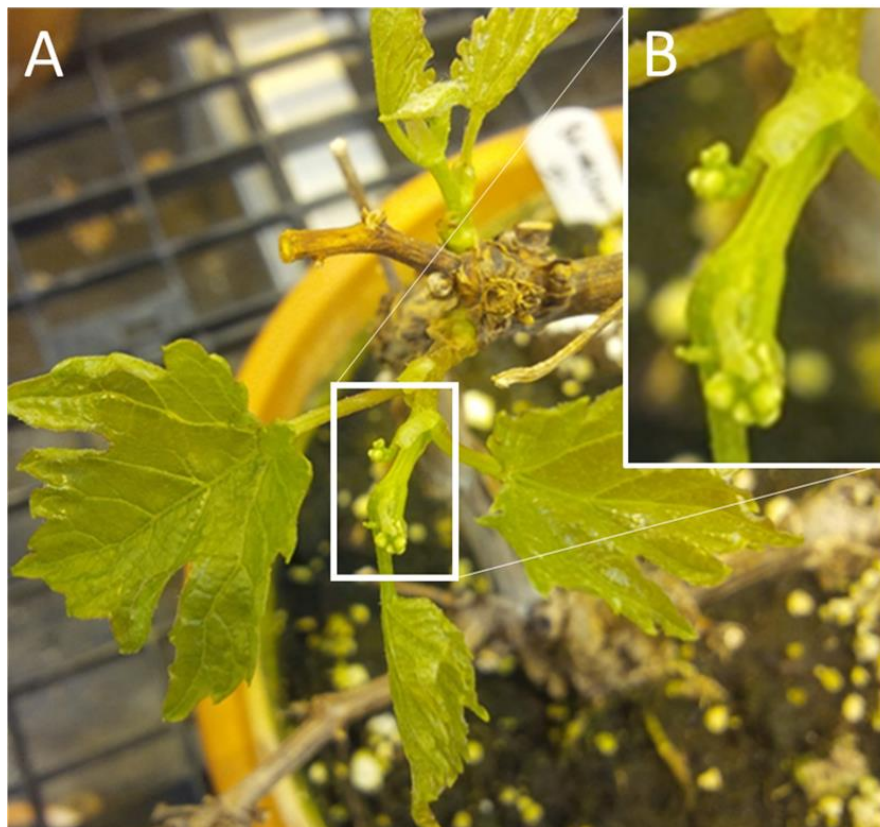


Figure 35. A) Plant resuming growth following induced dormancy, and B) Inflorescence showing normal development.



Figure 36. A) Cuttings of *Vitis* ‘ND Mutant 1’ showing profuse rooting, B) rooted cuttings, and C) propagule showing the same growth habit of the mother vine.

The ability of the plant to produce offspring was also investigated. Mature fruit was harvested. The resulting seeds were found to be underdeveloped and unviable. Through several fruiting cycles, the mother plant nor any propagule has produced fully developed seed, however only seed remnants. Genetic seedlessness cannot be ruled out, as the seedless characteristic is found within the background of one parental type ‘Valiant’. ‘Valiant’ was derived from *Vitis* ‘Fredonia’ pollinated with a *V. riparia* selection from Montana (Hemstad, 2015). ‘Fredonia’ has been shown to be a recessive seedless donor as it was the seed parent of the seedless grapes *Vitis* ‘Einset Seedless’ and *Vitis* ‘Suffolk Red’.

Though being seedless, pollen was collected from ‘ND mutant 1’ following vernalization. A single inflorescence from a pistillate grapevine (Regent x *V. riparia*, Unreleased) was pollinated as well as a single inflorescence from the parent vine ‘ND 733’ was emasculated and pollinated.

The pollination resulted in fruit and seed set producing 38 and 3 seeds, respectively. Seeds were treated with a 48-hour soak in water, followed by a 24-hour soak in a 2:5 solution of 3% hydrogen peroxide to water, followed by a 24-hour soak in 1000ppm gibberellic acid (GA<sub>3</sub>). Seeds were surface sterilized with bleach (0.6% sodium hypochlorite) and stratified for 30 days at 3°C (37.4°F) in moistened vermiculite. Sowing of seeds resulted in 15 and 3 seedlings, respectively.

### **Comparison of growth habit with a wild type S1 sibling**

#### *Materials and methods.*

To compare growth between the mutant and other similar vines, phenotypic measures were evaluated for mutant propagules and an S1 sibling of the same population. Two plants of each of ‘ND Mutant 1’ and an S1 derived sibling were evaluated for each of 5 stems. Each internode was measured to determine differences in internode length. Data was taken for four initial internodes prior to tip morphogenesis in mutant vines. The node at which the apical meristem was lost and a tendril structure was formed was determined by count. Individual stems not showing loss of the apical meristem at the 11<sup>th</sup> node were given a value of 11. The number of vegetative buds altered to inflorescence structures, number of converted flowers per stem, and number of converted flowers per node were also quantified for each vine. Mean values and standard deviations were calculated among sample stems within each genotype for each measure.

#### *Results.*

Measurement of stems were used to quantify differences in growth pattern between the determinant form vine and a wild-type S1 sibling (Table 41). As previously observed, the determinant form vine had abnormalities when compared to the wild type. All determinant form stems lost apical meristems following their conversion to tendril-like structures. The average

period of abscission was between nodes 6 and 7 whereas meristems were maintained past eleven nodes on all wild-type vines' stems. Determinant form vines also tended to convert lateral and resting buds to reproductive structures of singly borne flowers. Investigated determinant form vines' stems had on average 2.4 converted vegetative buds having on average 3.7 flowers per stem with an average of 1.2 singly borne flowers per converted bud, while no converted buds were observed on wild type stems. Additionally, internode length was less in determinant form vines.

Table 41. Effect of determinant form on growth characteristics.

Genotype	Internode length cm	Meristem loss <sup>y</sup> Node	Converted buds #	Converted flowers per stem #	Converted flowers per converted node <sup>x</sup> #
Determinant form	1.65 ± 0.86 <sup>z</sup>	6.6 ± 2.1	2.4 ± 1.8	3.7 ± 3.3	1.2 ± 0.7
S1 sibling	2.31 ± 1.14	11.0 ± 0.0	0.0 ± 0.0	0.0 ± 0.0	0.0 ± 0.0

<sup>z</sup> - mean ± standard deviation.

<sup>y</sup> - stems never losing apical meristems were set to value of 11.

<sup>x</sup> - stems with no converted flowers were set to 0.

### Future study and application

Further study must be done to determine the heritability of the unique determinate phenotype. Upon determination of the heritability of the phenotype, further investigations should be conducted to determine genetic and physiological cause of the accession's determinate nature. Comparisons should be made with the continuous flowering genotype *Vitis* 'Pixie' discovered in 2006. Though both vines exhibit continuous flowering capabilities the phenotypes of each are distinct and oppose one another. In contrast to the current natural mutant, the 'Pixie' vine demonstrates minimal lateral growth, has typical tendril like inflorescence structures, and retains morphologically typical buds. As proposed by Cousin and Tricoli (2006) further application of this genotype into accelerated backcrossing may be possible if the inheritance of the phenotype



could be confirmed. In addition, this discovery coupled with the recent sequencing of the *Vitis vinifera* genome may offer an excellent model organism for genetic and physiological study (Jaillon et al., 2007). In particular, further examination into the FLOWERING LOCUS T (FLT), TERMINAL FLOWER 1 (TFL1), LEAFY (LFY) and SUPPRESSOR OF OVEREXPRESSION OF CONSTANS 1 (SOC1) homologs gene families, previously described in *Arabidopsis* and *Populus* sp., should be considered as the expressed phenotype is more closely associated with their described effects when compared to those of the 'Pixie' phenotype. The overexpression of FLOWING LOCUS T1 (FT1) derived from *Populus trichocarpa* induced greatly changed morphology in plum (*Prunus domestica*) (Srinivasan et al., 2012). These alterations largely coincided with the contrasts between wild-type grapevines and the current determinant form as they resulted in continuous flowering habit and shrub form. Additionally, transformed plums required little to no chilling to promote bud break, the current determinant for maintains continuous growth through recurrent breaking of dormant resting buds without vernalization. TFL1, and its homologs forms of other species, generally opposes the effects of FT, promoting indeterminate growth, as down regulation of the gene results in determinant form as demonstrated in several species (Shannon and Meeks-Wagner, 1991; Pnueli et al., 1998; Repinski et al., 2012; Dhanasekar an Reddy, 2015).

Investigations into the TFL1 gene family in grapevine was initiated in 2006 by Boss et al. where the effects of a TFL1 homolog's effect on floral development was described. Sreekantan and Thomas (2006) also described the VvFT gene and additionally the VvMADS8 gene, a homolog of the SOC1 gene of *Arabidopsis*. The authors described the cycling of expression between VvFT and VvMADS8 as being responsible for induction and expression of flowering. VvMADS8 was found to express highly in axillary buds during the period of flower primordia

initiation while VvFT expression was relatively low. VvFT expression is largely associated with the expression of flowering and fruit development. In 2007, Carmona et al. investigated the genome of *V. vinifera* for possible homologs to LFT and TFL1. Through their research, they identified five relative genes. Three were relatives of the TFL1 gene. VvTFL1A was described to have qualities like TFL1 in meristem maintenance and the inhibition of meristem determination. The authors alluded that the three TFL1-like genes found in the *V. vinifera* genome may offer a redundancy mechanism. It is likely this 'ND Mutant1' is the result of a single or multiple alterations to FLT, TFL1, SOC1 related genes of *Vitis* resulting in a loss of reproductive meristem maintenance through the repression of TFL1-like genes or the over expression of FT1-like genes causing the differentiation of tissues to reproductive meristems prematurely and/or the repression of an undescribed FT2-like gene homolog. Further investigation of this mutant could be highly informative in both the reproductive physiology of grapevine, tissue differentiation, reproductive-vegetative cycling, and indeterminate growth habit of grapevine.

The lack of observable apical bud set is one of the defining characteristics of *Vitis* species and largely enables their vining habit and indeterminate nature. The discovered vine provides an excellent model system for the investigation of the linkage between indeterminate and determinant flowering in a perennial species, distinct from other annual plant based systems. Additionally, the mutant may have application in applied breeding by shortening generation cycle if the heritability of the trait is confirmed.

## CHAPTER V. OVERALL CONCLUSIONS

In the field study, contrasting responses were found in ‘Marquette’ and ‘St. Croix’ with a mediated response in ‘Frontenac Gris’. While ‘Marquette’ was relatively reactive to increases in temperatures, differing tissues of ‘Frontenac Gris’ and ‘St. Croix’ were relatively non-reactive under similar conditions. Temperature decline tended to signal increased rates of periderm development in ‘St. Croix’ while signaling increased rates of bud maturation in ‘Frontenac Gris’ and rapid growth cessation in ‘Marquette’ relative to the mean of tested cultivars when compared with alternate environments. In a related growth chamber study, the effect of differing temperatures was evaluated on a relatively diverse subset of genotypes important for cold-climate grapevine development. While field conditions fluctuated in real-time, growth chamber temperatures were adjusted to static values of 27°C and 10°C for the duration of growth chamber runs. All plants were held at 27°C prior to the application of temperature treatments, thus, unfortunately, the low temperature of 10°C was also confounded with a single temperature reduction, as no such temperature reduction was present in the 27°C treatment. Through the interpretation of the field based results following data reduction of both temperature and phenotypic trait data, it was determined that a portion of the differential responses of the investigated cultivars were attributable to increases and decreases in temperature. Trait trend relationships corresponding to the majority of variance in the phenotypic data significantly correlated with a temperature based axis having a large contribution to the variance in observed temperatures. This was associated with both the relative difference in temperature across contrasting environments, as well as contrasting rates of relative temperature change during periods of temperature increase or decrease.

With the knowledge that relative increases and decreases in temperature are likely to cause differences in trait expression among genotypes, the alterations to phenotypic expression of traits discovered in the controlled growth chambers experiment were likely influenced by the temperature reduction at the time of temperature treatment application. When the relative trait trends across the two temperatures were reduced from the resulting growth chamber phenotypic data, differences in relative similarity in reaction were more commonly found between that of 'Frontenac', the progenitor cultivar of the bud-sport mutant 'Frontenac Gris', in comparison with 'Marquette'. Across the two studies, relating to temperature, two axes were found to be in common. Both studies determined axes related to temperature induced differences in tip abscission progress as well as an axis relating contrasting effects on active growth rate, through the number of lateral shoots, with tissue maturation rate. In general, 'Frontenac' was found to be more similar in response to native *V. riparia* than was 'Marquette'. This was characterized by a reduction in rate of tip abscission progress under the imposed temperature decline. Under field conditions, similar observations were made between 'Frontenac Gris' and 'Marquette'. As temperature declined, 'Marquette' had an increase in tip abscission progress in comparison with either 'Frontenac Gris' or 'St. Croix' relative to other environments.

Relative rate of transition from active growth to tissue maturation was found to differ among tested cultivars in both experiments. Under controlled environmental alterations, 'Frontenac Gris' was, model dependent, more similar to *V. riparia* than was 'Marquette' in measures of the rate of transition from active growth to tissue maturation. Under controlled conditions, differences in trait responses between the two temperatures plateaued in wild-type vines, including 'Frontenac', while continued to increase late into the simulated season in non-wild-type vines including 'Marquette'. Similar responses were seen under field conditions

contrasting 'Frontenac Gris' and 'Marquette'. Under periods of temperature decline, the two cultivar showed similar relative responses in periderm development and bud maturation, as both generally differed from the responses of 'St. Croix'. However, the two cultivars had largely different relative responses as temperatures increased where tissue maturation was depressed in 'Marquette' relative to the other tested cultivars when relative to other environments.

Both 'Frontenac' and Marquette' were similar to *V. riparia* in the effect of temperature on relative timing of growth cessation and tissue maturation under controlled conditions relative to other tested vines. Upon a comparison of 'Frontenac Gris', 'Marquette', and 'St. Croix' under field conditions, relationships involving timing and a parabolic distortion from linear trends were not found to be of high importance as they did not involve the environmental axis relating the contrasting temperature trends among environments in 2012 with those of other years. This is reasonable as diversity in the trait may not have existed among the cultivars used for field evaluations.

The latent processes which were identified were interpreted to have relationships consistent with previously observed effects of ABA synthesis and likely its relative effects on water partitioning within the plant by alterations to symplasmic phloem unloading through alterations to plasmodesmal structure. In this current study, no quantification of ABA, symplasmic flow, or plasmodesmata measurements were taken. Future research would be needed to prove such hypotheses. While the basis is speculative at the current time, overall differences were found among the investigated cultivars. The traits identified were relatively consistent across the two experiments. The rate of acclimation, as it proceeded in exposure to differing temperatures, differed across genotypes. These differences were sufficient to separate wild *V. riparia* material from most hybrid accessions investigated. While earliness of acclimation response is imperative

to successful cultivars in northern production regions, the appropriate allocation of resources following the triggering of acclimation response was also found to be important. The inclusion of the identified traits for future breeding efforts will likely improve success in creating adapted cultivars for cold-climate use. Acclimation to winter conditions is a dynamic response manifesting in several alterations, leading to a condition that is relatively difficult to quantify in its entirety. The mimicking the generalized process observed in adapted material in the presence of dynamically applied stimuli may help to facilitate progress in such difficult adaptive traits while maintaining quantitative diversity in the trait among selected individuals. Such a method, used for background selection, when coupled with relatively well established methods to identify superior yield components and disease resistance characteristics may aid in stabilizing the production of high quality winegrapes in non-traditional growing regions by aiding in striking balances between regional climactic adaptation, overall agronomic compatibility, and improved as well as consistent wine quality. With the identification of similar traits under both field evaluation of mature vines and under growth chamber conditions with relatively small plantlets, the use of the described phenotyping method may facilitate rapid generation cycling under greenhouse conditions as a method to introgress adaptive traits into quality backgrounds.

Implementation of several experimental designs could be facilitated for quantification leading to selection. The use of an augmented design on seed derived progeny may be beneficial to maximize through-put of untested seedlings, as well as limit time and labor spent on propagation and propagule maintenance and allow for maximization of growth chamber space. Check vines should contain industry standards and parental types. Wild-type standards may be included as either replicated checks or non-replicated seedling populations to ensure directionality of results are understood.

To best allocate resources, the number of observations could likely be reduced. Several measures tended to have little influence on the overall solution, including stem length. Additionally particular measures were strongly correlated with others and provided little additional information, as in the case of the two included periderm development measures. Similarly, it may also be possible to reduce the number of observed photoperiodic times to reduce the overall run time of the trial and reduce phenotyping costs. However; general trends did rely heavily on the photoperiodic extremes, thus reductions may influence the interpretation or the ability to detect differences among cultivars.

Lastly, through the course of this investigation, a novel genotype was discovered. The determinant form vine may facilitate further expansion in investigations into the physiology of flowering and vegetative growth control within plants. Additionally, the vine may complement the current research to better understand vegetative and reproductive cycle signaling within perennial woody species. Lastly, this unique genotype may be further exploited to facilitate rapid generation cycling in grape breeding if heritability of the trait can be confirmed.

Overall, the included investigations demonstrated the influence temperature conditions of environments in determining the process of events upon the onset of fall conditions in *V. riparia* derived hybrid *Vitis*. It is likely, that in addition to previously described photoperiodic sensing of shortening daylength, the reactions of native vines to temperature regimes are also important for regional adaptation. Native vines were generally separable from other types based only on these observations. Additionally, this research has led to the development of an *ex situ* phenotyping methodology to enable the testing of new progeny based on such a process through determination of vine reactions. Overall, the inclusion of such methodologies for crop improvement for a wide array of difficult-to-quantify adaptation, resistance, quality, and developmental processes may

have benefit in *Vitis* as well as in other woody, perennial, or annual crops. Such methods may aid in preserving diversity in quantitative traits as compromises in trait similarities are made. Overall, the evaluation of process traits may aid in improving breeding for the future, especially when applied to the adaptation of germplasm to relatively non-traditional growing regions.



## LITERATURE CITED

- Andersson, C.A, and B. Bro. 2000. The N-way Toolbox for MATLAB. *Chemometrics & Intelligent Laboratory Systems*. 52(1):1-4.
- Bilska, A. and P. Sowiński. 2010. Closure of plasmodesmata in maize (*Zea mays*) at low temperature: a new mechanism for inhibition of photosynthesis. *Annals of Botany*. 106:675-686.
- Böhlenius, H. T. Huang, L. Charbonnel-Campaa, A.M. Brunner, S. Jansson, S.H. Strauss, and O. Nilsson. 2006. CO/FT regulatory module controls timing of flowering and seasonal growth cessation in trees. *Science*. 312:1040-1043.
- Boss P.K. and M.R. Thomas. 2002. Association of dwarfism and floral induction with a grape ‘green revolution’ mutation. *Nature*. 416:847-849.
- Boss P.K., L. Sreekantan, and M.R. Thomas. 2006. A grapevine TFL1 homologue can delay flowering and alter floral development when overexpressed in heterologous species. *Functional Plant Biology*. 33(1):31-41.
- Carbonell-Bejerano, P., E.S. María, R. Horres-Pérez, C. Royo, D. Lijavetzky, G. Bravo, J. Aguirreolea, M. Sánchez-Díaz, M.C. Antolín, and J.M. Martínez-Zapater. 2013. Thermotolerance responses in ripening berries of *Vitis vinifera* L. cv Muscat Hamburg. *Plant and Cell Physiology*. 54(7):1200-1216.
- Carmona, M.J., M. Calonje, and J.M. Martínez-Zapater. 2007. The FT/TFL1 gene family in grapevine. *Plant Molecular Biology*. 63:637-650.
- Chapman, S.C., J. Crossa, K.E. Basford, and P.M. Kroonenberg. 1997. Genotype by environment effects and selection for drought tolerance in tropical maize. II. Three-mode pattern analysis. *Euphytica*. 95(1):11-20.

- Cheng, W.H., A. Endo, L. Zhou, J. Penney, H.C. Chen, A. Arroyo, P. Leon, E. Nambara, T. Asami, M. Seo, T. Koshihara and J. Sheen. 2002. A unique short-chain dehydrogenase/reductase in *Arabidopsis* glucose signaling and abscisic acid biosynthesis and functions. *The Plant Cell*. 14:2723-2743.
- Chervin, C., A. El-Kereamy, J. Roustan, A. Latche, J. Lamon, and M. Bouzayen. 2004. Ethylene seems required for the berry development and ripening in grape, a non-climacteric fruit. *Plant Science*. 167(6):1301-1305.
- Christmann, A., E. Grill, and M. Meinhard. Abscisic acid signaling. p. 39-71. In: Hirt, H. and K. Shinozaki (eds.). Plant Responses to Abiotic Stress. 2004. Springer-Verlag. Berlin / Heidelberg, Germany.
- Conesa, A., J.M. Prats-Montalbán, S. Tarazona, M.J. Nueda, and A. Ferrer. 2010. A multiway approach to data integration in systems biology based on Tucker3 and N-PLS. *Chemometrics and Intelligent Laboratory Systems*. 104:101-111.
- Cooke, J.E.K, M.E. Eriksson, and O. Junttila. 2012. The dynamic nature of bud dormancy in trees: environmental control and molecular mechanisms. *Plant, Cell and Environment*. 35:1707-1728.
- Cousins P. and D. Tricoli. 2006. Pixie, a dwarf grapevine for teaching and research. <http://www.ars.usda.gov/SP2UserFiles/Program/305/July2007GrapeResearchWorkshop/Posters/Geneva.NewYork-PeterCousins.pdf>. Accessed 13 November 2014.
- Dami, I., B. Bordelon, D.C. Ferree, M. Brown, M.A. Ellis, R.N. Williams, and D. Doohan. 2005. Midwest grape production guide. Ohio State Univ. Extension. Bulletin No. 919.
- Dhanasekar, P. and K.S. Reddy. 2015. A novel mutation in TFL1 homolog affecting determinacy in cowpea (*Vigna unguiculata*). *Molecular Genetics and Genomics*. 290:55-65.

- Dyrby, M. D. Baunsgaard, R. Bro, and S.B. Engelsen. 2005. Multiway chemometric analysis of the metabolic response to toxins monitored by NMR. *Chemometrics and Intelligent Laboratory Systems*. 76:79-89.
- Fennell A., and E. Hoover. 1991. Photoperiod influences growth, bud dormancy, and cold acclimation in *Vitis labruscana* and *V. riparia*. *The Journal of the American Society for Horticultural Science*. 116(2):270-273.
- Fennell, A. and C. Wake. 1996. Use of <sup>1</sup>H-NMR to determine grape bud water state during the photoperiodic induction of dormancy. *The Journal of the American Society for Horticultural Science*. 121(6):1112-1116.
- Fennell A., K. Mathiason, and J. Luby. 2005. Genetic segregation for indicators of photoperiod control of dormancy induction in *Vitis* species. *Acta Horticulturae*. 689:533-539.
- Flores, F., M.T. Moreno, and J.I. Cubero. 1998. A comparison of univariate and multivariate methods to analyze G X E interaction. *Field Crops Research*. 56:271-286.
- Garris, A., L. Clark, C. Owens, S. McKay, J. Luby, K. Mathiason, and A. Fennell. 2009. Mapping of photoperiod induced growth cessation in the wild grape *Vitis riparia*. *The Journal of the American Society for Horticultural Science*. 134(2):261-272.
- Ghassemian, M., E. Nambara, S. Cutler, H. Kawaide, Y. Kamiya, P. McCourt. 2000. Regulation of abscisic acid signaling by the ethylene response pathway in *Arabidopsis*. *The Plant Cell*. 12:117-1126.
- Gomez-Cadenas, A., R. Zentella, M.K. Wlaker-Simmons, and T.H. Ho. 2001. Gibberellin/abscisic acid antagonism in barley aleurone cells: site of action of the protein kinase PKABA1 in relation to gibberellin signaling molecules. *The Plant Cell*. 13:667-679.

- Goodacre, R., D. Broadhurst, A.K. Smilde, B.S. Kristal, J.D. Baker, R. Beger, C. Bessant, S. Connor, G. Capuani, A. Craig, T. Ebbels, D.B. Kell, C. Manetti, J. Newton, G. Paternosto, R. Somorjai, M. Sjöström, J. Trygg, and F. Wulfert. 2007. Proposed minimum reporting standards for data analysis in metabolomics. *Metabolomics*. 3(3):231-241.
- Grant, N.T., I.E. Dami, T. Ji, D. Scullock, and J. Streeter. 2009. Variation in leaf and bud soluble sugar concentration among *Vitis* genotypes grown under two temperature regimes. *Canadian Journal of Plant Science*. 89(5):961-968.
- Greer, D.H., and C. Weston. 2010. Heat stress affects flowering, berry growth, sugar accumulation and photosynthesis of *Vitis vinifera* cv. Semillon grapevines grown in a controlled environment. *Functional Plant Biology*. 37(3):206-214.
- Hallauer, A.R., M.J. Carena, and J.B. Filho. 2010. Quantitative genetics in maize breeding. Springer Science+Business Media, LLC. 233 Spring Street, New York, NY 10013, USA.
- Hatterman-Valenti, H.M., C.P. Auwarter, and J.E. Stenger. 2016. Evaluation of cold-hardy grape cultivars for North Dakota and the North Dakota State University germplasm enhancement project. *Acta Horticulturae*. 1115:13-22.
- Heide, O.M. 2008. Interaction of photoperiod and temperature in the control of growth dormancy of *Prunus* species. *Scientia Horticulturae*. 115:309-314.
- Heide, O.M., and A.K. Prestrud. 2005. Low temperature, but not photoperiod, controls growth cessation and dormancy induction and release in apple and pear. *Tree Physiology*. 25:109-114.

- Hemstad, P. 2015. Grapevine breeding in the Midwest, p. 411-426. In: A. Reynolds (Ed.). Grapevine breeding programs for the wine industry. Woodhead Publishing. Waltham, MA.
- Hemstad, P., and J. Luby. 2008. Grapevine plant named 'Marquette'. U.S. Patent Plant 19579 P3, filed Oct 13 2006, and issued Dec 16, 2008.
- Hemstad, P.R., and J.J. Luby. 2000. Utilization of *V. riparia* for the development of new wine varieties with resistance to disease and extreme cold. *Acta Horticulturae*. 528:487-496.
- Ho, L.C., R.I. Grange, and A.J. Picken. 1987. An analysis of the accumulation of water and dry matter in tomato fruit. *Plant, Cell and Environment*. 10:157-162.
- Hotelling, H. 1933. Analysis of a complex of statistical variables into principal components. *Journal of Experimental Psychology* 24:417-441, 493-520.
- Hsu, C., J.P. Adams, H. Kim, K. No, C. Ma, S.H. Strauss, J. Drnevich, L. Vandervelde, J.D. Ellis, B. M. Rice, N. Wickett, L.E. Gunter, G.A. Tuskan, A.M. Brunner, G.P. Page, A. Barakat, J.E. Carlson, C.W. DePamphilis, D.S. Luthe, and C. Yuceer. 2011. FLOWERING LUCUS T duplication coordinates reproductive and vegetative growth in perennial poplar. *PNAS*. 108(26):10756-10761.
- Jaillon, O., J. Aury, B. Noel, A. Policriti, C. Clepet, A. Casagrande, N. Choisne, S. Aubourg, N. Vitulo, C. Jubin, A. Vezzi, F. Legeai, P. Huguency, C. Dasilva, D. Horner, E. Mica, D. Jublot, J. Poulain, C. Bruyere, A. Billault, B Segurens, M. Gouyvenoux, E. Ugarte, F. Cattonaro, V. Anthouard, V. Vico, C. DelFabbro, M. Alaux, G. Di Gaspero, V. Dumas, N. Felice, S. Paillard, I. Juman, M. Moroldo, S. Scalabrin, A.Canaguier, I. Le Clainche, G. Malacrida, E. Durand, G. Pesole, V. Laucou, P. Chatelet, D. Merdinoglu, M. Delledonne, M. Pezzotti, A. Lecharny, C. Scarpelli, F. Artiguenave, M. Enrico Pe, G.

- Valle, M. Morgante, M. Caboche, A. Adam-Blondon, J. Weissenbach, F. Quetier, and P. Wincker (2007) The grapevine genome sequence suggests ancestral hexaploidization in major angiosperm phyla. *Nature*. Vol. 449:463-468.
- Junttila, O., J. Nilsen, and B. Igeland. 2003. Effect of temperature on the induction of bud dormancy in ecotypes of *Betula pubescens* and *Betula pendula*. *Scandinavian Journal of Forest Research*. 18:208-217.
- Kalcsits, L.A., S. Silim, and K. Tanino. 2009. Warm temperature accelerates short photoperiod-induced growth cessation and dormancy induction in hybrid poplar (*Populus x spp.*). *Trees*. 23:971-979.
- Keller, M. and P.M. Shrestha. 2014. Solute accumulation differs in the vacuoles and apoplast of ripening grape berries. *Planta*. 239:633-642.
- Kenkel, N.C. and L. Orlóci. 1986. Applying metric and nonmetric multidimensional scaling to ecological studies: some new results. *Ecology*. 67(4):919-928.
- Kriedemann, P.E., B.R. Loveys, G.L. Fuller, and A.C. Leopold. 1972. Abscisic Acid and stomatal regulation. *Plant Physiology*. 49:842-847.
- Kroonenberg, P.M., ed (2008) Applied multiway data analysis. Hoboken, New Jersey: John Wiley & Sons, Inc.
- Kruskal, J.B. 1984. Multidimensional scaling by optimizing goodness of fit to a nonmetric hypothesis. *Psychometrika*. 29:1-27.
- Kuhn, N. L. Guan, Z.W. Dai, B. Wu, V. Lauvergeat, E. Gomès, S. Li, F. Godou, P. Arce-Johnson, and S. Delrot. 2013. Berry ripening: recently heard through the grapevine. *Journal of Experimental Botany*. doi:10.1093/jxb/ert395.

- Lagercrantz, U. 2009 At the end of the day: a common molecular mechanism for photoperiod responses in plants?. *Journal of Experimental Botany*. 60(9):2501-2515.
- Lang, A., 1990. Xylem, phloem and transpiration flows in developing apple fruits. *Journal of Experimental Botany*. 41:645-651.
- Lang, A. and M.R. Thorpe. 1989. Xylem, phloem and transpiration flows in a grape: application of a technique of measuring volume of attached fruits to high resolution using Archimedes' Principle. *Journal of Experimental Botany*. 40:1069-1078.
- Légère, A. and N. Samson. 1999. Relative influence of crop rotation, tillage, and weed management on weed associations in spring barley cropping systems. *Weed Science*. 47:112-122.
- Li, C., O. Junttila, A. Ernstsén, P. Heino, and E. Tapio Palva. 2003. Photoperiodic control of growth, cold acclimation and dormancy development in silver birch (*Betula pendula*) ecotypes. *Physiologia Plantarum*. 117:206-212.
- Li, C., T. Puhakainen, A. Welling, A. Viherä-Aarnio, A. Ernstsén, O. Junttila, P. Heino, and E.T. Palva. 2002. Cold acclimation response in silver birch (*Betula pendula*). Development of freezing tolerance in different tissues and climactic ecotypes. *Physiologia Plantarum*. 116:478-488.
- Luby and Hemstad, 2006. Grape plant named 'Frontenac gris'. US Plant Patent 16478 P3, filed Feb 2004, issued Apr 2006.
- Luciano, G. and T. Næs. 2009. Interpreting sensory data by combining principal component analysis and analysis of variance. *Food Quality and Preference*. 20:167-175.
- Mathiason, K., D. He, J. Grimplet, J. Venkateswari, D.W. Galbraith, E. Or, and A. Fennell. 2009. Transcript profiling in *Vitis riparia* during chilling requirement fulfillment reveals

- coordination of gene expression patterns with optimized bud break. *Functional and Integrative Genomics*. 9:81:96.
- Mori, K., H. Saito, N. Goto-Yamamoto, M. Kitayama, S. Kobayashi, S. Sugaya, H. Gemma, and K. Hashizume. 2005. Effects of abscisic acid treatment and night temperature on anthocyanin composition in Pinot noir grapes. *Vitis*. 44(4):161-165.
- Murcia, G., M. Pontin, H. Reinoso, R. Baraldi, G. Bertazza, S. Gómez-Talquenca, R. Bottini, and P. N. Piccoli. 2016. ABA and GA<sub>3</sub> increase carbon allocation in different organs of grapevine plants by inducing accumulation of non-structural carbohydrates in leaves, enhancement of phloem area and expression of sugar transporters. *Physiologia Plantarum*. 156:323-337.
- Myles, S., A.R. Boyko, C.L. Owens, P.J. Browin, B. Grassi, M.K. Aradhya, B. Prins, A. Reynolds, J. Chia, D. Ware, C.D. Bustamante, and E.S. Buckler. 2011. Genetic structure and domestication history of the grape. *PNAS*. 108(9):3530-3535.
- National Plant Germplasm System. 2009. Accessed May 5, 2009. <<http://www.ars-grin.gov/npgs/searchgrin.html>>.
- Nomikos, P., and J.F. MacGregor. 1995. Multivariate SPC charts for monitoring batch processes. *Technometrics*. 37(1):41-59.
- Nomme, K.M. and P.G. Harrison. 1991. A multivariate comparison of the seagrasses *Zostera narina* and *Zostera japonica* in monospecific mixed populations. *Canadian Journal of Botany*. 69(9):1984-1990
- Patrick, J.W. 1997. PHLOEM UNLOADING: Sieve element unloading and post-sieve element transport. *Annual Review of Plant Physiology and Plant Molecular Biology*. 48:191-222.



- Pearson, K. 1901. On lines and planes of closest fit to systems of points in space. *Philosophical Magazine, Sixth Series* 2:559-572.
- Pèros, J., G. Berger, A. Portemont, J. Boursiquot, and T. Lacombe. 2011. Genetic variation and biogeography of the disjunct *Vitis* subg. *Vitis* (*Vitaceae*). *Journal of Biogeography*. 38:471-486.
- Piepho, H. 1999. Stability analysis using the SAS system. *Agronomy Journal*. 91:154-160.
- Pnueli, L., L. Carmel-Goren, D. Hareven, T. Gutfinger, J. Alvarez, M. Ganal, D. Zamir, and E. Lifschitz. 1998. The SELF-PRUNING gene of tomato regulates vegetative to reproductive switching of sympodial meristems and is the ortholog of CEN and TFL1. *Development*. 125:1979-1989.
- Ruan, Y., D.J. Llewellyn, and R.T. Furbank. 2001. The control of single-celled cotton fiber elongation by developmentally reversible gating of plasmodesmata and coordinated expression of sucrose and K<sup>+</sup> Transporters and Expansin. *The Plant Cell*. 13:47-60.
- Schnabel B.J. and R.L. Wample. 1987. Dormancy and cold hardiness in *Vitis vinifera* L. cv. White Riesling as influenced by photoperiod and temperature. *American Journal of Enology and Viticulture*. 38(4):265-272.
- Shannon, S., and D.R. Meeks-Wagner. 1991. A mutation in the Arabidopsis TFL1 gene affects inflorescence meristem development. *The Plant Cell*. 3:877-892.
- Slovik, S., W. Daeter, W. Hartung. 1995. Compartmental redistribution and long-distance transport of abscisic acid (ABA) in plants as influenced by environmental changes in the rhizosphere – a biomathematical model. *Journal of Experimental Botany*. 46:881-894.

- Soolanayakanahally, R.Y, R.D. Guy, S.N. Silim, and M. Song. 2013. Timing of photoperiodic competency causes phenological mismatch in balsam poplar (*Populus balsamifera* L.). *Plant, Cell and Environment* 36:116-127.
- Sreekantan, L. and M.R. Thomas. 2006. VvFT and VvMADS8, the grapevine homologues of the floral integrators FT and SOC1, have unique expression patterns in grapevine that hasten flowering in *Arabidopsis*. *Functional Plant Biology*. 33(12):1129-1139.
- Srinivasan, C., C. Dardick, A. Callahan, and R. Scorza. 2012. Plum (*Prunus domestica*) trees transformed with poplar FT1 result in altered architecture, dormancy requirement, and continuous flowering. *Plos One*. 7(7) e40715.
- Stoner, J.D., D.L. Lorenz, G.J. Wiche, and R.M. Goldstein. Red River of the North basin, Minnesota, North Dakota, and South Dakota. *American Water Resources Association Water Resources Bulletin* 29(4):575-615.
- Sweetman, C., L.G. Deluc, G.R. Cramer, C.M. Ford, and K.L. Soole. 2009. Regulation of malate metabolism in grape berry and other developing fruits. *Phytochemistry*. 70:1329-1344.
- Swenson, E. 1982. Grapevine. U.S. Patent Plant 4,928, filed Feb 11, 1981, and issued Nov 9, 1982.
- Tanino, K.K, L. Kalcsits, S. Silim, E. Kendall, and G.R. Gray. 2010. Temperature-driven plasticity in growth cessation and dormancy development in deciduous woody plants: a working hypothesis suggesting how molecular and cellular function is affected by temperature during dormancy induction. *Plant Molecular Biology*. 73:49-65.
- Teh, S.K., W. Zheng, K. Ho, M. Teh, K. Yeoh, and Z. Huang. Near-infrared raman spectroscopy for early diagnosis and typing of adenocarcinoma in the stomach. *British Journal of Surgery*. 97:550-557.

- Tröndle, D., S. Schröder, H. Kassemeyer, C. Kiefer, M.A. Kock, and P. Nick. 2010. Molecular phylogeny of the genus *Vitis* (*Vitaceae*) based on plastid markers. *American Journal of Botany*. 97:1168-1178.
- Varela, M., J. Crossa, J. Rane, A.K. Joshi, and R. Trenthowan. 2006. Analysis of a three-way interaction including multi-attributes. *Australian Journal of Agriculture Research*. 57:1185-1193.
- Wake, C.M.F, and A. Fennell. 2000. Morphological, physiological and dormancy responses of three *Vitis* genotypes to short photoperiod. *Physiologia Plantarum* 109:203-210.
- Wan, Y., H.R. Schwaninger, A.M. Baldo, J.A. Labate, G. Zhong. 2013. A phylogenetic analysis of the grape genus (*Vitis* L.) reveals broad reticulation and concurrent diversification during Neogene and quaternary climate change. *BMC Evolutionary Biology*. 13:141.
- Wang, N., H. Zhang, and P.S. Nobel. Phloem-xylem water flow in developing cladodes of *Opuntia ficus-indica* during sink-to-source translocation. *Journal of Experimental Botany*. 48:675-682.
- Wilkinson, S. and W.J. Davies. 1997. Xylem sap pH increase: a drought signal received at the apoplastic face of the guard cell that involves the suppression of saturatable abscisic acid uptake by the epidermal symplast. *Plant Physiology*. 113:559-573.
- Wolpert, J.A. and G.S. Howell. 1985. Cold acclimation of Concord grapevines. II. Natural acclimation pattern and tissue moisture decline in canes and primary buds of bearing vines. *American Journal of Enology and Viticulture*. 36:189-194.
- Wolpert, J.A. and G.S. Howell. 1986. Cold acclimation of Concord grapevines III. Relationship between cold hardiness, tissue water content, and shoot maturation. *Vitis*. 25:151-159.

- Wright, S.T. and R.W. Hiron. 1969. Abscisic acid, the growth inhibitor induced in detached wheat leaves by a period of wilting. *Nature*. 224:719-720.
- Xie, Z., C.F. Forney, W. Xu, and S. Wang. 2009. Effects of root restriction on ultrastructure of phloem tissues in grape berry. *HortScience*. 44(5):1334-1339.
- Xiong, L. and J. Zhu. 2003. Regulation of abscisic acid biosynthesis. *Plant Physiology* 133:29-36.
- Zecca, G., J.R. Abbott, W. Sun, A. Spada, F. Sala, and F. Grassi. 2012. The timing and the mode of evolution of wild grapes (*Vitis*). *Molecular Phylogenetics and Evolution*. 62:732-747.
- Zeevaart, J.A.D. and R.A. Creelman. 1988. Metabolism and physiology of abscisic acid. *Annual Review of Plant Physiology and Plant Molecular Biology*. 39:439-473.
- Zhang, X., X. Wang, X. Wang, G. Xia, Q. Pan, R. Fan, F. Wu, X. Yu, and D. Zhang. 2006. A shift of phloem unloading from symplasmic to apoplasmic pathway is involved in developmental onset of ripening in grape berry. *Plant Physiology*. 142(1):220-232.
- Zheng, C., T. Halaly, A.K. Acheampong, Y. Takebayashi, Y. Jikumaru, Y. Kamiya, and E. Or. 2015. Abscisic acid (ABA) regulates grape bud dormancy, and dormancy release stimuli may act through modification of ABA metabolism. *Journal of Experimental Botany*. 66(5):1527-1542.

**APPENDIX A. TABLES**

Table A1. ANOVA for stem length.

SOV	Num DF	Den DF	F-Value	p-value
Run	1	12	75.64	<0.0001
Cultivar (Cult)	29	321	4.93	<0.0001
Run*Cult	29	321	2.62	<0.0001
Photoperiod (Photo)	10	120	134.05	<0.0001
Run*Photo	10	120	4.25	<0.0001
Cult*Photo	290	3102	1.31	0.0006
Run*Cult*Photo	290	3102	1.19	0.0178
Temperature (Temp)	1	12	464	<0.0001
Run*Temp	1	12	10.73	0.0066
Temp*Cult	29	321	2.29	0.0003
Run*Temp*Cult	29	321	1.07	0.3740
Temp*Photo	10	120	106.21	<0.0001
Run*Temp*Photo	10	120	4.5	<0.0001
Temp*Cult*Photo	290	3102	1.42	<0.0001
Run*Temp*Cult*Photo	290	3102	1.3	0.0008

Table A2. ANOVA for number of nodes.

SOV	Num DF	Den DF	F-Value	p-value
Run	1	12	99.68	<0.0001
Cultivar (Cult)	29	321	4.78	<0.0001
Run*Cult	29	321	2.4	0.0001
Photoperiod (Photo)	10	120	123.31	<0.0001
Run*Photo	10	120	6.84	<0.0001
Cult*Photo	290	3102	1.26	0.0027
Run*Cult*Photo	290	3102	1.23	0.0064
Temperature (Temp)	1	12	599.21	<0.0001
Run*Temp	1	12	51.31	<0.0001
Temp*Cult	29	321	3.14	<0.0001
Run*Temp*Cult	29	321	1.06	0.3924
Temp*Photo	10	120	64.91	<0.0001
Run*Temp*Photo	10	120	8.92	<0.0001
Temp*Cult*Photo	290	3102	1.4	<0.0001
Run*Temp*Cult*Photo	290	3102	1.18	0.0246

Table A3. ANOVA for number of mature nodes.

SOV	Num DF	Den DF	F-Value	p-value
Run	1	12	1.39	0.2611
Cultivar (Cult)	29	321	4.54	<0.0001
Run*Cult	29	321	1.24	0.1855
Photoperiod (Photo)	10	120	251.38	<0.0001
Run*Photo	10	120	7.45	<0.0001
Cult*Photo	290	3102	1.67	<0.0001
Run*Cult*Photo	290	3102	1.15	0.0453
Temperature (Temp)	1	12	387.22	<0.0001
Run*Temp	1	12	5.36	0.0391
Temp*Cult	29	321	2.95	<0.0001
Run*Temp*Cult	29	321	1.28	0.1570
Temp*Photo	10	120	64.92	<0.0001
Run*Temp*Photo	10	120	7.32	<0.0001
Temp*Cult*Photo	290	3102	1.56	<0.0001
Run*Temp*Cult*Photo	290	3102	1.07	0.2016

Table A4. ANOVA for number of lateral shoots.

SOV	Num DF	Den DF	F-Value	p-value
Run	1	12	240.24	<0.0001
Cultivar (Cult)	29	321	4.87	<0.0001
Run*Cult	29	321	2.92	<0.0001
Photoperiod (Photo)	10	120	82.09	<0.0001
Run*Photo	10	120	19.55	<0.0001
Cult*Photo	290	3102	1.2	0.0162
Run*Cult*Photo	290	3102	1.25	0.0039
Temperature (Temp)	1	12	352.72	<0.0001
Run*Temp	1	12	102.02	<0.0001
Temp*Cult	29	321	4.24	<0.0001
Run*Temp*Cult	29	321	2.03	0.0017
Temp*Photo	10	120	43.47	<0.0001
Run*Temp*Photo	10	120	9.67	<0.0001
Temp*Cult*Photo	290	3102	1.44	<0.0001
Run*Temp*Cult*Photo	290	3102	1.09	0.1521

Table A5. ANOVA for tip abscission progress.

SOV	Num DF	Den DF	F-Value	p-value
Run	1	12	0.56	0.4681
Cultivar (Cult)	29	321	4.42	<0.0001
Run*Cult	29	321	1.99	0.0023
Photoperiod (Photo)	10	120	316.33	<0.0001
Run*Photo	10	120	3.36	0.0007
Cult*Photo	290	3102	1.53	<0.0001
Run*Cult*Photo	290	3102	1.11	0.1054
Temperature (Temp)	1	12	8.65	0.0124
Run*Temp	1	12	4.32	0.0598
Temp*Cult	29	321	3.2	<0.0001
Run*Temp*Cult	29	321	2.29	0.0003
Temp*Photo	10	120	18.19	<0.0001
Run*Temp*Photo	10	120	5.69	<0.0001
Temp*Cult*Photo	290	3102	1.51	<0.0001
Run*Temp*Cult*Photo	290	3102	1.2	0.0154

Table A6. ANOVA for periderm development (length of shoot).

SOV	Num DF	Den DF	F-Value	p-value
Run	1	12	0.01	0.9113
Cultivar (Cult)	29	321	3.63	<0.0001
Run*Cult	29	321	1.09	0.3484
Photoperiod (Photo)	10	120	116.17	<0.0001
Run*Photo	10	120	4.48	<0.0001
Cult*Photo	290	3102	1.98	<0.0001
Run*Cult*Photo	290	3102	1.14	0.0641
Temperature (Temp)	1	12	231.08	<0.0001
Run*Temp	1	12	2.86	0.1168
Temp*Cult	29	321	2.61	<0.0001
Run*Temp*Cult	29	321	0.76	0.8134
Temp*Photo	10	120	59.31	<0.0001
Run*Temp*Photo	10	120	6.74	<0.0001
Temp*Cult*Photo	290	3102	1.78	<0.0001
Run*Temp*Cult*Photo	290	3102	1.03	0.3633

Table A7. ANOVA for periderm development (nodes enveloped).

SOV	Num DF	Den DF	F-Value	p-value
Run	1	12	0.16	0.6923
Cultivar (Cult)	29	321	3.62	<0.0001
Run*Cult	29	321	1.15	0.2790
Photoperiod (Photo)	10	120	159.2	<0.0001
Run*Photo	10	120	5.97	<0.0001
Cult*Photo	290	3102	1.76	<0.0001
Run*Cult*Photo	290	3102	1.19	0.0168
Temperature (Temp)	1	12	314.69	<0.0001
Run*Temp	1	12	9.84	0.0086
Temp*Cult	29	321	2.75	<0.0001
Run*Temp*Cult	29	321	0.99	0.4880
Temp*Photo	10	120	68.07	<0.0001
Run*Temp*Photo	10	120	9.23	<0.0001
Temp*Cult*Photo	290	3102	1.81	<0.0001
Run*Temp*Cult*Photo	290	3102	1.05	0.2716



Table A8. Factor weights of predictor variables for non-rotated SVD axis 1.

Temperature	Photoperiod (h)	L	N	MAT	LAT	TIP	PL	PN
<i>10°C</i>		----- Weight x 10 <sup>2</sup> -----						
	15	-0.321	-0.690	-0.061	-0.246	2.328	-0.525	-0.483
	14.5	-0.187	-0.549	-0.258	0.144	2.163	-0.681	-0.633
	14	0.012	-0.303	-0.328	0.579	1.699	-0.847	-0.812
	13.5	0.195	-0.070	-0.350	0.632	1.446	-0.977	-0.875
	13	0.184	0.155	-0.498	0.742	1.025	-0.878	-0.730
	12.5	0.190	0.299	-0.341	0.367	-0.231	-0.186	-0.098
	12	0.245	0.362	-0.318	0.362	-0.902	0.198	0.053
	11.5	0.119	0.305	0.244	-0.250	-1.602	0.639	0.543
	11	-0.016	0.225	0.516	-0.527	-2.052	0.978	0.876
	10.5	-0.137	0.174	0.671	-0.773	-2.136	1.128	1.073
	10	-0.282	0.092	0.723	-1.031	-1.737	1.151	1.086
<i>27°C</i>								
	15	0.321	0.690	0.061	0.246	-2.328	0.525	0.483
	14.5	0.187	0.549	0.258	-0.144	-2.163	0.681	0.633
	14	-0.012	0.303	0.328	-0.579	-1.699	0.847	0.812
	13.5	-0.195	0.070	0.350	-0.632	-1.446	0.977	0.875
	13	-0.184	-0.155	0.498	-0.742	-1.025	0.878	0.730
	12.5	-0.190	-0.299	0.341	-0.367	0.231	0.186	0.098
	12	-0.245	-0.362	0.318	-0.362	0.902	-0.198	-0.053
	11.5	-0.119	-0.305	-0.244	0.250	1.602	-0.639	-0.543
	11	0.016	-0.225	-0.516	0.527	2.052	-0.978	-0.876
	10.5	0.137	-0.174	-0.671	0.773	2.136	-1.128	-1.073
	10	0.282	-0.092	-0.723	1.031	1.737	-1.151	-1.086

L = Stem length, N = Number of nodes, MAT = Number of mature nodes, LAT = Number of lateral shoots, TIP = Progress toward tip abscission, PL = Length of periderm development, and PN = Periderm development in number of nodes.




 hue indicates an increasingly negative association with the axis.  
 hue indicates an increasingly positive association with the axis.

Table A9. Factor weights of predictor variables for non-rotated SVD axis 2.

Temperature	Photoperiod (h)	L	N	MAT	LAT	TIP	PL	PN
<i>10°C</i>		----- Weight x 10 <sup>2</sup> -----						
	15	-1.007	-1.406	1.032	-1.975	0.914	1.387	1.055
	14.5	-1.080	-1.428	0.916	-1.728	1.114	1.271	0.937
	14	-0.946	-1.263	0.900	-1.293	0.667	1.152	0.783
	13.5	-0.672	-0.903	0.687	-0.891	0.284	0.959	0.537
	13	-0.298	-0.241	0.068	-0.105	0.241	0.315	0.020
	12.5	0.318	0.397	-0.232	0.513	-0.196	-0.411	-0.388
	12	0.826	0.910	-0.823	1.308	-0.127	-1.120	-0.975
	11.5	0.870	1.077	-0.594	1.220	-0.617	-1.144	-0.812
	11	0.843	1.161	-0.653	1.236	-1.098	-0.931	-0.559
	10.5	0.666	0.940	-0.621	0.915	-0.745	-0.794	-0.359
	10	0.479	0.756	-0.679	0.802	-0.436	-0.687	-0.237
<i>27°C</i>								
	15	1.007	1.406	-1.032	1.975	-0.914	-1.387	-1.055
	14.5	1.080	1.428	-0.916	1.728	-1.114	-1.271	-0.937
	14	0.946	1.263	-0.900	1.293	-0.667	-1.152	-0.783
	13.5	0.672	0.903	-0.687	0.891	-0.284	-0.959	-0.537
	13	0.298	0.241	-0.068	0.105	-0.241	-0.315	-0.020
	12.5	-0.318	-0.397	0.232	-0.513	0.196	0.411	0.388
	12	-0.826	-0.910	0.823	-1.308	0.127	1.120	0.975
	11.5	-0.870	-1.077	0.594	-1.220	0.617	1.144	0.812
	11	-0.843	-1.161	0.653	-1.236	1.098	0.931	0.559
	10.5	-0.666	-0.940	0.621	-0.915	0.745	0.794	0.359
	10	-0.479	-0.756	0.679	-0.802	0.436	0.687	0.237

L = Stem length, N = Number of nodes, MAT = Number of mature nodes, LAT = Number of lateral shoots, TIP = Progress toward tip abscission, PL = Length of periderm development, and PN = Periderm development in number of nodes.

 hue indicates an increasingly negative association with the axis.



 hue indicates an increasingly positive association with the axis.

Table A10. Factor weights of predictor variables for non-rotated SVD axis 3.

Temperature	Photoperiod (h)	L	N	MAT	LAT	TIP	PL	PN
<i>10°C</i>		----- Weight x 10 <sup>2</sup> -----						
	15	-1.395	-1.136	1.599	-1.155	-0.105	1.206	0.985
	14.5	-0.648	-0.413	1.166	-1.132	-1.213	1.286	0.956
	14	-0.071	0.353	0.237	0.000	-1.290	0.659	0.109
	13.5	0.878	0.895	-0.493	1.331	-1.884	-0.060	-0.666
	13	1.914	1.987	-1.998	2.599	-1.376	-0.913	-2.213
	12.5	2.179	2.153	-2.119	3.117	-0.849	-1.844	-2.639
	12	1.304	1.212	-1.308	1.510	-0.362	-1.078	-1.277
	11.5	-0.007	0.011	0.080	-0.375	-0.842	0.281	0.853
	11	-0.752	-0.784	0.753	-1.424	0.563	0.348	1.295
	10.5	-1.494	-1.972	0.706	-2.010	3.041	0.273	1.454
	10	-1.909	-2.306	1.373	-2.463	4.321	-0.158	1.141
<i>27°C</i>								
	15	1.395	1.136	-1.599	1.155	0.105	-1.206	-0.985
	14.5	0.648	0.413	-1.166	1.132	1.213	-1.286	-0.956
	14	0.071	-0.353	-0.237	0.000	1.290	-0.659	-0.109
	13.5	-0.878	-0.895	0.493	-1.331	1.884	0.060	0.666
	13	-1.914	-1.987	1.998	-2.599	1.376	0.913	2.213
	12.5	-2.179	-2.153	2.119	-3.117	0.849	1.844	2.639
	12	-1.304	-1.212	1.308	-1.510	0.362	1.078	1.277
	11.5	0.007	-0.011	-0.080	0.375	0.842	-0.281	-0.853
	11	0.752	0.784	-0.753	1.424	-0.563	-0.348	-1.295
	10.5	1.494	1.972	-0.706	2.010	-3.041	-0.273	-1.454
	10	1.909	2.306	-1.373	2.463	-4.321	0.158	-1.141

L = Stem length, N = Number of nodes, MAT = Number of mature nodes, LAT = Number of lateral shoots, TIP = Progress toward tip abscission, PL = Length of periderm development, and PN = Periderm development in number of nodes.

 hue indicates an increasingly negative association with the axis.



 hue indicates an increasingly positive association with the axis.

Table A11. Factor weights of predictor variables for rotated SVD axis 1.

Temperature	Photoperiod (h)	L	N	MAT	LAT	TIP	PL	PN
<i>10°C</i>		----- Weight x 10 <sup>2</sup> -----						
	15	0.042	-0.385	-0.465	0.043	2.285	-0.807	-0.712
	14.5	-0.023	-0.437	-0.544	0.416	2.417	-0.978	-0.851
	14	0.020	-0.399	-0.369	0.545	1.984	-0.977	-0.803
	13.5	-0.049	-0.311	-0.201	0.252	1.890	-0.916	-0.664
	13	-0.326	-0.371	0.043	0.037	1.352	-0.605	-0.127
	12.5	-0.383	-0.270	0.222	-0.454	-0.003	0.298	0.590
	12	-0.095	0.043	0.024	-0.030	-0.777	0.460	0.374
	11.5	0.127	0.304	0.208	-0.130	-1.333	0.531	0.293
	11	0.190	0.436	0.294	-0.124	-2.139	0.843	0.502
	10.5	0.266	0.694	0.457	-0.211	-2.865	1.008	0.652
	10	0.231	0.699	0.332	-0.344	-2.810	1.144	0.748
<i>27°C</i>								
	15	-0.042	0.385	0.465	-0.043	-2.285	0.807	0.712
	14.5	0.023	0.437	0.544	-0.416	-2.417	0.978	0.851
	14	-0.020	0.399	0.369	-0.545	-1.984	0.977	0.803
	13.5	0.049	0.311	0.201	-0.252	-1.890	0.916	0.664
	13	0.326	0.371	-0.043	-0.037	-1.352	0.605	0.127
	12.5	0.383	0.270	-0.222	0.454	0.003	-0.298	-0.590
	12	0.095	-0.043	-0.024	0.030	0.777	-0.460	-0.374
	11.5	-0.127	-0.304	-0.208	0.130	1.333	-0.531	-0.293
	11	-0.190	-0.436	-0.294	0.124	2.139	-0.843	-0.502
	10.5	-0.266	-0.694	-0.457	0.211	2.865	-1.008	-0.652
	10	-0.231	-0.699	-0.332	0.344	2.810	-1.144	-0.748

L = Stem length, N = Number of nodes, MAT = Number of mature nodes, LAT = Number of lateral shoots, TIP = Progress toward tip abscission, PL = Length of periderm development, and PN = Periderm development in number of nodes.

 hue indicates an increasingly negative association with the axis.



 hue indicates an increasingly positive association with the axis.

Table A12. Factor weights of predictor variables for rotated SVD axis 2.

Temperature	Photoperiod (h)	L	N	MAT	LAT	TIP	PL	PN
<i>10°C</i>		----- Weight x 10 <sup>2</sup> -----						
	15	-1.202	-1.571	1.246	-2.125	0.952	1.529	1.170
	14.5	-1.166	-1.487	1.064	-1.867	0.989	1.421	1.046
	14	-0.946	-1.208	0.916	-1.264	0.523	1.210	0.769
	13.5	-0.536	-0.768	0.600	-0.676	0.052	0.915	0.413
	13	-0.019	0.047	-0.229	0.284	0.071	0.158	-0.314
	12.5	0.629	0.706	-0.540	0.960	-0.321	-0.674	-0.761
	12	1.009	1.083	-1.008	1.518	-0.202	-1.255	-1.145
	11.5	0.863	1.075	-0.569	1.147	-0.773	-1.075	-0.668
	11	0.728	1.044	-0.526	1.007	-1.061	-0.845	-0.347
	10.5	0.443	0.655	-0.497	0.600	-0.364	-0.716	-0.121
	10	0.197	0.424	-0.458	0.417	0.134	-0.670	-0.044
<i>27°C</i>								
	15	1.202	1.571	-1.246	2.125	-0.952	-1.529	-1.170
	14.5	1.166	1.487	-1.064	1.867	-0.989	-1.421	-1.046
	14	0.946	1.208	-0.916	1.264	-0.523	-1.210	-0.769
	13.5	0.536	0.768	-0.600	0.676	-0.052	-0.915	-0.413
	13	0.019	-0.047	0.229	-0.284	-0.071	-0.158	0.314
	12.5	-0.629	-0.706	0.540	-0.960	0.321	0.674	0.761
	12	-1.009	-1.083	1.008	-1.518	0.202	1.255	1.145
	11.5	-0.863	-1.075	0.569	-1.147	0.773	1.075	0.668
	11	-0.728	-1.044	0.526	-1.007	1.061	0.845	0.347
	10.5	-0.443	-0.655	0.497	-0.600	0.364	0.716	0.121
	10	-0.197	-0.424	0.458	-0.417	-0.134	0.670	0.044

L = Stem length, N = Number of nodes, MAT = Number of mature nodes, LAT = Number of lateral shoots, TIP = Progress toward tip abscission, PL = Length of periderm development, and PN = Periderm development in number of nodes.

 hue indicates an increasingly negative association with the axis.



 hue indicates an increasingly positive association with the axis.

Table A13. Factor weights of predictor variables for rotated SVD axis 3.

Temperature	Photoperiod (h)	L	N	MAT	LAT	TIP	PL	PN
<i>10°C</i>		----- Weight x 10 <sup>2</sup> -----						
	15	-1.270	-1.062	1.362	-0.884	0.374	0.815	0.664
	14.5	-0.512	-0.333	0.916	-0.796	-0.756	0.868	0.614
	14	0.072	0.441	0.012	0.338	-0.886	0.242	-0.219
	13.5	0.985	0.965	-0.661	1.564	-1.464	-0.450	-0.941
	13	1.918	1.972	-2.047	2.690	-1.083	-1.145	-2.306
	12.5	2.084	2.076	-2.078	2.998	-0.843	-1.750	-2.489
	12	1.190	1.120	-1.213	1.348	-0.562	-0.816	-1.065
	11.5	-0.101	-0.064	0.225	-0.598	-1.132	0.599	1.074
	11	-0.842	-0.858	0.948	-1.674	0.161	0.720	1.544
	10.5	-1.558	-1.973	0.939	-2.251	2.456	0.668	1.718
	10	-1.966	-2.287	1.596	-2.734	3.737	0.248	1.405
<i>27°C</i>								
	15	1.270	1.062	-1.362	0.884	-0.374	-0.815	-0.664
	14.5	0.512	0.333	-0.916	0.796	0.756	-0.868	-0.614
	14	-0.072	-0.441	-0.012	-0.338	0.886	-0.242	0.219
	13.5	-0.985	-0.965	0.661	-1.564	1.464	0.450	0.941
	13	-1.918	-1.972	2.047	-2.690	1.083	1.145	2.306
	12.5	-2.084	-2.076	2.078	-2.998	0.843	1.750	2.489
	12	-1.190	-1.120	1.213	-1.348	0.562	0.816	1.065
	11.5	0.101	0.064	-0.225	0.598	1.132	-0.599	-1.074
	11	0.842	0.858	-0.948	1.674	-0.161	-0.720	-1.544
	10.5	1.558	1.973	-0.939	2.251	-2.456	-0.668	-1.718
	10	1.966	2.287	-1.596	2.734	-3.737	-0.248	-1.405

L = Stem length, N = Number of nodes, MAT = Number of mature nodes, LAT = Number of lateral shoots, TIP = Progress toward tip abscission, PL = Length of periderm development, and PN = Periderm development in number of nodes.

 hue indicates an increasingly negative association with the axis.



 hue indicates an increasingly positive association with the axis.

Table A14. Factor weights of predictor variables for Tucker axis 1.

Temperature	Photoperiod (h)	L	N	MAT	LAT	TIP	PL	PN
<i>10°C</i>		----- Weight x 10 <sup>2</sup> -----						
	15	-0.260	-0.610	-0.150	0.050	2.120	-0.600	-0.530
	14.5	-0.170	-0.510	-0.260	0.220	2.150	-0.750	-0.660
	14	-0.030	-0.320	-0.370	0.400	1.900	-0.840	-0.740
	13.5	0.110	-0.120	-0.460	0.570	1.600	-0.910	-0.790
	13	0.280	0.170	-0.520	0.720	0.970	-0.870	-0.760
	12.5	0.310	0.370	-0.300	0.480	-0.210	-0.350	-0.300
	12	0.260	0.460	-0.070	0.200	-1.080	0.120	0.110
	11.5	0.050	0.310	0.280	-0.290	-1.620	0.680	0.600
	11	-0.080	0.220	0.510	-0.610	-2.000	1.050	0.920
	10.5	-0.210	0.080	0.650	-0.840	-2.010	1.240	1.090
	10	-0.270	-0.020	0.680	-0.900	-1.820	1.240	1.090
<i>27°C</i>								
	15	0.260	0.610	0.150	-0.050	-2.120	0.600	0.530
	14.5	0.170	0.510	0.260	-0.220	-2.150	0.750	0.660
	14	0.030	0.320	0.370	-0.400	-1.900	0.840	0.740
	13.5	-0.110	0.120	0.460	-0.570	-1.600	0.910	0.790
	13	-0.280	-0.170	0.520	-0.720	-0.970	0.870	0.760
	12.5	-0.310	-0.370	0.300	-0.480	0.210	0.350	0.300
	12	-0.260	-0.460	0.070	-0.200	1.080	-0.120	-0.110
	11.5	-0.050	-0.310	-0.280	0.290	1.620	-0.680	-0.600
	11	0.080	-0.220	-0.510	0.610	2.000	-1.050	-0.920
	10.5	0.210	-0.080	-0.650	0.840	2.010	-1.240	-1.090
	10	0.270	0.020	-0.680	0.900	1.820	-1.240	-1.090

L = Stem length, N = Number of nodes, MAT = Number of mature nodes, LAT = Number of lateral shoots, TIP = Progress toward tip abscission, PL = Length of periderm development, and PN = Periderm development in number of nodes.

 hue indicates an increasingly negative association with the axis.



 hue indicates an increasingly positive association with the axis.

Table A15. Factor weights of predictor variables for Tucker axis 2.

Temperature	Photoperiod (h)	L	N	MAT	LAT	TIP	PL	PN
<i>10°C</i>		----- Weight x 10 <sup>2</sup> -----						
	15	-1.250	-1.540	1.180	-1.940	0.980	1.380	1.190
	14.5	-1.170	-1.450	1.100	-1.810	0.960	1.270	1.090
	14	-0.920	-1.140	0.850	-1.400	0.820	0.960	0.830
	13.5	-0.640	-0.820	0.580	-0.960	0.660	0.640	0.550
	13	-0.170	-0.240	0.120	-0.220	0.340	0.090	0.080
	12.5	0.400	0.470	-0.410	0.660	-0.170	-0.510	-0.440
	12	0.760	0.930	-0.740	1.200	-0.530	-0.880	-0.750
	11.5	0.810	1.010	-0.750	1.240	-0.710	-0.860	-0.740
	11	0.850	1.080	-0.780	1.290	-0.840	-0.870	-0.740
	10.5	0.730	0.940	-0.650	1.090	-0.810	-0.700	-0.600
	10	0.580	0.760	-0.500	0.850	-0.710	-0.530	-0.450
<i>27°C</i>								
	15	1.250	1.540	-1.180	1.940	-0.980	-1.380	-1.190
	14.5	1.170	1.450	-1.100	1.810	-0.960	-1.270	-1.090
	14	0.920	1.140	-0.850	1.400	-0.820	-0.960	-0.830
	13.5	0.640	0.820	-0.580	0.960	-0.660	-0.640	-0.550
	13	0.170	0.240	-0.120	0.220	-0.340	-0.090	-0.080
	12.5	-0.400	-0.470	0.410	-0.660	0.170	0.510	0.440
	12	-0.760	-0.930	0.740	-1.200	0.530	0.880	0.750
	11.5	-0.810	-1.010	0.750	-1.240	0.710	0.860	0.740
	11	-0.850	-1.080	0.780	-1.290	0.840	0.870	0.740
	10.5	-0.730	-0.940	0.650	-1.090	0.810	0.700	0.600
	10	-0.580	-0.760	0.500	-0.850	0.710	0.530	0.450

L = Stem length, N = Number of nodes, MAT = Number of mature nodes, LAT = Number of lateral shoots, TIP = Progress toward tip abscission, PL = Length of periderm development, and PN = Periderm development in number of nodes.

 hue indicates an increasingly negative association with the axis.



 hue indicates an increasingly positive association with the axis.



Table A16. Factor weights of predictor variables for Tucker axis 3.

Temperature	Photoperiod (h)	L	N	MAT	LAT	TIP	PL	PN
<i>10°C</i>		----- Weight x 10 <sup>2</sup> -----						
	15	1.200	1.310	-1.370	2.130	0.170	-1.850	-1.600
	14.5	0.610	0.570	-0.830	1.240	0.730	-1.240	-1.070
	14	-0.220	-0.440	-0.040	-0.060	1.340	-0.310	-0.270
	13.5	-1.010	-1.410	0.730	-1.310	1.880	0.610	0.510
	13	-1.970	-2.560	1.690	-2.870	2.380	1.790	1.530
	12.5	-1.870	-2.330	1.750	-2.890	1.590	2.020	1.730
	12	-1.420	-1.680	1.440	-2.320	0.650	1.790	1.540
	11.5	0.010	0.160	0.200	-0.220	-0.980	0.440	0.390
	11	0.900	1.310	-0.580	1.090	-2.020	-0.390	-0.320
	10.5	1.710	2.320	-1.320	2.320	-2.760	-1.220	-1.040
	10	2.060	2.750	-1.670	2.880	-2.970	-1.650	-1.400
<i>27°C</i>								
	15	-1.200	-1.310	1.370	-2.130	-0.170	1.850	1.600
	14.5	-0.610	-0.570	0.830	-1.240	-0.730	1.240	1.070
	14	0.220	0.440	0.040	0.060	-1.340	0.310	0.270
	13.5	1.010	1.410	-0.730	1.310	-1.880	-0.610	-0.510
	13	1.970	2.560	-1.690	2.870	-2.380	-1.790	-1.530
	12.5	1.870	2.330	-1.750	2.890	-1.590	-2.020	-1.730
	12	1.420	1.680	-1.440	2.320	-0.650	-1.790	-1.540
	11.5	-0.010	-0.160	-0.200	0.220	0.980	-0.440	-0.390
	11	-0.900	-1.310	0.580	-1.090	2.020	0.390	0.320
	10.5	-1.710	-2.320	1.320	-2.320	2.760	1.220	1.040
	10	-2.060	-2.750	1.670	-2.880	2.970	1.650	1.400

L = Stem length, N = Number of nodes, MAT = Number of mature nodes, LAT = Number of lateral shoots, TIP = Progress toward tip abscission, PL = Length of periderm development, and PN = Periderm development in number of nodes.

 hue indicates an increasingly negative association with the axis.



 hue indicates an increasingly positive association with the axis.

Table A17. Factor weights of predictor variables for mode-rotated Tucker axis 1.

Temperature	Photoperiod (h)	L	N	MAT	LAT	TIP	PL	PN
<i>10°C</i>		----- Weight x 10 <sup>2</sup> -----						
	15	-0.010	-0.340	-0.440	0.490	2.160	-0.990	-0.870
	14.5	-0.110	-0.480	-0.380	0.380	2.370	-0.950	-0.830
	14	-0.210	-0.590	-0.250	0.180	2.320	-0.770	-0.680
	13.5	-0.310	-0.670	-0.120	-0.010	2.200	-0.570	-0.510
	13	-0.400	-0.700	0.080	-0.280	1.720	-0.220	-0.200
	12.5	-0.270	-0.350	0.240	-0.400	0.300	0.260	0.220
	12	-0.120	0.000	0.310	-0.410	-0.870	0.580	0.510
	11.5	0.150	0.460	0.230	-0.190	-1.930	0.670	0.600
	11	0.330	0.760	0.190	-0.060	-2.630	0.750	0.660
	10.5	0.450	0.940	0.100	0.100	-2.880	0.680	0.610
	10	0.490	0.960	0.030	0.200	-2.760	0.570	0.510
<i>27°C</i>								
	15	0.010	0.340	0.440	-0.490	-2.160	0.990	0.870
	14.5	0.110	0.480	0.380	-0.380	-2.370	0.950	0.830
	14	0.210	0.590	0.250	-0.180	-2.320	0.770	0.680
	13.5	0.310	0.670	0.120	0.010	-2.200	0.570	0.510
	13	0.400	0.700	-0.080	0.280	-1.720	0.220	0.200
	12.5	0.270	0.350	-0.240	0.400	-0.300	-0.260	-0.220
	12	0.120	0.000	-0.310	0.410	0.870	-0.580	-0.510
	11.5	-0.150	-0.460	-0.230	0.190	1.930	-0.670	-0.600
	11	-0.330	-0.760	-0.190	0.060	2.630	-0.750	-0.660
	10.5	-0.450	-0.940	-0.100	-0.100	2.880	-0.680	-0.610
	10	-0.490	-0.960	-0.030	-0.200	2.760	-0.570	-0.510

L = Stem length, N = Number of nodes, MAT = Number of mature nodes, LAT = Number of lateral shoots, TIP = Progress toward tip abscission, PL = Length of periderm development, and PN = Periderm development in number of nodes.

 hue indicates an increasingly negative association with the axis.



 hue indicates an increasingly positive association with the axis.

Table A18. Factor weights of predictor variables for mode-rotated Tucker axis 2.

Temperature	Photoperiod (h)	L	N	MAT	LAT	TIP	PL	PN
<i>10°C</i>		----- Weight x 10 <sup>2</sup> -----						
	15	-1.470	-1.760	1.470	-2.370	0.800	1.790	1.540
	14.5	-1.260	-1.510	1.270	-2.050	0.660	1.550	1.340
	14	-0.840	-1.000	0.850	-1.370	0.400	1.050	0.910
	13.5	-0.410	-0.470	0.420	-0.680	0.140	0.530	0.460
	13	0.260	0.320	-0.230	0.390	-0.250	-0.260	-0.220
	12.5	0.790	0.960	-0.770	1.260	-0.510	-0.930	-0.800
	12	1.050	1.260	-1.040	1.680	-0.600	-1.260	-1.080
	11.5	0.780	0.930	-0.790	1.270	-0.390	-0.970	-0.840
	11	0.640	0.750	-0.650	1.050	-0.260	-0.810	-0.700
	10.5	0.350	0.400	-0.370	0.590	-0.070	-0.480	-0.410
	10	0.120	0.130	-0.150	0.230	0.070	-0.210	-0.180
<i>27°C</i>								
	15	1.470	1.760	-1.470	2.370	-0.800	-1.790	-1.540
	14.5	1.260	1.510	-1.270	2.050	-0.660	-1.550	-1.340
	14	0.840	1.000	-0.850	1.370	-0.400	-1.050	-0.910
	13.5	0.410	0.470	-0.420	0.680	-0.140	-0.530	-0.460
	13	-0.260	-0.320	0.230	-0.390	0.250	0.260	0.220
	12.5	-0.790	-0.960	0.770	-1.260	0.510	0.930	0.800
	12	-1.050	-1.260	1.040	-1.680	0.600	1.260	1.080
	11.5	-0.780	-0.930	0.790	-1.270	0.390	0.970	0.840
	11	-0.640	-0.750	0.650	-1.050	0.260	0.810	0.700
	10.5	-0.350	-0.400	0.370	-0.590	0.070	0.480	0.410
	10	-0.120	-0.130	0.150	-0.230	-0.070	0.210	0.180

L = Stem length, N = Number of nodes, MAT = Number of mature nodes, LAT = Number of lateral shoots, TIP = Progress toward tip abscission, PL = Length of periderm development, and PN = Periderm development in number of nodes.

 hue indicates an increasingly negative association with the axis.


 hue indicates an increasingly positive association with the axis.

Table A19. Factor weights of predictor variables for mode-rotated Tucker axis 3.

Temperature	Photoperiod (h)	L	N	MAT	LAT	TIP	PL	PN
<i>10°C</i>		----- Weight x 10 <sup>2</sup> -----						
	15	0.950	1.120	-0.980	1.570	-0.380	-1.230	-1.060
	14.5	0.390	0.420	-0.460	0.720	0.120	-0.640	-0.550
	14	-0.360	-0.520	0.250	-0.460	0.730	0.190	0.160
	13.5	-1.090	-1.410	0.940	-1.580	1.310	0.990	0.850
	13	-1.940	-2.450	1.760	-2.930	1.920	1.960	1.680
	12.5	-1.750	-2.180	1.640	-2.700	1.500	1.880	1.620
	12	-1.250	-1.520	1.210	-1.970	0.870	1.440	1.240
	11.5	0.150	0.230	-0.060	0.140	-0.480	0.010	0.010
	11	1.020	1.340	-0.860	1.460	-1.330	-0.880	-0.750
	10.5	1.780	2.290	-1.560	2.630	-2.010	-1.680	-1.440
	10	2.100	2.680	-1.870	3.120	-2.250	-2.040	-1.750
<i>27°C</i>								
	15	-0.950	-1.120	0.980	-1.570	0.380	1.230	1.060
	14.5	-0.390	-0.420	0.460	-0.720	-0.120	0.640	0.550
	14	0.360	0.520	-0.250	0.460	-0.730	-0.190	-0.160
	13.5	1.090	1.410	-0.940	1.580	-1.310	-0.990	-0.850
	13	1.940	2.450	-1.760	2.930	-1.920	-1.960	-1.680
	12.5	1.750	2.180	-1.640	2.700	-1.500	-1.880	-1.620
	12	1.250	1.520	-1.210	1.970	-0.870	-1.440	-1.240
	11.5	-0.150	-0.230	0.060	-0.140	0.480	-0.010	-0.010
	11	-1.020	-1.340	0.860	-1.460	1.330	0.880	0.750
	10.5	-1.780	-2.290	1.560	-2.630	2.010	1.680	1.440
	10	-2.100	-2.680	1.870	-3.120	2.250	2.040	1.750

L = Stem length, N = Number of nodes, MAT = Number of mature nodes, LAT = Number of lateral shoots, TIP = Progress toward tip abscission, PL = Length of periderm development, and PN = Periderm development in number of nodes.




 hue indicates an increasingly negative association with the axis.  
 hue indicates an increasingly positive association with the axis.

Table A20. Factor weights of predictor variables for core-rotated Tucker axis 1.

Temperature	Photoperiod (h)	L	N	MAT	LAT	TIP	PL	PN
<i>10°C</i>		----- Weight x 10 <sup>2</sup> -----						
	15	-0.970	-1.220	0.890	-1.480	0.900	1.010	0.870
	14.5	-1.020	-1.280	0.920	-1.530	1.000	1.030	0.880
	14	-0.940	-1.200	0.840	-1.400	0.990	0.920	0.790
	13.5	-0.830	-1.070	0.730	-1.230	0.950	0.780	0.670
	13	-0.570	-0.750	0.480	-0.810	0.770	0.480	0.410
	12.5	0.010	-0.020	-0.040	0.050	0.160	-0.080	-0.070
	12	0.450	0.560	-0.430	0.710	-0.350	-0.510	-0.440
	11.5	0.790	1.010	-0.710	1.180	-0.820	-0.780	-0.670
	11	1.020	1.310	-0.900	1.510	-1.140	-0.970	-0.830
	10.5	1.070	1.380	-0.920	1.560	-1.260	-0.980	-0.840
	10	0.990	1.290	-0.850	1.440	-1.210	-0.890	-0.770
<i>27°C</i>								
	15	0.970	1.220	-0.890	1.480	-0.900	-1.010	-0.870
	14.5	1.020	1.280	-0.920	1.530	-1.000	-1.030	-0.880
	14	0.940	1.200	-0.840	1.400	-0.990	-0.920	-0.790
	13.5	0.830	1.070	-0.730	1.230	-0.950	-0.780	-0.670
	13	0.570	0.750	-0.480	0.810	-0.770	-0.480	-0.410
	12.5	-0.010	0.020	0.040	-0.050	-0.160	0.080	0.070
	12	-0.450	-0.560	0.430	-0.710	0.350	0.510	0.440
	11.5	-0.790	-1.010	0.710	-1.180	0.820	0.780	0.670
	11	-1.020	-1.310	0.900	-1.510	1.140	0.970	0.830
	10.5	-1.070	-1.380	0.920	-1.560	1.260	0.980	0.840
	10	-0.990	-1.290	0.850	-1.440	1.210	0.890	0.770

L = Stem length, N = Number of nodes, MAT = Number of mature nodes, LAT = Number of lateral shoots, TIP = Progress toward tip abscission, PL = Length of periderm development, and PN = Periderm development in number of nodes.

 hue indicates an increasingly negative association with the axis.


 hue indicates an increasingly positive association with the axis.

Table A21. Factor weights of predictor variables for core-rotated Tucker axis 2.

Temperature	Photoperiod (h)	L	N	MAT	LAT	TIP	PL	PN
<i>10°C</i>		----- Weight x 10 <sup>2</sup> -----						
	15	0.020	0.340	0.420	-0.480	-2.110	0.960	0.850
	14.5	0.040	0.390	0.420	-0.460	-2.250	0.990	0.870
	14	0.070	0.400	0.370	-0.380	-2.130	0.890	0.780
	13.5	0.100	0.410	0.300	-0.290	-1.950	0.770	0.680
	13	0.120	0.350	0.160	-0.130	-1.430	0.490	0.430
	12.5	0.080	0.100	-0.060	0.110	-0.120	-0.060	-0.050
	12	0.030	-0.110	-0.230	0.270	0.920	-0.470	-0.420
	11.5	-0.050	-0.330	-0.310	0.330	1.790	-0.750	-0.660
	11	-0.110	-0.480	-0.380	0.380	2.360	-0.950	-0.830
	10.5	-0.140	-0.540	-0.370	0.350	2.530	-0.970	-0.850
	10	-0.150	-0.530	-0.330	0.300	2.380	-0.890	-0.780
<i>27°C</i>								
	15	-0.020	-0.340	-0.420	0.480	2.110	-0.960	-0.850
	14.5	-0.040	-0.390	-0.420	0.460	2.250	-0.990	-0.870
	14	-0.070	-0.400	-0.370	0.380	2.130	-0.890	-0.780
	13.5	-0.100	-0.410	-0.300	0.290	1.950	-0.770	-0.680
	13	-0.120	-0.350	-0.160	0.130	1.430	-0.490	-0.430
	12.5	-0.080	-0.100	0.060	-0.110	0.120	0.060	0.050
	12	-0.030	0.110	0.230	-0.270	-0.920	0.470	0.420
	11.5	0.050	0.330	0.310	-0.330	-1.790	0.750	0.660
	11	0.110	0.480	0.380	-0.380	-2.360	0.950	0.830
	10.5	0.140	0.540	0.370	-0.350	-2.530	0.970	0.850
	10	0.150	0.530	0.330	-0.300	-2.380	0.890	0.780

L = Stem length, N = Number of nodes, MAT = Number of mature nodes, LAT = Number of lateral shoots, TIP = Progress toward tip abscission, PL = Length of periderm development, and PN = Periderm development in number of nodes.





 hue indicates an increasingly negative association with the axis.  
 hue indicates an increasingly positive association with the axis.

Table A22. Factor weights of predictor variables for core-rotated Tucker axis 3.

Temperature	Photoperiod (h)	L	N	MAT	LAT	TIP	PL	PN
<i>10°C</i>		----- Weight x 10 <sup>2</sup> -----						
	15	1.460	1.690	-1.530	2.430	-0.450	-1.930	-1.670
	14.5	0.860	0.940	-0.970	1.510	0.080	-1.300	-1.120
	14	-0.020	-0.130	-0.140	0.150	0.740	-0.320	-0.280
	13.5	-0.860	-1.160	0.670	-1.170	1.350	0.630	0.540
	13	-1.910	-2.430	1.700	-2.850	2.020	1.870	1.600
	12.5	-1.940	-2.400	1.820	-3.000	1.600	2.110	1.810
	12	-1.570	-1.890	1.550	-2.510	0.950	1.870	1.610
	11.5	-0.170	-0.110	0.280	-0.400	-0.480	0.470	0.410
	11	0.710	1.000	-0.500	0.910	-1.370	-0.400	-0.340
	10.5	1.530	2.020	-1.260	2.170	-2.090	-1.270	-1.090
	10	1.910	2.490	-1.640	2.770	-2.350	-1.720	-1.470
<i>27°C</i>								
	15	-1.460	-1.690	1.530	-2.430	0.450	1.930	1.670
	14.5	-0.860	-0.940	0.970	-1.510	-0.080	1.300	1.120
	14	0.020	0.130	0.140	-0.150	-0.740	0.320	0.280
	13.5	0.860	1.160	-0.670	1.170	-1.350	-0.630	-0.540
	13	1.910	2.430	-1.700	2.850	-2.020	-1.870	-1.600
	12.5	1.940	2.400	-1.820	3.000	-1.600	-2.110	-1.810
	12	1.570	1.890	-1.550	2.510	-0.950	-1.870	-1.610
	11.5	0.170	0.110	-0.280	0.400	0.480	-0.470	-0.410
	11	-0.710	-1.000	0.500	-0.910	1.370	0.400	0.340
	10.5	-1.530	-2.020	1.260	-2.170	2.090	1.270	1.090
	10	-1.910	-2.490	1.640	-2.770	2.350	1.720	1.470

L = Stem length, N = Number of nodes, MAT = Number of mature nodes, LAT = Number of lateral shoots, TIP = Progress toward tip abscission, PL = Length of periderm development, and PN = Periderm development in number of nodes.

 hue indicates an increasingly negative association with the axis.

 hue indicates an increasingly positive association with the axis.

## APPENDIX B. FIGURES

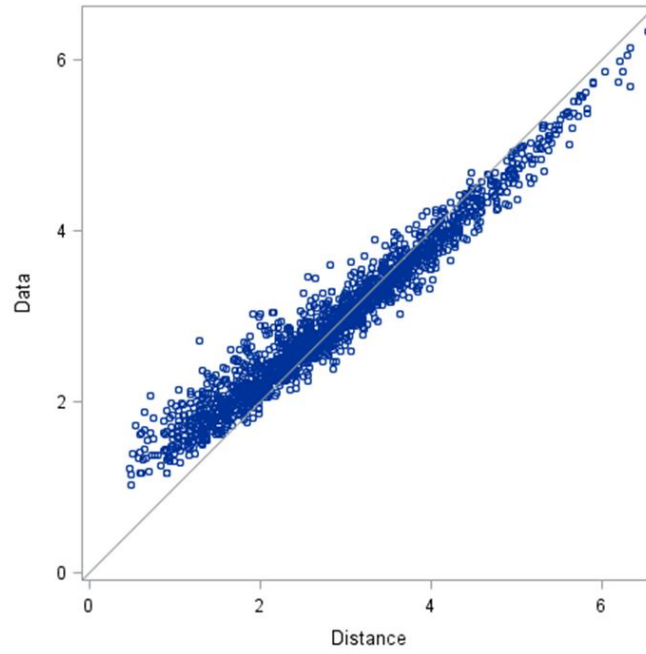


Figure B1. Metric-MDS three axis solution fit.

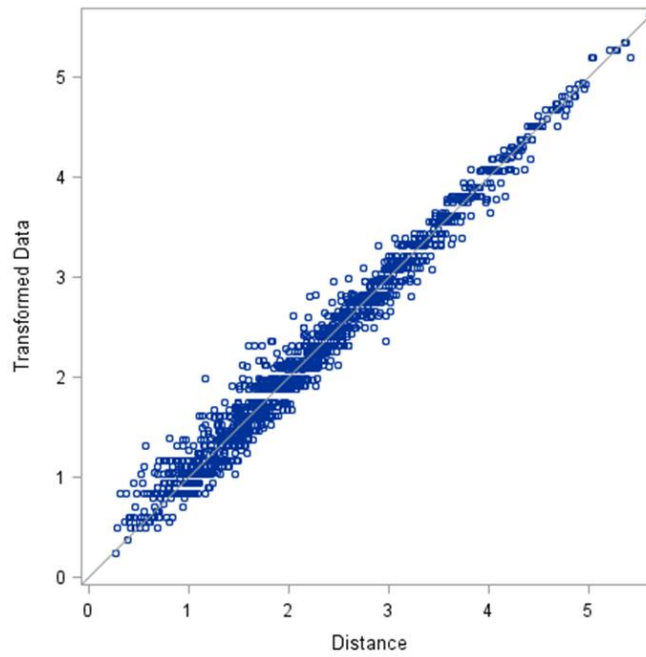


Figure B2. NMS three axis solution fit.



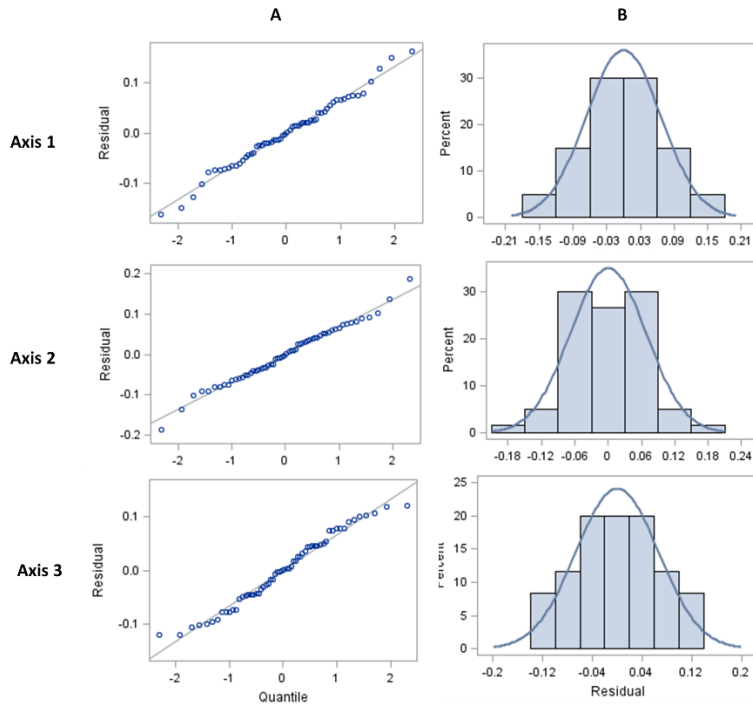


Figure B3. SVD A.) quartile-quartile plot and B.) distribution of residuals from ANOVA of each retained axis.

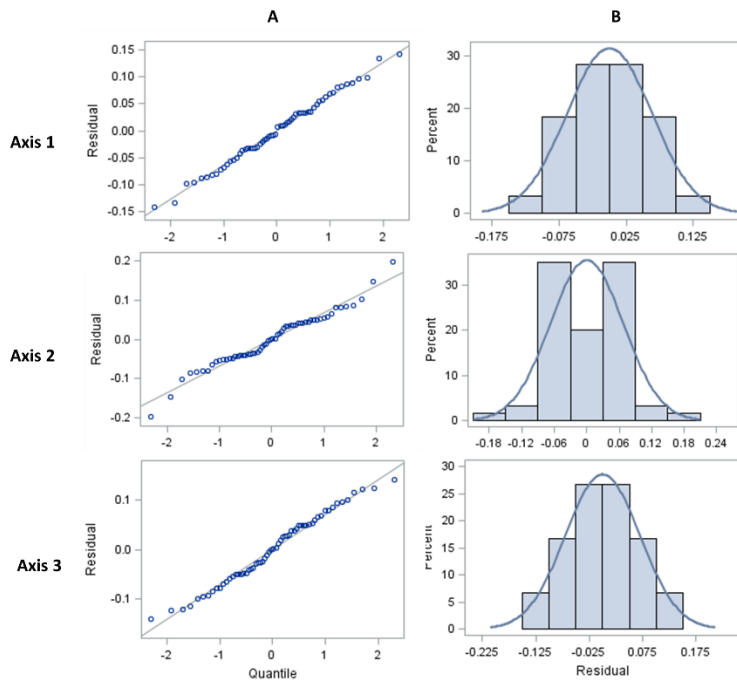


Figure B4. Varimax rotated SVD A.) quartile-quartile plot and B.) distribution of residuals from ANOVA of each retained axis.

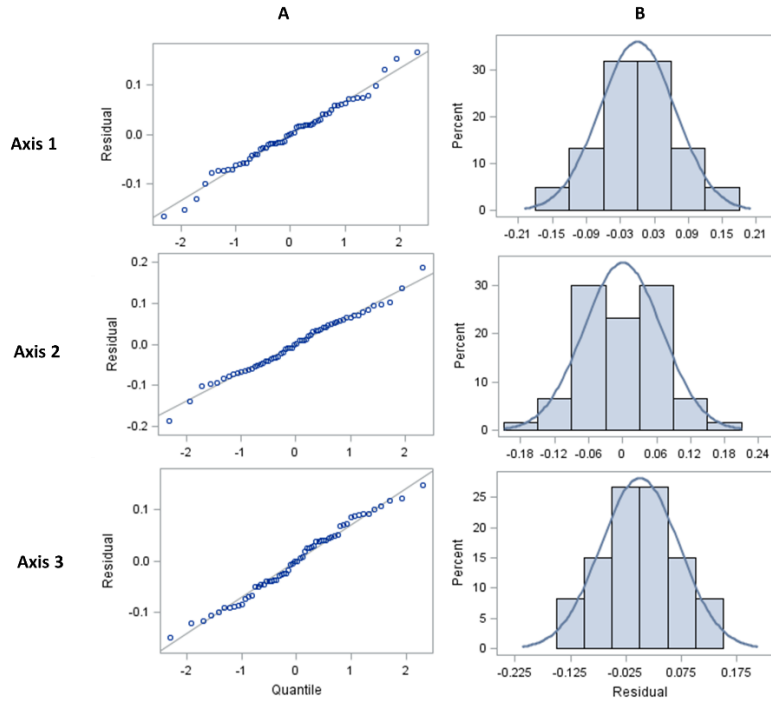


Figure B5. Tucker decomposition A.) quartile-quartile plot and B.) distribution of residuals from ANOVA of each retained axis.

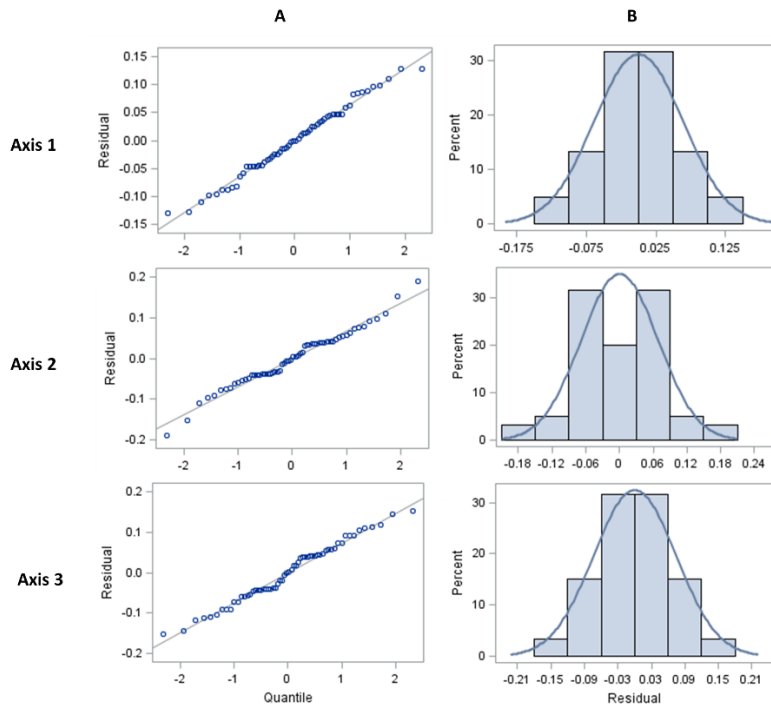


Figure B6. Mode-rotated Tucker A.) quartile-quartile plot and B.) distribution of residuals from ANOVA of each retained axis.

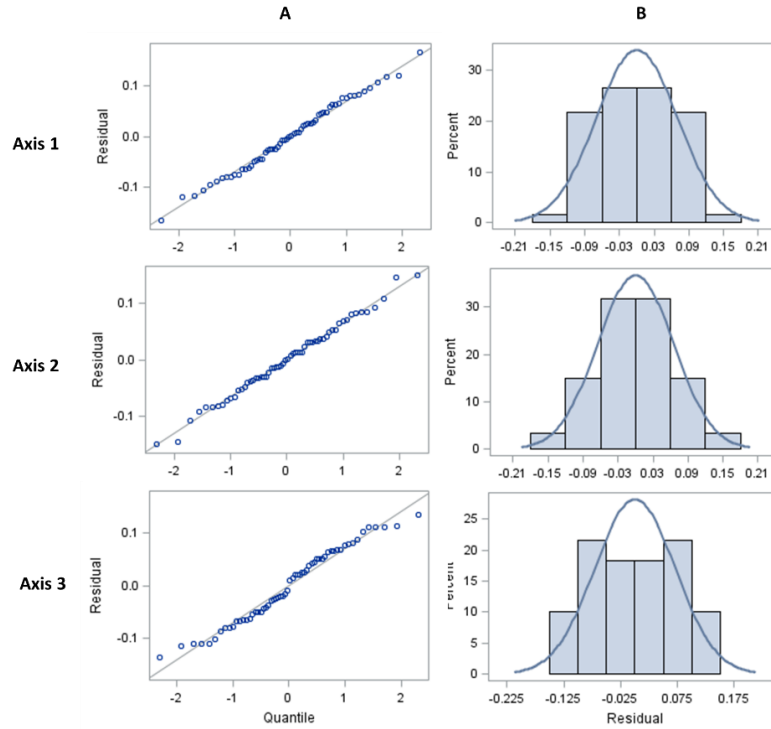


Figure B7. Core-rotated Tucker A.) quartile-quartile plot and B.) distribution of residuals from ANOVA of each retained axis.

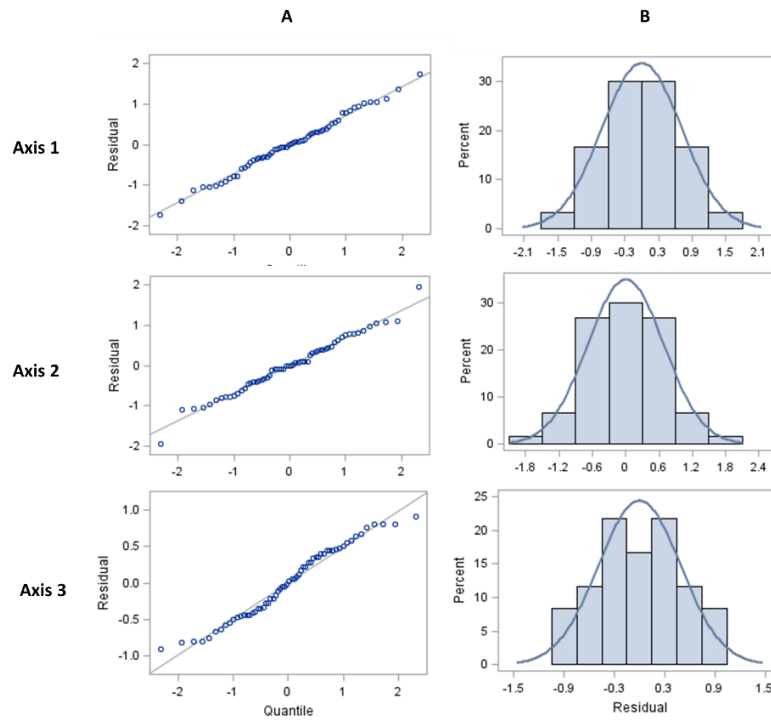


Figure B8. Metric-MDS A.) quartile-quartile plot and B.) distribution of residuals from ANOVA of each retained axis.

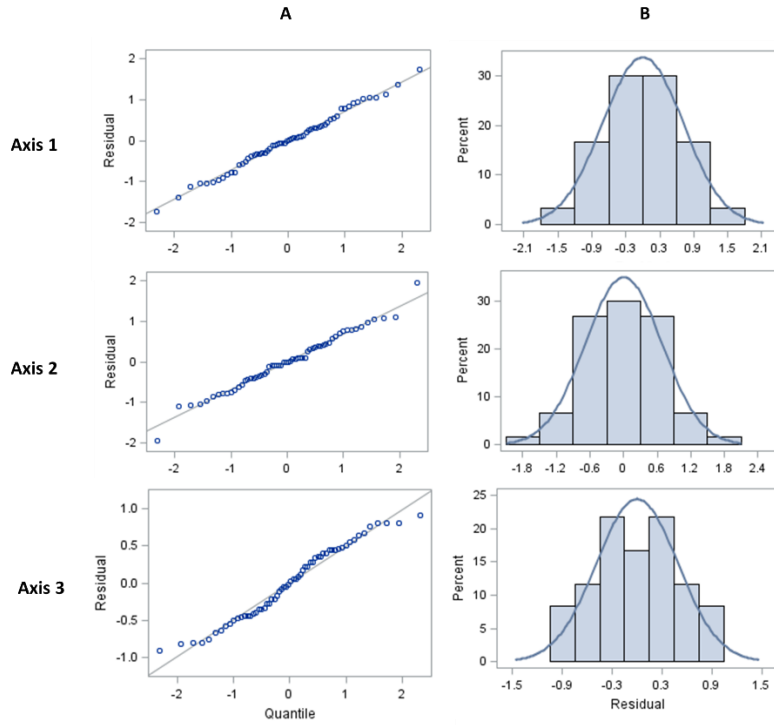


Figure B9. NMS A.) quartile-quartile plot and B.) distribution of residuals from ANOVA of each retained axis.

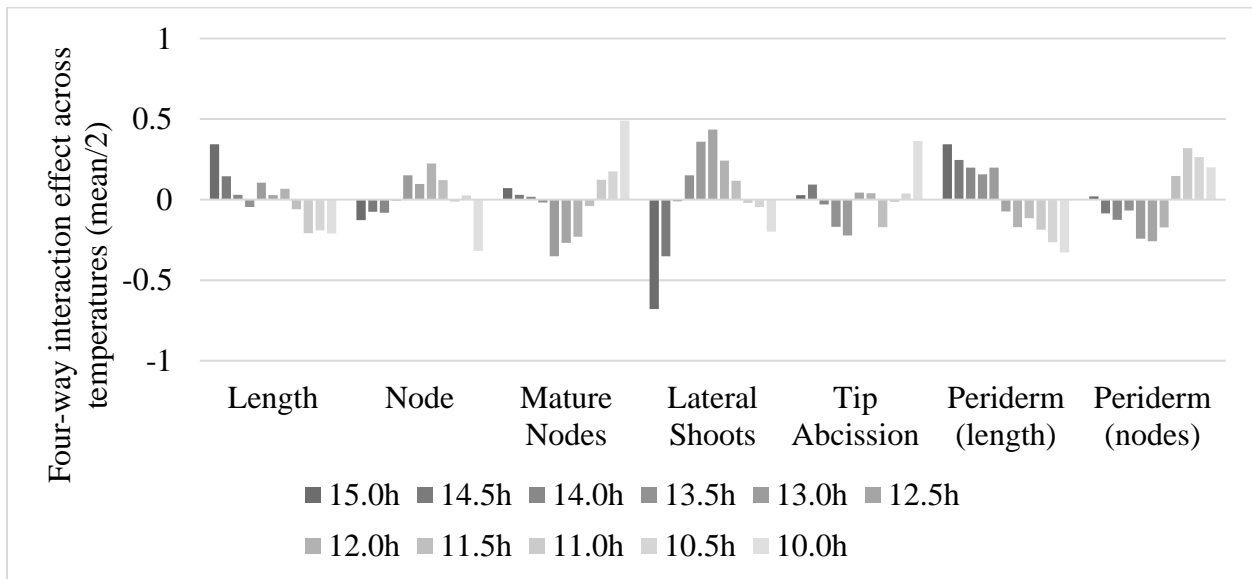


Figure B10. Plotted mean four-way interaction effect trends averaged across tested '64'.

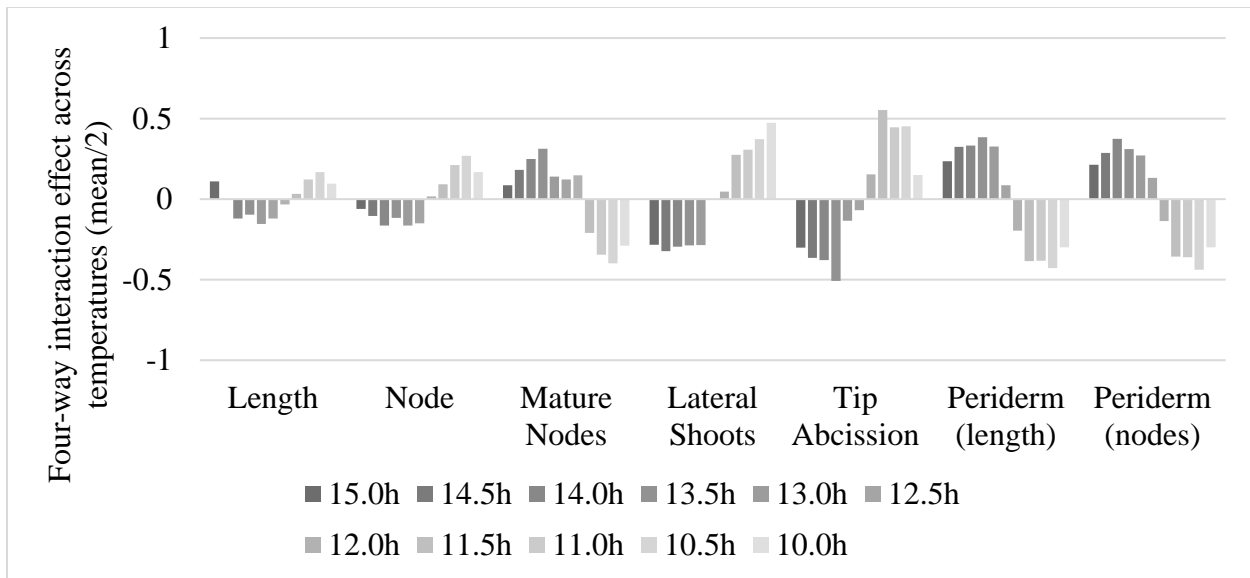


Figure B11. Plotted mean four-way interaction effect trends averaged across tested '73'.

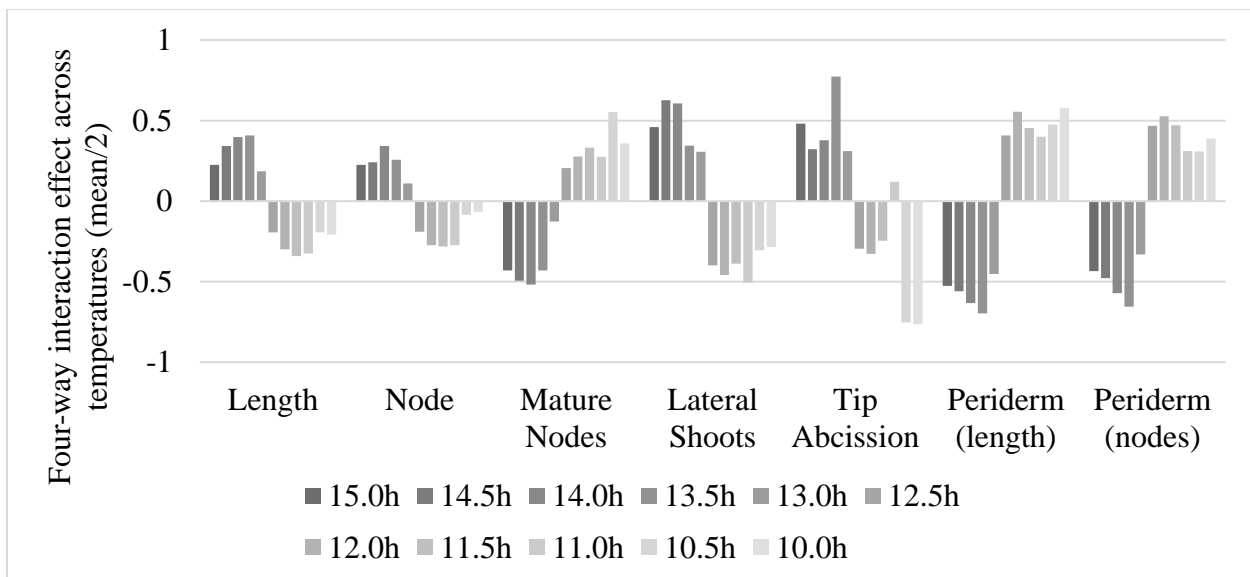


Figure B12. Plotted mean four-way interaction effect trends averaged across tested '900'.

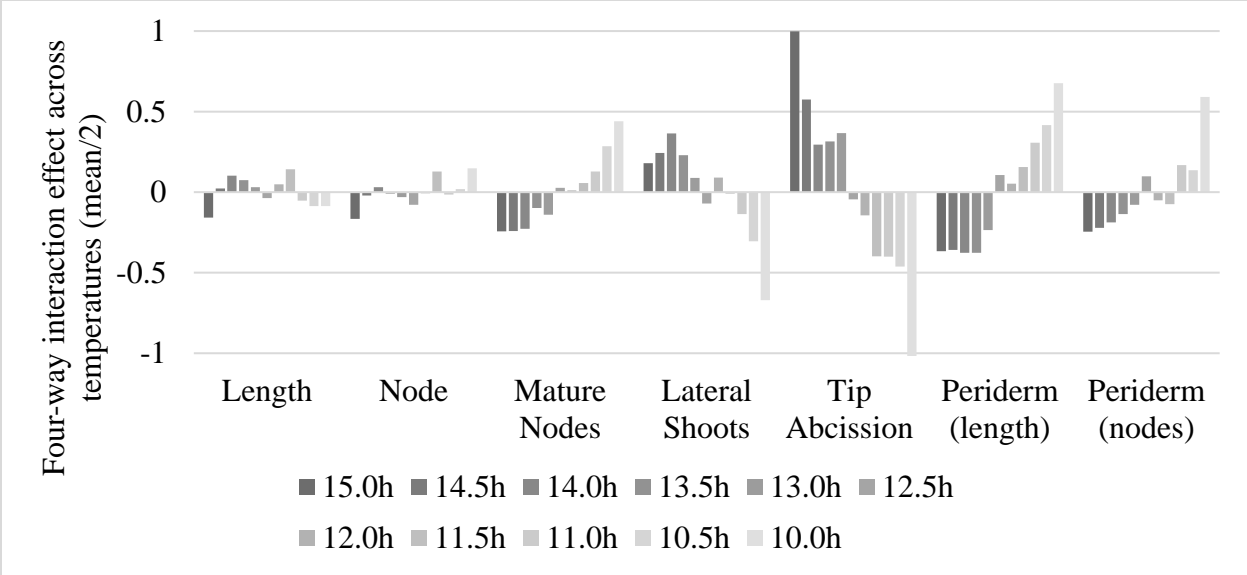


Figure B13. Plotted mean four-way interaction effect trends averaged across tested '903'.

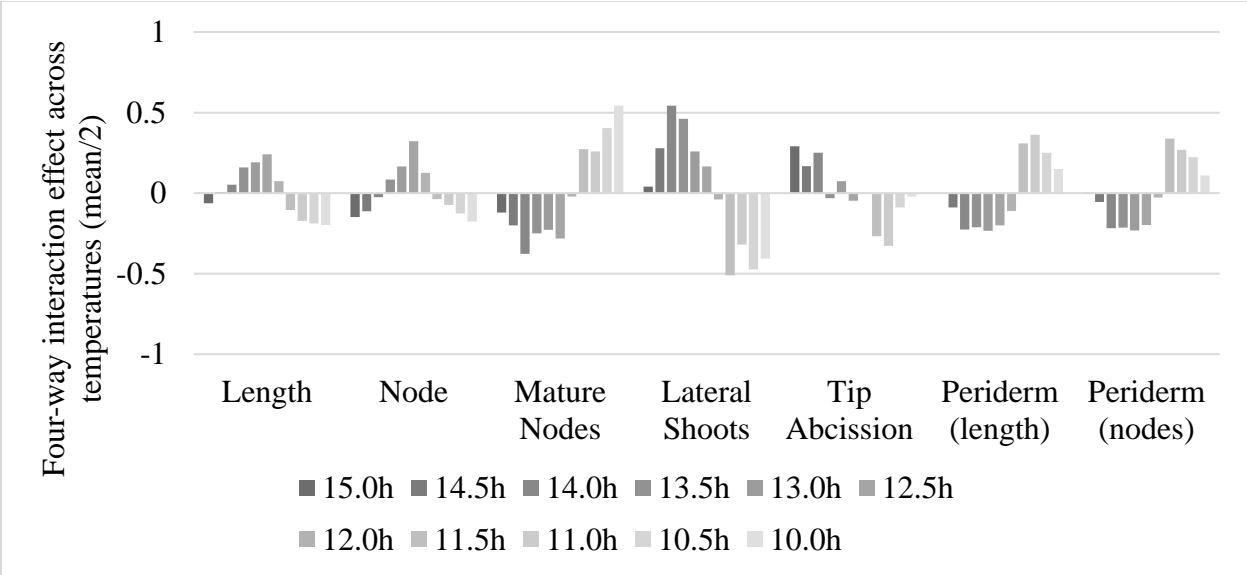


Figure B14. Plotted mean four-way interaction effect trends averaged across tested '906'.

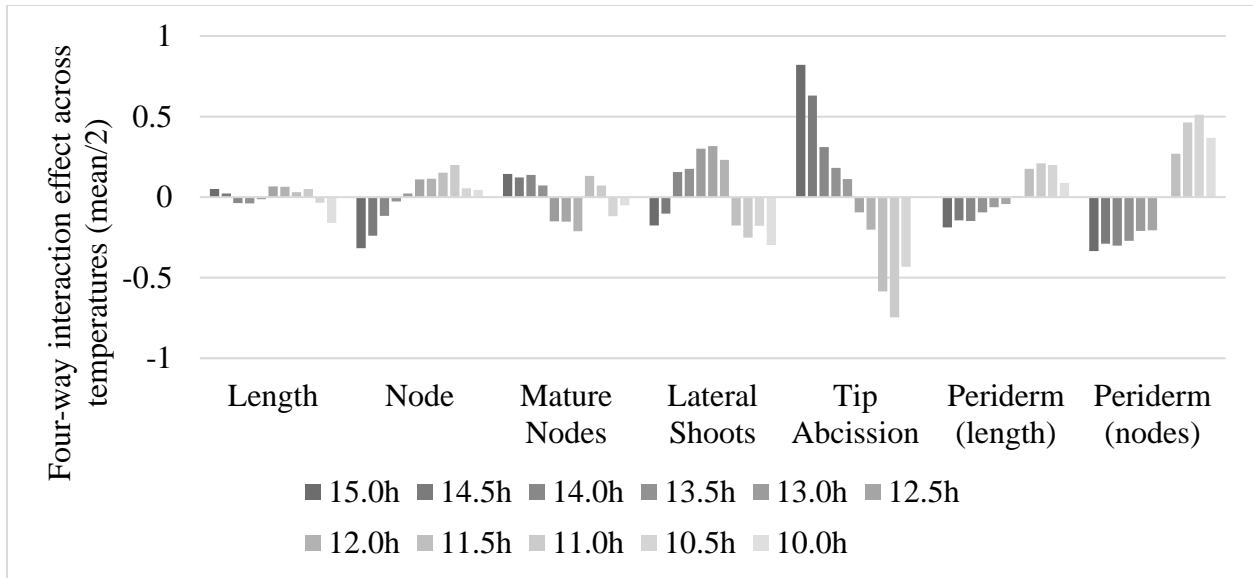


Figure B15. Plotted mean four-way interaction effect trends averaged across tested '909'.

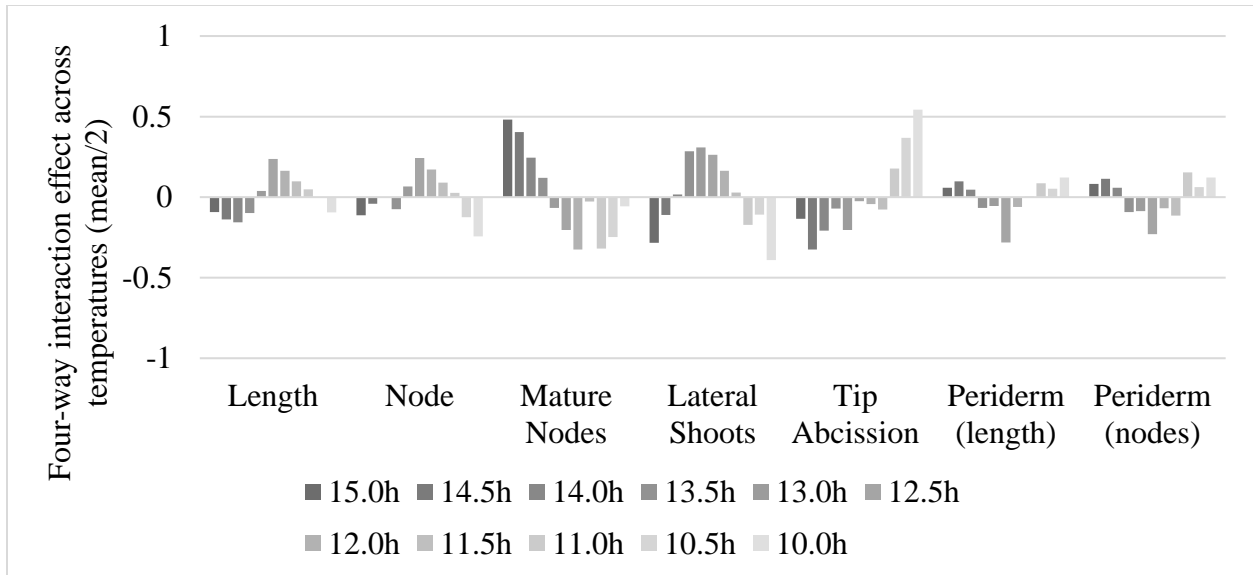


Figure B16. Plotted mean four-way interaction effect trends averaged across tested '911'.

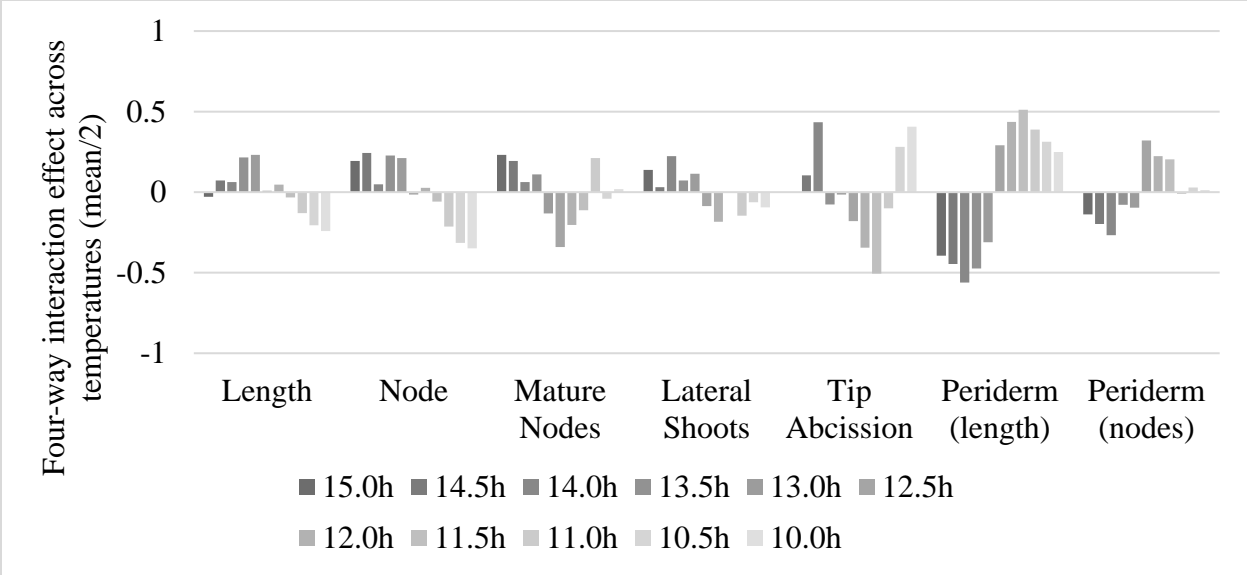


Figure B17. Plotted mean four-way interaction effect trends averaged across tested '913'.

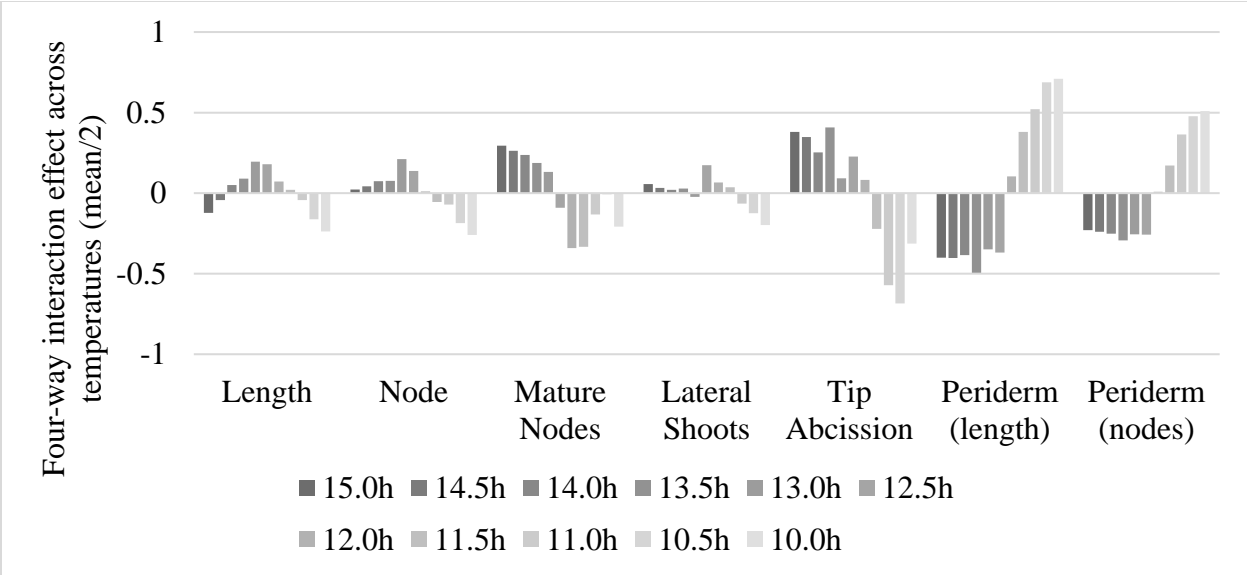


Figure B18. Plotted mean four-way interaction effect trends averaged across tested '914'.



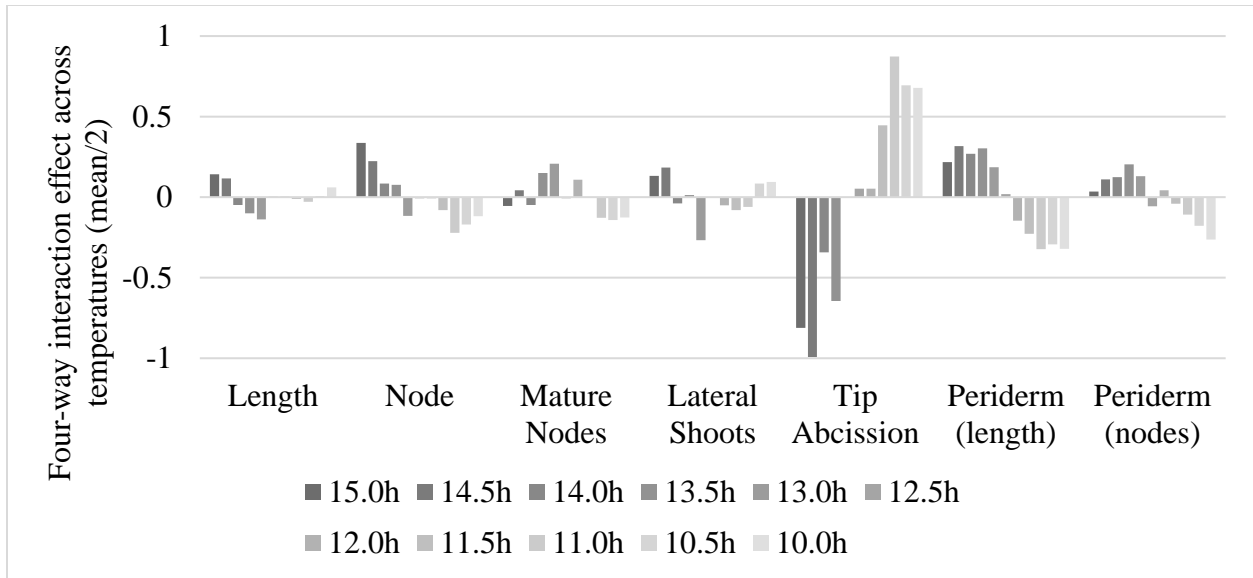


Figure B19. Plotted mean four-way interaction effect trends averaged across tested '917'.

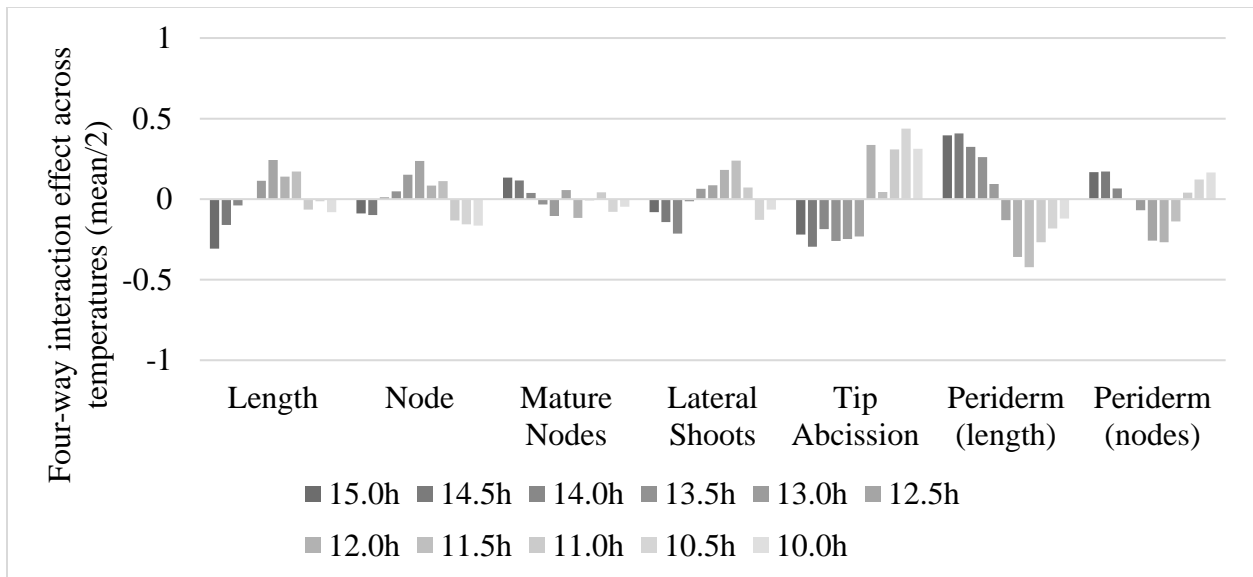


Figure B20. Plotted mean four-way interaction effect trends averaged across tested '920'.

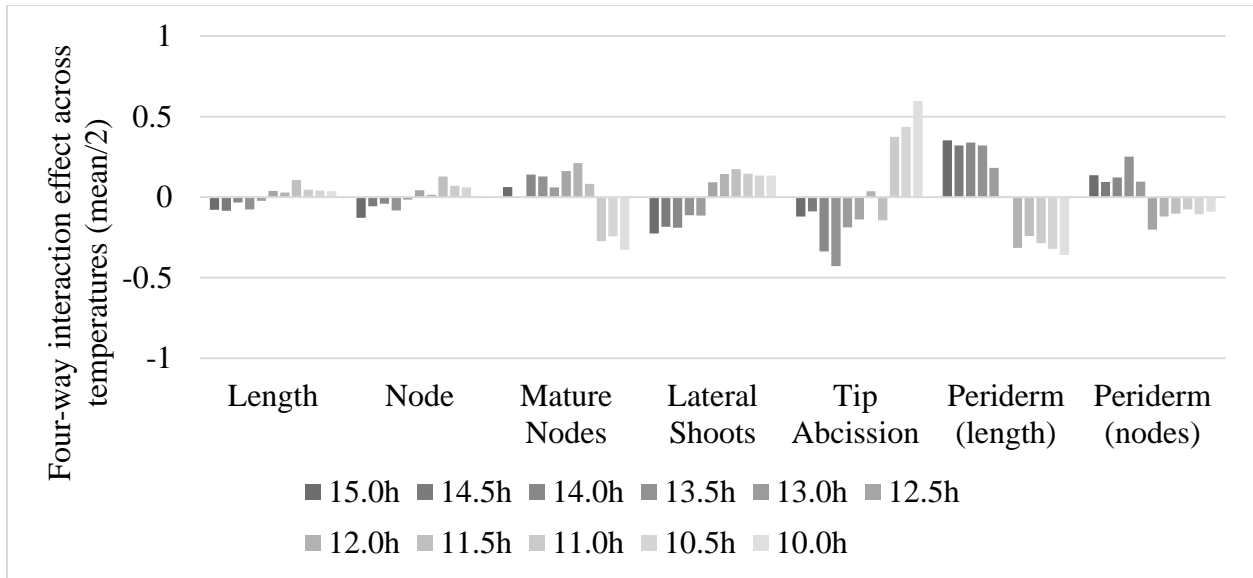


Figure B21. Plotted mean four-way interaction effect trends averaged across tested '924'.

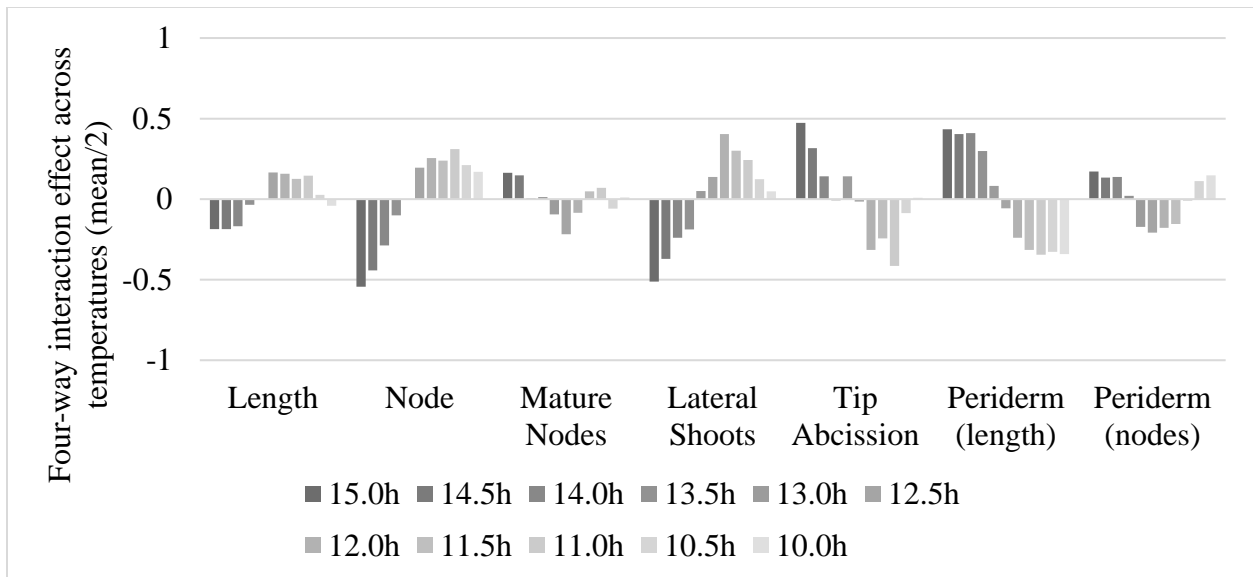


Figure B22. Plotted mean four-way interaction effect trends averaged across tested '936'.

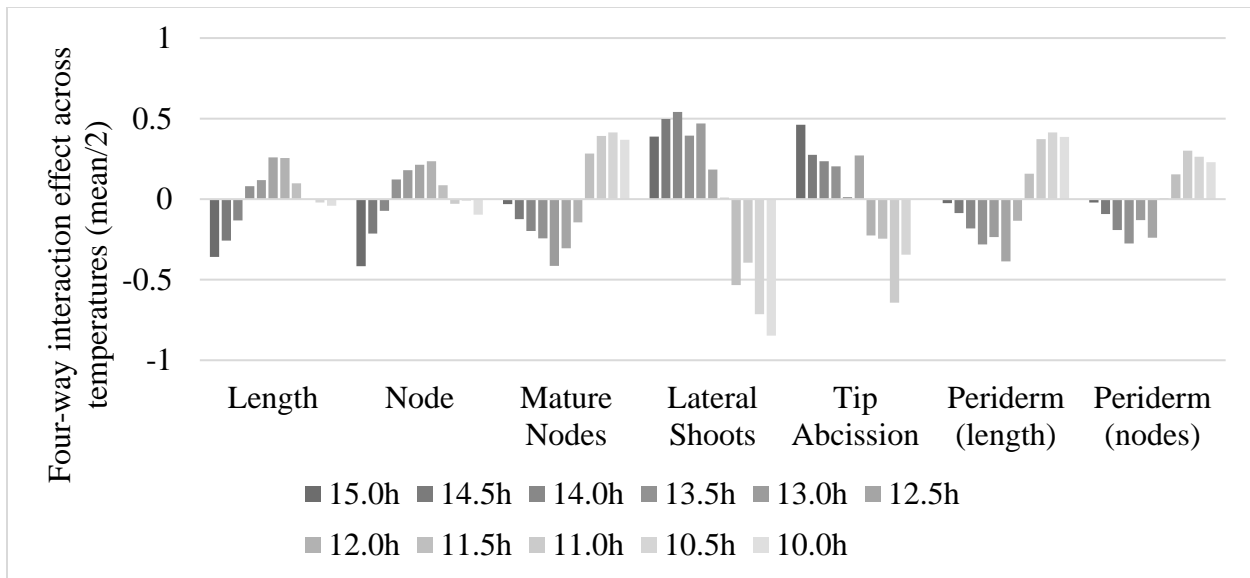


Figure B23. Plotted mean four-way interaction effect trends averaged across tested '937'.

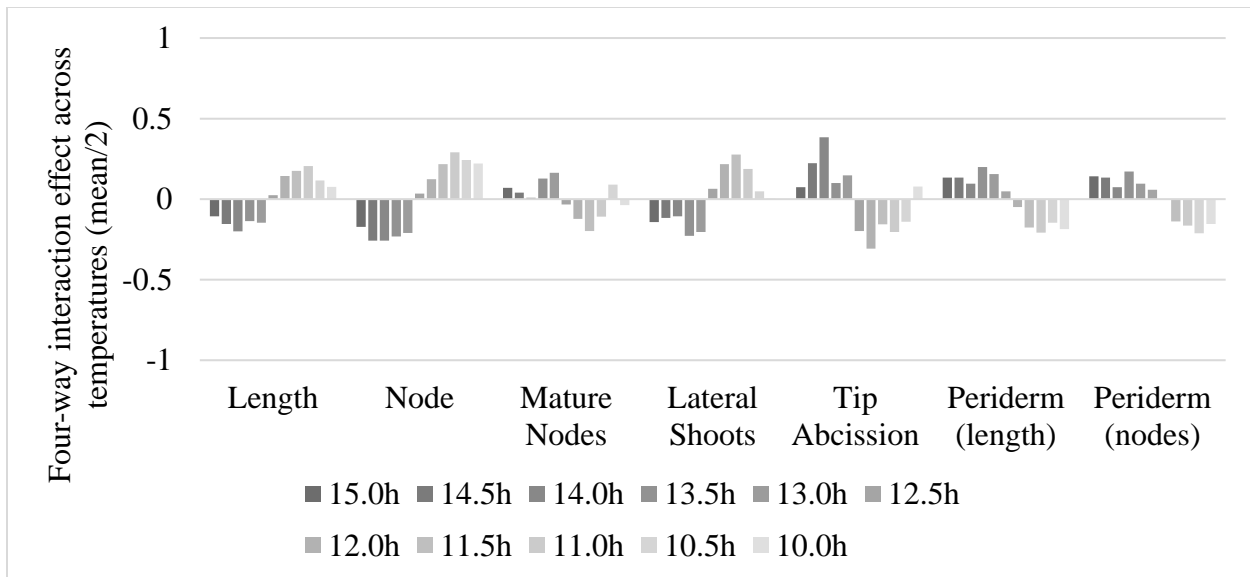


Figure B24. Plotted mean four-way interaction effect trends averaged across tested '938'.

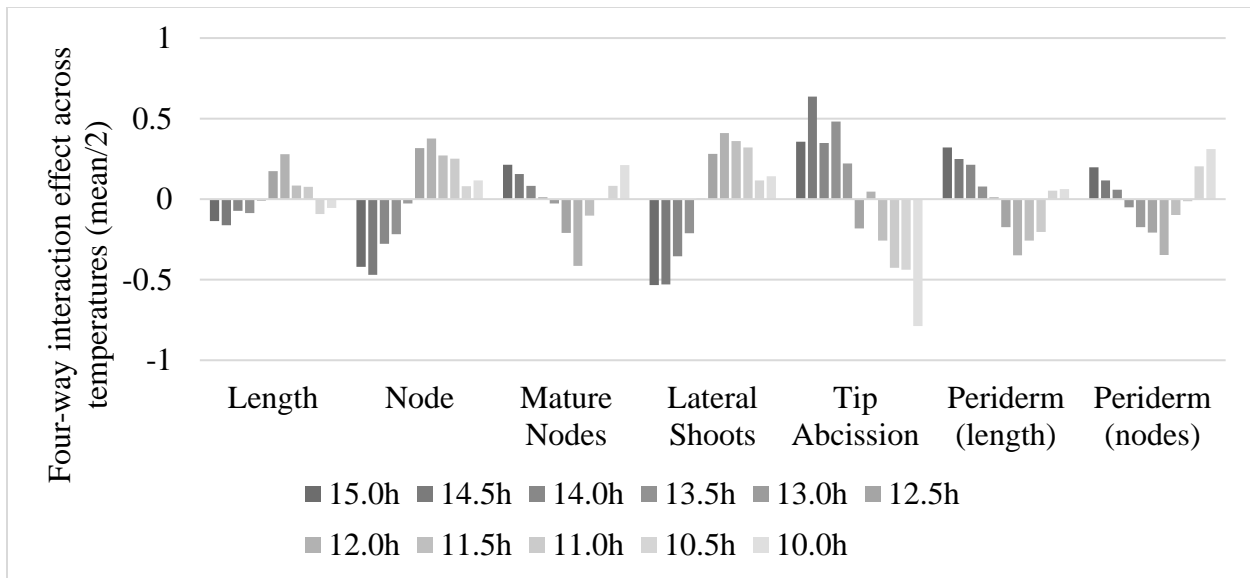


Figure B25. Plotted mean four-way interaction effect trends averaged across tested '939'.

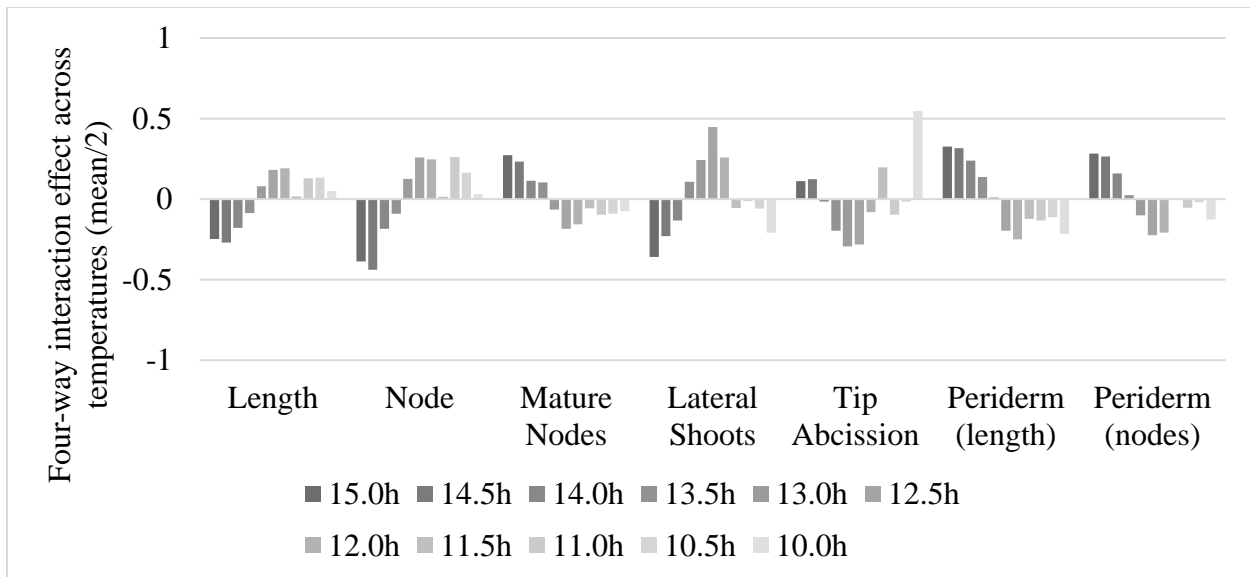


Figure B26. Plotted mean four-way interaction effect trends averaged across tested '940'.

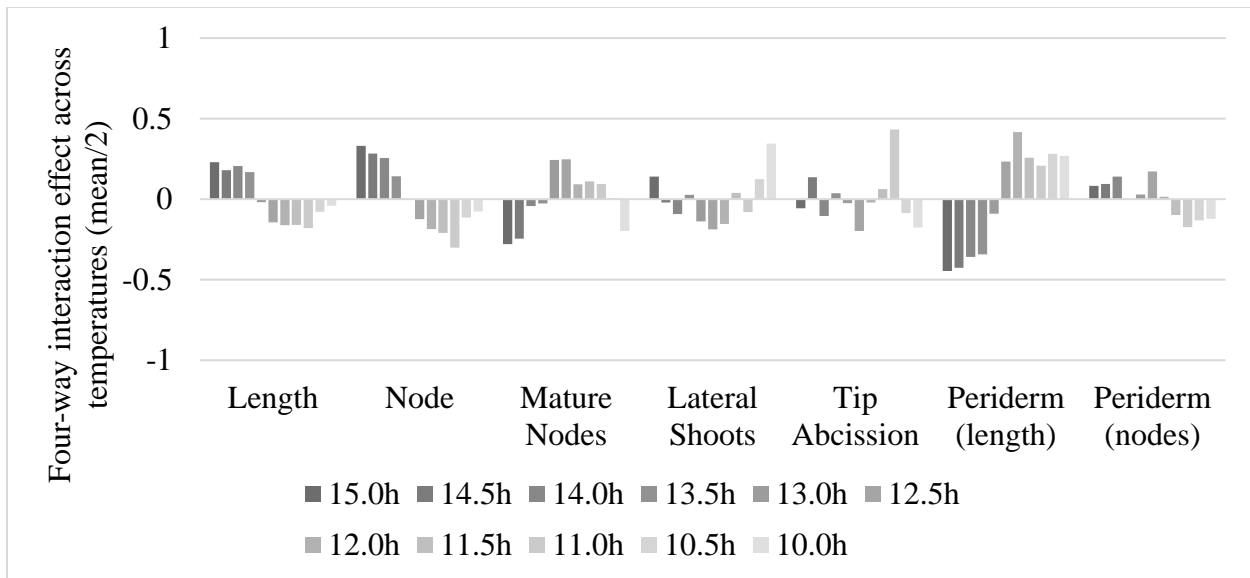


Figure B27. Plotted mean four-way interaction effect trends averaged across tested '956'.

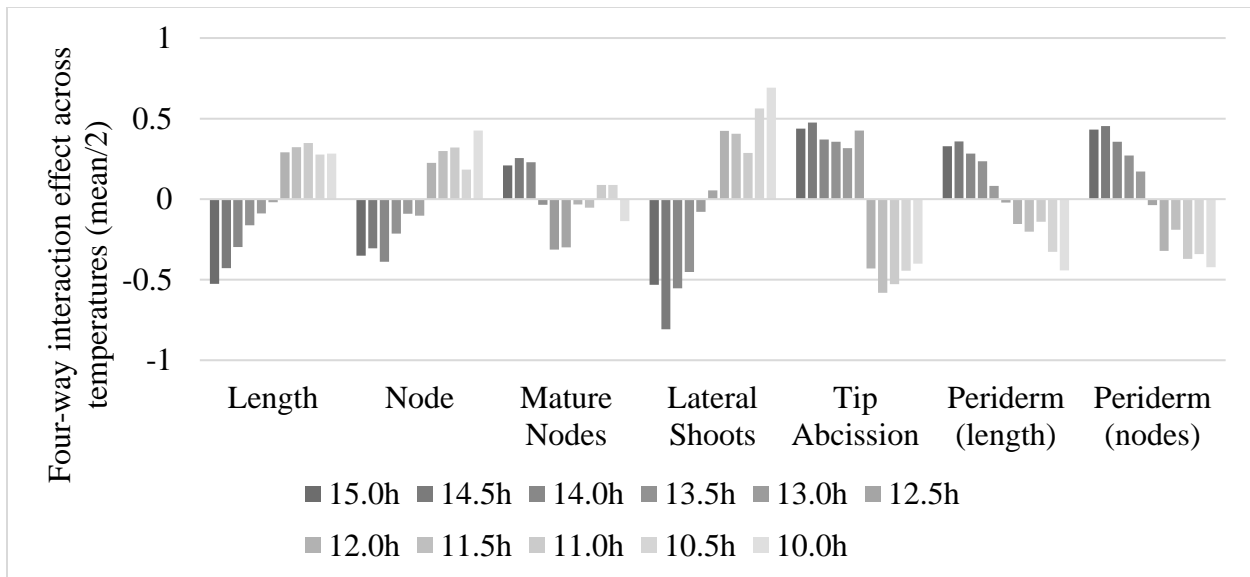


Figure B28. Plotted mean four-way interaction effect trends averaged across tested '958'.

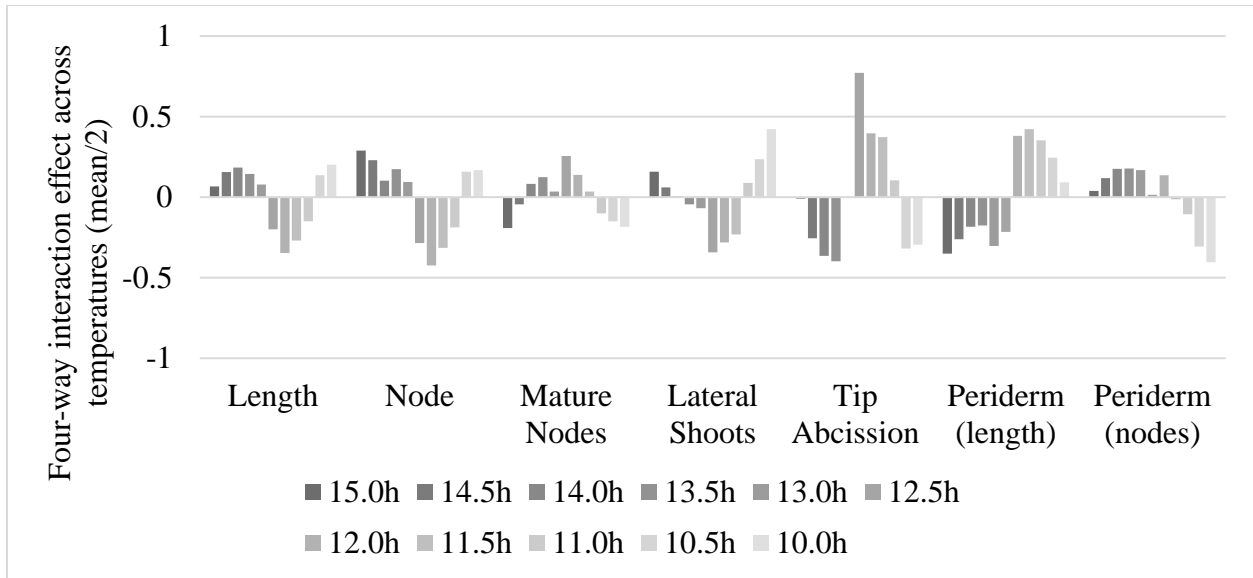


Figure B29. Plotted mean four-way interaction effect trends averaged across tested '961'.

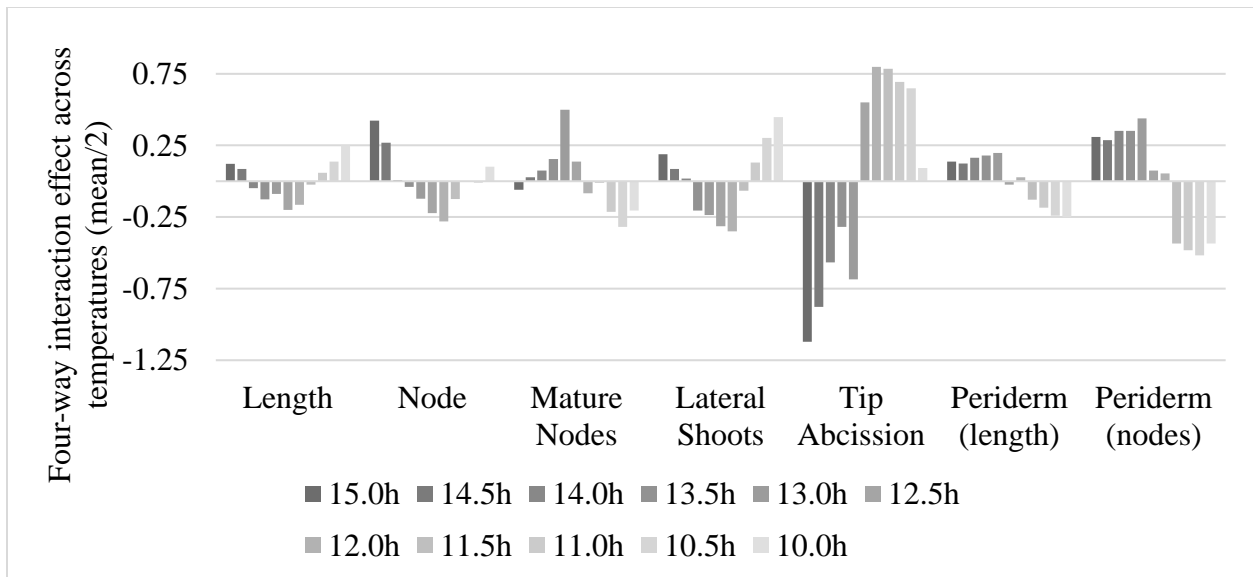


Figure B30. Plotted mean four-way interaction effect trends averaged across tested '962'.

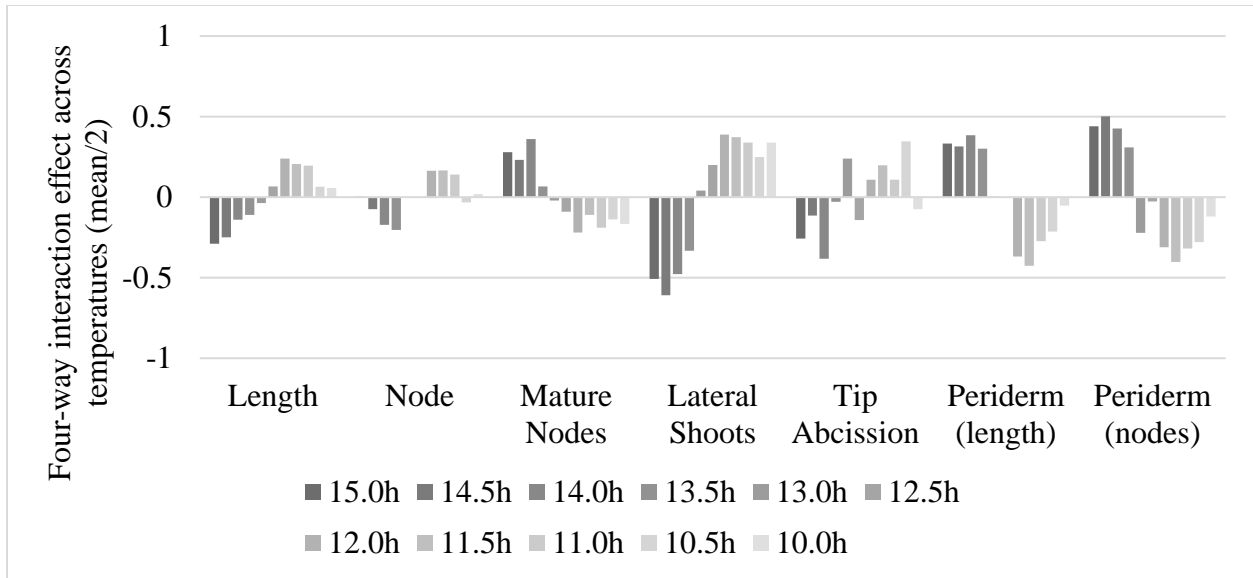


Figure B31. Plotted mean four-way interaction effect trends averaged across tested '965'.

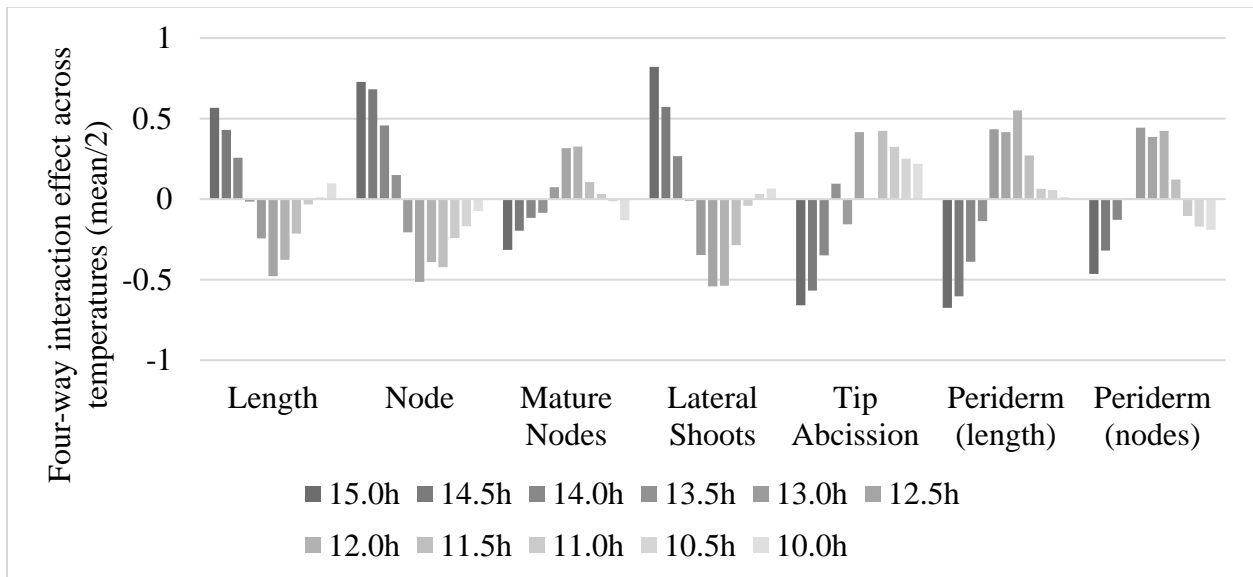


Figure B32. Plotted mean four-way interaction effect trends averaged across tested '1001'.

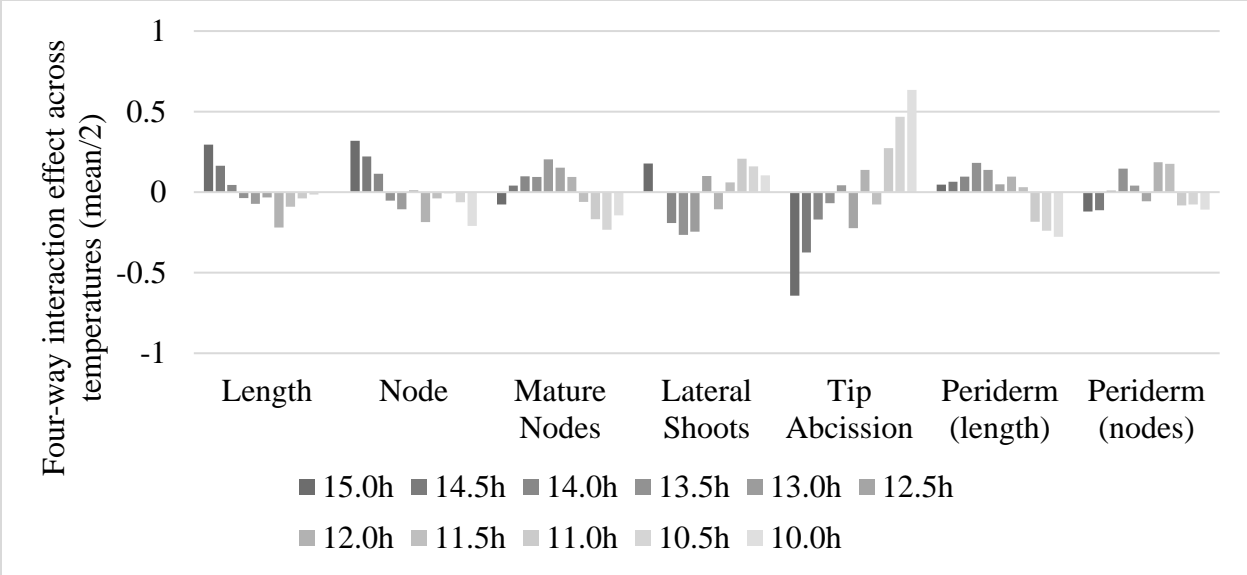


Figure B33. Plotted mean four-way interaction effect trends averaged across tested '1002'.

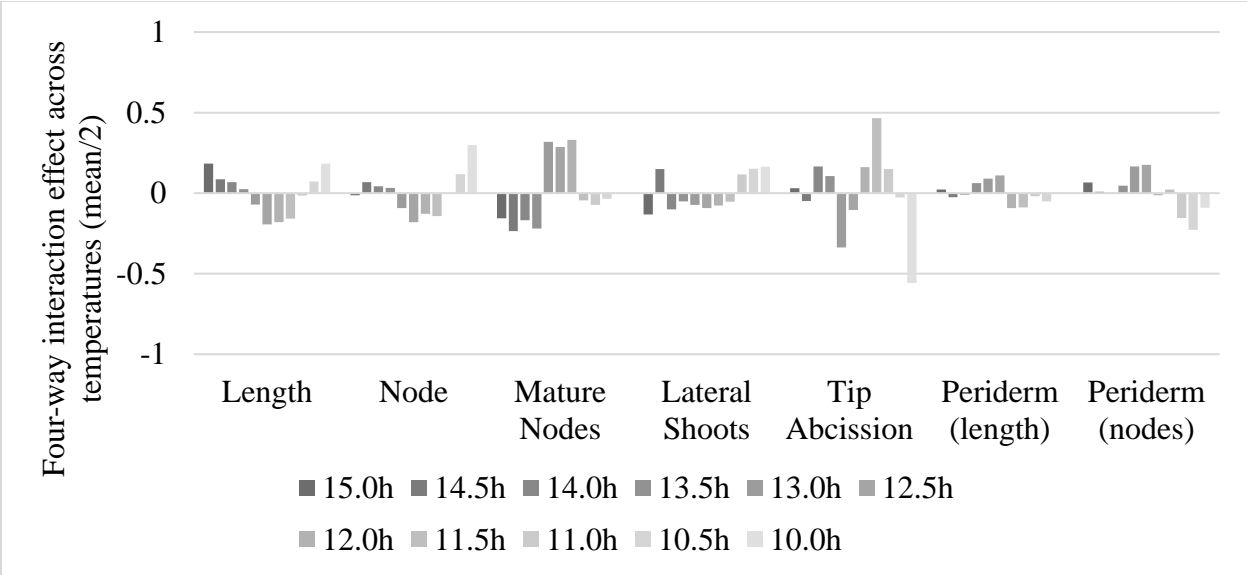


Figure B34. Plotted mean four-way interaction effect trends averaged across tested '1003'.



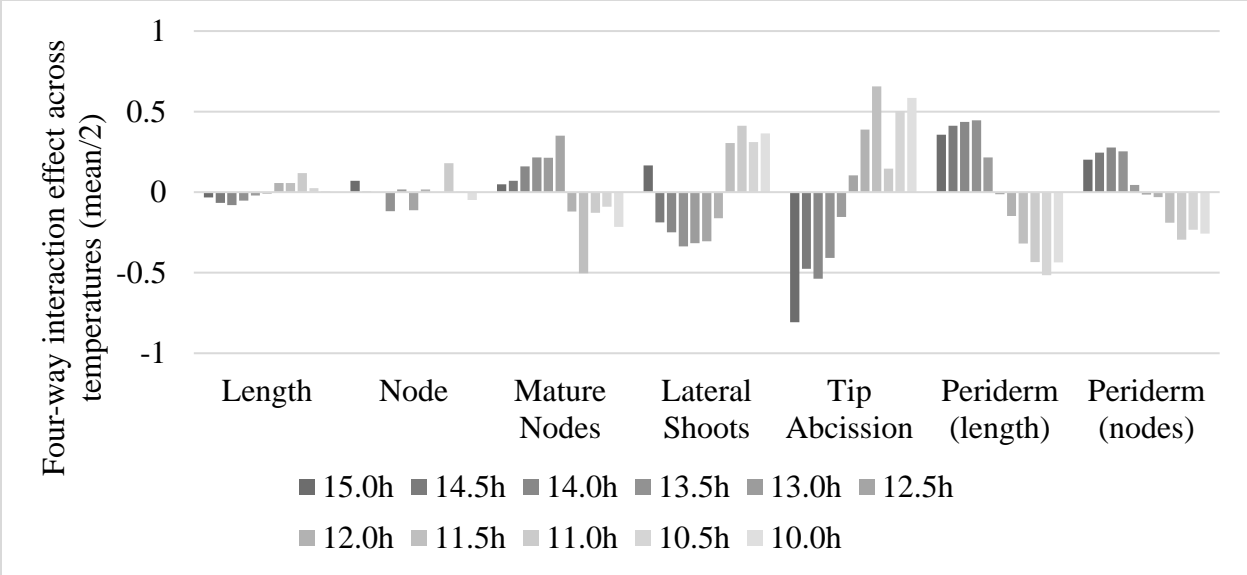


Figure B35. Plotted mean four-way interaction effect trends averaged across tested 'Frontenac'.

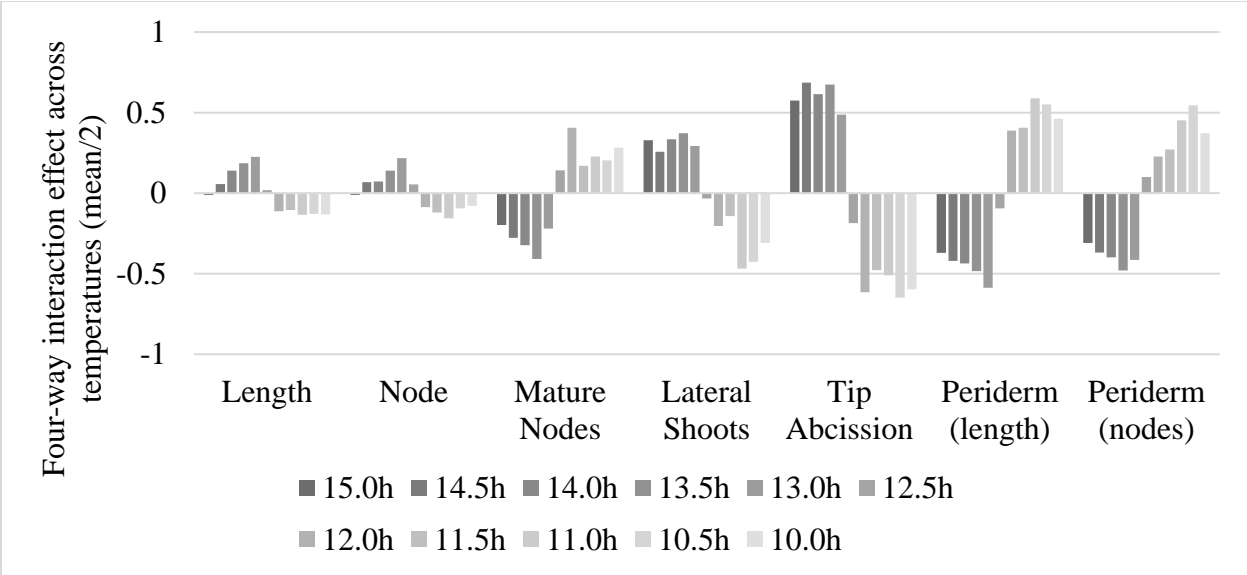


Figure B36. Plotted mean four-way interaction effect trends averaged across tested 'MN 1131'.

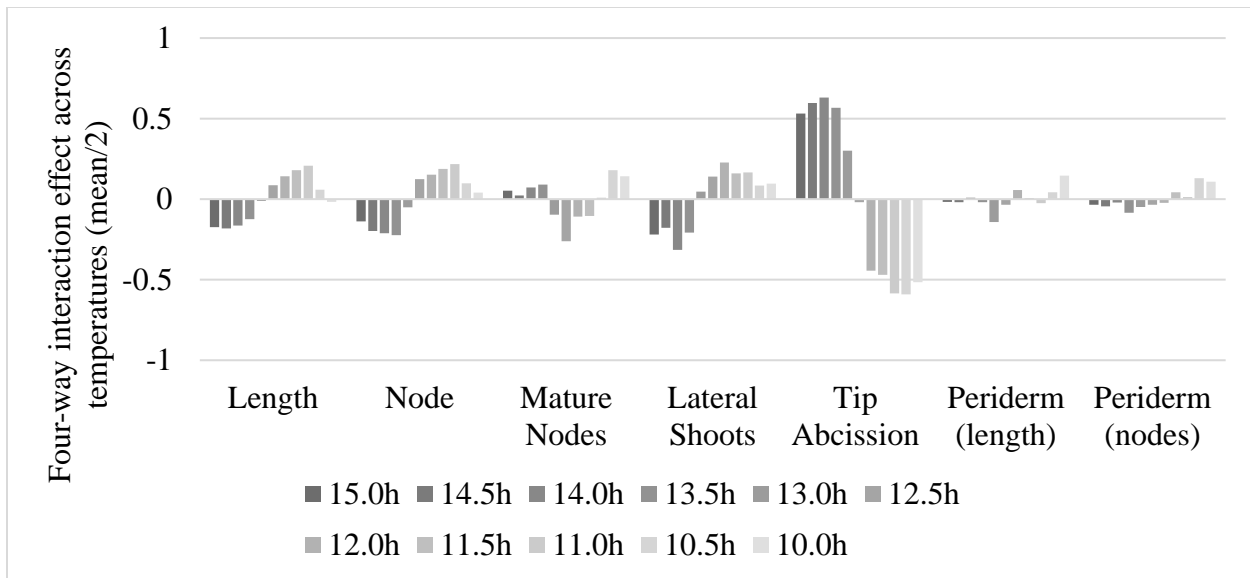


Figure B37. Plotted mean four-way interaction effect trends averaged across tested 'Marquette'.

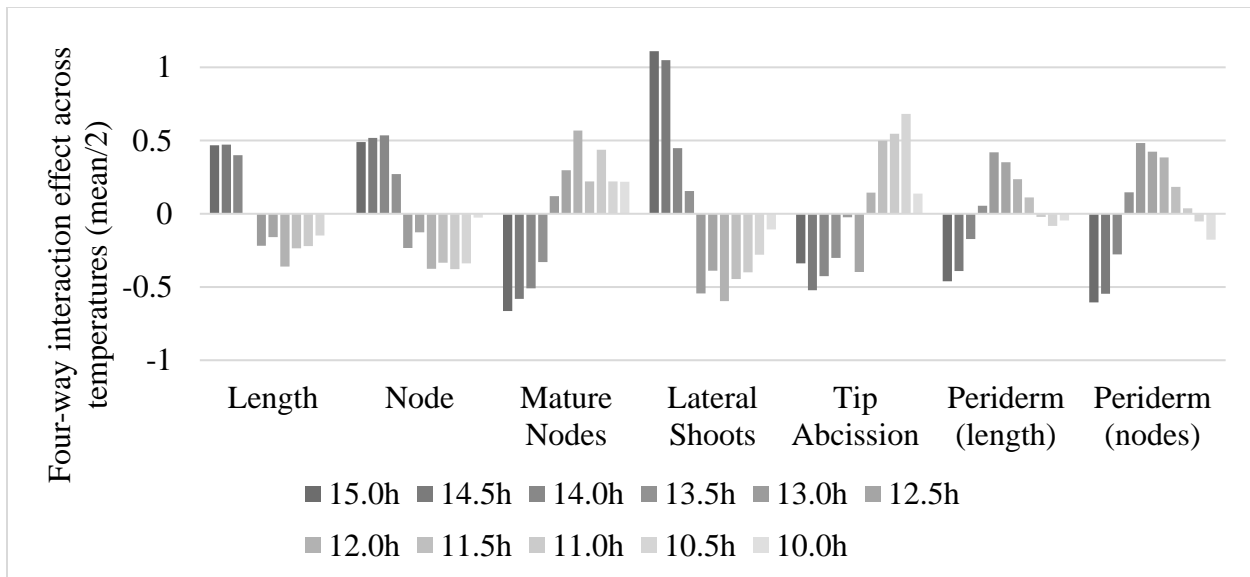


Figure B38. Plotted mean four-way interaction effect trends averaged across tested '1004'.

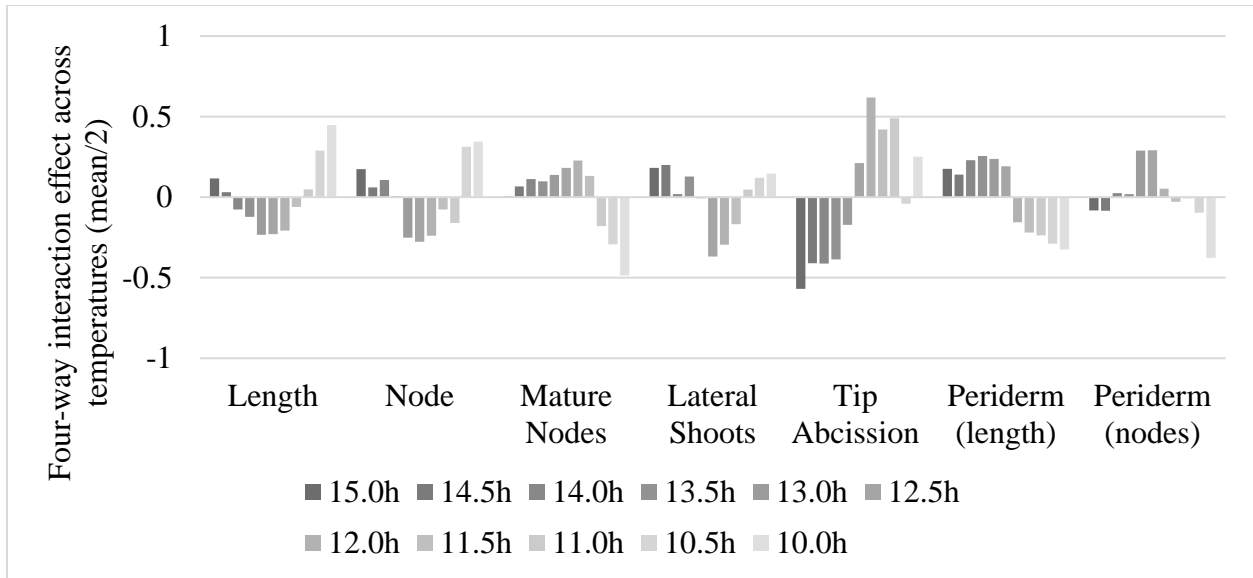


Figure B39. Plotted mean four-way interaction effect trends averaged across tested 'SD 62-8-160'.

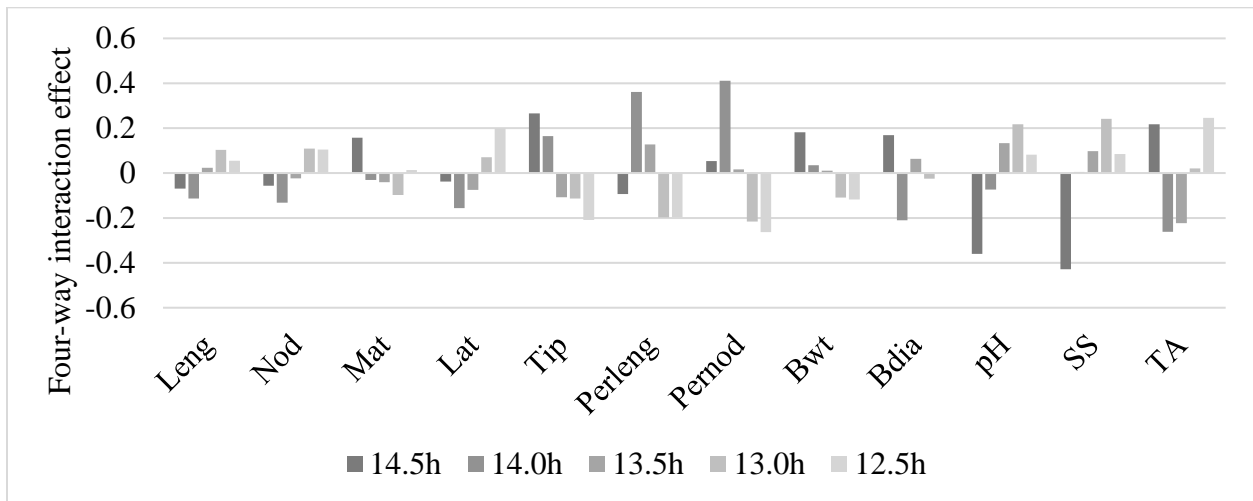


Figure B40. Plotted mean four-way interaction effect trends for averaged 'St. Croix' in Absaraka, ND in 2012. Leng, stem length; Nod, number of nodes; Mat, number of mature buds; Lat, number of lateral shoots; Tip, tip abscission progress; Perleng, periderm development as length of stem; Pernod, periderm development as number of nodes; Bwt, berry weight; Bdia, berry diameter; pH, juice pH; SS, juice soluble solid; TA, juice titratable acidity.

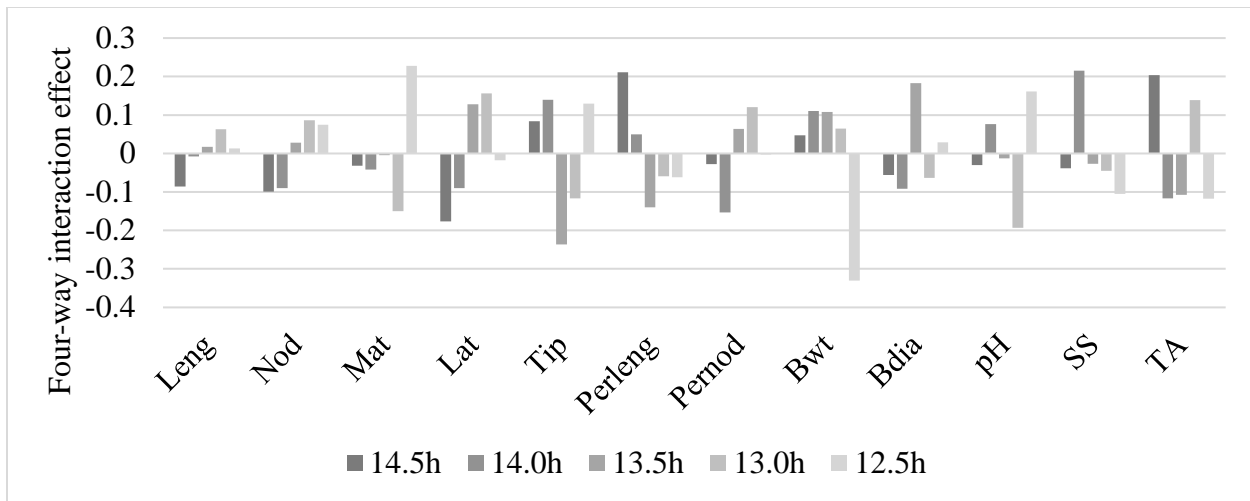


Figure B41. Plotted mean four-way interaction effect trends for averaged ‘St. Croix’ in Wyndmere, ND in 2012. Leng, stem length; Nod, number of nodes; Mat, number of mature buds; Lat, number of lateral shoots; Tip, tip abscission progress; Perleng, periderm development as length of stem; Pernod, periderm development as number of nodes; Bwt, berry weight; Bdia, berry diameter; pH, juice pH; SS, juice soluble solid; TA, juice titratable acidity.

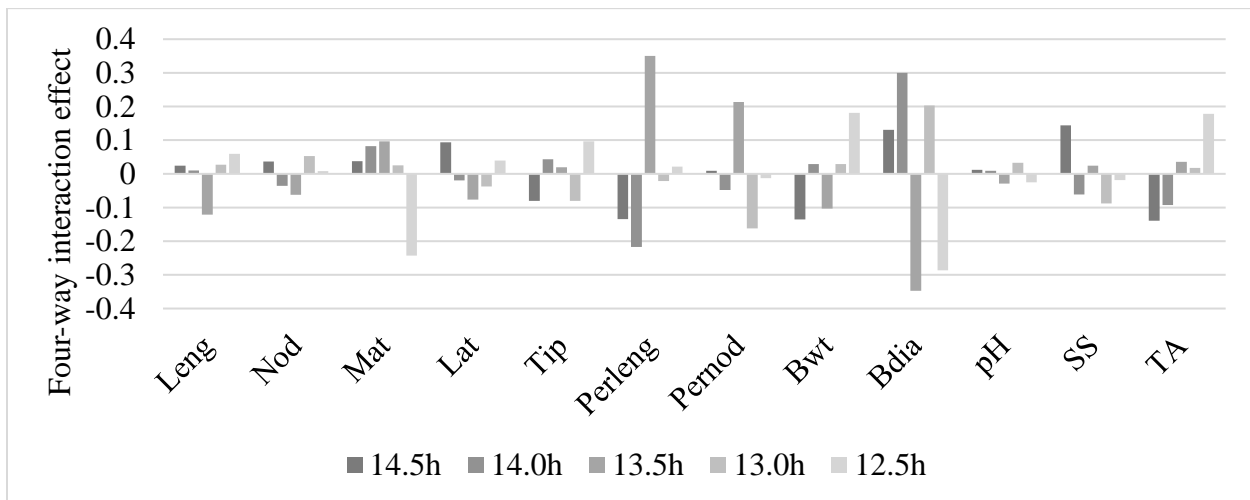


Figure B42. Plotted mean four-way interaction effect trends for averaged ‘St. Croix’ in Absaraka, ND in 2013. Leng, stem length; Nod, number of nodes; Mat, number of mature buds; Lat, number of lateral shoots; Tip, tip abscission progress; Perleng, periderm development as length of stem; Pernod, periderm development as number of nodes; Bwt, berry weight; Bdia, berry diameter; pH, juice pH; SS, juice soluble solid; TA, juice titratable acidity.

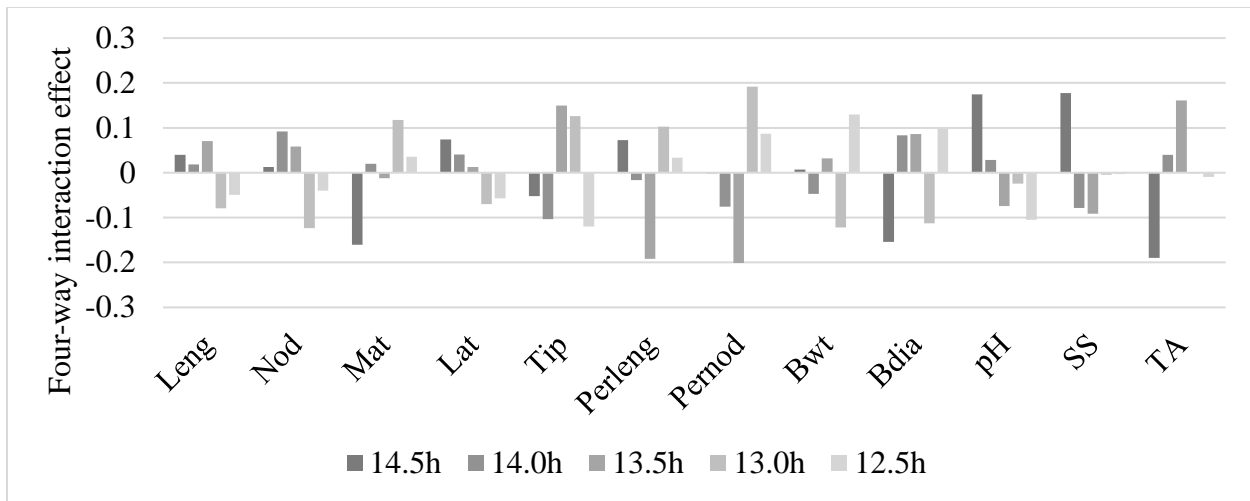


Figure B43. Plotted mean four-way interaction effect trends for averaged ‘St. Croix’ in Wyndmere, ND in 2013. Leng, stem length; Nod, number of nodes; Mat, number of mature buds; Lat, number of lateral shoots; Tip, tip abscission progress; Perleng, periderm development as length of stem; Pernod, periderm development as number of nodes; Bwt, berry weight; Bdia, berry diameter; pH, juice pH; SS, juice soluble solid; TA, juice titratable acidity.

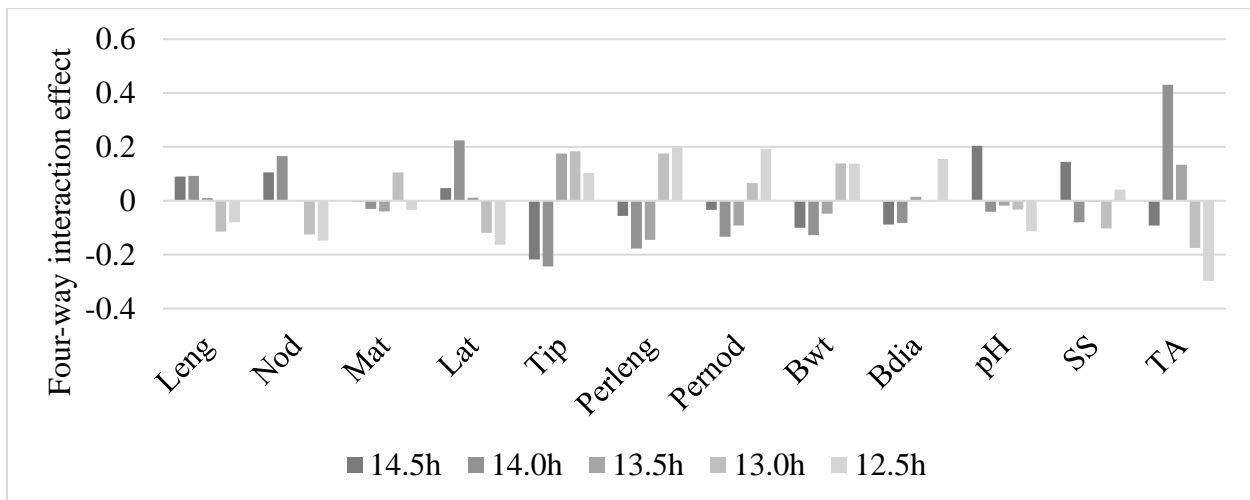


Figure B44. Plotted mean four-way interaction effect trends for averaged ‘St. Croix’ in Absaraka, ND in 2014. Leng, stem length; Nod, number of nodes; Mat, number of mature buds; Lat, number of lateral shoots; Tip, tip abscission progress; Perleng, periderm development as length of stem; Pernod, periderm development as number of nodes; Bwt, berry weight; Bdia, berry diameter; pH, juice pH; SS, juice soluble solid; TA, juice titratable acidity.

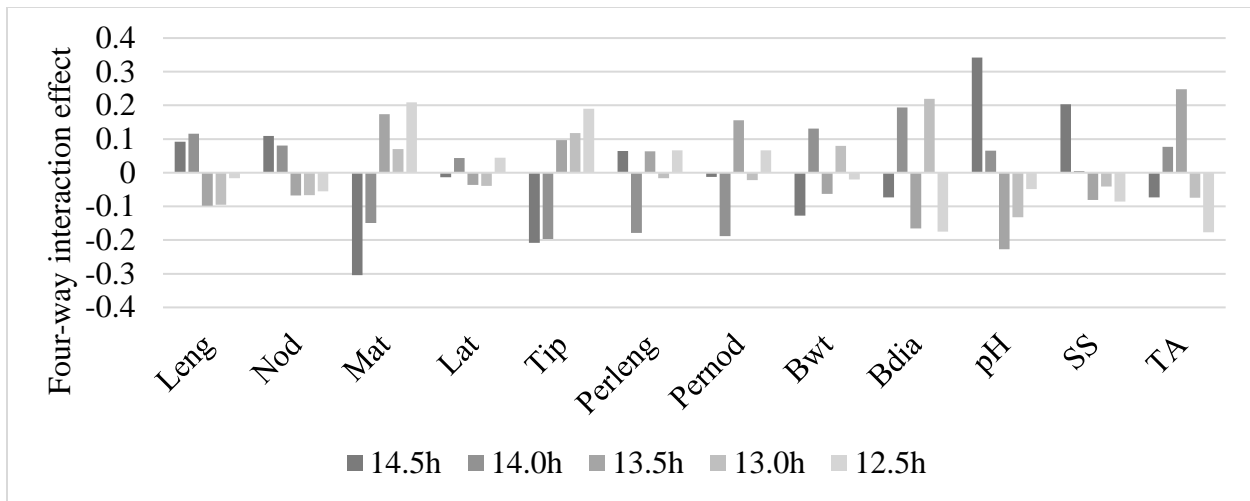


Figure B45. Plotted mean four-way interaction effect trends for averaged ‘Marquette’ in Absaraka, ND in 2012. Leng, stem length; Nod, number of nodes; Mat, number of mature buds; Lat, number of lateral shoots; Tip, tip abscission progress; Perleng, periderm development as length of stem; Pernod, periderm development as number of nodes; Bwt, berry weight; Bdia, berry diameter; pH, juice pH; SS, juice soluble solid; TA, juice titratable acidity.

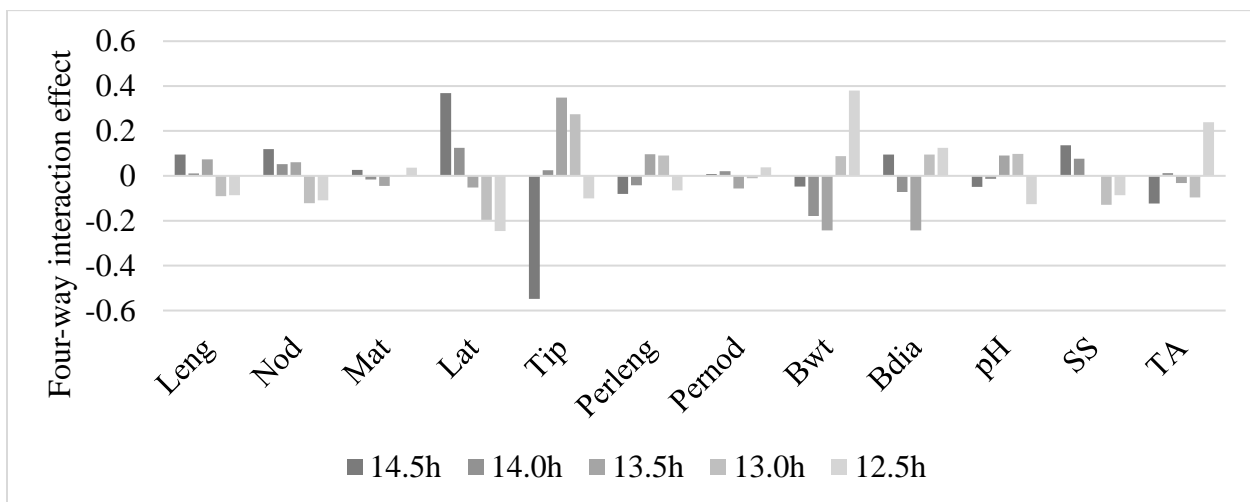


Figure B46. Plotted mean four-way interaction effect trends for averaged ‘Marquette’ in Wyndmere, ND in 2012. Leng, stem length; Nod, number of nodes; Mat, number of mature buds; Lat, number of lateral shoots; Tip, tip abscission progress; Perleng, periderm development as length of stem; Pernod, periderm development as number of nodes; Bwt, berry weight; Bdia, berry diameter; pH, juice pH; SS, juice soluble solid; TA, juice titratable acidity.

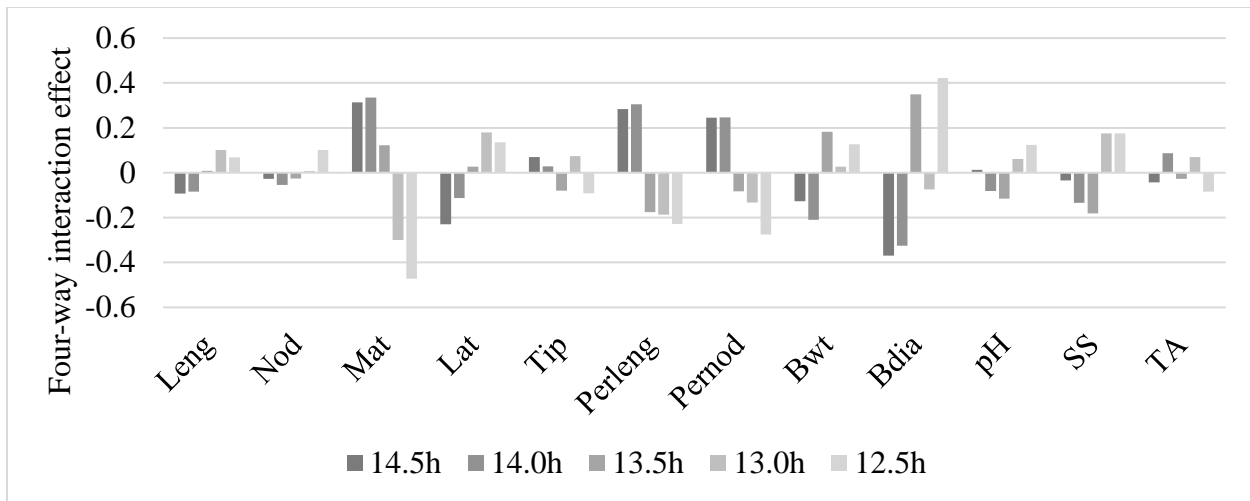


Figure B47. Plotted mean four-way interaction effect trends for averaged ‘Marquette’ in Absaraka, ND in 2013. Leng, stem length; Nod, number of nodes; Mat, number of mature buds; Lat, number of lateral shoots; Tip, tip abscission progress; Perleng, periderm development as length of stem; Pernod, periderm development as number of nodes; Bwt, berry weight; Bdia, berry diameter; pH, juice pH; SS, juice soluble solid; TA, juice titratable acidity.

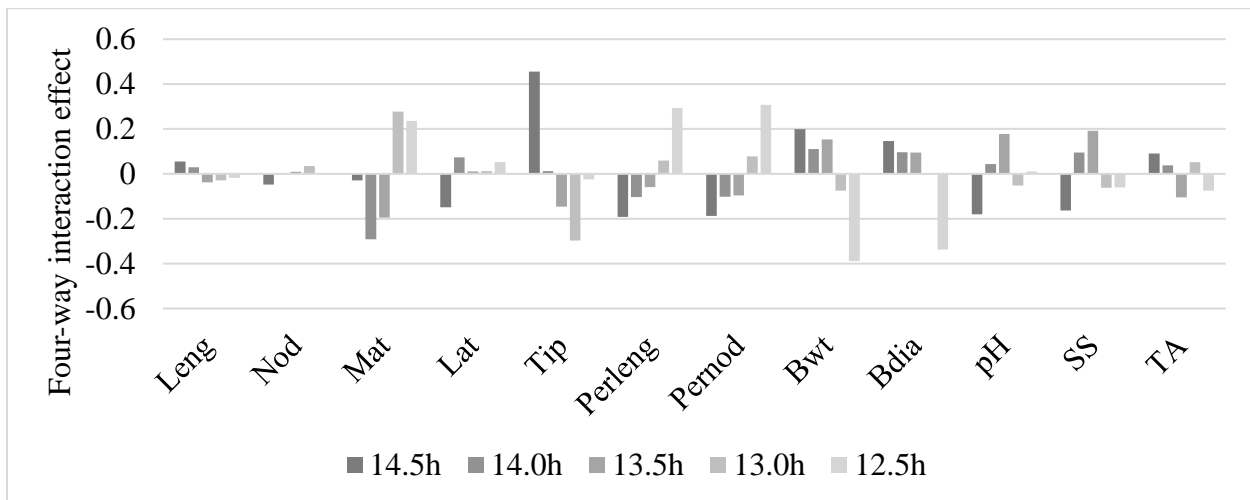


Figure B48. Plotted mean four-way interaction effect trends for averaged ‘Marquette’ in Wyndmere, ND in 2013. Leng, stem length; Nod, number of nodes; Mat, number of mature buds; Lat, number of lateral shoots; Tip, tip abscission progress; Perleng, periderm development as length of stem; Pernod, periderm development as number of nodes; Bwt, berry weight; Bdia, berry diameter; pH, juice pH; SS, juice soluble solid; TA, juice titratable acidity.

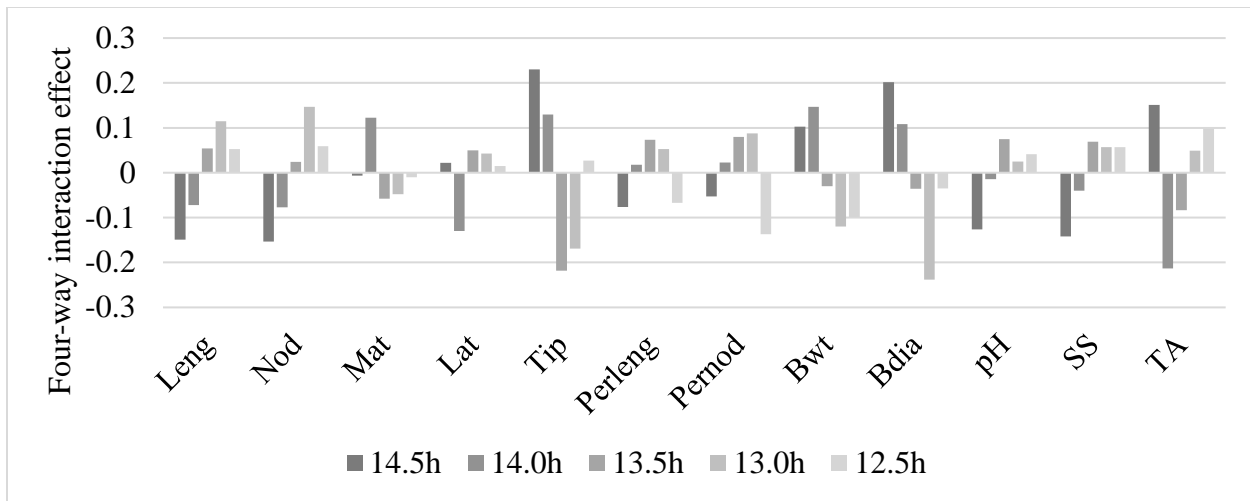


Figure B49. Plotted mean four-way interaction effect trends for averaged ‘Marquette’ in Absaraka, ND in 2014. Leng, stem length; Nod, number of nodes; Mat, number of mature buds; Lat, number of lateral shoots; Tip, tip abscission progress; Perleng, periderm development as length of stem; Pernod, periderm development as number of nodes; Bwt, berry weight; Bdia, berry diameter; pH, juice pH; SS, juice soluble solid; TA, juice titratable acidity.

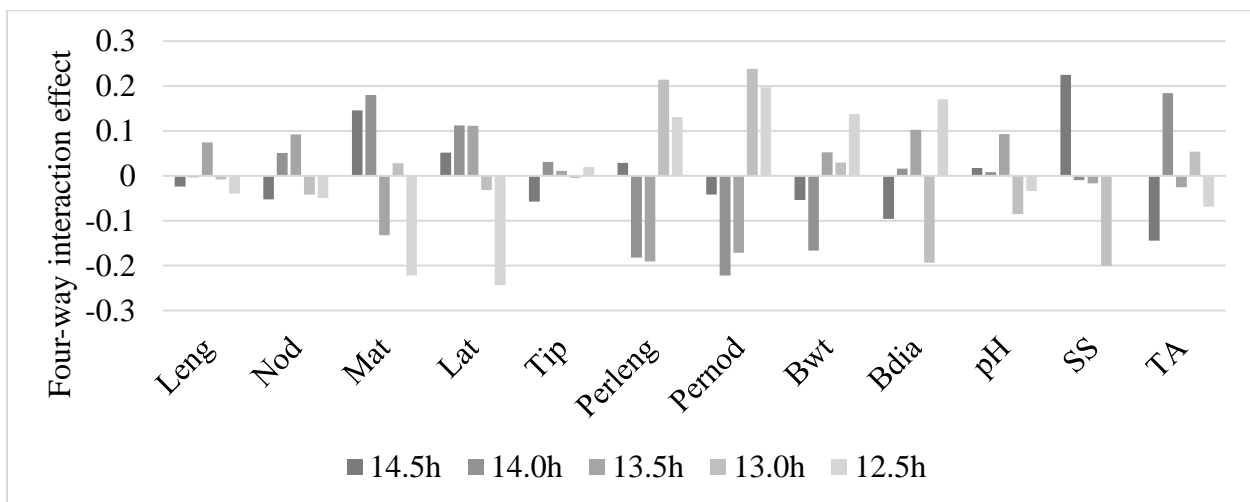


Figure B50. Plotted mean four-way interaction effect trends for averaged ‘Frontenac Gris’ in Absaraka, ND in 2012. Leng, stem length; Nod, number of nodes; Mat, number of mature buds; Lat, number of lateral shoots; Tip, tip abscission progress; Perleng, periderm development as length of stem; Pernod, periderm development as number of nodes; Bwt, berry weight; Bdia, berry diameter; pH, juice pH; SS, juice soluble solid; TA, juice titratable acidity.



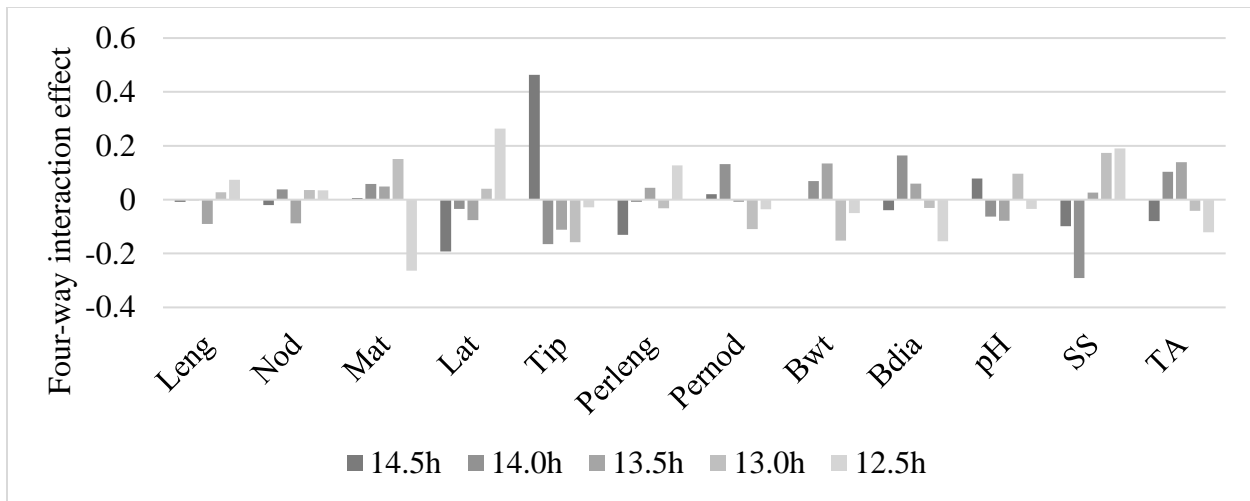


Figure B51. Plotted mean four-way interaction effect trends for averaged 'Frontenac Gris' in Wyndmere, ND in 2012. Leng, stem length; Nod, number of nodes; Mat, number of mature buds; Lat, number of lateral shoots; Tip, tip abscission progress; Perleng, periderm development as length of stem; Pernod, periderm development as number of nodes; Bwt, berry weight; Bdia, berry diameter; pH, juice pH; SS, juice soluble solid; TA, juice titratable acidity.

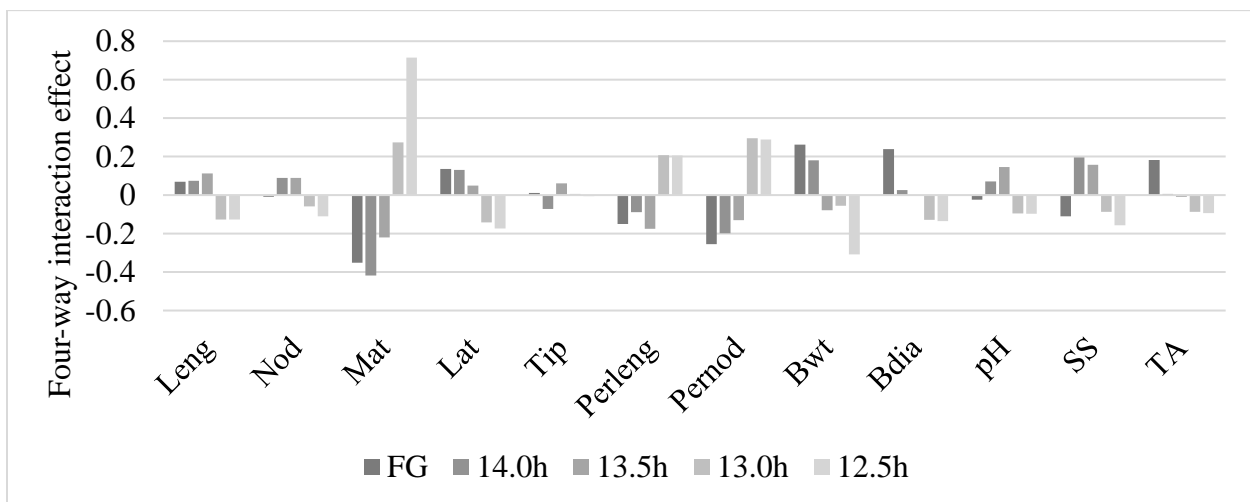


Figure B52. Plotted mean four-way interaction effect trends for averaged 'Frontenac Gris' in Absaraka, ND in 2013. Leng, stem length; Nod, number of nodes; Mat, number of mature buds; Lat, number of lateral shoots; Tip, tip abscission progress; Perleng, periderm development as length of stem; Pernod, periderm development as number of nodes; Bwt, berry weight; Bdia, berry diameter; pH, juice pH; SS, juice soluble solid; TA, juice titratable acidity.

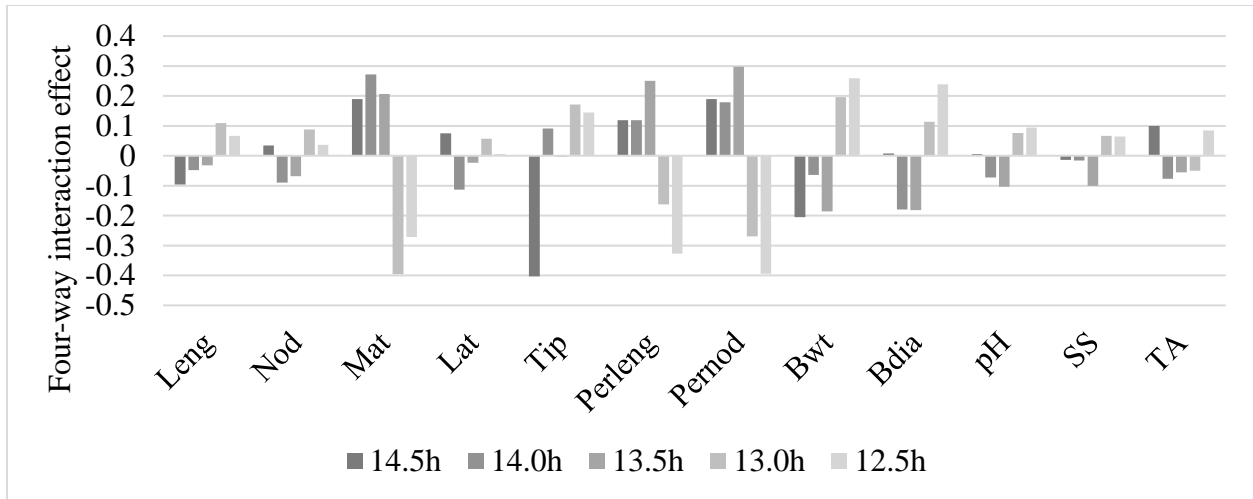


Figure B53. Plotted mean four-way interaction effect trends for averaged ‘Frontenac Gris’ in Wyndmere, ND in 2013. Leng, stem length; Nod, number of nodes; Mat, number of mature buds; Lat, number of lateral shoots; Tip, tip abscission progress; Perleng, periderm development as length of stem; Pernod, periderm development as number of nodes; Bwt, berry weight; Bdia, berry diameter; pH, juice pH; SS, juice soluble solid; TA, juice titratable acidity.

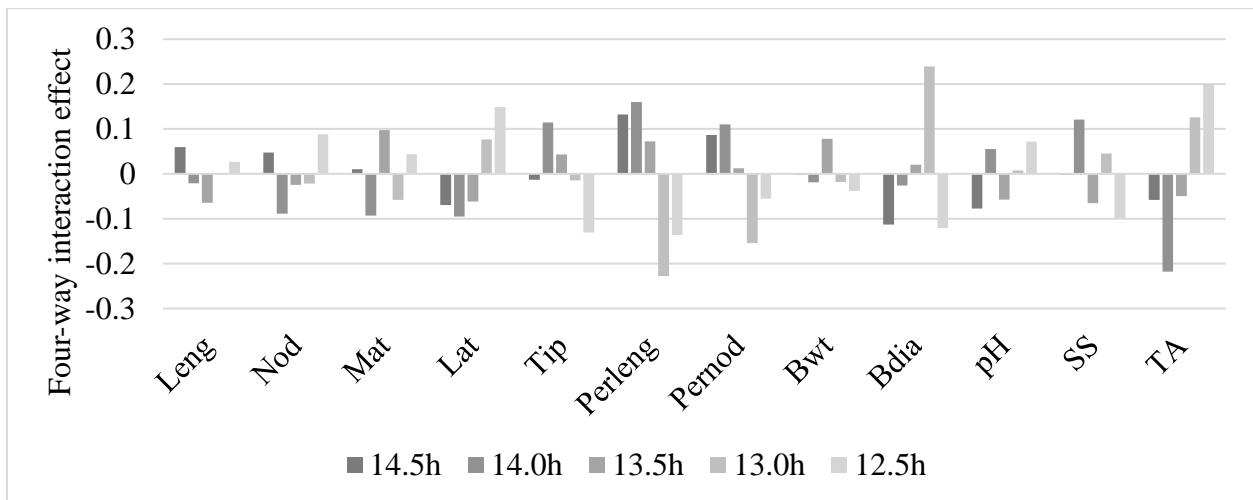


Figure B54. Plotted mean four-way interaction effect trends for averaged ‘Frontenac Gris’ in Absaraka, ND in 2014. Leng, stem length; Nod, number of nodes; Mat, number of mature buds; Lat, number of lateral shoots; Tip, tip abscission progress; Perleng, periderm development as length of stem; Pernod, periderm development as number of nodes; Bwt, berry weight; Bdia, berry diameter; pH, juice pH; SS, juice soluble solid; TA, juice titratable acidity.

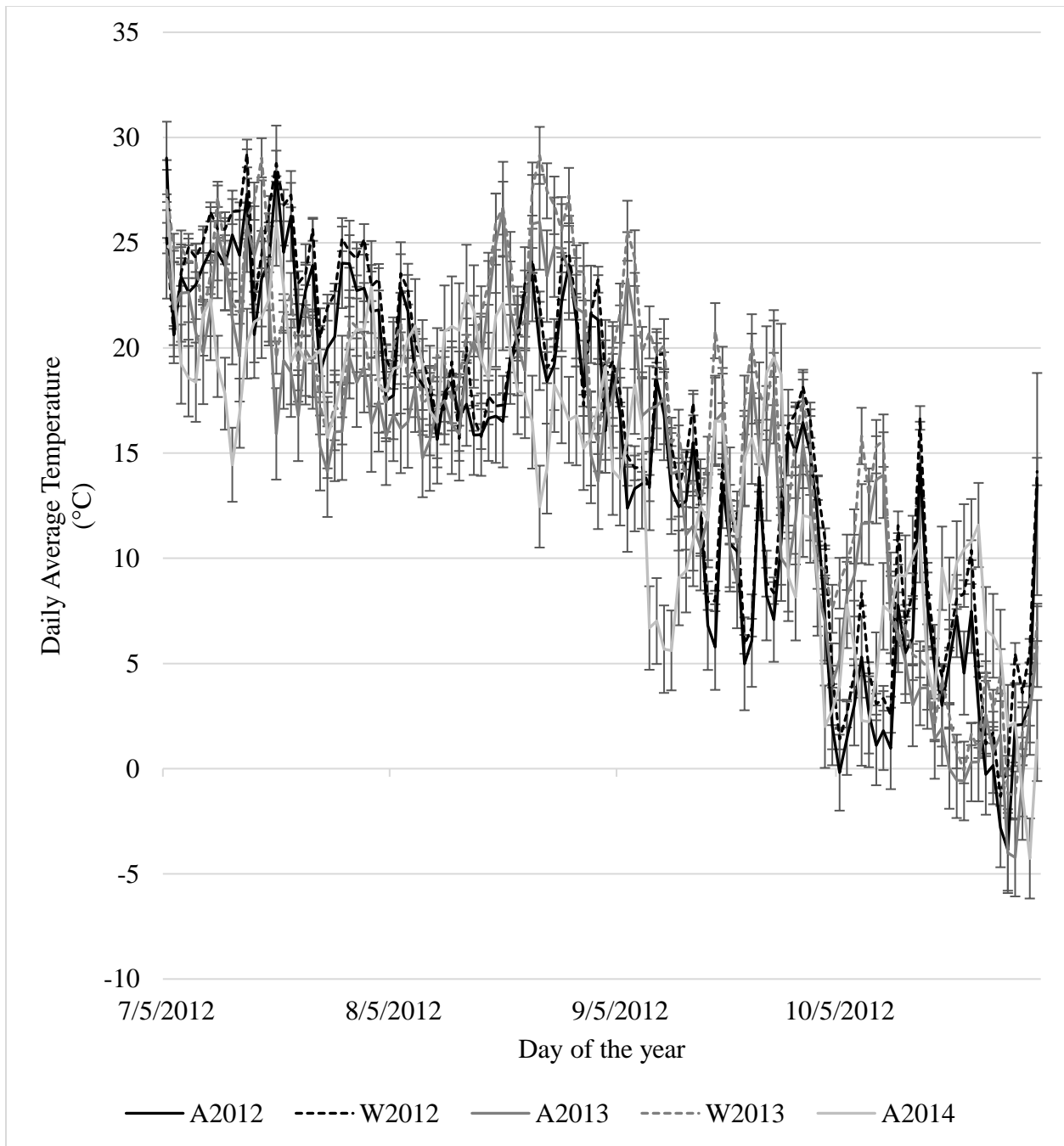


Figure B55. Daily average temperatures in Absaraka, ND (A) and Wyndmere ND (W) in 2012 – 2014. Error bars indicate +/- one standard deviation from the mean of the sampled data loggers (n=9) within each environment.